**DOCTOR OF PHILOSOPHY**

# Biohydrogen production in Escherichia coli – a synthetic biology approach

Kelly, Ciaran L.

*Award date:*
2014

DOCTOR OF PHILOSOPHY

# Biohydrogen production in Escherichia coli – a synthetic biology approach

Ciaran L. Kelly

2014

University of Dundee

# Biohydrogen Production in *Escherichia coli* – A Synthetic Biology Approach

Ciarán L Kelly

September 2013


Thesis submitted to the University of Dundee in partial fulfilment of the requirements for the degree of Doctor of Philosophy

**Table of Contents**

**Table of Figures**

**Table of Tables**

**Acknowledgements**

Well, I wasn't always certain I'd ever get to this stage of finishing the thesis, so a massive thank you is firstly owed to my supervisor, Frank Sargent. You've given me advice and guidance when I've really needed it and more importantly when I didn't know I needed it! I thank you for letting me work in your lab, for your patience in allowing me the freedom to go off on slight tangents at points throughout this project (and the "subtle" nudges in the right direction when I needed them as well) and importantly for encouraging me to take advantage of all of the different opportunities available as a PhD student in the College of Life Sciences in Dundee. I hope I've done your original ideas for the project some kind of justice.

I also need to thank Tracy Palmer for all of her help during my PhD, for doing a great job as Head of Division and for all of the good-humoured slagging matches in the bay! MMB has been an amazing place to spend four years learning how to do science properly and I'd like to thank everyone who's played a part in making it so easy, interesting and fun! I've made some amazing friends for life here and genuinely feel like I could thank every single person in the division (if only for putting up with my singing and constant pranks). But I want to specifically thank Holger Kneuper, Grant Buchanan, Jennifer McDowall, Rebecca Keller, Max Fritsch and Conny Pinske for showing me so many techniques and giving me so much advice over the course of my PhD. Thank you to our collaborators Paul Fyfe in Bill Hunter's group, Fraser Armstrong at the University of Oxford and Alison Parkin at the University of York as well as Colin Hammond in Tom Owen-Hughes' lab. I also need to say a special thank you to our amazing lab manager, Jackie Heilbronn, who does far too much for everyone in the division, makes ordering a breeze and still is able to smile through it all! Thanks as well to the secretarial staff over the 4 years (Tricia, Geri, Claire and Louise) for sorting out transport, accommodation and conferences.

Finally I'd like to thank those closest to me. To my friends, thanks for putting up with me, the eternal-student bum! To my family, Aoife, Niamh and my two heroes, my Mam and Dad, I can't thank you enough for all of the support and encouragement you've given me to get me to where I am today. I could not have any more admiration for how strong you've been over the last couple of extremely difficult years and keeping me focused at times when it's not been easy. And of course I can't finish without thanking Lisa. As most people who know me will happily confirm, I can be a nightmare at times: loud; silly; and very opinionated! You've given me so much love and support over the last 3 years (despite initially finding me annoying in first year), as well as a lot of fun and I'm very lucky you still want to hang around with me!

**Declaration**

I declare that I am the author of this thesis and that, unless otherwise stated, all references cited have been consulted; that the work of which this thesis is a record has been performed by me, and that it has not been previously accepted for a higher degree: where the thesis is based upon joint research, the nature and extent of my individual contribution is defined.

**Ciarán L Kelly**

**Abstract**

In the 21st Century molecular hydrogen ($H_2$) has become an essential industrial commodity. It is widely heralded as an exciting alternative to petroleum-based transportation fuels and also plays indispensable roles in many other important industrial processes, including hydrogenation of fats and oils, methanol production, and ammonia production – an essential component of agricultural fertilizers.

Biohydrogen (Bio-$H_2$) is molecular hydrogen produced by microorganisms and is an exciting prospect as a fully renewable, commercially-viable second-generation biofuel. Bio-$H_2$ can be produced at ambient temperatures by metal-dependent hydrogenase enzymes, with potentially no CO or $H_2S$ contamination, and is a carbon neutral/positive process.

*Escherichia coli* naturally produces Bio-$H_2$ during mixed-acid fermentation via its own endogenous nickel-dependent hydrogenase enzymes. The main aim of this project is to enhance Bio-$H_2$ production by *E. coli,* and to achieve this goal a number of alternative synthetic biology approaches were investigated. A synthetic [FeFe]-hydrogenase based on a thermostable NADH-dependent hydrogenase was designed, constructed and expressed in *E. coli*. The structure and activity of the synthetic hydrogenase has been characterised *in vitro* using a number of techniques including autoradiography, spectroscopy, SEC-MALLS, protein-film voltammetry and $H_2$ production assays. Metabolic engineering of various *E. coli* strains and directed protein evolution has been carried out to integrate this synthetic hydrogenase activity into cellular metabolism and the resulting strains were characterised using metabolomics and standard microbiological approaches.

Another approach used in this project involved the construction and expression of active $H_2$-producing synthetic chimeric metalloenzymes, which combined the catalytic activity of two different enzymes: thiosulfate reductase from *Salmonella*; and *E. coli* Hyd-2. The activity of this synthetic fusion enzyme could be improved by increasing/maintaining the proton motive force across the cytoplasmic membrane, through the heterologous expression of a proton-pumping proteorhodopsin. Finally the bidirectionality of *E. coli* Hyd-2, i.e. $H_2$ oxidation and $H_2$ production, was demonstrated, suggesting that it may operate as a quinol release valve *in vivo*.

**Publications**

F. Sargent, F. A. Davidson, C. L. Kelly, R. Binny, N. Christodoulides, D. Gibson, E. Johansson, K. Kozyrska, L. Licandro Lado, J. MacCallum, R. Montague, B. Ortmann, R. Owen, S.J. Coulthurst, L. Dupuy, A. R. Prescott and T. Palmer (2013) "A synthetic system for expression of components of a bacterial microcompartment", Microbiology, published online 6 Sep 2013

C. L. Kelly, A. Parkin, L. Flanagan, T. Palmer and F. Sargent (in preparation) "Design and testing of a synthetic [FeFe]-hydrogenase", submitting to ACS Synthetic Biology

**Conferences and Presentations**

SB6.0: The Sixth International Meeting on Synthetic Biology, Imperial College London, London, UK. July 2013. Poster Presentation: "Synthetic Biology approaches to Biohydrogen Production in *E. coli*". Awarded General Travel Grant by the Biochemical Society and by the Northern Research Partnership.

Biochemical Society YLS Symposium: Protein Evolution and Engineering, Leeds University, UK. August 2011. Co-Chair of a Session

SB5.0: The Fifth International Meeting on Synthetic Biology, Stanford University, California, USA. June 2011. Poster Presentation: "Biohydrogen Production: Synthetically-Designed Hydrogenase Expression in *E. coli*". Awarded Young Researcher Travel Grant by the BioBricks Foundation

Northern Research Partnership Graduate Student Symposium, University of Dundee, UK. January 2011. First Place for Poster Presentation: "Engineered Biohydrogen Production in *Escherichia coli*"

The 9th International Hydrogenase Conference, Uppsala University, Sweden. June – July 2010. Poster Presentation: "Engineered Biohydrogen Production in Enteric Bacteria". Awarded Scientific Meeting Travel Grant by the Society for General Microbiology

**Abbreviations**

| | |
|---|---|
| Å | Ångstrom (0.1 nm) |
| A | absorbance |
| ADP | adenosine diphosphate |
| Amp | ampicillin |
| ATP | adenosine triphosphate |
| Bio-H2 | biohydrogen |
| BLAST | basic local alignment search tool |
| bp | base pairs |
| BSA | bovine serum albumin |
| BV | benzyl viologen |
| Cml | chloramphenicol |
| C-terminal | carboxy-terminal |
| CTP | cytidine triphosphate |
| DMSO | dimethyl sulphoxide |
| DNA | deoxyribonucleic acid |
| DNase | deoxyribonuclease |
| dNTP | deoxynucleoside triphosphate |
| DTT | dithiothreitol |
| EDTA | ethylenediamine tetraacetic acid |
| EPR | electron paramagnetic resonance |
| FAD | flavin adenine dinucleotide |
| FeS | iron-sulphur |
| FHL | formate hydrogenlyase |
| FMN | flavin mononucleotide |
| g | gram |
| x g | relative centrifugal force |
| gDNA | genomic DNA |
| GFP | green fluorescent protein |
| GTP | guanosine triphosphate |

| | |
|---|---|
| h | hour |
| H | proton |
| $H_2$ | molecular hydrogen |
| Hyd-1 | hydrogenase-1 |
| Hyd-2 | hydrogenase-2 |
| Hyd-3 | hydrogenase-3 |
| IMAC | immobilised metal-ion affinity chromatography |
| IPTG | isopropyl β-D thiogalactopyranoside |
| Kan | kanamycin |
| kb | kilobases |
| kDa | kilodaltons |
| LB | Luria-Bertani medium |
| m | milli |
| M | molar |
| MGD | molybdopterin guanine dinucleotide |
| µ | micro |
| min | minute |
| MMS | methyl methanesulfonate |
| mol | mole |
| mRNA | messenger RNA |
| MV | methyl viologen |
| $NAD^+$ | nicotinamide adenine dinucleotide |
| NADH | nicotinamide adenine dinucleotide - reduced form |
| $NADP^+$ | nicotinamide adenine dinucleotide phosphate |
| NADPH | nicotinamide adenine dinucleotide phosphate - reduced form |
| N-terminal | amino terminal |
| nm | nanometre |
| NMR | nuclear magnetic resonance |
| NTP | nucleotide triphosphate |
| OD | optical density |
| PAGE | polyacrylamide gel electrophoresis |

| | |
|---|---|
| PCR | polymerase chain reaction |
| PFE | protein film electrochemistry |
| $P_i$ | inorganic phosphate |
| pmf (Δp) | proton motive force |
| psi | pounds per square inch |
| Tat | twin-arginine translocase |
| rpm | rotations per minute |
| SDS | sodium dodecyl sulphate |
| TM | transmembrane |
| TMAO | trimethylamine N-oxide |
| Tris | Tris(hydroxymethyl)aminomethane |
| TTP | thymidine triphosphate |
| UV | ultraviolet |
| Vis | visible |
| v/v | volume per volume |
| w/v | weight per volume |

**Amino-acid abbreviations**

| | | |
|---|---|---|
| Alanine | A | Ala |
| Arginine | R | Arg |
| Asparagine | N | Asn |
| Aspartate | D | Asp |
| Cysteine | C | Cys |
| Glutamate | E | Glu |
| Glutamine | Q | Gln |
| Glycine | G | Gly |
| Histidine | H | His |
| Isoleucine | I | Ile |
| Leucine | L | Leu |
| Lysine | K | Lys |
| Methionine | M | Met |
| Phenylalanine | F | Phe |
| Proline | P | Pro |
| Serine | S | Ser |
| Threonine | T | Thr |
| Tryptophan | W | Trp |
| Tyrosine | Y | Tyr |
| Valine | V | Val |
| | | |
| Any | X | |

# 1. Introduction

## 1.1 Energy supply and demand in the 21st Century

Climate Change is an unequivocal, urgent global issue. Global mean atmospheric temperature is rising and this has many effects around the world. Sea levels have already risen by 15-20 cm on average over the last century (Meyssignac and Cazenave, 2012), glaciers are retreating and extreme fluctuations in temperature and rainfall are increasing (Solomon and (eds.), 2007). Human health has already been hugely affected as a direct result of these physical symptoms of an ailing planet (Campbell-Lendrum and Woodruff, 2007). This has now been conclusively attributed to anthropogenic greenhouse gas (GHG) emissions (Solomon and (eds.), 2007).

The world population is conservatively projected to reach 9.6 billion people by 2050 (UN Department of Economic and Social Affairs, 2013), creating a massive corresponding increase in world energy consumption demand. We have already seen a doubling of the average annual world energy consumption from 1980 to 2005 and this increase in demand shows no sign of stopping. World energy consumption demands are projected to increase by over a third by 2035, mostly driven by emerging economies such as India and China (60% rise in demand by 2035) (IEA, 2012).

The energy sector is responsible for over two thirds of global GHG emissions, due to its continuing dependence on fossil fuels (IEA, 2013). It is therefore clear that our heavy reliance on fossil fuels as energy sources must be reduced and alternative carbon-neutral energy sources must be developed.

There are worrying signs, however, amid current global economic uncertainties that climate change is not as high a political priority. It will be interesting to monitor developments in Ireland over the next 20 years, which has implemented many progressive green policies in the past two decades. Now, however, the discovery of Ireland's first commercially viable oil field, Barryroe off the west coast of Ireland (1.7 billion barrels, of which at least 270 million can be recovered), is viewed as the possible saviour of Ireland’s bankrupt economy, and measures are underway to rapidly exploit this not-so-white knight.

Evidence of this abandonment of many admirable global policies to tackle climate change came from the recent International Energy Authority’s special report on climate and energy where they concluded that the agreed global target to limit the anthropogenic rise in temperature to 2 °C, will not be met based on current proposals (3.6 °C – 5.3 °C more likely) and intensive action is required before 2020 (IEA, 2013).

With the rejection of nuclear power in many countries around the world, the options available to supply sustainable, carbon-neutral (or even carbon negative) energy sources include various

renewable energy sources such as wind, tidal, solar and hydroelectric, as well as biofuel energy sources such as biodiesel, biobutanol, biohydrogen, biomethane and bioethanol. In order to achieve this necessary development of greener energy sources, subsidies for fossil fuels however must be reduced ($523 billion in 2011, six times the amount of renewables subsidies: $88 billion) and carbon prices increased (fallen from €20/tonne in 2008 to €3.5/tonne in 2013), otherwise the incentive to develop sustainable energy sources will not exist (IEA, 2013).

First-generation biofuels used food crops as substrates for biofuel production (e.g. biodiesel or bioethanol). This is extremely controversial as it firstly drives up the price of foods such as wheat and sugar, but it also means that more land is needed to grow crops and therefore many first-generation biofuels actually lead to a net increase in GHG emissions and cannot be regarded as sustainable (Searchinger*, et al.*, 2008; Danielsen*, et al.*, 2009). Second-generation biofuels were developed to avoid this "food versus fuel" conundrum, as they do not use food crops as their main substrate. The ideal second-generation biofuels are those that use a variety of waste products as the substrate for biofuel production. Fourth-generation biofuels are now in development, which essentially integrate carbon capture and sequestration steps into the biofuel production process.

## 1.2 $H_2$ as an industrial commodity

Molecular hydrogen ($H_2$) in the 21st Century has become an essential industrial commodity. It plays indispensable roles in many important industrial processes (Figure 1.1), including the hydrogenation of fats and oils, methanol production, and ammonia production – an essential component of agricultural fertilizers. As legal requirements for cleaner automotive fuels rightly continue to get stricter around the world, $H_2$ is also used in refineries to remove dangerous pollutants, such as organic sulfur from crude oil, through a process called hydrodesulfurisation, as well as in the conversion of heavy crude oil to lighter fuels.

Moreover, due to its high energy density by weight, $H_2$ is widely heralded as an exciting alternative to petroleum-based transportation fuels, as it can be used directly in Proton Exchange Membrane (P.E.M.) fuel cells to generate electricity, with water vapour as its only emission, thus reducing greenhouse gas emissions from transportation.

The majority of $H_2$ is currently produced through steam-methane reformation (SMR), which requires a large energy input and produces large amounts of greenhouse gas emissions (Environmental Protection Agency, 2008) (Figure 1.1). Worldwide ammonia production in 2009 for example, required the production of 23 million metric tons of $H_2$, resulting in 198 million metric tons of $CO_2$ emissions, or 0.7% of global $CO_2$ emissions (Environmental Protection Agency, 2008; Geological Survey, 2011). The current unsustainable methods of $H_2$ production, in combination with issues such as hydrogen purification and storage as well as the high cost of fuel-cell technology mean that a number of significant economic and environmental hurdles must be surmounted before a fully-fledged "hydrogen economy" becomes a reality (Turner, 2004).

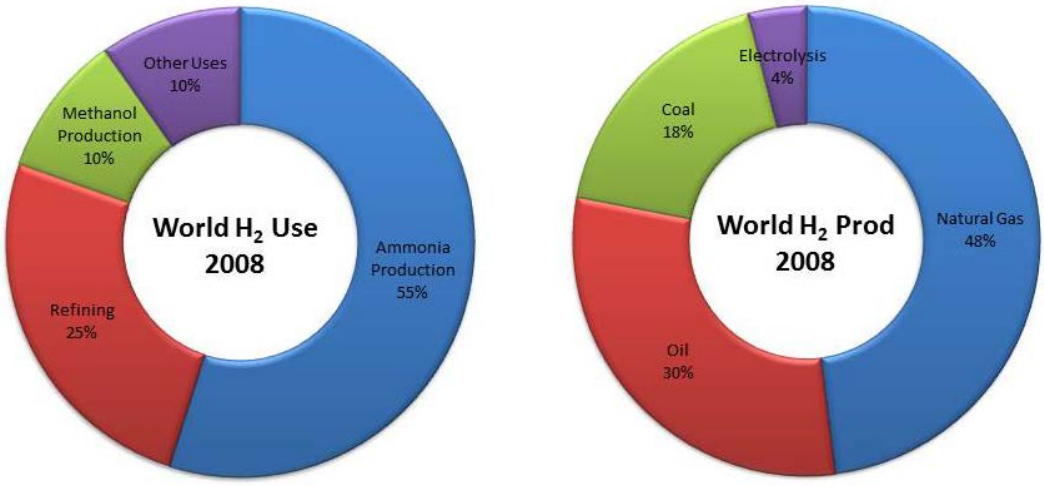


**Figure 1.1 Worldwide $H_2$ demand and production methods, 2008.** The majority of $H_2$ is used by the fertiliser industry to produce ammonia. The main method of $H_2$ production is steam-methane reformation (SMR) and other fossil-fuel production methods. (Environmental Protection Agency, 2008)

## 1.3 **Biohydrogen**

Biohydrogen (Bio-$H_2$), hydrogen produced biologically from sustainable sources, is an exciting candidate for use as a commercially-viable second-generation biofuel. Bio-$H_2$ can be produced at ambient temperatures, often with no CO or $H_2S$ contamination, and is a carbon neutral process. Bio-$H_2$ truly is sustainable and reduces GHG emissions by 57-73% and non-renewable energy use by 65-79% when compared to SMR (Manish and Banerjee, 2008). Bio-$H_2$ can be considered carbon neutral as although $CO_2$ is often released during biohydrogen production from biomass, this biomass has always been recently cultivated using $CO_2$ fixed from the atmosphere. This is in stark contrast to the combustion of fossil fuels, where the carbon has been sequestered and locked down over millions of years only to be rapidly released as $CO_2$ over tens of years. The fact that the $CO_2$ release occurs during Bio-$H_2$ production, and not at the combustion stage of the carbon cycle, means that immediate carbon capture and sequestration could be integrated into production to make Bio-$H_2$ a carbon-negative process (Hallenbeck and Ghosh, 2012).

Many microorganisms naturally produce $H_2$. In the absence of $O_2$, they reduce protons to dispose of excess reducing equivalents and reoxidise their coenzymes. Photosynthetic microorganisms such as microalgae, cyanobacteria and purple non-sulphur bacteria (PNSB), use sunlight to produce $H_2$ through either “direct” or “indirect” photolysis and also in an oxygenic/non-oxygenic manner. Microalgae such as *Chlamydomonas reinhardtii* (Melis*, et al.*, 2000), and cyanobacteria such as *Synechococcus sp.* (Howarth and Codd, 1985), *Synechocystis sp.* strain PCC 6803 (Howarth and Codd, 1985) and *Anabaena variabilis* (Happe*, et al.*, 2000) can produce $H_2$ during oxygenic photosynthesis. Direct photolysis occurs when the light energy absorbed by Photosystem II (PSII) is used to reduce the intermediate electron carrier, plastoquinone, which then transfers these electrons through the cytochrome $b_6$/f complex, plastocyanin, Photosystem I (PSI) and finally to ferredoxin (Fd), which is ultimately reoxidised to produce $H_2$ (Ghirardi*, et al.*, 2009). Indirect photolysis occurs in some filamentous cyanobacterial strains that are capable of forming heterocysts, where $H_2$ is a by-product of $N_2$ fixation. Purple non-sulphur bacteria such as various *Rhodobacter sp.* (Ghirardi*, et al.*, 2009) are also capable of $H_2$ production, with extremely high yields, during $N_2$ fixation, however these bacteria are non-oxygenic and they perform cyclic photosynthesis.

Various obligate and facultative anaerobic bacteria are capable of $H_2$ production during so-called “dark fermentation” (no light required). Indeed it has been suggested that fermentative-Bio-$H_2$ production is the most promising approach to commercial Bio-$H_2$ production (Levin*, et al.*, 2004). Many species of *Clostridiaceae* have been reported to produce $H_2$ with modest

yields, including *C. butyricum CGS5* (2.78 mol $H_2$ $mol^{-1}$ sucrose) (Chen*, et al.*, 2005), *C. saccharoperbutylacetonicum* ATCC 27021 (2.7 mol $H_2$ $mol^{-1}$ lactose (Ferchichi*, et al.*, 2005) and *C. thermolacticum* DSM 2910 (2.1-3 mol $H_2$ $mol^{-1}$ lactose) (Collet*, et al.*, 2004). The other well studied family of fermentative, $H_2$-producing bacteria are *Enterobacteriaceae*. Well studied members of this family include various *Escherichia coli* strains (2 mol $H_2$ $mol^{-1}$ glucose) (Bisaillon*, et al.*, 2006) and (1 mol $H_2$ $mol^{-1}$ formate) (Yoshida*, et al.*, 2005), *Citrobacter sp.* Y19 (2.49 mol $H_2$ $mol^{-1}$ glucose) (Oh*, et al.*, 2003) and *Klebsiella pneumonia*. Other bacterial species that produce $H_2$ during fermentation included some thermophilic organisms such as *Caldicellulosiruptor saccharolyticus* DSM8903 (5.9 mol $H_2$ $mol^{-1}$ sucrose) (van Niel*, et al.*, 2003) and *Thermotoga maritima* (Verhagen*, et al.*, 1999).

## 1.4 **Hydrogenases**

### 1.4.1 Hydrogenase fundamentals and their discovery

The observation that a wide variety of organisms from all three Domains of life, and many different environmental niches, were capable of producing $H_2$ led to intense research from 1930 onwards into the mechanisms involved. The term "hydrogenase" was coined by Stephenson and Stickland in 1931, as they described an enzyme that "activates" molecular hydrogen in different bacteria, including *Escherichia coli* (Stephenson and Stickland, 1931). Hydrogenases catalyse the reversible reaction $H_2 \leftrightarrow 2H^+ + 2e^-$ (Stephenson and Stickland, 1932; Green and Stickland, 1934). In the 1930s, 40s and 50s, they were viewed by many in the scientific community as an ideal "simple" model enzyme to study. The partial purification of hydrogenases from the cell was essential to allow their true characterisation (Joklik, 1950b; Gest, 1952; Krasna*, et al.*, 1960), but the fact that they were only partially purifiable indicated that they were not all localised in the cytoplasm (Ackrell*, et al.*, 1966). Hydrogenases were found to be reversibly (Joklik, 1950b; Joklik, 1950a; Gest, 1952) or irreversibly (Abeles, 1964) inactivated by $O_2$, and other oxidising agents, and many organisms were found to have more than one hydrogenase activity (Ackrell*, et al.*, 1966). However, the nature of the assumed cofactors responsible for the catalytic activity remained elusive for many years, and early attempts to dissociate them from the protein structure were unsuccessful (Gest, 1952; Krasna*, et al.*, 1960).

Many hydrogenases have now been purified to homogeneity and the identity of their essential cofactors confirmed. Hydrogenases are thus divided into three phylogenetically distinct classes of enzyme, based on the metal content of their active sites. They are the [NiFe]-hydrogenases, the [FeFe]-hydrogenases and the Fe-only (FeS-cluster free) hydrogenases. Nitrogenases also produce $H_2$ during $N_2$ fixation (reviewed in Vignais and Billoud, 2007), but this reaction is not reversible and usually has a lower rate of catalytic activity than true hydrogenases.

### 1.4.2 [NiFe]-hydrogenases

It was known since the 1940s that iron was important for hydrogen metabolism in bacteria (Waring and Werkman, 1944; Gray and Gest, 1965). Iron was subsequently shown to be an essential component of purified hydrogenases as well as iron-sulfur complexes (Nicholas*, et al.*, 1960; Sadana and Rittenberg, 1963; Sadana and Rittenberg, 1964; Legall*, et al.*, 1971; Nakos and Mortenson, 1971). Nickel, however, was not conclusively proven to be a true hydrogenase cofactor until the 1980s.

It was known that nickel was essential for chemolithotrophic growth on $H_2$ (Bartha and Ordal, 1965), but it required the use of improved characterisation techniques, such as electron paramagnetic resonance (EPR) spectroscopy, *in vivo* radiolabelling, immunochemical, and advances in molecular genetics, to demonstrate conclusively that some hydrogenases contain nickel (Lancaster, 1980; Diekert*, et al.*, 1981; LeGall*, et al.*, 1982; Sawers and Boxer, 1986; Waugh and Boxer, 1986). The crystal structure of two [NiFe]-hydrogenases: *Desulfovibrio gigas* (Volbeda*, et al.*, 1995) (Volbeda*, et al.*, 1996); and *Desulfovibrio vulgaris* Miyazaki (Higuchi*, et al.*, 1997) further elucidated the structure of the polypeptide-backbone, active site and FeS clusters. The catalytic complex of all [NiFe]-hydrogenases consists of an αβ heterodimer and this catalytic core is sometimes found in complex with other subunits.

The *Desulfovibrio gigas* [NiFe]-hydrogenase structure (Volbeda*, et al.*, 1995) was resolved to 2.85 Å resolution. The large (α) and small (β) subunits interacted extensively over a surface of 3,500 Å (Volbeda*, et al.*, 1995). The large 60 kDa subunit contains the deeply buried active site. The active site was shown to be ligated by four cysteines, Cys68 and Cys533 are bridging ligands of both metal ions, while Cys65 and Cys530 are bound to the Ni atom alone (Volbeda*, et al.*, 1995). The identity of the other metal was suggested to be Fe however could not be confirmed in this study (Volbeda*, et al.*, 1995). This was confirmed in a later study (Volbeda*, et al.*, 1996), which also showed the presence of a bridging oxygen species between Ni and Fe (suggesting this was a crystal of an inactive [NiFe]-hydrogenase) and that the Fe atom binds three diatomic ligands, which were shown by infrared analysis to be two $CN^-$ and one CO ligands, a finding that was later confirmed using Fourier transform infrared (FTIR) spectroscopy (Fichtner*, et al.*, 2006). The identity of the bridging ligand between the Ni and Fe atoms was controversial for many years, until it was shown to be a hydroxo species in the 'ready' or 'Ni-B' (EPR) state and a hydro-peroxide in the 'unready' or 'Ni-A'/'Ni-$S_U$' state (Volbeda*, et al.*, 2005). A hydrophobic channel for $H_2$ diffusion connects the [NiFe] active site to the protein surface (Fontecilla-Camps*, et al.*, 2007). A $Mg^{2+}$ ion was also found in large subunit of some [NiFe]-hydrogenases (Higuchi*, et al.*, 1997).

The small 28 kDa subunit was found to be structurally similar to a Clostridial flavodoxin and consisted of three FeS clusters: the proximal [4Fe-4S] cluster (6.1 Å from [NiFe] active site); the medial [3Fe-4S] cluster (5.7 Å from the proximal cluster) and the distal [4Fe-4S] cluster (5.2 Å from the medial cluster) (Volbeda*, et al.*, 1995). These FeS clusters align nicely to pass electrons from the active site to the electron acceptor, with the previously unseen histidine ligand of the distal cluster suggested to play a role in interaction with its cytochrome $c_3$ partner (Volbeda*, et al.*, 1995).

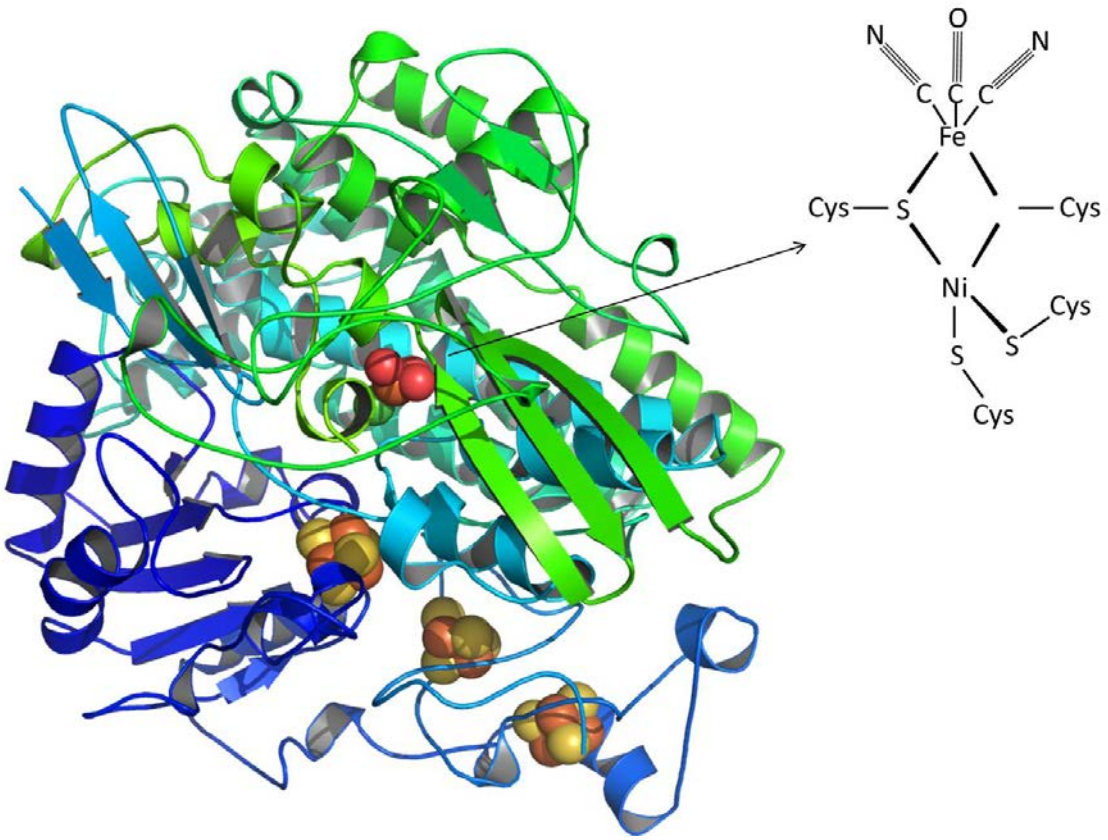


**Figure 1.2 X-Ray Structure of [NiFe]-hydrogenase from *Desulfovibrio gigas*.** The active site consists of a Ni and Fe core ligated by four cysteines and the Fe atom has three diatomic ligands (2 x $CN^-$ and 1 x CO). (Volbeda, *et al.*, 1995)

[NiFe]-hydrogenases are very diverse in their physiological roles in their native organisms (reviewed in Vignais and Billoud, 2007). Most are involved exclusively in $H_2$ uptake from the environment and eventually pass the electrons from $H_2$ oxidation to various terminal electron acceptors such as fumarate or $O_2$. Bidirectional $NAD(P)^+$-linked hydrogenases are capable of reducing or oxidising $NAD(P)^+$ and NAD(P)H, respectively, depending on the cellular redox environment. Some membrane-bound [NiFe]-hydrogenases produce $H_2$ during fermentation to remove excess reducing equivalents and some of these are thought to have an associated energy-conserving proton pumping activity. A subgroup of the [NiFe]-hydrogenases has been identified that contain selenocysteine in their active sites (Garcin*, et al.*, 1999) and these are called [NiFeSe]-hydrogenases.

### 1.4.2.1 NiFe active site maturation

The accessory proteins essential for [NiFe]-hydrogenase large subunit maturation were first identified through classic genetic studies in *E. coli*. Researchers found that certain mutations, located in regions of the chromosome distinct from the genes encoding the structural subunits of the [NiFe]-hydrogenases, led to a pleiotropic loss in hydrogenase activity. These regions were eventually found to contain the *hyp* genes, *hypA-E* and *hypF* (Lutz*, et al.*, 1991). HypD contains a [4Fe-4S] cluster, acts as a scaffold protein and forms a (hetero)tetramer with HypC, HypE & HypF (Soboh*, et al.*, 2012; Stripp*, et al.*, 2013). These co-ordinate the two $CN^-$ ligands, which are derived from carbamoyl phosphate (Paschos*, et al.*, 2001; Petkun*, et al.*, 2011), and the CO ligand, the origin of which is still unknown (Forzi*, et al.*, 2007; Forzi and Sawers, 2007b; Lenz*, et al.*, 2007) to the Fe atom (Soboh*, et al.*, 2012). HypC then transfers this immature structure into an apo-form of the large subunit. The Ni atom is then inserted into the large subunits by the complex containing the nickel binding proteins HypA and HypB (also a GTPase) (Forzi and Sawers, 2007b; Chan*, et al.*, 2012a; Chan*, et al.*, 2012b), and some researchers believe SlyD has a role here too. Finally, a dedicated protease catalyses cleavage of a short C-terminal peptide from the large subunit, which renders the process reversible and assembly of the holoenzyme is completed (Forzi and Sawers, 2007a).

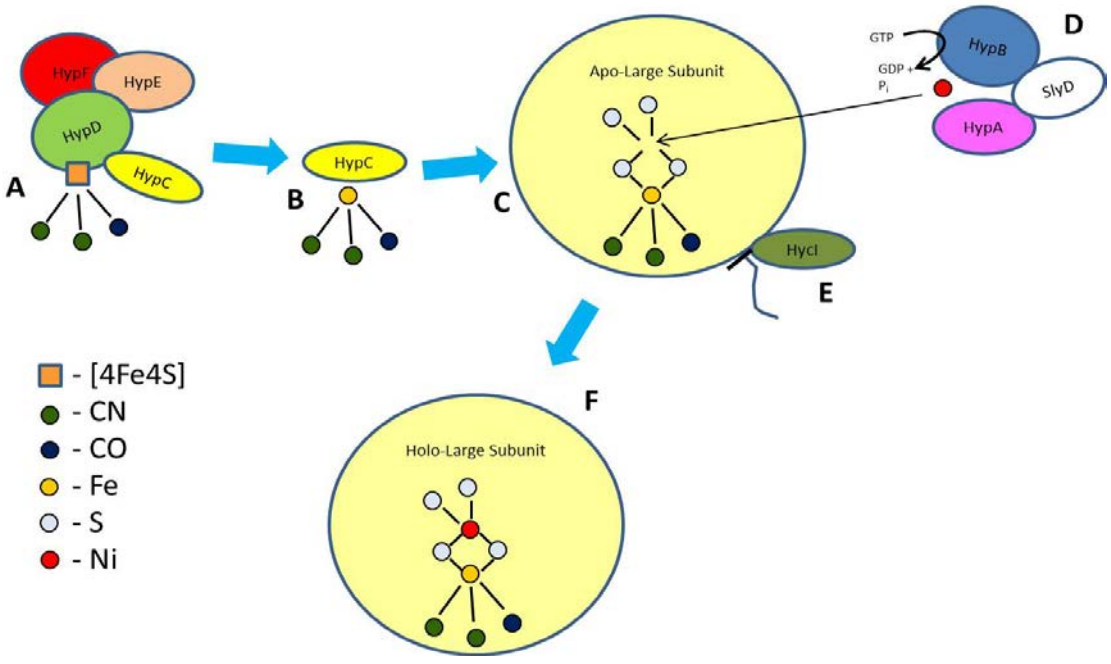


**Figure 1.3 The [NiFe] active-site maturation machinery.** A. HypC, D, E & F form a tetramer and the CO and CN ligands are assembled on a [4Fe-4S] cluster on HypD. B. HypC accepts the Fe, CO, CN scaffold. C. HypC inserts this into the large [NiFe]-hydrogenase subunit. D. HypB in combination with HypA and SlyD inserts the Ni cofactor onto the scaffold in the large subunit completing the active site. E. A system-specific protease cleaves off the C terminal peptide of the large subunit. F. The holoenzyme is complete.

### 1.4.3 [FeFe]-hydrogenases

In 1984, the hydrogenases of *Clostridium pasteurianium* were both shown to only contain iron and sulphur and no nickel (Adams and Mortenson, 1984). A similar finding was made with a periplasmic hydrogenase from *Desulfovibrio vulgaris* (Huynh*, et al.*, 1984). Further characterisation of previously suspected [FeFe]-hydrogenases indicated the presence of 20 gram atoms of Fe and 18 atoms of $S^{2-}$ per mole of protein (Adams*, et al.*, 1989). It was further shown that each active site contained 6 Fe atoms per active-site (Fauque*, et al.*, 1988; Adams*, et al.*, 1989; Filipiak*, et al.*, 1989), suggesting that the active site or H-cluster was in fact a modified [4Fe-4S] cluster with additional iron atoms. A complicating factor in the classification/characterisation of these hydrogenases was the heterogeneity of the enzyme complexes between different organisms. Over 140 [FeFe]-hydrogenases have now been characterised and examples of monomers, heterodimers, heterotrimers and heterotetramers have all been reported (reviewed in Vignais and Billoud, 2007). These nickel-free [FeFe]-hydrogenases typically display much higher catalytic rates than [NiFe]-hydrogenases (reviewed in Adams, 1990). Most are thought to be involved in $H_2$ production (reviewed in Adams, 1990), as is reflected by their catalytic bias in hydrogenase assays, although the physiological role of the periplasmic [FeFe]-hydrogenase from *Desulfovibrio vulgaris* Hildenborough has now been shown to be $H_2$ uptake (Pohorelic*, et al.*, 2002). [FeFe]-hydrogenases are the only hydrogenases found so far amongst eukaryotes.

The first crystal structures of [FeFe]-hydrogenases were published at the end of the 1990s (Peters*, et al.*, 1998; Nicolet*, et al.*, 1999). It was known through various spectroscopic studies, that the Fe and S of hydrogenase I of *Clostridium pasteurianum* (*Cp*I) were organised into 5 distinct metal clusters (Peters*, et al.*, 1998). The authors proposed that there were four different domains to the enzyme. The first large (60 kDa) active site-containing domain makes up 2/3 of the total protein. It is arranged in 2 lobes, each consisting of a four strand β sheet with five α helices per lobe. The active site or H cluster lies at the interface between each lobe. It consists of a [4Fe-4S] cluster bridged via a single cysteinyl S (Cys300) to the [FeFe] core. This cysteinyl S is the only covalent ligand of the active site to the protein backbone, a characteristic noticed previously with the active site of sulphite reductase. The [4Fe-4S] cluster is ligated by four cysteines (Cys300, Cys355, Cys499 and Cys503). The two Fe atoms are held 2.62 Å apart and each Fe atom has 5 ligands. These were tentatively identified as two $CO/CN^-$ ligands; one bridging $CO/CN^-$; and two bridging S atoms (bound to another unknown atom).

The next domain, closest to active site and interacting with it, contains two [4Fe-4S] clusters (each ligated by four cysteines). The first [4Fe-4S] cluster (FS4A) lies 9 Å (edge to edge) from

the FeS cluster of the H-cluster with the second (FS4B) 10 Å away from it. The other two domains contain the third and fourth FeS clusters. The third [4Fe-4S] cluster (FS4C), which is ligated by a histidine (His94) and three cysteines and it is situated 8 Å from the FS4B cluster. The final FeS cluster is a 2Fe-2S cluster (FS2) and it is ligated by four cysteines. It lies 11 Å from FS4B and 17 Å from FS4C. These last two FeS clusters (FS4C and FS2) are both located near the protein surface and therefore likely to be involved in accepting electrons from the physiological electron donor.

The crystal structure (resolution: 1.6 Å) of the periplasmic [FeFe]-hydrogenase from *Desulfovibrio desulfuricans* showed some subtle differences to that of *Cp*I and answered some remaining questions (Nicolet*, et al.*, 1999). Its structure, apart from a ferredoxin-like domain had a very novel fold. It contained three FeS clusters, all of which were of the [4Fe-4S] variety. This structure was able to confirm that the non-protein ligands of the Fe atom were two CO and two $CN^-$ (1 each per Fe) ligands. Erroneously, the authors suggested that the two bridging S of the two Fe atoms was a propanedithiol bridge. This has now been shown to be an aminedithiolate bridge (Nicolet*, et al.*, 2001). It was also suggested, as a result of its empty coordination sphere and its proximity to both Lys237 and hydrophobic channel to the protein surface, that the second Fe atom is involved in $H_2$ binding (Nicolet*, et al.*, 1999).

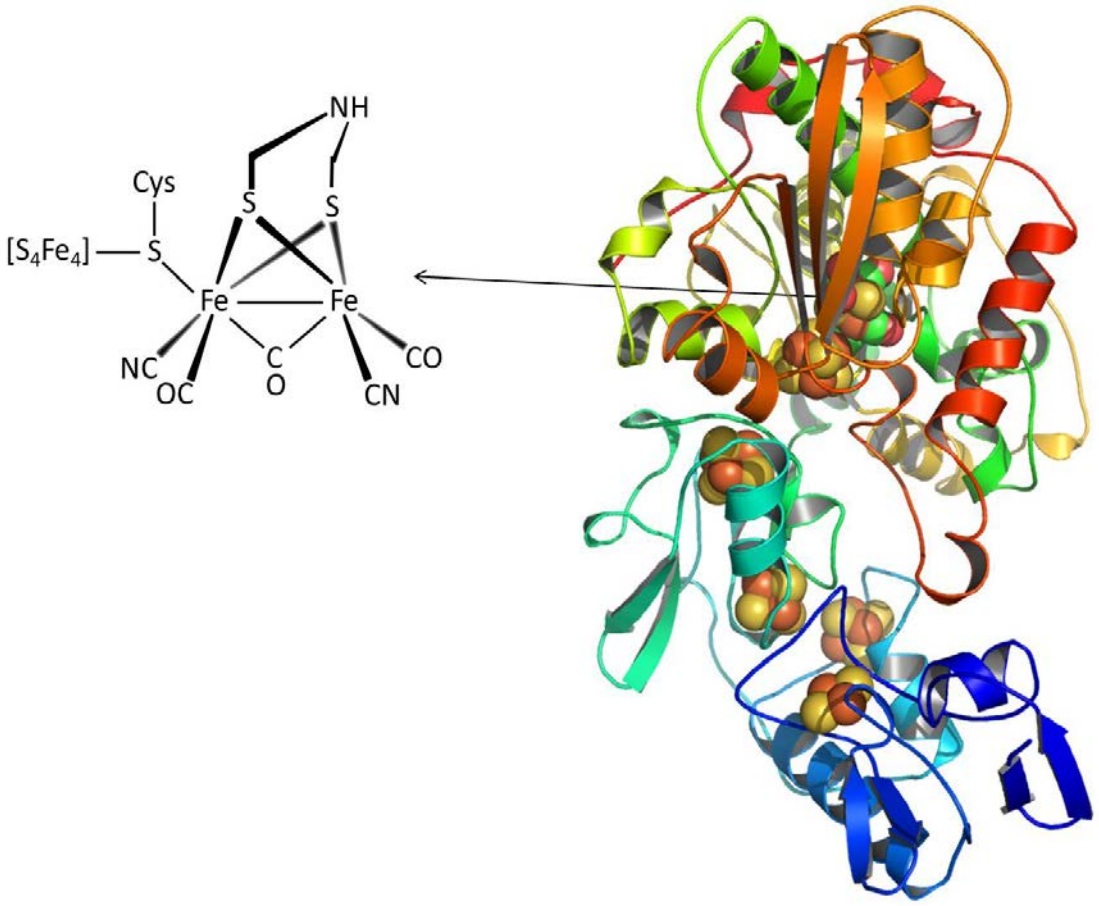


**Figure 1.4 The crystal structure of the [FeFe]-hydrogenase from *Clostridium pasteurianum*.** The [FeFe] active site is highlighted and the FeS clusters can also be seen. (Peters, *et al.*, 1998)

### 1.4.3.1 FeFe active site assembly

Assembly of the metals and non-protein ligands into the active sites of hydrogenases are not spontaneous events. Elaborate networks of accessory proteins are required to assemble and insert the cofactors. The accessory proteins essential for holoenzyme maturation of [FeFe]-hydrogenases have been identified as HydE, HydF, and HydG (Posewitz*, et al.*, 2005). HydF is thought to act as the scaffold for H-cluster assembly (McGlynn*, et al.*, 2008) and has been shown to bind one [4Fe-4S] and hydrolyse GTP to GDP (Brazzolotto*, et al.*, 2006). HydE, a radical S-adenosylmethionine **(**SAM) enzyme, binds two [4Fe-4S] clusters and synthesizes the bridging dithiolate group on a 2Fe core of apo-HydF (Rubach*, et al.*, 2005). HydG, another radical SAM enzyme, binds one [4Fe-4S] cluster and uses tyrosine to synthesise the CO and $CN^-$ ligands for each Fe atom (Shepard*, et al.*, 2010a). HydF then transfers the mature active site into the large hydrogenase subunit, leading to catalytically-competent hydrogenase (Mulder*, et al.*, 2010; Mulder*, et al.*, 2011). The GTPase activity of HydF is thought to be essential for the interactions between HydE, HydG and HydF, possibly through the induction of conformational changes in HydF (Shepard*, et al.*, 2010b).

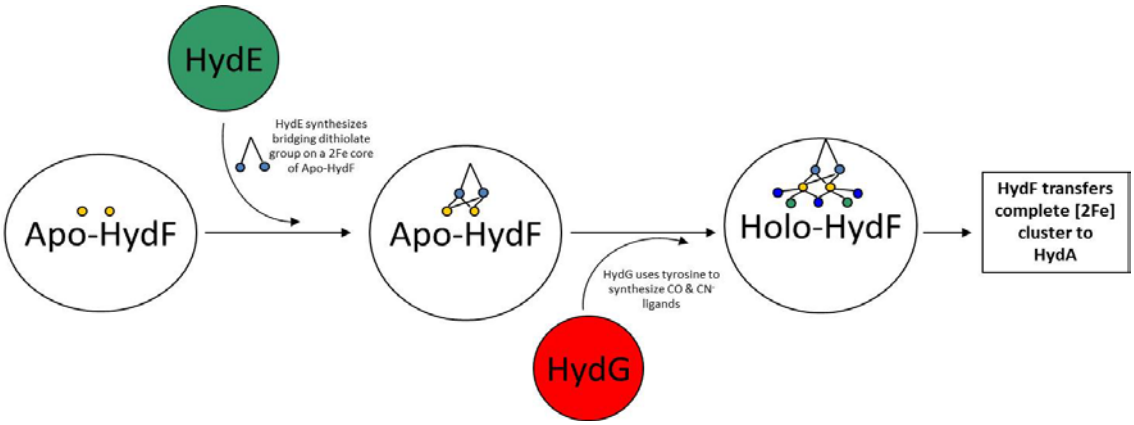


**Figure 1.5 The maturation enzymes required for construction of the [FeFe] active site.** HydF acts as a scaffold for H-cluster assembly. HydE and HydG, two radical SAM enzymes synthesise the bridging dithiolate group onto the 2Fe core of HydF and then the CO and CN ligands. Finally once fully assembled, the [FeFe] active site is transferred into the large subunit.

### 1.4.4 FeS-cluster free hydrogenases

The third phylogenetic class of hydrogenases are the [Fe]-only/FeS-cluster free hydrogenases. They were discovered in methanogenic archaea (Zirngibl*, et al.*, 1992; Hartmann*, et al.*, 1996) and initially thought be metal-free hydrogenases. A crystal structure revealed a unique structure and catalytic mechanism compared to the [NiFe] and [FeFe] classes of enzymes (Shima*, et al.*, 2008). The enzyme is a homodimer and its active site is found on the surface of the enzyme. It simultaneously binds both methylenetetrahydromethanopterin and protons, allowing them to react directly. This this direct binding of both substrates to the same active site on the surface of the protein removes the necessity for FeS clusters to relay electrons.

### 1.4.5 Hydrogenases couple $H_2$–oxidation to a variety of physiological electron donors and acceptors

[NiFe] and [FeFe]-hydrogenases are involved in a wide variety of biochemical processes, depending on the environmental niche of the host organism and the local redox requirements. Because of this, ten classes of hydrogenases are now proposed (reviewed in Vignais and Billoud, 2007). For example, the [NiFe]-hydrogenase of *Desulfovibrio vulgaris* is a respiratory "uptake" enzyme and as such oxidises $H_2$ and transfers the electrons to cytochrome $c_3$ , which subsequently is used to reduce Fe(III) or U(VI) (Elias*, et al.*, 2004). Likewise, membrane-bound [NiFe] hydrogenases have been described that link hydrogen oxidation directly to quinone reduction. In addition, ferredoxin has been known to play an essential role in $H_2$ metabolism in certain microorganisms for many years. In *Clostridium pasteurianium* and *Micrococcus lactilyticus*, ferredoxin accepts electrons from pyruvate:ferredoxin oxidoreductase (PFOR) and passes those to an [FeFe]-hydrogenase to produce $H_2$. Ferredoxin also plays a role in $H_2$ oxidation as the intermediate electron carrier for $H_2$-dependent reduction of nitrite and hydroxylamine (Valentine and Wolfe, 1963; Gray and Gest, 1965). *Chlamydomonas reinhardtii* has a reversible [FeFe]-hydrogenase that is capable of coupling $NADP^+/NAD^+$ reduction directly to $H_2$ oxidation in the dark, but can switch to $H_2$ production with NADPH/NADH as electron donors when in the light (Abeles, 1964). Some hydrogenases produce $H_2$ during fermentation with formate as the sole electron donor (Sawers, 2005).

### 1.4.6 Inhibitors of hydrogenases

The catalytic activity of all hydrogenases can be inhibited either reversibly or irreversibly by a number of molecules/compounds. Molecular oxygen is the best studied and probably the most relevant to any discussion of hydrogenases (Joklik, 1950a; Joklik, 1950b; Gest, 1952). $O_2$ binds to the active site of both [NiFe]- and [FeFe]-hydrogenases. The majority of [NiFe] enzymes can

be reactivated upon reduction with a strong reducing agent such as dithionite or upon prolonged exposure to $H_2$. Some [NiFe]-hydrogenases are able to perform this reduction extremely quickly (and are therefore named oxygen-tolerant hydrogenases) due to the presence of a unique [4Fe3S] proximal cluster (Goris*, et al.*, 2011; Parkin*, et al.*, 2012; Parkin and Sargent, 2012; Evans*, et al.*, 2013). However, all [FeFe]-hydrogenases characterised until now are sensitive to $O_2$ and irreversibly inactivated by it. This inactivation is thought to be the result of the formation of a reactive oxygen species-like superoxide, which leads to instability and degradation of the H-cluster (Lambertz*, et al.*, 2011). Other strong oxidising agents such as ferricyanide, iodine and hydrogen peroxide are also capable of inactivating hydrogenases, however most are reversible. Indeed the deliberate/accidental oxidation of certain [FeFe]-hydrogenases with something other than $O_2$ (e.g. ferricyanide) can allow them to form the $H_{ox}$ inactive state, which protects from $O_2$ attack and can be reactivated upon $H_2$ exposure (Miyake*, et al.*, 2013). Carbon monoxide has long been shown to inhibit hydrogenase activity (Joklik, 1950a) and recently it was shown that aldehydes such as formaldehyde could also reversibly inhibit them (Wait*, et al.*, 2011). Other known inhibitors of hydrogenases include heavy metals such as copper sulphate (Sawers and Boxer, 1986), mercury, azide (Sawers and Boxer, 1986), N-bromosuccinimide (NBS) (Sawers and Boxer, 1986), acetylene (Sun*, et al.*, 1992) and nitric oxide (NO) (Berlier*, et al.*, 1987).

## 1.5 *E. coli* expresses three hydrogenases under anaerobic conditions

The *E. coli* chromosome contains genes for four [NiFe]-hydrogenases, three of which have been biochemically characterised (Figure 1.6). Hyd-1, Hyd-2 and Hyd-3 are encoded by the *hya*, *hyb* and *hyc* operons respectively (Figure 1.7). The *hyf* operon, encoding Hyd-4, appears to be cryptic in *E. coli* K-12 and has not been found to be expressed under laboratory conditions tested so far. Hyd-1 and Hyd-2 are membrane-bound, periplasmic-facing hydrogen uptake enzymes, while Hyd-3 is a loosely membrane-attached, cytoplasmic-facing hydrogen-producing enzyme (Section 1.5.3). Due to their periplasmic localisation and extensive cofactor content, Hyd-1 and Hyd-2 are both substrates of the twin-arginine translocation system (Tat), which transports folded proteins across the cytoplasmic membrane (Sargent, *et al.*, 1998b; Weiner, *et al.*, 1998; Rodrigue, *et al.*, 1999; Sargent, *et al.*, 1999; Berks, *et al.*, 2000; Jack, *et al.*, 2004).

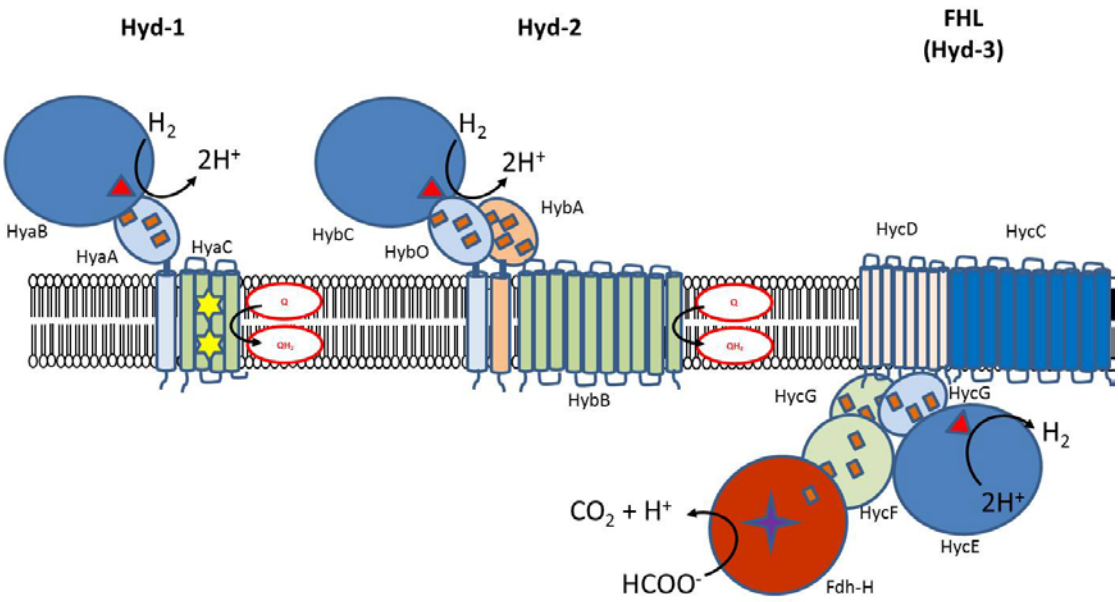


**Figure 1.6 The three [NiFe]-hydrogenases of *E. coli*. Hyd-1 and Hyd-2 are predominantly $H_2$ uptake enzymes whereas FHL produces $H_2$ from formate.**

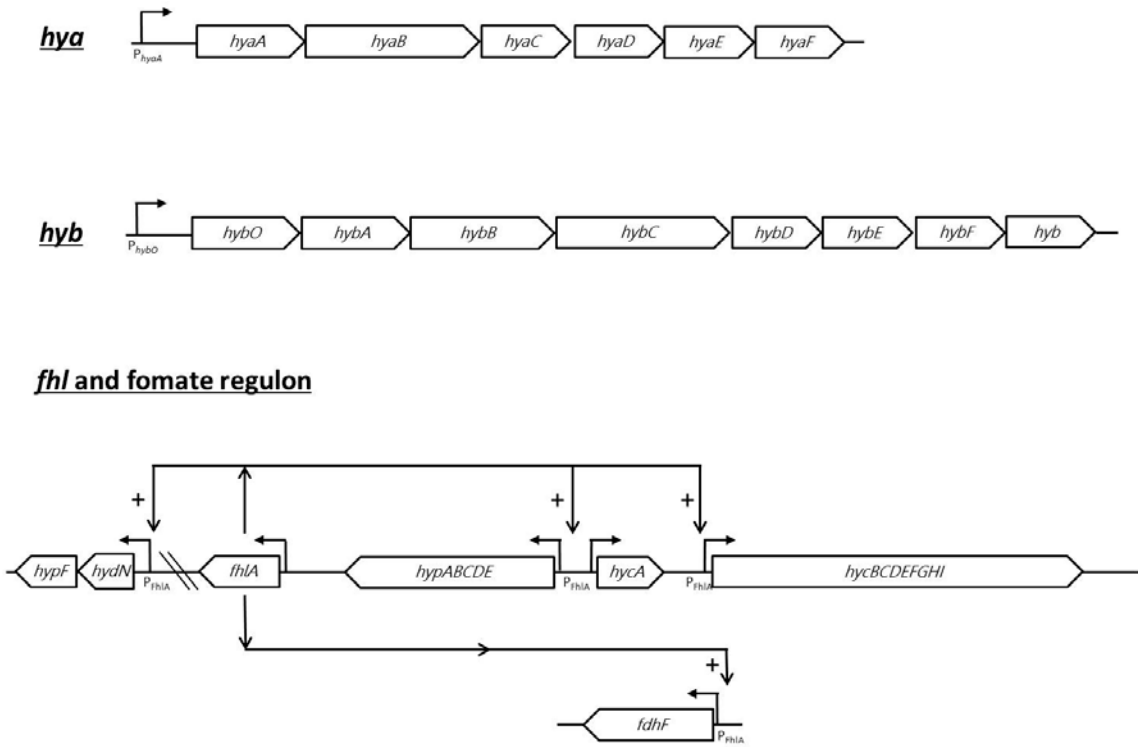


**Figure 1.7 The *hya*, *hyb* and *fhl* operons of *E. coli*.** The *hya* operon encodes Hyd-1, the *hyb* operon encodes Hyd-2 and the *hyc* operon and *fdhF* gene encode the FHL complex. FhlA is the transcriptional activator of the formate regulon and it regulates expression of the FHL-encoding genes in addition to the *hyp* operon.

### 1.5.1 The operons encoding Hyd-1 and Hyd-2

The *hya* operon is comprised of six genes: *hyaABCDEF* (Menon*, et al.*, 1991) (Figure 1.7A). Two of the genes, *hyaA* and *hyaB*, encode the small and large structural subunits of Hyd-1, respectively, however native levels of hydrogenase activity require the expression of all six *hya* genes (Menon*, et al.*, 1991). The gene product of *hyaC* is a *b*-type cytochrome with a calculated molecular mass of 27.6 kDa and contains four hydrophobic transmembrane domains (Menon*, et al.*, 1990; Volbeda*, et al.*, 2013). HyaC is most likely a ubiquinone reductase, transferring electrons from the core hydrogenase in the periplasm to quinone at the cytoplasmic side of the membrane. The *hyaD* gene encodes a protease required for C-terminal processing of the Hyd-1 large subunit. The gene product of *hyaE* has been shown to interact specifically with HyaA and prevents its premature transport by the Tat machinery (Dubini and Sargent, 2003). The gene *hyaF* is thought to encode a maturase involved in nickel incorporation into Hyd-1 active site, but is not essential, as a Δ*hyaF* mutant retains two thirds of the Hyd-1 activity of the wild-type strain (Dubini*, et al.*, 2002) and this reduction in Hyd-1 activity can be rescued by the addition nickel to the growth media (Menon*, et al.*, 1991).

Hyd-1 forms a large membrane-attached complex with a molecular mass of 200 kDa, consisting of two large (64 kDa) subunits and two small (35 kDa) subunits (Sawers and Boxer, 1986), which is consistent with the recently solved crystal structure of Hyd-1, which shows the

enzyme is a physiologically-active dimer of heterodimers (Volbeda*, et al.*, 2012). An important feature of $O_2$-tolerant [NiFe]-hydrogenases is the unique [4Fe-3S] proximal cluster, ligated by six conserved cysteine residues, that are capable of donating two electrons to the oxidised [NiFe] active site to help reduce and remove attacking $O_2$ (Fritsch*, et al.*, 2011; Goris*, et al.*, 2011; Parkin and Sargent, 2012). The crystal structure of Hyd-1 with its b-type cytochrome (HyaC) was also recently solved (Volbeda*, et al.*, 2013) (Figure 1.8).

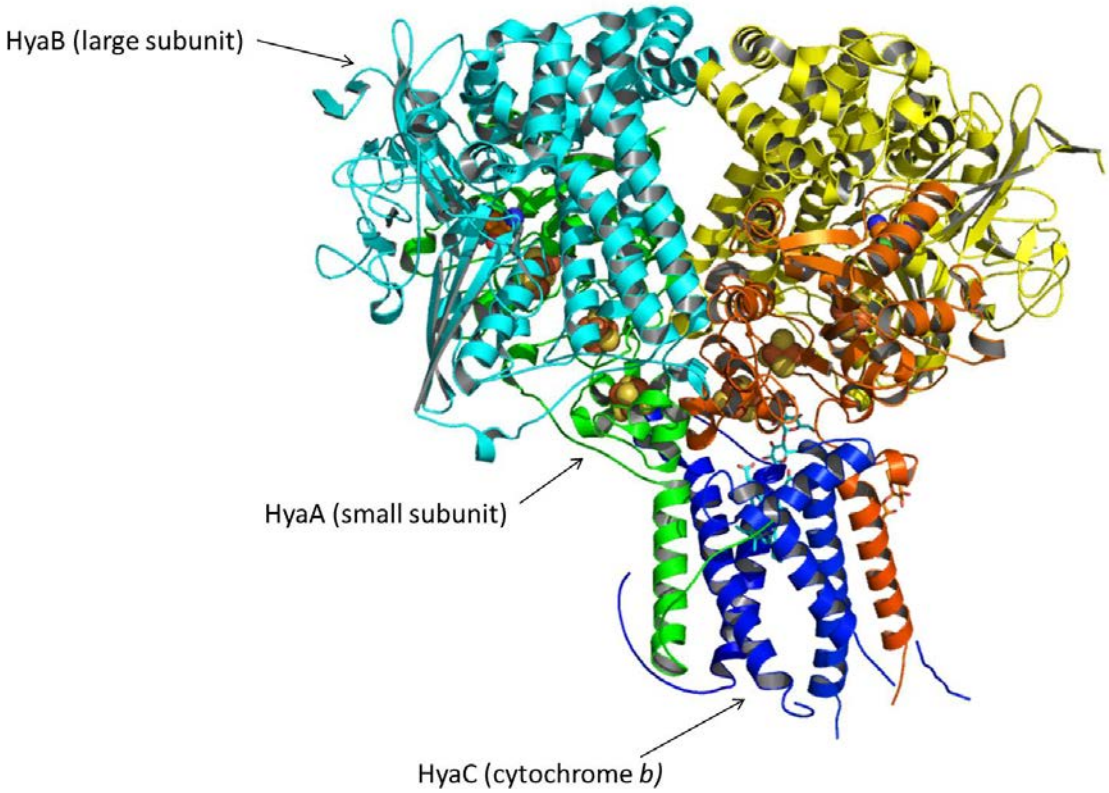


**Figure 1.8 Crystal Structure of *E. coli* hydrogenase-1 with its *b*-type cytochrome**

The *hyb* operon is comprised of eight genes, *hybOABCDEFG* (Figure 1.7B) (Sargent*, et al.*, 1998a). The large subunit is encoded by *hybC* (Menon*, et al.*, 1994). Originally the identity of the gene encoding the small subunit of Hyd-2 was suggested to be *hybA*, as it contains cysteines capable of ligating FeS and it possesses an N-terminal twin-arginine signal peptide (Menon*, et al.*, 1994). It was later shown that an open reading frame existed immediately upstream of *hybA* and that this gene, named *hybO,* encoded the small subunit (Sargent*, et al.*, 1998a). The original paper which suggested HybA was the small subunit claimed that expression of *hybA-G* (i.e. no *hybO* expression necessary) was sufficient to restore wild type levels of Hyd-2 activity in Δ*hybA-G* mutants (Menon*, et al.*, 1991), which is controversial. The gene products of *hybB* and *hybA* are essential for $H_2$-dependent quinone reduction by Hyd-2 (Menon*, et al.*, 1994; Dubini*, et al.*, 2002). The *hybB* gene is thought to encode a large integral membrane protein with ten transmembrane domains (Menon*, et al.*, 1994) and shares 40%

overall sequence identity to the Hmc cytochrome of *Desulfovibrio vulgaris*. The *hybA* gene is thought to encode a periplasmic-facing 16Fe ferredoxin. The gene product of *hybD* shares 40% sequence identity to HyaD, and therefore assumed to play an essential role in Hyd-2 processing. The products of *hybE*, *hybF*, and *hybG* are still poorly understood but are thought to act as chaperones for cofactor assembly or protein translocation (Dubini*, et al.*, 2002). HybE shares homology with known Tat chaperones (e.g. 26% sequence identity and 38% sequence similarity with HoxT from *Ralstonia eutropha*), and is involved in proofreading the HybOC complex before Tat-mediated translocation (Dubini and Sargent, 2003; Jack*, et al.*, 2004). HybF and HybG are homologs of HypA and HypC and are specifically involved in large subunit maturation of both Hyd-1 and Hyd-2 (Blokesch*, et al.*, 2002; Blokesch*, et al.*, 2004; Butland*, et al.*, 2006).

Hyd-2 is a periplasm-facing and membrane-attached enzyme with a molecular mass of 180 kDa. The core active hydrogenase fragment was released from the membranes using tryptic digestion and an active dimer-of-heterodimers was isolated (Ballantine and Boxer, 1986). The small subunit of the non-trypsin treated enzyme has a molecular mass of 35 kDa, and the trypsin treatment removed a 5 kDa stretch of polypeptide thought to be the short hydrophobic transmembrane helix that anchors Hyd-2 to the membrane on the periplasmic side, to give a 30 kDa tryptic fragment (Ballantine and Boxer, 1986; Dubini*, et al.*, 2002). In its native form, HybOC forms a large respiratory complex with HybA and HybB (Figure 1.6) and this association with HybA and HybB is essential for $H_2$-dependent fumarate reduction and growth on hydrogen and fumarate alone (Dubini*, et al.*, 2002).

### 1.5.2 The physiological roles of Hyd-1 and Hyd-2

The physiological role of Hyd-2 has been firmly established as a $H_2$-uptake hydrogenase under anaerobic respiratory conditions. Expression of the *hyb* operon is strongly induced in anaerobic conditions, which is predominantly regulated by FNR, ArcBA and to a lesser extent IscR (Richard*, et al.*, 1999; Giel*, et al.*, 2006). The expression of the *hyb* operon is also affected by catabolite repression (Richard*, et al.*, 1999). It is responsible for the majority (92%) of hydrogenase activity in membranes purified from grown cells under anaerobic respiratory conditions (Sawers and Boxer, 1986). It can catalyse the $H_2$-dependent reduction of a wide variety of artificial electron acceptors including MV and BV, and, *via* quinols, can form one half of short electron transport chains driving $H_2$-dependent reduction of many respiratory electron acceptors, including fumarate, DMSO and nitrate (Laurinavichene and Tsygankov, 2001). Hyd-2 most active under reducing/anaerobic conditions, and is inactive under aerobic conditions (Laurinavichene*, et al.*, 2001; Lukey*, et al.*, 2010). This maximal activity during anaerobic

respiratory conditions correlates neatly with the amount of protein found in cells grown anerobically on $H_2$ or glycerol with fumarate as the terminal electron acceptor (Sawers*, et al.*, 1985).

The physiological role of Hyd-1 has remained somewhat elusive. Biochemical studies on Hyd-1 have been performed and showed that it was capable of $H_2$-dependent reduction of BV (Sawers and Boxer, 1986) *in vitro*, as well as, *via* quinols as one half of a membrane-bound electron transfer chain, being able to couple $H_2$ oxidation to the reduction of $O_2$, DMSO and nitrate (Laurinavichene and Tsygankov, 2001; Laurinavichene and Tsygankov, 2003). Hyd-1 is also capable of sustaining $H_2$ uptake activity in more oxidising conditions than Hyd-2, as well as showing tolerance to $O_2$ attack (Lukey*, et al.*, 2010). The ability of Hyd-1 to tolerate $O_2$ has led to suggestions that it may play a role as an $O_2$ scavenger during microaerobic conditions (Laurinavichene*, et al.*, 2001). This hypothesis is intriguing when it is considered that the two genes at the 3' end of the *hya* operon, *appC* and *appB*, encode cytochrome *bd* II oxidase (Dassa*, et al.*, 1991). Perhaps Hyd-1 is involved in supplying reduced quinols (from the oxidation of $H_2$) for this oxidase upon the onset of aerobiosis or under fluctuating environmental conditions.

Many theories on the physiological role of Hyd-1 are based on gene expression studies. These studies take advantage of transcriptional fusions between the *hyaA* promoter ($P_{hyaA}$) and *lacZ*, for example (Richard*, et al.*, 1999). The expression of *hya* is repressed by IscR under aerobic conditions (Giel*, et al.*, 2006) and strongly induced in anaerobic conditions (Brondsted and Atlung, 1994; Nesbit*, et al.*, 2012; Pinske*, et al.*, 2012). ArcA and AppY antagonise the binding of IscR to $P_{hya}$ (ArcA and IscR DNA-binding sites overlap and the binding of one to DNA prevents the binding of the other) (Nesbit*, et al.*, 2012). The *hya* operon is transcribed at a much higher level than the *hyb* operon (Richard*, et al.*, 1999) and yet only contributes 8% of total membrane hydrogenase activity, as assayed using BV (Sawers and Boxer, 1986; Menon*, et al.*, 1991). It was shown that a *hyaA*'-'*lacZ* translational fusion had only 5% of the activity of a transcriptional fusion, indicating that post transcriptional regulation played an important role in determining the amount of Hyd-1 in the cell (Pinske*, et al.*, 2012). Another possible role for Hyd-1, and one that has been shown in *Salmonella*, is that it plays a role in $H_2$ re-uptake during fermentative conditions, thus acting to conserve energy (the so-called "hydrogen cycling" hypothesis). In *Salmonella* the expression of *hyaA* is highest under anaerobic conditions when cells are grown on glucose (i.e. fermentatively) and a 25% reduction in growth rate is observed in Δ*hya* mutants (Zbell*, et al.*, 2007). No similar growth rate defect was observed with *E. coli* Δ*hya* mutants when grown in rich media supplemented with glucose (Menon*, et al.*, 1991). The addition of formate to growth media was found to induce *hya* expression (Brondsted and

Atlung, 1994) and cellular levels of Hyd-1 enzyme (Sawers*, et al.*, 1985), however *hya* expression is actually higher in anaerobic respiratory conditions (Brondsted and Atlung, 1994; Richard*, et al.*, 1999), which led to the suggestion that perhaps Hyd-1 acts as an intermediate electron transport protein operating between formate hydrogenlyase and fumarate reductase (or another terminal reductase) (Francis*, et al.*, 1990; Brondsted and Atlung, 1994).

### 1.5.3 Hyd-3, a component of the formate hydrogenlyase complex

Hyd-3 is the [NiFe]-hydrogenase component of the formate hydrogenlyase complex (FHL). FHL is a large membrane-attached complex of at least seven-proteins that is responsible for $H_2$ production during mixed-acid fermentation by *E. coli* (Section 1.6.1). The enzyme couples formate oxidation at the cytoplasmic side of the membrane directly to proton reduction, also at the cytoplasmic side of the membrane.

#### 1.5.3.1 Expression

The *hyc* operon consists of 9 genes: *hycABCDEFGHI* (Figure 1.7C). The structural subunits of FHL are encoded by six of these genes (*hycBCDEFG*) and another gene, *fdhF,* which is transcribed elsewhere on the *E. coli* chromosome (reviewed in Sawers, 2005). The gene product of *fdhF* is the formate dehydrogenase responsible for formate oxidation during $H_2$ production (Fdh-H) (Boyington*, et al.*, 1997). The *hycB* gene encodes the predicted small subunit (molecular mass of 21.8 kDa) ferredoxin-like subunit of FdhF (Sauter*, et al.*, 1992). The *hycE* gene encodes the [NiFe] hydrogenase large subunit (the catalytic subunit of Hyd-3) (Rossmann*, et al.*, 1994). The *hycG* gene encodes an FeS cluster-containing protein, which is the best candidate for a small subunit partner for HycE (Sauter*, et al.*, 1992). The *hycC* and *hycD* genes encode predicted integral membrane proteins, while *hycF* is thought to encode another ferredoxin-like electron transfer subunit (Sauter*, et al.*, 1992).

The *hycA* gene product is not part of the enzyme complex but instead is a repressor of *hyc* operon expression (Sauter*, et al.*, 1992). Likewise, the *hycI* gene product is not part of the enzyme but encodes the HycE specific endopeptidase involved in C-terminal processing of the large subunit after Ni cofactor insertion. The function of the *hycH* gene product remains unknown (Sauter*, et al.*, 1992). The *fdhF* gene and the *hyc* operon are regulated by both FNR and the presence of formate. These genes have upstream regulatory sequences to which FhlA, the formate-associated transcriptional activator, can bind when formate is present. The *fhlA* gene itself is expressed at low levels in all conditions due to its own constitutive weak promoter. This is boosted further during anaerobic conditions as *fhlA* sits downstream of the *hypABCDE* operon and when the *hyp* operon is induced by FNR under anaerobic conditions,

*fhlA* is also co-transcribed with *hyp* (Sawers, 2005). The FhlA transcriptional activator is activated by formate, which binds to one domain of FhlA ($K_m$ of FhlA for formate = 0.5 mM (Hopper and Bock, 1995)). This binding increases the affinity of FhlA's DNA-binding domain to the regulatory sequences of the formate regulon. FhlA subsequently aids the recruitment of $\sigma^{54}$ (NtrA), which induces the transcription of genes with $\sigma^{54}$-dependent promoters (Leonhartsberger*, et al.*, 2000). Transcription of *fhlA* itself increases in a positive feedback circuit (Sawers, 2005). HycA (the *hyc* operon repressor) and OxyS, a small mRNA expressed in oxidative stress conditions, inhibit FhlA activity and *fhlA* mRNA translation to further regulate this formate regulon (Sawers, 2005).

#### 1.5.3.2 Biochemical data and physiological role of FHL

There is very little structural information on the entire FHL complex and most of the individual subunits, as the complex is unstable after purification and has proved recalcitrant to purification. It is thought to be membrane anchored by the integral membrane subunits HycC and HycD but is oriented towards the cytoplasm (Figure 1.6) (Rossmann*, et al.*, 1994). HycC, HycD, HycE, HycF, and HycG share sequence identity with Nqo12, Nqo8, Nqo4, Nqo9, and Nqo2, respectively, of prokaryotic respiratory Complex I (NADH dehydrogenase), the crystal structure of which was recently solved (**Error! Reference source not found.**) (Efremov and Sazanov, 2012; Baradaran*, et al.*, 2013). This allows the structures of these FHL subunits to be predicted and physiological roles to be inferred. The crystal structure of Fdh-H has also been solved (Boyington*, et al.*, 1997). FdhF contains selenocysteine, *bis*-molybdopterin guanine dinucleotide (MGD) and a [4Fe-4S] cluster (Figure 1.10) (Boyington*, et al.*, 1997).

The physiological role of the FHL complex is to catalyse the oxidation of formate and concurrent reduction of protons to produce $H_2$ during mixed-acid fermentation. At physiological pH, formate is charged and so not freely membrane permeable ($pK_a$ = 3.75). Formate produced in the cell cytoplasm during anaerobic metabolism is exported to prevent acidification using the formate channels, FocA (Suppmann and Sawers, 1994), FocB, and possibly another unknown formate transporter. Under anaerobic respiratory conditions when electron acceptors such as nitrate, TMAO or exogenous fumarate are present, this extracellular formate is oxidised by respiratory formate dehydrogenases Fdh-N or Fdh-O (Axley*, et al.*, 1990)), which are membrane-bound but periplasmically-localised formate dehydrogenases. However, if no electron acceptors are present, the build-up of secreted formate, acetate and lactate can cause the extracellular pH to drop below 6.8, at which point the formate is re-imported into the cell, activates FhlA, and ultimately is oxidised to produce $H_2$ by FHL (Sawers, 2005).

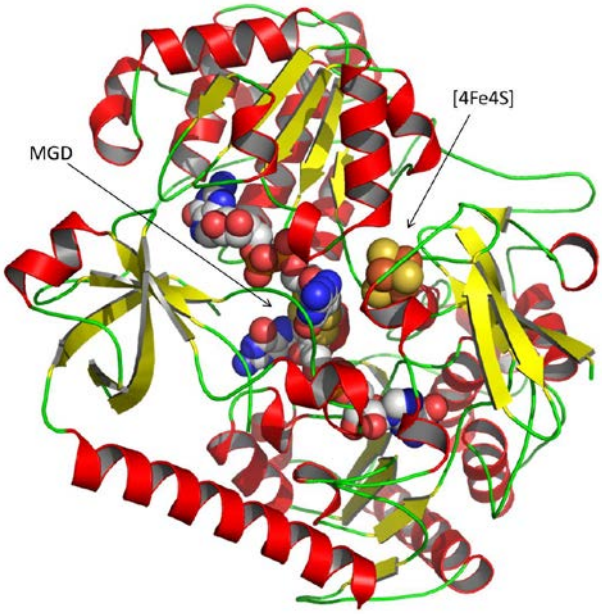


**Figure 1.10 The crystal structure of Fdh-H.** The MGD cofactor and [4Fe-4S] cluster are highlighted. This is the enzyme responsible for formate oxidation during mixed-acid fermentation and forms part of the FHL complex. (Boyington, *et al.,* 1997)

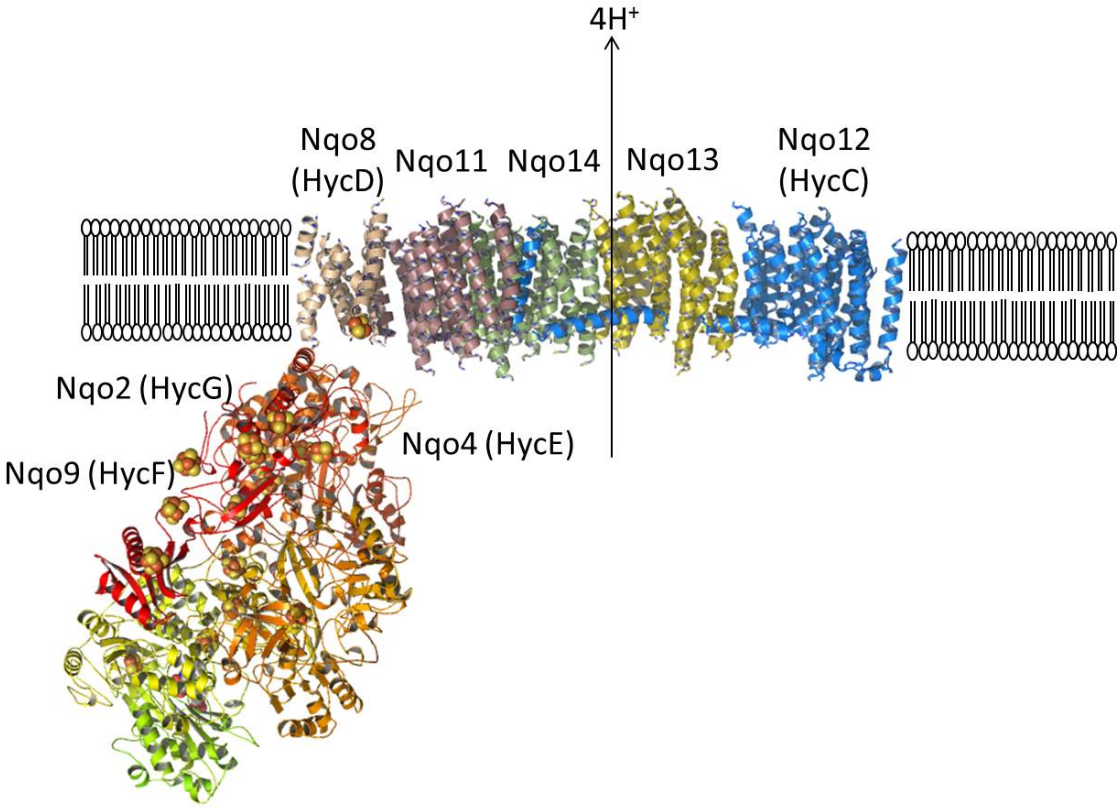


**Figure 1.9 The crystal structure of respiratory complex I from *Thermus thermophiles*.** The FHL homologues of Hqo2, 9, 4, 8 and 12 are indicated. (Baradaran, *et al.*, 2013)

### 1.5.4 Other genes involved in hydrogenase expression, biosynthesis and maturation

In addition to the specific machinery dedicated to active site assembly and insertion, many other systems are essential to successfully load the other cofactors found in hydrogenase enzymes. The iron-sulphur machinery of *E. coli* is essential for the assembly and insertion of FeS clusters into the small and large subunits of hydrogenases. The main pathways for these are the Isc (encoded by *iscRSUA*) and Suf (encoded by *sufABCDSE*) pathways, which operate under normal and oxidative stress conditions respectively and have been studied and reviewed extensively (Johnson*, et al.*, 2005; Ayala-Castro*, et al.*, 2008; Fontecave and Ollagnier-de-Choudens, 2008; Lill, 2009; Vinella*, et al.*, 2009). The sulphur of FeS clusters is supplied in the form of sulphide, which is delivered by a cysteine desulfurase, IscS/SufS. The FeS clusters are assembled on the scaffold proteins IscU/SufU (U-type carrier protein) or IscA/SufA (a type II A-type carrier protein), which accepts the sulphide and the iron. One protein shown to be involved in iron delivery is CyaY, which has been shown to bind iron and also interact with IscU and IscS (Layer*, et al.*, 2006). The electrons required for the reduction of the sulphide to sulphur is supplied by ferredoxin and finally the insertion of the assembled FeS cluster into the target protein requires the action of an ATPase. In the Isc machinery this is carried out by HscA, with its chaperone, HscB (Reyda*, et al.*, 2009), and in the Suf machinery, this is carried out by SufC (Saini*, et al.*, 2010). It has recently been shown that IscU, IscA and a type I A-type carrier protein, ErpA, are essential for FeS cluster assembly and insertion into the small subunits of both *E. coli* Hyd-1 and Hyd-2, but SufA is not required (Pinske and Sawers, 2012a; Pinske and Sawers, 2012b).

The uptake of nickel is of course essential for the activity of all [NiFe]-hydrogenases and is catalysed by the Nik machinery (encoded by the *nikABCDER* operon) (Navarro*, et al.*, 1993; Eitinger and Mandrand-Berthelot, 2000). NikA is the periplasmic Ni-binding component of the Nickel ABC transporter, NikR is the repressor of the operon, NikB & C are the membrane components of the ABC transporter and NikD & E bind ATP, which energises the transporter. Iron uptake is poorly understood in *E. coli*. Candidates for proteins involved in Fe uptake for use in hydrogenases etc. include MntH, a $Mn^{2+}/Fe^{2+}:H^{+}$ symporter (Makui*, et al.*, 2000) and the FeoAB system, which takes up ferrous iron (Kammler*, et al.*, 1993; Cartron*, et al.*, 2006).

Finally, the radical SAM enzymes involved in H-cluster maturation, HydE and HydG, require the production of S-adenosyl-L-methionine. This is carried out by the products of the *met* genes and involves one additional reaction to the de novo methionine biosynthesis pathway. MetJ is a transcriptional repressor and when bound to S-adenosyl-L-methionine represses the expression of this operon. MetA catalyses the first step and converts L-homoserine to O-

succinyl-L-homoserine (Born and Blanchard, 1999), which in combination with L-cysteine is converted to succinate and L-cystathionine in a reaction catalysed by MetB (Holbrook*, et al.*, 1990). L-cystathionine is further converted to L-homocysteine (catalysed by MetC) (Rowbury and Woods, 1964; Laber*, et al.*, 1996). The final step in the methionine biosynthesis pathway occurs by two possible routes, catalysed by either MetE or MetH (Whitfield*, et al.*, 1970; Gonzalez*, et al.*, 1992). S-adenosylmethionine (AdoMet) is produced by MetK, the methionine adenosyltransferase (Markham*, et al.*, 1980).

## 1.6 **$H_2$ production in the anaerobic metabolism of *E. coli***

### 1.6.1 Mixed Acid Fermentation in *E. coli*

#### 1.6.1.1 Glycolysis

Hydrogen production from the oxidation of formate, catalysed by the FHL complex, is one of the final steps in mixed-acid fermentation in *E. coli.* Essentially mixed-acid fermentation can be divided into two half pathways: (1) glycolysis, where glucose or other carbon sources are oxidised to pyruvate, thus producing ATP; and (2) the reduction of pyruvate to a variety of reduced fermentation products, including organic acids, ethanol, $CO_2$ and $H_2$, in order to consume reducing equivalents and maintain a redox balance. The reactions of mixed-acid fermentation proceed according to a small set of basic biochemical rules: the thermodynamic favourability of individual reactions; the availability of enzymes capable of catalysing a specific chemical reaction; and the physiochemical properties of intermediate/final metabolites produced during fermentation (reviewed in Bar-Even*, et al.*, 2012).

Glycolysis is essential for all chemoheterotrophs. *E. coli* primarily uses the Embden-Mayerhoff-Parnas (EMP) glycolytic pathway to oxidise glucose to pyruvate (Figure 1.11) (reviewed in Fraenkel, 1996). Glycolysis can be thought of as the thermodynamically favourable rearrangement of electrons in order to release chemical energy, ATP (reviewed in Bar-Even*, et al.*, 2012). The oxidation of glucose *via* the EMP pathway results in a net production of two ATP molecules per molecule of glucose. The glucose is transported into the cell by the PEP-dependent phosphotransferase system (PTS), which results in the consumption of one ATP molecule and concurrent phosphorylation of glucose to glucose 6-phosphate. The addition of a charged phosphate moiety to substrates is common during glycolysis, as it both reduces the permeability of small uncharged molecules (thus preventing leakage through cytoplasmic membrane and loss of C and energy sources) (Westheimer, 1987) and often increases the affinity of an enzyme for a particular substrate (Bar-Even*, et al.*, 2011). Glucose 6-phosphate is first isomerised to fructose 6-phosphate by phosphohexose isomerase (Pgi) before fructose 6-

phosphate is then further phosphorylated resulting in fructose 1,6-biphosphate by phosphofructokinase (PfkA). the 6-carbon fructose 1,6-biphosphate is then split into two 3-carbon molecules by fructose 1,6-phosphate aldolase (FbaB), yielding one molecule of glyceraldehyde 3-phosphate and one molecule of dihydroxyacetone phosphate. Dihydroxyacetone phosphate can be isomerised to glyceraldehyde 3-phosphate by triose phosphate isomerase (TpiA).

The next steps in glycolysis involve the recovery of the energy already invested in the phosphorylation events, and the release of maximum energy through additional electron rearrangement. Glyceraldehyde 3-phosphate is oxidised and phosphorylated in a complicated reaction catalysed by glyceraldehyde 3-phosphate dehydrogenase (GapA). The resulting 1,3-bisphosphoglycerate molecule is a substrate of phosphoglycerate kinase (Pgk), which generates ATP and 3-phosphoglycerate. Phosphoglycerate mutase (GpmA) rearranges 3-phosphoglycerate into 2-phosphoglycerate, which can be dehydrated by enolase (Eno) resulting in phosphoenolpyruvate (PEP). Finally, pyruvate kinase (PykA/PykF) generates pyruvate from phosphoenolpyruvate together with a second molecule of ATP.

Two molecules of 3-carbon glyceraldehyde 3-phosphate are generated in the first half of glycolysis (consuming 2 $\times$ ATP), and the second half of glycolysis generates 2 $\times$ ATP for each glyceraldehyde 3-phosphate oxidised to 3-carbon pyruvate, this gives a net gain of 2 ATP for every 6-carbon glucose molecule consumed.

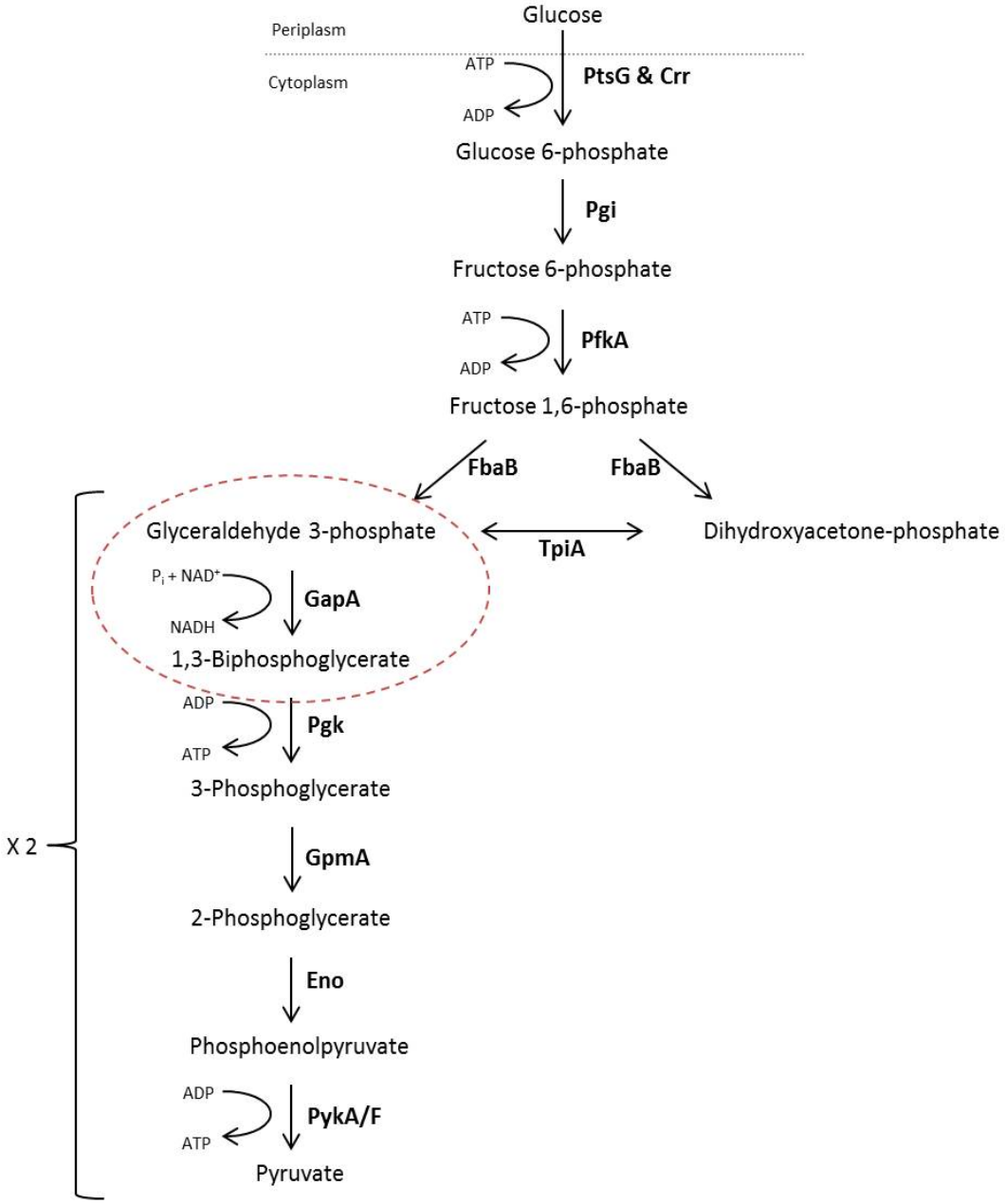


**Figure 1.11 The Embden-Mayerhoff-Parnas pathway of glycolysis, typical of *Escherichia coli* and *Salmonella*.** Enzyme abbreviations: PtsG & Crr: components of the PEP-dependent phosphotransferase system; Pgi: phosphoglucose isomerase; PfkA: phosphofructokinase; FbaB: fructose biphosphate aldolase; TpiA: triose phosphate isomerase; GapA: glyceraldehyde 3-phosphate dehydrogenase; Pgk: phosphoglycerate kinase; GpmA: phosphoglycerate mutase; Eno: enolase; PykA/F: pyruvate kinase. The reduction of $NAD^+$ is highlighted in the dashed oval. Two glyceraldehyde 3-phosphate molecules are oxidised per molecule of glucose consumed.

Alternatives to the EMP pathway of glycolysis are also found in *E. coli*. Sugar acids such as gluconate and glucuronate, which are often found in the intestine, are oxidised *via* the Entner-Doudoroff (ED) pathway (Peekhaus and Conway, 1998). The ED pathway is thought to predate the EMP pathway (Romano and Conway, 1996) and is highly conserved in prokaryotes. In the ED pathway, substrates such as gluconate are only phosphorylated once (instead of twice in EMP pathway), converted to 2-keto-3-deoxy-6-phosphogluconate (KDPG) by 6-phosphogluconate dehydratase (Edd), which is then cleaved into one pyruvate molecule and one glyceraldehyde-3-phosphate molecule by KDPG aldolase (Eda). As only G3P (and not pyruvate) can be used for substrate-level phosphorylation, the net production from the ED glycolysis pathway is only one ATP molecule per gluconate oxidised, instead of two from the EMP pathway (Flamholz*, et al.*, 2013).

In addition to energy conservation through ATP formation during glycolysis, some carbon flux must also flow through the pentose phosphate pathway in order to produce essential precursor metabolites and supply the reducing equivalent NADPH (Kruger and von Schaewen, 2003). Substrates for the essential pentose phosphate pathway can originate from either the EMP pathway (glucose/fructose 6-phosphate) or from the ED pathway (gluconate 6-phosphate) and intermediate metabolites can also be redirected back into the ED/EMP pathways of glycolysis if required (Sprenger, 1995; Kruger and von Schaewen, 2003).

#### 1.6.1.2 Reduction of pyruvate and organic acid production

Glycolysis generates reducing equivalents, in the form of two NADH molecules *per* glucose, which act as electron carriers. These must be re-oxidised in order to re-generate $NAD^+$ so that glycolysis can continue. *E. coli* deals with this by reducing pyruvate and excreting the final products out of the cell (reviewed in Böck and Sawers, 1996) (Figure 1.12). The first step of pyruvate metabolism during mixed-acid fermentation can proceed in one of two different directions. First, pyruvate can be cleaved to formate and acetyl-CoA, which is catalysed by the pyruvate formatelyase (Pfl) complex and, unlike the aerobically-expressed pyruvate dehydrogenase (PDH), results in no NADH production (Knappe and Sawers, 1990). Alternatively, pyruvate can be reduced to lactate by an NADH-dependent lactate dehydrogenase (LdhA), an enzyme that is produced during the late exponential and stationary phases of growth.

Formate is the sole precursor for $H_2$ production, which is catalysed by the FHL complex (Section 1.5.3). Acetyl-CoA itself can be further metabolised to produce two different fermentation products: acetate and ethanol, each with their own distinct advantage to the fermenting cell. Acetate production occurs through the reversible phosphotransacetylase

(PTA) - acetate kinase (Ack) pathway. Phosphotransacetylase (Pta) forms a homohexameric complex (Campos-Bermudez*, et al.*, 2010) and catalyses the reaction: Acetyl-CoA + Pi ↔ Acetyl-phosphate + CoA. It is allosterically regulated by pyruvate and PEP, which ensures the reaction proceeds in the forward direction (acetyl-phosphate synthesis) (Campos-Bermudez*, et al.*, 2010). Acetate kinase has been purified as a homodimer (Fox and Roseman, 1986) and due to its lower $K_m$ for acetyl phosphate, preferentially catalyses the production of acetate and the transfer of the phosphate group to ADP yielding one molecule of ATP per molecule of pyruvate. No NADH reducing equivalents are consumed however during acetate production.

The main mechanism for consumption of these reducing equivalents occurs as a result of the reduction Acetyl-CoA to ethanol *via* acetylaldehyde. In *E. coli* this reaction is catalysed by one enzyme in alcohol dehydrogenase (AdhE), a multimeric enzyme complex (20 - 60 subunits, each 96 kDa) (Kessler*, et al.*, 1991). NADH is the electron donor for both of these reactions, with one NADH molecule being oxidised to $NAD^+$ at each step. Housing both reactions in one enzyme helps prevent release of potentially toxic acetaldehyde (ethanal) into the cell cytoplasm. Ethanol is the most highly reduced fermentation product and is released into the extracellular melieu. Its essential role in $NAD^+$ regeneration can be demonstrated by the fact that Δ*adhE* mutants are unable to grow fermentatively (Lorowitz and Clark, 1982; Cunningham and Clark, 1986). The expression of *adhE* is regulated by anaerobiosis and, in particular, the redox state of the cell. The expression of *adhE* seems to correlate with the concentration of cellular NADH concentration (Leonardo*, et al.*, 1993).

The other possible routes for the consumption of NADH generated during glycolysis are through the production of lactate and succinate, however these are generally secondary to ethanol production. Lactate production occurs during late stationary phase of fermentation cultures, thus is not the main mechanism of $NAD^+$ regeneration. Only one of the three lactate dehydrogenase expressed in *E. coli* are involved in mixed-acid fermentation, D-(-)-nLDH/LdhA. This soluble lactate dehydrogenase with a molecular mass of 115 kDa, binds pyruvate at two sites: the catalytic active site; and a site for allosteric control (Tarmy and Kaplan, 1968a; Tarmy and Kaplan, 1968b). Indeed, LdhA is only activated upon pyruvate binding , which cannot occur unless the cytoplasmic concentration of pyruvate is higher than 7 mM ($K_m$ for pyruvate: 7 mM) (Tarmy and Kaplan, 1968a). This only occurs late in fermentation when the high extracellular concentrations of acetate, formate and ethanol slow these pathways and pyruvate accumulates (Clark*, et al.*, 1988). NADH is the reducing agent and is oxidised to $NAD^+$. Its non-essential role in *E. coli* mixed-acid fermentation was shown by the fact that Δ*ldhA* mutants are not necessary for fermentative growth (Clark*, et al.*, 1988).

The other normally minor contributor to NADH reoxidation occurs during succinate production, which normally accounts for only 5 – 10% of total fermentation products (reviewed in Böck and Sawers, 1996). PEP (not pyruvate) is the substrate for succinate production during mixed-acid fermentation and perhaps this is why succinate production is only a minor fermentation product, as its overproduction would yield less ATP per molecule of glucose oxidised. Indeed many biotechnological approaches to increase succinate production by *E. coli* during mixed-acid fermentation rely on the introduction of an ATP production step into the succinate production pathway (Zhang*, et al.*, 2009a; Zhang*, et al.*, 2009b). PEP is carboxylated to oxaloacetate using the $CO_2$ produced during fermentation by FHL, the availability of which also limits succinate production. Oxaloacetate is further reduced via malate dehydrogenase & fumarate reductase, consuming one NADH molecule, resulting in succinate (Zhang*, et al.*, 2009a; Zhang*, et al.*, 2009b).

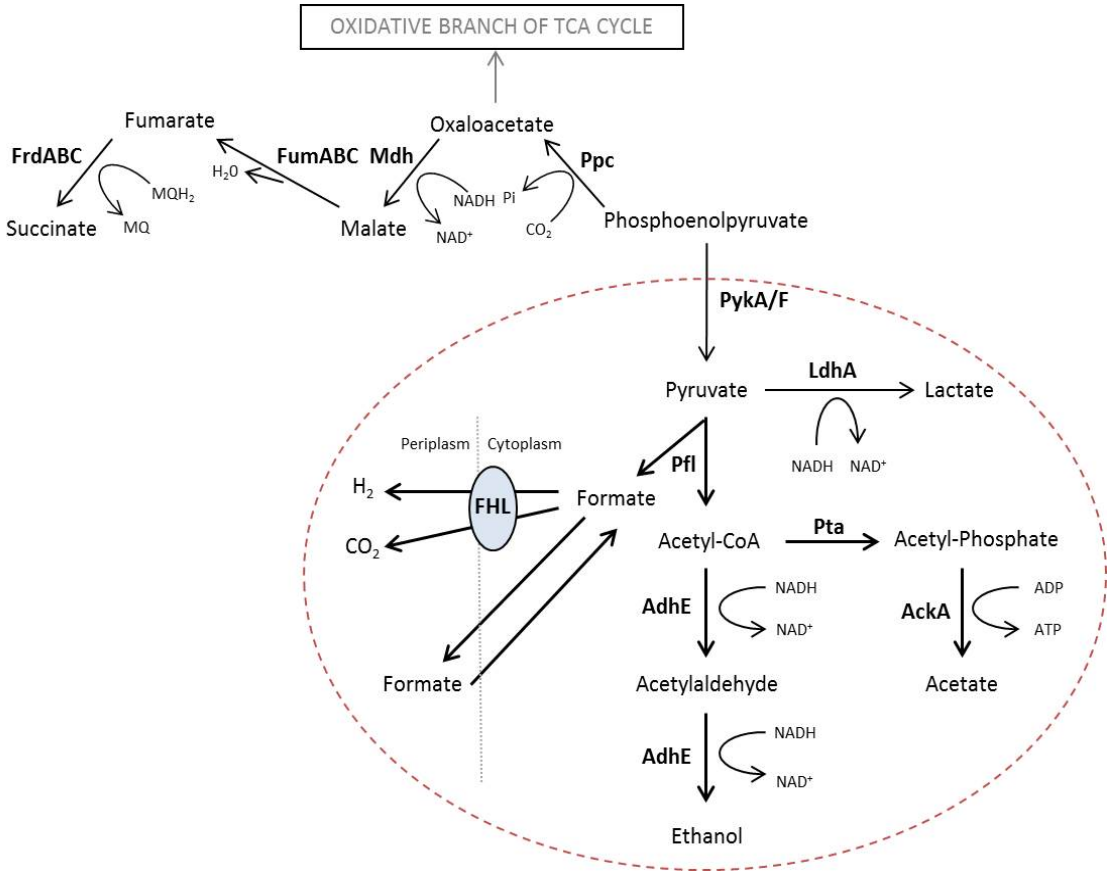


**Figure 1.12 The reductive pathways of mixed-acid fermentation in *E. coli*.** Enzyme abbreviations: PykA/F: pyruvate kinase; LdhA: lactate dehydrogenase; Pta: phosphotransacetylase; AdhE: alcohol dehydrogenase; Pfl: pyruvate formate lyase; Ppc: phosphoenolpyruvate carboxylase; Mdh: malate dehydrogenase; FumABC: fumarase; and FrdABC: fumarate reductase. The oxidative pathway of the TCA cycle halting at α-ketoglutarate is not shown for simplicity

#### 1.6.1.3 Alternative carbon sources as substrates for mixed-acid fermentation

The end products of mixed-acid fermentation have different oxidation states (or degrees of reduction), which is the hypothetical charge a compound would have if all bonds were ionic. Carbon compounds also have varying degrees of reduction/oxidation states. As mixed-acid fermentation is a redox neutral process, *E. coli* can adjust the amount of each fermentation product to maintain redox balance (Alam and Clark, 1989). However a trade-off between NADH oxidation and ATP production always exists. For example, more reduced sugars and sugar alcohols (relative to glucose) may be fermented by *E. coli*, however these must be oxidised before they can enter glycolysis, resulting in the production of one more molecule of NADH, which is then balanced by the production of more ethanol or lactate, which results in less acetate being produced during sugar alcohol fermentations and hence less ATP. On the other hand, more oxidised sugars, such as gluconate, can be fermented by *E. coli* with less $NAD^+$ regeneration required and hence more acetate and ATP is produced. These substrates however, enter lower glycolysis through the ED pathway, meaning a net production of only one ATP per glucose instead of two in the EMP pathway (Flamholz*, et al.*, 2013).

It has also been shown that the efflux of one of these organic acids, lactate, from the bacterial cytoplasm to the extracellular medium can be coupled to the symport of protons, thus generating an electrochemical proton gradient (Ten Brink and Konings, 1980; Verdoni*, et al.*, 1990), which can be used to drive ATP synthesis. A similar system is proposed for formate through the FocA channel (Suppmann and Sawers, 1994), although this formate:proton symport may only operate during formate uptake (thus actually collapsing the proton gradient) (Lu*, et al.*, 2011). If the concentration of extracellular organic acid was reduced, for example through syntrophic consumption by another organism (McInerney*, et al.*, 2009), this could allow for sustained organic acid efflux and therefore allow even greater yields of ATP to be generated.

### 1.6.2 Fermentation in other organisms

Other members of the Enterobacteriaceae are capable of alternative forms of fermentation. *Klebsiella oxytoca* for example is capable of fermenting glycerol (Lin, 1976), something *E. coli* is thought unable to do. Certain *Klebsiella spp.* and *Clostridia spp.* are known to perform a type of fermentation called acetone-butanol fermentation, whereby they produce 2,3-butanediol as the predominant electron sink for the regeneration of $NAD^+$ and $NADP^+$ (Jones and Woods, 1986; Böck and Sawers, 1996). Amongst many of the differences between mixed-acid fermentation in *E. coli* and the *Clostridial* acetone-butanol fermentation is the existence of a pyruvate:ferredoxin oxidoreductase instead of pyruvate formatelyase, which both oxidises

pyruvate to acetyl-CoA and reduces ferredoxin, which is then used as the electron donor for hydrogen production (Jones and Woods, 1986).

### 1.6.3 Biohydrogen production during mixed-acid fermentation

For every mol of glucose hydrolysed, 12 mol of $H_2$ could potentially be produced ($C_6H_{12}O_6$ + $6H_2O \leftrightarrow 6CO_2 + 12H_2$). However, much more typical yields of 2 – 4 mol of $H_2$ per mol of glucose are usually observed in $H_2$-producing organisms (Davila-Vazquez*, et al.*, 2008). This is close to the theoretical maximum of 4 mol $H_2$ per mol of glucose oxidised (1/3 of pyruvate generated during glycolysis converted into formate), if acetate is the sole end product: $C_6H_{12}O_6$ + $2H_2O \rightarrow 2CH_3COOH + 4H_2 + 2CO_2$. Of course this theoretical maximum is never achieved in native strains as acetate is never the sole fermentation product and some carbon must be assimilated into biomass. Furthermore factors such as the $pH_2$ can have inhibitory effects on hydrogenase activity (Chong*, et al.*, 2009), thus creating a bottleneck in metabolic flux through these enzymes, which is relieved by producing other fermentation products.

It has been suggested that in order for biohydrogen to become commercially viable, yields of $H_2$ must reach 60-80% efficiency, which is equivalent to over 7 mol $H_2$ per mol of glucose (Benemann, 1996). Other studies have focussed on the rate of $H_2$ production necessary and therefore the size of a reaction vessel that would be necessary to power a PEM fuel cell large enough to power an average house (Levin*, et al.*, 2004). They concluded that a 10-fold increase in the rate of $H_2$ production would allow a home to store a reasonably-sized bioreactor (e.g. one that could fit comfortably in the basement) to supply such a PEM fuel cell (Levin*, et al.*, 2004).

## 1.7 **Synthetic biology**

### 1.7.1 An overview of synthetic biology and the development of tools for synthetic biology projects

Synthetic biology encompasses the design and engineering of novel biological parts as well as the reengineering of existing biological parts, which are then combined to construct new synthetic devices and systems. The use of the word engineering in this definition is significant as in addition to a “drive to make” (Schyfter, 2013), a central aim of synthetic biology is to standardise biological parts so they be exchanged in a “plug and play” fashion. Biological parts are physical DNA sequences such as transcriptional promoters, ribosome-binding sites, linker/insulator sequences between parts, polypeptide coding sequences, non-polypeptide coding sequences (e.g. sRNA regulatory sequences, ribosome encoding sequences etc.) and

transcriptional terminators. These parts can then be combined to construct devices/systems in a chosen host organism, termed a chassis. Synthetic biology projects therefore often overlap with aspects of metabolic engineering, protein engineering and pathway engineering, which has led to some disputes over its definition (Stephanopoulos, 2012), however many researchers in the field now happily group these fields under the umbrella of synthetic biology (Nielsen and Keasling, 2011).

Technologies developed through synthetic biology research and industries that service this sector already generate significant revenue, the value of which is expected to reach $10.8 billion by 2016 (Kitney and Freemont, 2012). One could argue that synthetic biology is a rebranding of a number of fields that have suffered from bad publicity over the last twenty years, including genetically modified organisms (GMOs) and nanotechnology. In an attempt to pro-actively engage with the public and hopefully generate public backing for new technologies that emerge from synthetic biology, a large section of the synthetic biology community are engaged in “human practices” research (Brown, 2009). A related motivation sees an increased emphasis on building in safety and control mechanisms to any new synthetic system or organism (Moe-Behrens*, et al.*, 2013).

An idealised synthetic biology project can be divided into a number of steps (Figure 1.13) (Arpino*, et al.*, 2013). It starts with the *in silico* design of the desired parts, pathways and overall synthetic system, which can be followed by modelling studies on the hypothetical pathways and system, the results of which should guide further refinement of the individual parts.. The next step involves the *in vitro* construction of each individual part and the combination of these parts to assemble in the final synthetic pathways and systems. Finally the performance of these parts, pathways and systems can be tested and fully characterised both *in vitro* and *in vivo* and if required, further refinement of non-optimal parts performed. In order for these processes to become easy, quick and affordable, many tools are being developed to assist *in silico* design of parts and devices and the *in vitro* construction and combination of large sequences of DNA, as well as the construction of vast libraries of individual parts with specific characteristics.

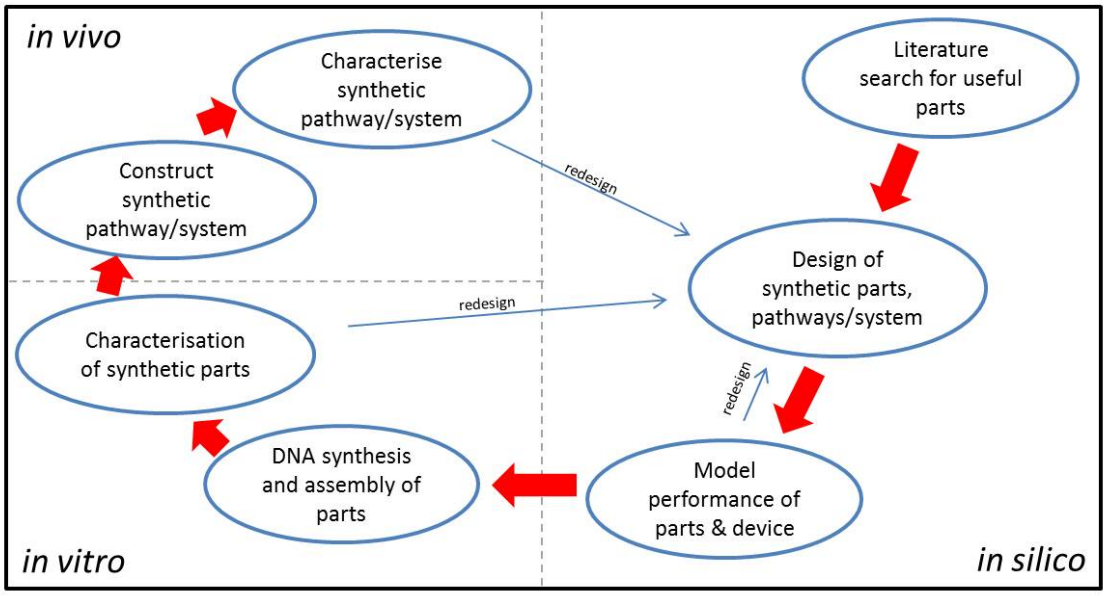


**Figure 1.13 A theoretical workflow chart for a typical synthetic biology project.** *In silico*, *in vitro* and *in vivo* approaches are combined and at each stage, redesign and optimisation may be required.

Many computer-aided design (CAD) tools specifically for synthetic biology have been developed to allow *in silico* part, pathway and system design and modelling. Programs such as J5 Device Editor (Hillson*, et al.*, 2012) facilitate the automated design of DNA assembly and part manipulation. Other programs, such as PIGEON, allow the visualisation of constructs with combinations of individual parts (Bhatia and Densmore, 2013). EUGENE allows for the construction of synthetic devices (pathway/system) from a wide selection of defined parts, based on constraints set by the individual user (e.g. level of output signal etc.) (Bilitchenko*, et al.*, 2011). The ribosome-binding site calculator developed by Salis and Voigt is an invaluable tool for the design (or testing) of ribosome-binding sites with defined translation initiation rates, based on the surrounding DNA sequence (Salis, 2011). A final example of a synthetic biology CAD tool is TinkerCell (Chandran*, et al.*, 2009), which allows the design and testing of intricate genetic circuits and synthetic devices. This software also allows the integration of modelling programs into its interface and also guides the final construction of the individual DNA sequences. A standardised visual language for synthetic parts, the Synthetic Biology Open Language (SBOL), has also been developed and has widely adopted (Galdzicki*, et al.*, 2011).

The construction of vast libraries of useful biological parts, many of which are stored in a central “Biobrick” repository (Registry of standard biological parts, Cambridge, Massachusetts) and available to synthetic biology researchers is both noble and invaluable. Libraries of synthetic promoters have been constructed and their strength of transcriptional initiation characterised (Davis*, et al.*, 2011; Brewster*, et al.*, 2012; Pasotti*, et al.*, 2012; Temme*, et al.*,

2012). Similar libraries of synthetic ribosome-binding sites have also been developed with translation initiation rates measured in combination with a wide variety of promoters and coding sequences (Salis*, et al.*, 2009; Temme*, et al.*, 2012). Transcriptional terminators have also been developed (Temme*, et al.*, 2012; Chen*, et al.*, 2013) as well as insulating (linker) sequences between individual parts, to ensure minimal interference with promoters, RBSs and terminators (Lou*, et al.*, 2012). Libraries of expression vectors have also been constructed specifically for biobrick cloning compatibility (Lee*, et al.*, 2011), while other researchers are developing a standard European vector, pSEVA, which would allow exchange of modular parts (selection markers, origins of replication, multiple cloning sites etc.), which looks promising (Silva-Rocha*, et al.*, 2013). As a last example of synthetic parts many researchers have developed libraries of polymerase-encoding genes, which when combined with promoter libraries allow for fully tunable levels of gene expression (Shis and Bennett, 2013).

The greatest revolution, and possibly the driving force, behind synthetic biology has been the development of cheaper high-throughput DNA synthesis (<$0.28 per base pair) and assembly technologies (Carlson, 2009). Synthetic DNA constructs can now be designed *in silico,* based on the vast amount of genomic information available, ordered and assembled in days. Assembly methods such as the Biobrick assembly standard (Knight, 2003) are now being replaced with high-throughput one-step assembly methods such as Gibson assembly (Gibson, 2009) and Golden-Gate assembly (Engler*, et al.*, 2009). New techniques allowing rapid recombination and DNA shuffling (Coco*, et al.*, 2001; Bloom*, et al.*, 2005; Edwards*, et al.*, 2008; Bloom and Arnold, 2009; Wang*, et al.*, 2012) and microfluidics based DNA mutant library construction (Szita*, et al.*, 2010), mean it is possible to construct novel synthetic parts with completely new functions (Altamirano*, et al.*, 2000). These technologies also enable expression of metagenomic sequences in a chassis such as *E. coli*.

### 1.7.2 Construction of synthetic genetic circuits

A longstanding aim of many in the field of synthetic biology is to construct synthetic genetic circuits where the expression of specific genes is regulated in response to specific inputs (Hasty*, et al.*, 2002). Riboswitches are small regulatory RNAs (aptamers) that can bind specific DNA or RNA sequence, thus inhibiting transcription or translation of these sequences, and whose action is controlled allosterically through the binding of a specific metabolite or ions (Hollands*, et al.*, 2012). Synthetic riboswitches have been constructed to control transcription/translation of any desired sequence (Bayer and Smolke, 2005; Wachsmuth*, et al.*, 2013). Riboswitches, recombinases, repressors, libraries of promoters and terminators, have been combined in the construction many interesting genetic circuits in bacteria and yeast,

such as synthetic circuits with the ability to count the application of a specific input (Friedland*, et al.*, 2009) or genetic circuits/toggle switches that can oscillate gene expression over multiple cycles (Elowitz and Leibler, 2000; Gardner*, et al.*, 2000; Atkinson*, et al.*, 2003; Fung*, et al.*, 2005). Decision making capabilities in the form of artificial logic gates that can respond to a variety of inputs have been constructed and can be orthologous or modular in nature (Yokobayashi*, et al.*, 2002; van Hijum*, et al.*, 2009). More complicated genetic circuits that can both record and store information over many generations (Bonnet*, et al.*, 2012) and the combination of synthetic biological logic gates and synthetic DNA data storage (Siuti*, et al.*, 2013) have also been developed.

### 1.7.3 From synthetic circuits to synthetic organisms

Synthetic genetic circuits to date focus on a maximum of two inputs to control the expression a small number of output genes and have mostly been used as proofs of principle in synthetic biology. More complex synthetic biology projects have also been carried out. The expansion of the genetic code is one of the most impressive and ground-breaking achievements of synthetic biology to date, allowing the *in vivo*, site-specific incorporation of non-natural amino acids into a wide variety of proteins and is being used in many areas of fundamental biological research, as well as the construction of new functional proteins and bio-materials (Davis and Chin, 2012). The Schultz lab were the first to successfully construct DNA sequences encoding many useful non-natural amino acids, through the construction of unique tRNA/tRNA synthetase pairs (Wang*, et al.*, 2001; Chin*, et al.*, 2002a; Chin*, et al.*, 2002b; Santoro*, et al.*, 2002; Wang*, et al.*, 2002; Zhang*, et al.*, 2002). Synthetic orthogonal ribosomes were developed by the Chin lab, which recognise alternative Shine Dalgarno sequences to that recognised by the native ribosome (Rackham and Chin, 2005). This allows polypeptides with non-natural amino acids to be synthesised independently to native protein production (reviewed in Chin, 2011). The expansion of the genetic code took another huge leap forward with the development of a synthetic form of nucleic acid known as XNA by the Holliger lab (Pinheiro*, et al.*, 2012; Pinheiro*, et al.*, 2013).

Synthetic spatial organisation of cellular enzymes is another exciting area of research in synthetic biology. A variety of scaffolds have been constructed to bring enzymes closer together in order to increase reaction rates. These include various protein scaffolds (Dueber*, et al.*, 2009; Agapakis*, et al.*, 2010) as well as RNA scaffolds (Delebecque*, et al.*, 2011; reviewed in Thodey and Smolke, 2011). Empty proteinaceous bacterial microcompartments, such as that used in the propanediol utilisation (Pdu) pathway of *Salmonella* have been synthetically expressed in a variety of chasses and a variety of proteins can be targeted into this

microcompartment using a short signal peptide (reviewed in Parsons*, et al.*, 2010; Frank*, et al.*, 2013). Another bacterial microcompartment, the $CO_2$ fixing microcompartment (carboxysome) from *Thiobacillus neapolitanus* has been heterologously expressed in an *E. coli* chassis and is functional at $CO_2$ fixing both *in vivo* and *in vitro* (Bonacci*, et al.*, 2012).

The next development in synthetic biology is sure to be the construction of a fully synthetic organism. An extremely well-publicised first attempt in the "creation" of a synthetic bacterium was recently published (Gibson*, et al.*, 2010). This team assembled a stripped down version of the *Mycoplasma mycoides* genome, both to understand the minimal set of genes required for life and to provide an ideal and robust platform for future synthetic biology devices (Gibson*, et al.*, 2010). This project also led to the development of the high-throughput DNA assembly method known as Gibson assembly (Gibson, 2009). Recently a number of groups have started engineering the Gram-negative soil bacterium *Pseudomonas putida* as a specialised synthetic biology chassis (Poblete-Castro*, et al.*, 2012).

## 1.8 **Aims**

The aim of this thesis was to explore different approaches to enhancing biohydrogen production in *E. coli*. This will involve combining modern synthetic biology concepts with traditional molecular biology and metabolic engineering technologies. The research has the following specific objectives.

**1.** To design, construct and characterise a synthetic [FeFe]-hydrogenase

**2.** To integrate a synthetic NADH-dependent hydrogenase into the central metabolism of *E. coli*

**3.** To re-purpose *E. coli* Hyd-2 for respiratory $H_2$ production using chimeric enzymes

**4.** To examine the use of glycerol as substrate for $H_2$ production by *E. coli*

# 2. *In vitro* characterisation of a synthetic [FeFe]-hydrogenase

## 2.1.1 Introduction

### 2.1.1.1 Heterologous expression of hydrogenases to increase $H_2$ production

In order for biohydrogen production to become commercially viable, $H_2$ yields must be increased to close to the maximum theoretical yield of $H_2$. Heterologous expression of hydrogenases from other $H_2$-producing organisms is an attractive strategy to improve $H_2$ yields. Non-native hydrogenases with alternative catalytic properties, cellular localisations, or substrate specificities may offer an advantage over native hydrogenases. [FeFe]-hydrogenases have $H_2$-production activities that are 10 – 100 times greater than [NiFe]-hydrogenases and are therefore attractive candidates for enhanced $H_2$ production projects (Adams, 1990; Frey, 2002). Recent identification and elucidation of the roles of each of the [FeFe]-hydrogenase accessory maturases, HydE, HydF, and HydG (Posewitz*, et al.*, 2004), has allowed successful co-expression of these maturases and a variety of non-native [FeFe]-hydrogenases in *E. coli*, resulting in active enzyme (Posewitz*, et al.*, 2004; King*, et al.*, 2006). Most of these studies were, however, designed to investigate the H-cluster maturation proteins and used hydrogenases such as those from *Clostridium acetobutylicum* or *Chlamydomonas reinhardtii*, whose natural electron donor is reduced ferredoxin. Ferredoxin is an electron carrier that does not appear to form a central part of *E. coli* metabolism. $NAD^+$/NADH are the main electron carriers used by *E. coli* during glycolysis and fermentation and a hydrogenase that could accept electrons from NADH would therefore be desirable.

### 2.1.1.2 An NADH-dependent [FeFe]-hydrogenase with high specific activities

*Thermoanaerobacter tengcongensis (Tte*; recently reclassified as *Caldanaerobacter tengcongensis*) is a thermophilic Gram-negative bacterium found in hot springs in China (Xue*, et al.*, 2001) that expresses two hydrogenases, one of which has been described as a soluble [FeFe]-hydrogenase that produces $H_2$ with NADH as the sole electron donor (Soboh*, et al.*, 2004). The enzyme was originally purified under anaerobic conditions and consisted of a four subunit complex: HydA; HydB; HydC and HydD. The genes encoding these products were identified and were found to be organised a single gene cluster: *TTE0890-TTE0894*, which corresponds to: *hydC;* a gene of unknown function – product not found in purified enzyme; *hydD; hydB;* and *hydA*, respectively. HydA is the large 64 kDa H-cluster-containing catalytic subunit predicted to contain an additional three [4Fe-4S] clusters and one [2Fe-2S] cluster. HydB is a large 65 kDa diaphorase subunit, with sequence similarity to NADH dehydrogenases and 65% overall sequence identity with HydB from *Thermotoga maritima* (Verhagen*, et al.*, 1999). It is thought to contain a flavin a part of the NAD(H)-binding site, three [4Fe-4S] clusters and one [2Fe-2S] cluster. HydC has a molecular mass of 20 kDa and shares 47% overall

sequence identity to HndA of *Desulfovibrio fructosovorans* and is thought to ligate a single [2Fe-2S] cluster. HydD has a molecular mass of 14 kDa and shares 36% sequence identity with HndB of *Desulfovibrio fructosovorans* and is likely to ligate an FeS cluster (Soboh*, et al.*, 2004). The purified enzyme displayed high $H_2$ oxidation and production rates with methyl viologen (MV) as the artificial electron acceptor/donor (both at 1700 U; 1U = µmol $H_2$ $min^{-1}$ $mg^{-1}$) and with $NAD^+$/NADH as electron acceptor/donor (5/10 U respectively). The purified enzyme was found to contain FMN at the ratio of 1 mol FMN per mol enzyme and an excess of FMN was required in all buffers during purification for significantly-increased hydrogenase activity (Soboh*, et al.*, 2004).

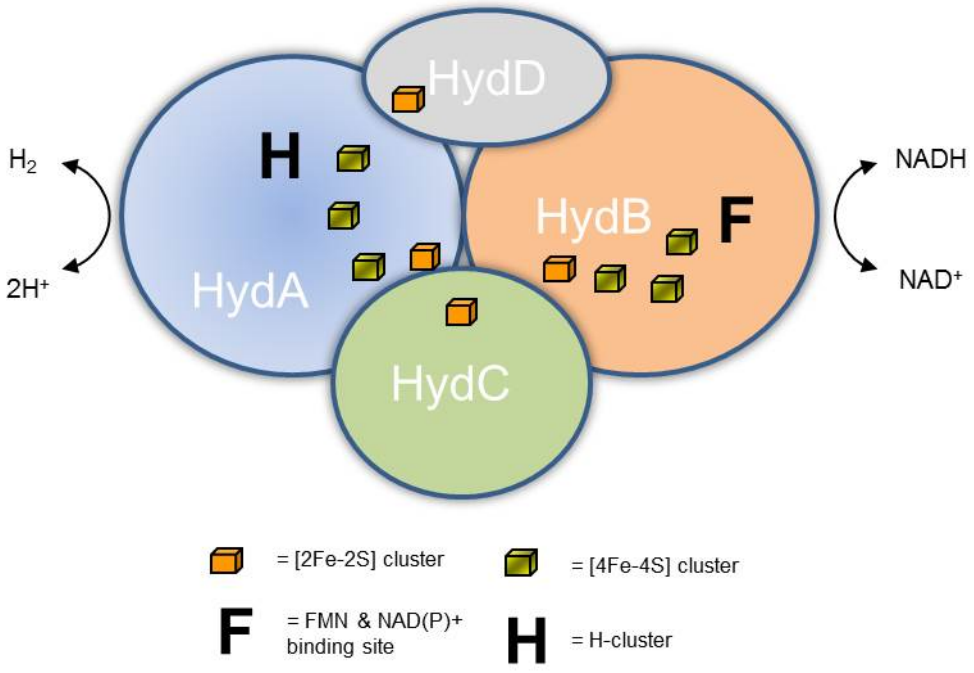


**Figure 2.1 Schematic of *Ca. tengcongensis* NADH-dependent [FeFe]-hydrogenase.** The exact type of FeS cluster in HydD is still unknown but shown here as [2Fe-2S] cluster.

## 2.2 Aims

This Chapter aims to construct, express and characterise a synthetic NADH-dependent $H_2$-producing [FeFe]-hydrogenase. This requires design of a synthetic operon encoding the hydrogenase structural genes, as well as provision of essential maturation proteins that will help build the [FeFe] catalytic centre in an *E. coli* chassis. Full comprehensive characterisation of each synthetic construct is planned, including both physical characterisation of all parts as well as functional characterisation of the synthetic hydrogenase enzyme.

## 2.3 **Results**

### 2.3.1 The design, construction and expression of a synthetic [FeFe]-hydrogenase operon

As a starting point, the soluble, thermostable NADH-dependent [FeFe]-hydrogenase operon of *Thermoanaerobacter tengcongensis* (*Tte*; recently reclassified as *Caldanaerobacter tengcongensis*) was chosen (Soboh*, et al.*, 2004). The constituent parts chosen to build a synthetic operon were the five genes *hydC*, *TTE0891, hydD, hydB,* and *hydA*. The primary amino acid sequences were back translated into DNA sequence, which was then codon optimised to ensure efficient translation in an *E. coli* chassis using the OPTIMIZER software (Puigbo*, et al.*, 2007). This gave final codon adaptation indices (CAIs), which is a comparison between the codon usage in a given DNA sequence and a reference set of highly expressed genes from the same species (Sharp and Li, 1987), for each gene of 0.759 for *hydC*; 0.742 for *tte0891*; 0.796 for *hydD*; 0.768 for *hydB*; and 0.747 for *hydA* (for comparison, a score of 0 = very different and unlikely to be translated in new host, while a score of 1 = identical to codon usage of new host and very likely to be translated). This indicates that heterologous expression of all synthetic genes should be successful in an *E. coli* K-12 chassis based on known tRNA abundances. In addition, sequences were designed so that commonly-used restriction sites were omitted.

A synthetic RBS and spacer sequence was included upstream of each synthetic gene: AGGAGGAAAAAAA. This sequence (along with the sequence upstream of the RBS and spacer, and the coding sequence itself) was analysed using the RBS CALCULATOR software (Salis*, et al.*, 2009), which allows the efficiency of translation initiation to be predicted. This software uses a thermodynamic model to quantify the free energies involved in the rate limiting step of translation initiation (calculated from the Gibbs free energies associated with mRNA secondary structure, 16S rRNA binding, etc.). The translation initiation rates (based on experimental validation of predictive model with transcriptional fusions of a library of RBSs to *rfp*; given in fluorescence units) and the $\Delta G_{total}$ (the difference in Gibbs free energies between the separate mRNA transcript and free 30S complex and the 30S assembled pre-initiation complex on the mRNA transcript; measured in kcal/mol) are shown in Table 2.1. All genes except *hydB* show strong translation initiation rates and very favourable $\Delta G_{total}$ values, indicating that this synthetic construct should be translated efficiently in *E. coli*. The *hydB* gene sequence appears to suffer from very strong mRNA secondary structure. These results show the sequence upstream of the RBS as well as the coding sequence itself can affect translation initiation.

| | Translation initiation rate (Au) | $\Delta G_{total}$ (kcal/mol) | $\Delta G_{mRNA:rRNA}$ (kcal/mol) | $\Delta G_{mRNA}$ (kcal/mol) |
|---|---|---|---|---|
| ***hydC*** | 51287.28 | -6.71 | -11.98 | -5.79 |
| ***TTE0891*** | 129028.73 | -8.76 | -13.38 | -5.14 |
| ***hydD*** | 258037.37 | -10.30 | -17.38 | -7.60 |
| ***hydB*** | 1778.21 | 0.76 | -12.38 | -13.66 |
| ***hydA*** | 30703.96 | -5.57 | -12.38 | -7.33 |

**Table 2.1 Analysis of the RBS and spacer used upstream of each gene in synthetic hydrogenase operon using RBS CALCULATOR**. Translation initiation rate is based on experimental validation with transcriptional fusion of a library of RBSs to *rfp* of predictive model. $\Delta G_{total}$ shows how energetically favourable the formation of the pre-initiation complex is. $\Delta G_{mRNA:rRNA}$ shows how energetically favourable the binding of the 16S rRNA is. $\Delta G_{mRNA}$ shows how strong the secondary structure mRNA transcript is folded. The same RBS and spacer sequence was used before each gene, AGGAGGAAAAAAA. RBS CALCULATOR was published by (Salis*, et al.*, 2009)

The five synthetic sequences were then brought together to form a synthetic operon in which the natural gene order (*hydC*, *TTE0891, hydD, hydB,* and *hydA*) was maintained. Finally, unique restriction site sequences were chosen to separate each gene at which point the design phase was considered complete (Figure 2.2). The complete 5,104 bp operon was then synthesised and assembled as a service by Biomatik Corp (USA).

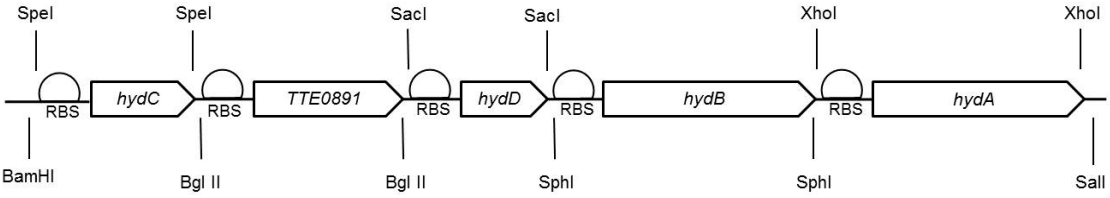


**Figure 2.2 The final synthetic construct encoding the *Ca. tengcongensis* [FeFe]-hydrogenase.** Each gene in the native *TTE0890-0894* operon was codon-optimised for expression in *E. coli* and has its own upstream synthetic RBS and spacer. Unique restriction enzyme sites were inserted to allow simple subcloning.

Once complete, the synthetic operon was subcloned into the *E. coli* expression vector, pUNI-PROM (Jack*, et al.*, 2004), which contains both the commonly used inducible T7 promoter ($P_{T7lac}$) and the constitutive promoter of the *E. coli tat* operon ($P_{tat}$) giving the final construct pUNI-Tte-Hyd (Figure 2.3A). The *tat* promoter is a well characterised promoter that conveys constitutive expression of genes under its regulation in both aerobic and anaerobic respiratory conditions (900 Miller units when studied *in situ* with a RBS and spacer sequence AGAGGAACATGT and the *lacZ* reporter gene placed downstream) as well as under fermentative conditions (430 Miller units) (Jack*, et al.*, 2001).

In order to validate that each gene in the synthetic operon was being correctly transcribed and translated the engineered restriction sites were used to modify the pUNI-Tte-Hyd plasmid. A bank of six new plasmids were constructed each carrying specific gene deletions. These were termed pUNI-Tte-HydΔ*hydC*, pUNI-Tte-HydΔ*TTE0891*, pUNI-Tte-HydΔ*hydD,* pUNI-Tte-HydΔ*hydB,* pUNI-Tte-HydΔ*hydA*, and pUNI-Tte-HydΔ*hydAB.* The seven synthetic constructs were next used in $^{35}$S-Methionine radiolabelling experiments. *E. coli* strain K38 (containing plasmid pGP1-2, a temperature-sensitive plasmid that encodes T7 polymerase) was transformed separately with pUNI-Tte-Hyd, pUNI-Tte-HydΔ*hydC*, pUNI-Tte-HydΔ*tte0891*, pUNI-Tte-HydΔ*hydD*, pUNI-Tte-HydΔ*hydB*, pUNI-Tte-HydΔ*hydA*, and pUNI-Tte-HydΔ*hydAB* respectively. Cultures of M9 minimal medium lacking cysteine and methionine were labelled *in vivo* for 15 min by the addition of $^{35}$S-methionine. Samples were then analysed by SDS-PAGE (12% w/v polyacrylamide gels), fixed, and visualised by autoradiography. Clear, radiolabelled protein bands could be assigned to each synthetic gene product (Figure 2.3B), confirming both transcription and translation of each gene in the *E. coli* chassis.

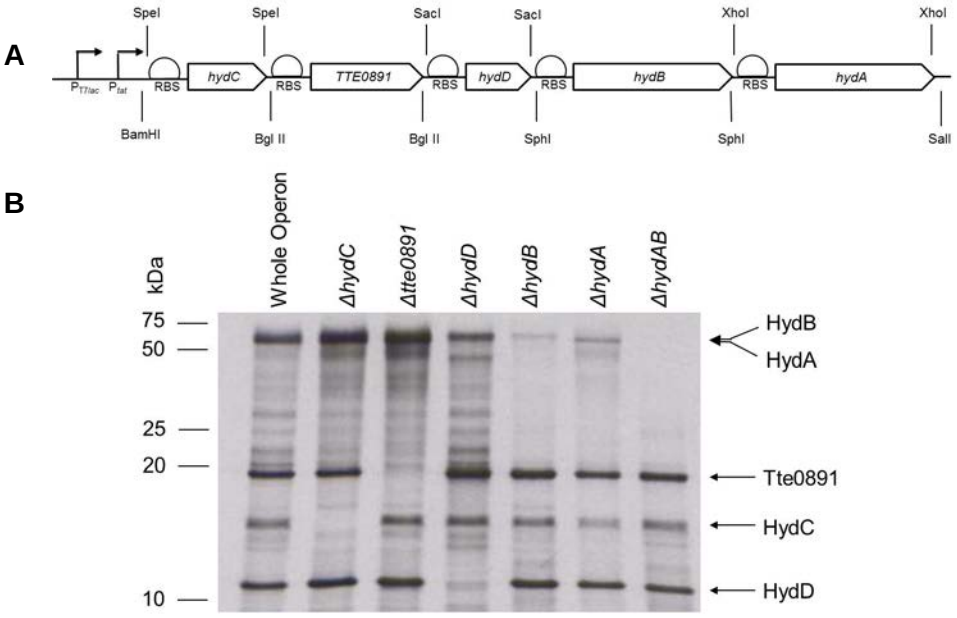


**Figure 2.3 $^{35}$S-methionine radiolabelling confirms production of all gene products from the synthetic operon.** *E. coli* strain K38/pGP1-2 was transformed with plasmids: pUNI-Tte-Hyd; pUNI-Tte-HydΔ*hydC*; pUNI-Tte-HydΔ*tte0891*; pUNI-Tte-HydΔ*hydD*; pUNI-Tte-HydΔ*hydB*; pUNI-Tte-HydΔ*hydA*; and pUNI-Tte-HydΔ*hydAB* and minimal M9 cultures lacking cysteine and methionine were labelled for 15 min by the addition of $^{35}$S-methionine. Protein samples were then separated by SDS-PAGE (12% w/v polyacrylamide), fixed, and visualised by autoradiography.

### 2.3.2 The design, construction & expression of a synthetic [FeFe] active-site maturase operon

A complex suite of maturation proteins are required in order to both assemble and insert the [FeFe] active site into the large catalytic subunit of HydA. While the Hyp accessory proteins, required for assembly of the [$NiFeCO_2CN$] cofactor in a [NiFe]-hydrogenase, appear to the species-specific the same cannot be said of the genes required for H-cluster assembly. The γ-Proteobacterium *Shewanella oneidensis* is closely related to *E. coli* but encodes a periplasmic [FeFe]-hydrogenase in its genome. Co-expressed with the [FeFe]-hydrogenase structural genes are four open reading frames *SO_3923* (*hydG*), *SO_3924* (a gene of unknown function – *hydX*), *SO_3925* (*hydE*), and *SO_3926* (*hydF*), that are thought to encode maturation proteins for H-cluster assembly. Indeed, during the course of this work, *Sh. oneidensis* and its *hydGXEF* genes have been successfully used in heterologous expression studies of [FeFe]-hydrogenases (Kuchenreuther*, et al.*, 2010).

Initially, the codon usage of the native *Sh. oneidensis hydGXEF* genes was analysed using OPTIMIZER (Puigbo*, et al.*, 2007). The codon adaptation indices for *hydG*, *hydX*, *hydE*, and *hydF* were all above the lower threshold figure of 0.3 (0.413; 0.337; 0.319; and 0.323 respectively), meaning all genes could be translated in *E. coli*. The four gene operon containing *SO_3923* (*hydG*); *SO_3924* (*hydX*); *SO_3925* (*hydE*) and *SO_3926* (*hydF*) was amplified by PCR from *Sh. oneidensis* genomic DNA and subsequently cloned directly into pUNI-PROM ($Amp^R$; $P_{T7lac}$; $P_{tat}$) and pSU-PROM ($Kan^R$; $P_{tat}$) (Jack*, et al.*, 2004), with only one engineered RBS and spacer before the first gene in the operon, to give the plasmids pUNI-Sh-EFG and pSU-Sh-EFG (Figure 2.4A).

To examine the translational efficiency of the cloned genes, the pUNI-Sh-EFG plasmid was used in a radiolabelling experiment in the *E. coli* chassis. Unfortunately, not all gene products could be confidently identified using this method. Only two prominent bands were evident migrating at 52 and 43 kDa (Figure 2.4B). In comparison, the predicted sizes of the *hydGXEF* gene products are 52 kDa, 23.5, 39.5 and 43 kDa respectively.

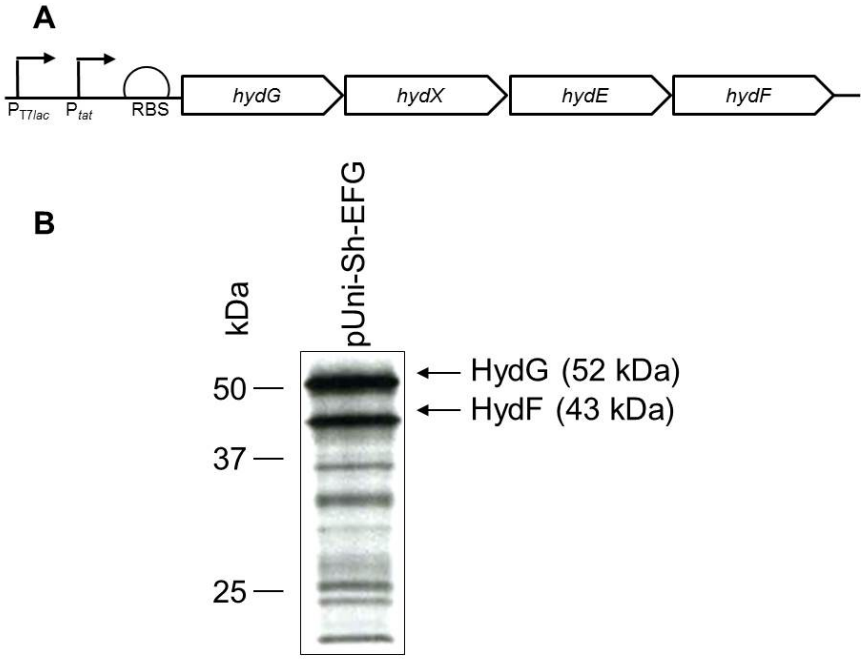


**Figure 2.4 $^{35}$S-methionine radiolabelling indicates problems with translation of *Shewanella* genes in *E. coli*.** *E. coli* strain K38/pGP1-2 was transformed with pUNI-Sh-EFG and cultures of M9 minimal medium lacking cysteine and methionine were labelled for 15 min by the addition of $^{35}$S-methionine. Protein samples were then separated by SDS-PAGE (14% w/v polyacrylamide), fixed, and visualised by autoradiography. HydG has a predicted molecular mass of 52 kDa, HydF has a predicted molecular mass of 43 kDa. HydE has a predicted molecular mass of 39.5 kDa and HydX has a predicted molecular mass of 23.5 kDa.

In an attempt to identify which genes were being translated a set of restriction digests were performed. The pUNI-Sh-EFG vector was digested with XhoI, which will remove a portion of the final gene in the operon *SO_3926* (*hydF*). Subsequent radiolabelling experiments established that the prominent band migrating at 43 kDa was HydF. Next, the pUNI-Sh-EFG vector was digested with SacI, which will remove a portion of the first gene in the operon *SO_3923* (*hydG*). In this case the prominent band migrating at 52 kDa was identified as HydG. Interestingly, therefore, despite transcription being driven from a single T7 promoter in this experiment, it is the first and last genes of the four-cistron operon that are most efficiently translated and the most stable in the cell. Expression of neither *SO_3924* (*hydX*) nor *SO_3925* (*hydE*) could be confirmed by this method (Figure 2.5).

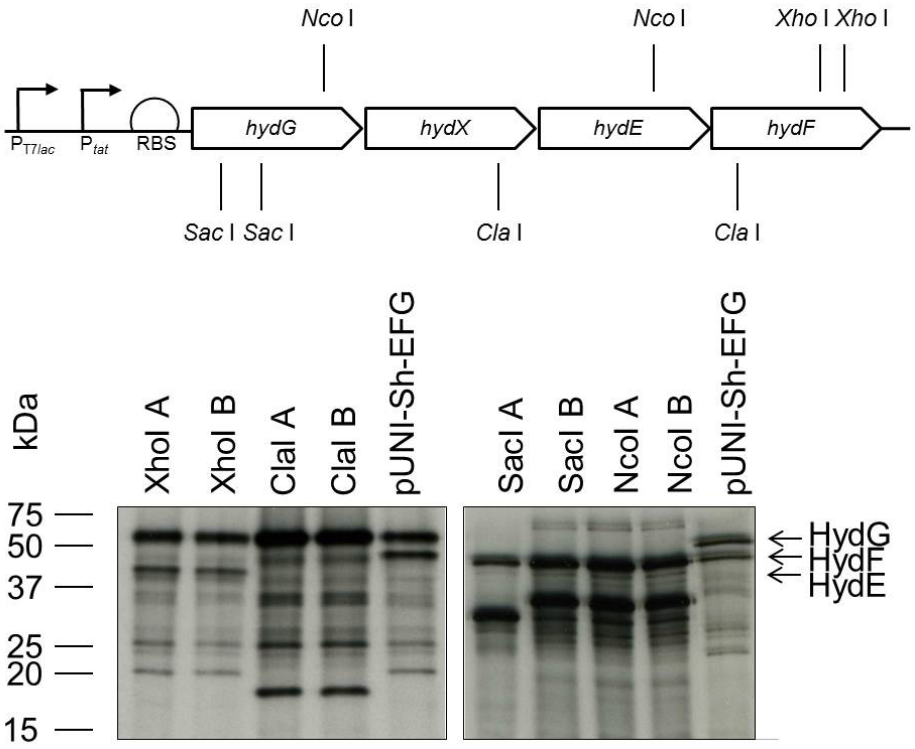


**Figure 2.5 The *hydE* gene is not translated efficiently in the *E. coli* chassis.** *E. coli* strain K38/pGP1-2 was transformed with plasmids: pUNI-Sh-EFG; pUNI-Sh-EFG$_{SacI}$; pUNI-Sh-EFG$_{ClaI}$; pUNI-pUNI-Sh-EFG$_{XhoI}$; pUNI-Sh-EFG$_{NcoI}$ and minimal M9 cultures lacking cysteine and methionine were labelled for 15 min by the addition of $^{35}$S-methionine. Protein samples were then separated by SDS-PAGE (14% w/v polyacrylamide), fixed, and visualised by autoradiography. pUNI-Sh-EFG$_{XhoI}$ allows identification of HydF (predicted molecular mass of 43 kDa). pUNI-Sh-EFG$_{SacI}$ and pUNI-Sh-EFG$_{NcoI}$ allows identification of HydG (predicted molecular mass of 52 kDa). pUNI-Sh-EFG$_{ClaI}$ allows identification of HydE (predicted molecular mass of 39.5 kDa). HydX has a predicted molecular mass of 23.5 kDa but could not be identified.

### 2.3.3 Optimising expression of the H-cluster maturation genes

Although HydG and HydF are being produced from the pUNI-Sh-EFG vector, this is unlikely to be sufficient to assemble the active site H-cluster. The activity of HydE is essential for maturation, as mutation of its three anion-binding residues reduced [FeFe]-hydrogenase activity (Nicolet*, et al.*, 2008) and its similarity to other AdoMet radical proteins suggests it is responsible for the synthesis of the bridging aminedithiolate ligand on the 2Fe scaffold of HydF (Nicolet*, et al.*, 2010; Peters and Broderick, 2012). In an attempt to induce expression of *hydE*, and remove some of the native regulatory elements possibly hidden in the native *Sh. oneidensis* operon structure, it was decided to clone both halves of the operon *(hydGX* and *hydEF*) separately into the dual expression vector pACYC-Duet. The pACYC-Duet vector has two multiple cloning sites both under the control of separate $P_{T7lac}$ promoters and also contains *lacI*, encoding the repressor of the *lac* operon. Each half-operon was amplified by PCR and cloned with the initial gene in each half enjoying the same RBS and spacer sequence (AGGAGGAAAAAAA). The resultant plasmid, pDuet-Sh-GX-EF, was then analysed by $^{35}$S-Methionine radiolabelling experiments. In this case, crucially, all the major maturation genes were found to be transcribed and translated (Figure 2.6).

Next, the entire RBS–spacer-*hydGX*-$Term_{T7}$-*hydEF* DNA fragment from pDuet-Sh-GX-EF was subcloned into pSU23 (Bartolome*, et al.*, 1991), which, unlike pACYC-Duet, does not encode the LacI repressor. This lead to increased expression levels relative to pDuet-Sh-GX-EF as observed by radiolabelling experiments (Figure 2.6). Finally, as repression or careful induction of expression of *S. oneidensis* operon was not thought to be required, the *E. coli tat* promoter ($P_{tat}$) was introduced upstream of the first gene to yield pSUtat-Sh-GX-EF. This removed the need to co-express with a plasmid encoding T7 polymerase (e.g. pGP1-2),

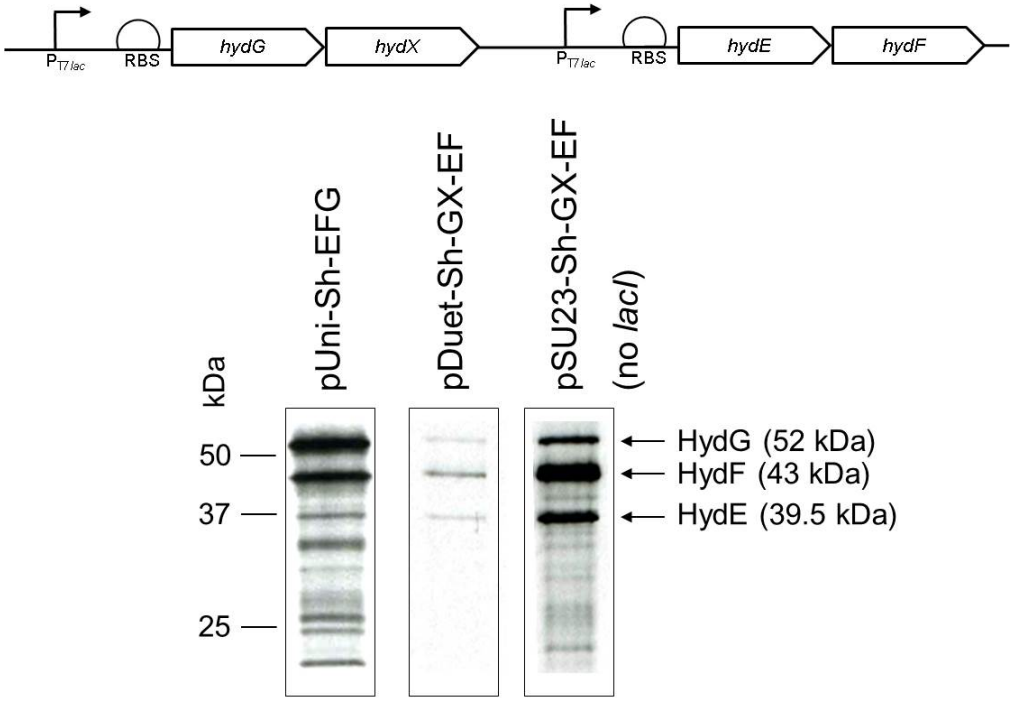


**Figure 2.6 $^{35}$S-methionine radiolabelling confirmed the production of each maturation gene after optimisation.** *E. coli* strain K38/pGP1-2 was transformed with plasmids: pDuet-Sh-GX-EF; pSU23-Sh-GX-EF and minimal M9 cultures lacking cysteine and methionine (supplemented with 10 mM IPTG; necessary to induce expression of genes on pDuet-Sh-GX-EF plasmid; not necessary for pUNI-Sh-EFG or pSU23-Sh-GX-EF however) were labelled for 15 min by the addition of $^{35}$S-methionine. Protein samples were then separated by SDS-PAGE (14% w/v polyacrylamide), fixed, and visualised by autoradiography.

### 2.3.4 Purification and structural characterisation of a synthetic hydrogenase complex

To facilitate *in vitro* characterisation of the synthetic *Ca. tengcongensis* [FeFe] hydrogenase complex, the plasmid pUNI-Tte-$Hyd_{hisC}$ was constructed, which is identical to the pUNI-Tte-Hyd vector except that it encodes a version of HydC that carries an N-terminal hexa-Histidine tag. In theory, any intact complex could then be easily purified using immobilised metal affinity chromatography (IMAC). During the course of this work, an increase in the activity of a heterologously-expressed [FeFe]-hydrogenases has been reported when expressed in an *E. coli iscR* mutant (Kuchenreuther*, et al.*, 2010). As a result the *E. coli* strain PK4854 (as MG1655 Δ*iscR*) was chosen as the host strain for all subsequent experiments.

PK4854 was transformed with pSUtat-Sh-GX-EF and pUNI-Tte-$Hyd_{hisC}$ and this was used to inoculate 5 litre anaerobic LB cultures supplemented with 0.4 % (w/v) glucose, 2 mM cysteine, 2 mM ferric ammonium citrate and the appropriate antibiotics. The cultures were incubated at 37 °C for ~16 hours before the cells were harvested and then lysed using either BPER (contains detergent) or sonication. The resultant crude cell extract was loaded to a $Ni^{2+}$ Sepharose™ high performance column (GE Healthcare), washed and bound proteins eluted by the application of an imidazole gradient. As [FeFe]-hydrogenases are notoriously sensitive to irreversible inactivation by $O_2$, all buffers were maintained as anaerobic as possible by degassing and constant bubbling with $N_2$. In addition, cell pellets and crude extracts were flushed with Ar throughout the purification protocol. Aliquots of individual peak fractions were immediately flushed with Ar, aliquoted and flash frozen in liquid $N_2$ before being stored under Ar at -80 °C.

Individual peak aliquots were analysed by SDS-PAGE (Figure 2.9). Strong bands corresponding to the expected sizes of each of the four subunits of the synthetic [FeFe] hydrogenase were observed and the identification of each subunit was further confirmed by tryptic peptide mass-fingerprinting (HydA, HydB and HydD). The identification of HydC was confirmed by western immunoblotting using an α-pentaHis antibody (Figure 2.8).

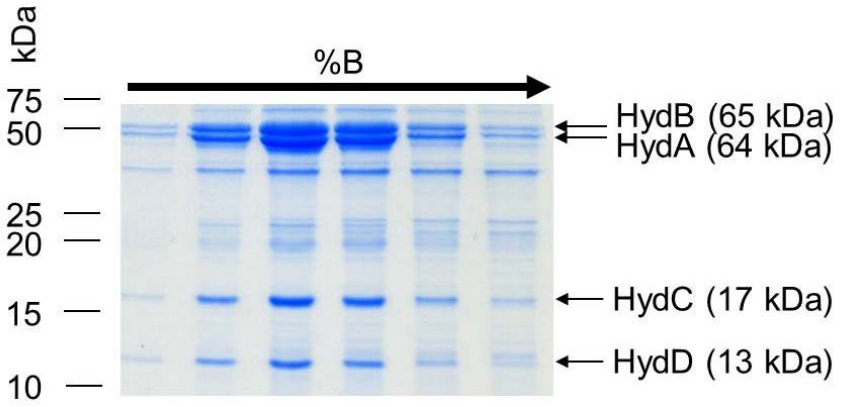


**Figure 2.9 Purification of synthetic [FeFe]-hydrogenase using IMAC.** *E. coli* strain PK4854 (Δ*iscR*) was transformed with plasmids: pUNI-Tte-$Hyd_{hisC}$ and pSUtat-Sh-GX-EF. This was used to inoculate 5 litre overnight, anaerobic cultures of L.B. supplemented with 0.4 % (w/v) glucose, 2 mM cysteine, 2 mM ferric ammonium citrate and the appropriate antibiotics. Cells were harvested and lysed using sonication. Crude cell extract was loaded onto a HisTrap™ HP column and eluted by an imidazole gradient (buffer B: 1 M imidazole). All steps were carried out under Ar. Peak fractions were collected, separated on 14% SDS-PAGE gel and visualised after staining with Coomassie Blue. Each subunit was identified using tryptic peptide mass fingerprinting.

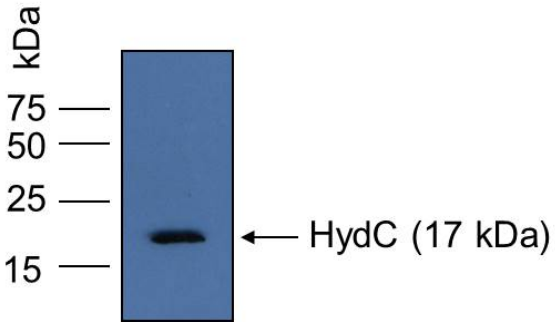


**Figure 2.8 Identification of HydC confirmed by α-His immunoblotting.** Purified hydrogenase was separated on a 14% SDS-PAGE gel, followed by a semi-dry transfer to nitrocellulose membrane and the band corresponding to HydC confirmed by immunoblotting using an α-pentaHis antibody.

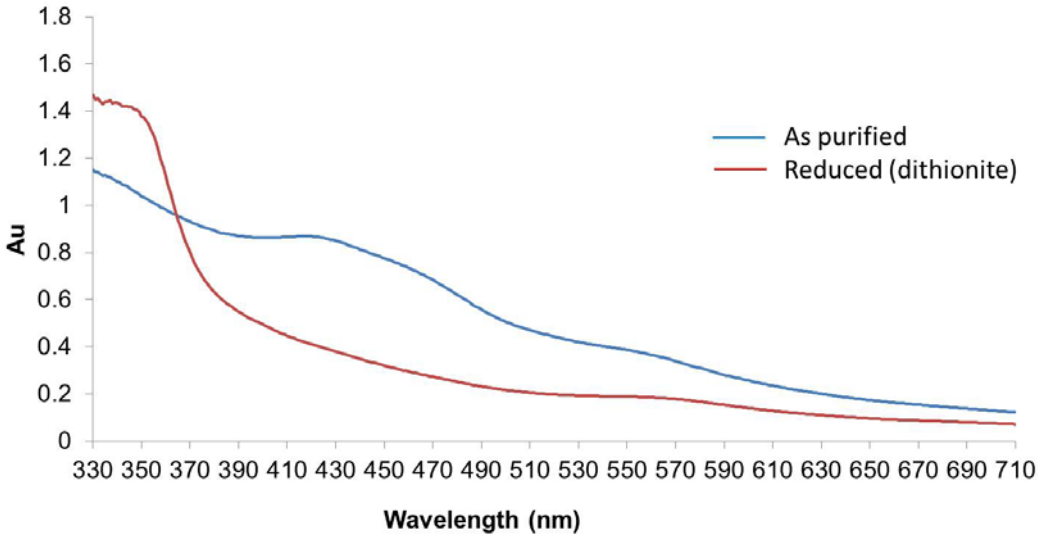


**Figure 2.7 Visible-light spectroscopy of purified enzyme shows characteristic FeS-cluster shoulders at 420 and 450 nm.** Purified enzyme was diluted 1:1 with 100 mM sodium phosphate buffer pH 6.0 and analysed over wavelengths from 330 to 710 nm.

A collaboration with Prof. Bill Hunter's Structural Biology group at the University of Dundee was initiated to investigate the structure of the synthetic hydrogenase. A number of purifications, followed by size-exclusion chromatography (S.E.C.) and crystallisation screens with a wide variety of conditions were performed, however no crystals were obtained.

During S.E.C. the enzyme complex was observed to elute at a volume indicating it had a molecular mass of approximately 320 kDa, which was approximately double the expected molecular mass of the four subunit enzyme. This merited further investigation. Size-exclusion chromatography – multi-angle laser light scattering (SEC-MALLS) experiments were carried out on purified enzyme from cells that had been lysed using the BPER chemical cocktail. The protein was concentrated and resolved on a MAbPac SEC– 1 (Dionex). The column was linked in series to two detectors: a laser photometer that continuously fires a laser at the eluent, thus scattering the beam and measuring the intensity of the scattered beam at different angles; and a refractive-index detector that determines accurate relative sample concentration. This allows information such as molecular mass, polydispersity and the radius of the complex to be accurately calculated. The purified enzyme appeared to form a stable large monodisperse complex containing each of the four subunits (confirmed by SDS-PAGE; Figure 2.11). The enzyme purified using the BPER lysis method, forms a monodisperse complex with a molecular weight of 325 kDa (±0.1%) and has a radius of 11.9 nm (±3.3%) (Figure 2.10).

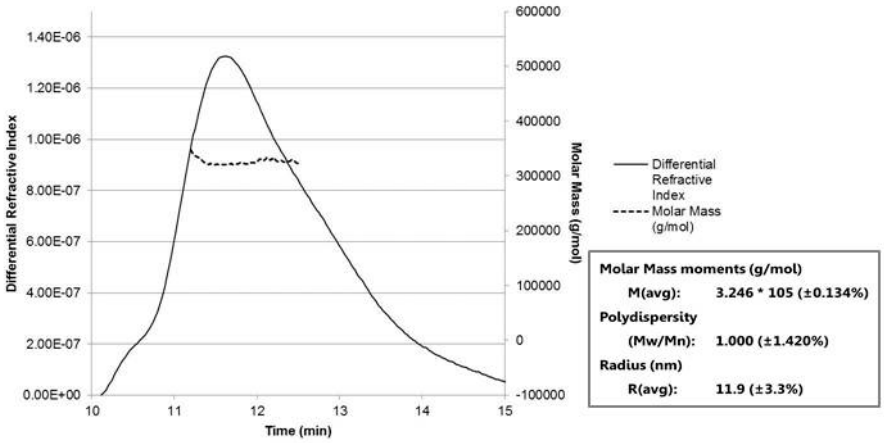


**Figure 2.10 SEC-MALLS analysis of the purified synthetic hydrogenase complex.** After Ni-IMAC, 1 mg of enzyme purified using the BPER method of lysis was loaded onto a MAbPac SEC–1 **(Dionex) column**. The molar mass of the eluent was calculated from light-scattering and differential refractive index measurements. The continuous line represents the absorbance at 280 nm of the eluent against time and the dotted line represents the weight-average molecular weight of the species in the eluent. The purified enzyme forms a monodisperse complex containing all four subunits, with a radius of 11.9 nm.

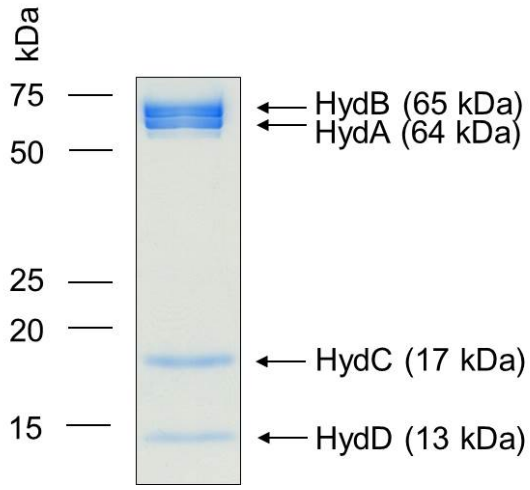


**Figure 2.11 SDS-PAGE analysis of the synthetic enzyme following SEC-MALLS.** The peak fraction from SEC-MALLS analysis was collected, concentrated and separated on 12% SDS polyacrylamide gel, followed by staining with Instant Blue™ Coomassie stain.

### 2.3.5 Purified synthetic hydrogenase displays $H_2$-oxidation and $H_2$-reduction activity *in vitro*

The next stage in the functional characterisation of the synthetic hydrogenase was to assay its ability to either oxidise or evolve $H_2$ with an artificial electron acceptor or donor. Benzyl viologen (BV) was chosen as the electron acceptor as its standard reduction potential ($E^{0'}$ -348 mV) is above that of the $H^+/½\ H_2$ redox couple ($E^{0'}$ -420 mV) and methyl viologen (MV) as the electron donor ($E^{0'}$ -443 mV) as it is a stronger reducing agent. For BV reduction, one activity unit (U) is defined as 1 µmol BV reduced $min^{-1}$ $mg^{-1}$ cells. For MV-dependent $H_2$ production, one unit (U) is defined as 1 µmol $H_2$ evolved $min^{-1}$ $mg^{-1}$ cells.

Synthetic enzyme purified from cells co-expressing pSUtat-Sh-GX-EF and lysed by sonication, catalysed the reduction of BV with $H_2$ as the electron donor, with a specific activity of 38 U (when assayed in pH 8.0 Tricine buffer) or 24 U (pH 8.0 Tris HCl) (Figure 2.12B). This was >40 times higher (0.6 U) than enzyme purified from cells co-expressing the pSU23-Sh-GX-EF (and T7 polymerase-encoding pGP1-2) lysed using BPER, even when all steps were performed in an MBraun Labstar™ anaerobic glove box. Trace activity was observed when enzyme was purified from cells co-expressing the original *Sh. oneidensis* accessory plasmid, pSU-Sh-EFG (0.01 U).

Synthetic *Ca. tengcongensis* [FeFe]-hydrogenase purified using the sonication method also demonstrated good $H_2$-evolution activity with reduced MV as the artificial electron donor (5 U) (Figure 2.12A). Again, this was much higher than the rate observed for enzyme purified from cells lysed with BPER and co-expressing the original *Sh. oneidensis* accessory plasmid, pSU-Sh-EFG (0.8 U).

Disappointingly, no NADH-dependent production of $H_2$ was observed under a number of different assay conditions, despite $H_2$ production with the artificial electron donor MV being demonstrated. Synthetic *Ca. tengcongensis* [FeFe]-hydrogenase was also unable to catalyse the oxidation/reduction of $NADH/NAD^+$ during spectroscopic experiments (absorbance of NADH monitored at 340 nm).

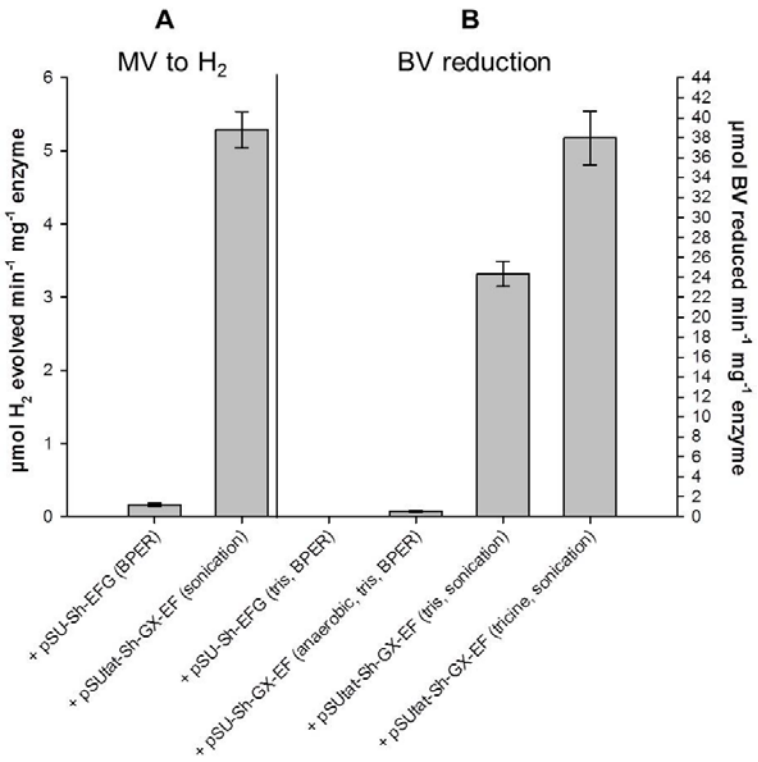


**Figure 2.12 Purified synthetic [FeFe]-hydrogenase displays hydrogenase activity *in vitro* .** After Ni-IMAC, purified enzyme from cells coexpressing one of the three accessory plasmids: pSU-Sh-EFG; pSU23-Sh-GX-EF; or pSUtat-Sh-GX-EF, and lysed either by sonication or using Bacteria Protein Extraction Reagent (BPER) was assayed for hydrogenase activity. (a) Methyl viologen (MV)-dependent $H_2$ production was measured in a modified Clark-type electrode. 100 mM sodium phosphate buffer pH 6.0 was added to the reaction chamber, to which 12.5 mM MV and 650 µM sodium dithionite was added. The reaction was initiated by the addition of 10 µg of purified *Tte* enzyme. (b) Benzyl viologen (BV) reduction ($H_2$ oxidation) was monitored at 578 nm in a UV-vis spectrometer. 1 ml quartz cuvettes were filled with $H_2$-saturated buffer (50 mM Tris HCl pH 8.0 or 50 mM Tricine pH 8.0) and 13 mM BV. This was titrated with sodium dithionite to an absorbance of 0.4 - 0.7 and the reaction started by the addition of 20 µg of purified *Ca. tengcongensis* enzyme. Error bars represent the standard error of three independent experiments.

### 2.3.6 Investigation of possible bifurcating mechanism of *Ca. tengcongensis* hydrogenase

It was recently shown that the soluble [FeFe]-hydrogenase from *Thermotoga maritima* has an interesting bifurcating mechanism of hydrogen production, where it uses reduced ferredoxin in combination with NADH, synergistically, as electron donors for $H_2$ (Schut and Adams, 2009). The reduced ferredoxin is a product of the oxidation of pyruvate to acetyl-CoA catalysed by the pyruvate ferredoxin oxidoreductase.

Pyruvate ($CH_3COCOO^-$) + CoA + $2Fd^{ox}$ $\leftrightarrow$ acetyl-CoA + $CO_2$ + $2H^+$ + $2Fd^{red}$

Indeed, in the course of this research a number of other studies have described or suggested a bifurcating mechanism of $H_2$ metabolism in certain [FeFe]-hydrogenases (Huang*, et al.*, 2012; Rydzak*, et al.*, 2012; Schuchmann and Muller, 2012).

The three subunits HydA, B and C of the *Th. maritima* [FeFe] hydrogenase share high sequence identity and similarity to the *Ca.tengcongensis* hydrogenase subunits (HydA, B and C): *Ca. tengcongensis* HydA has 43% overall sequence identity and 59% overall similarity with *Th. maritima* HydA; *Ca.tengcongensis* HydB shares 56% identity and 71% similarity with *Th. maritima* HydB; and *Ca. tengcongensis* Hyd C shares 48% identity and 70% similarity with *Th. maritima* HydC. It was therefore decided to investigate whether a similar mechanism was involved in $H_2$ production by the *Ca.tengcongensis* enzyme.

The gene *TM0927* (encoding a ferredoxin (Fd)) and the operon *TM0015-TM0018* (encoding the γ, δ, α & β subunits of a pyruvate-ferredoxin oxidoreductase (POR)) were cloned from *Th. maritima* genomic DNA into pUNI-PROM expression vectors. Successful heterologous expression of both the *Th. maritima* ferredoxin-encoding gene and the POR-encoding operon was confirmed using $^{35}$S-methionine radiolabelling (Figure 2.13A). Both pyruvate-ferredoxin oxidoreductase and ferredoxin were purified using IMAC and the pyruvate-oxidation/coenzymeA-acetylation activity of POR was assayed (2 µmol BV reduced $min^{-1}$ $mg^{-1}$). Furthermore, size-exclusion chromatography (and SDS-PAGE analysis) of the purified His-tagged POR complex on its own (Figure 2.13 B and C) and when co-expressed with a non-affinity-tagged Fd (Figure 2.13 B and D) indicated a probable interaction between the heterologously-expressed POR and Fd. *In vivo* assays where the *Ca.tengcongensis* hydrogenase and the *Th. maritima* POR/$Fd^{red}$ system were combined to test for $H_2$ production in a bifurcating-dependent manner were initiated, but were inconclusive upon cessation of experimental work.

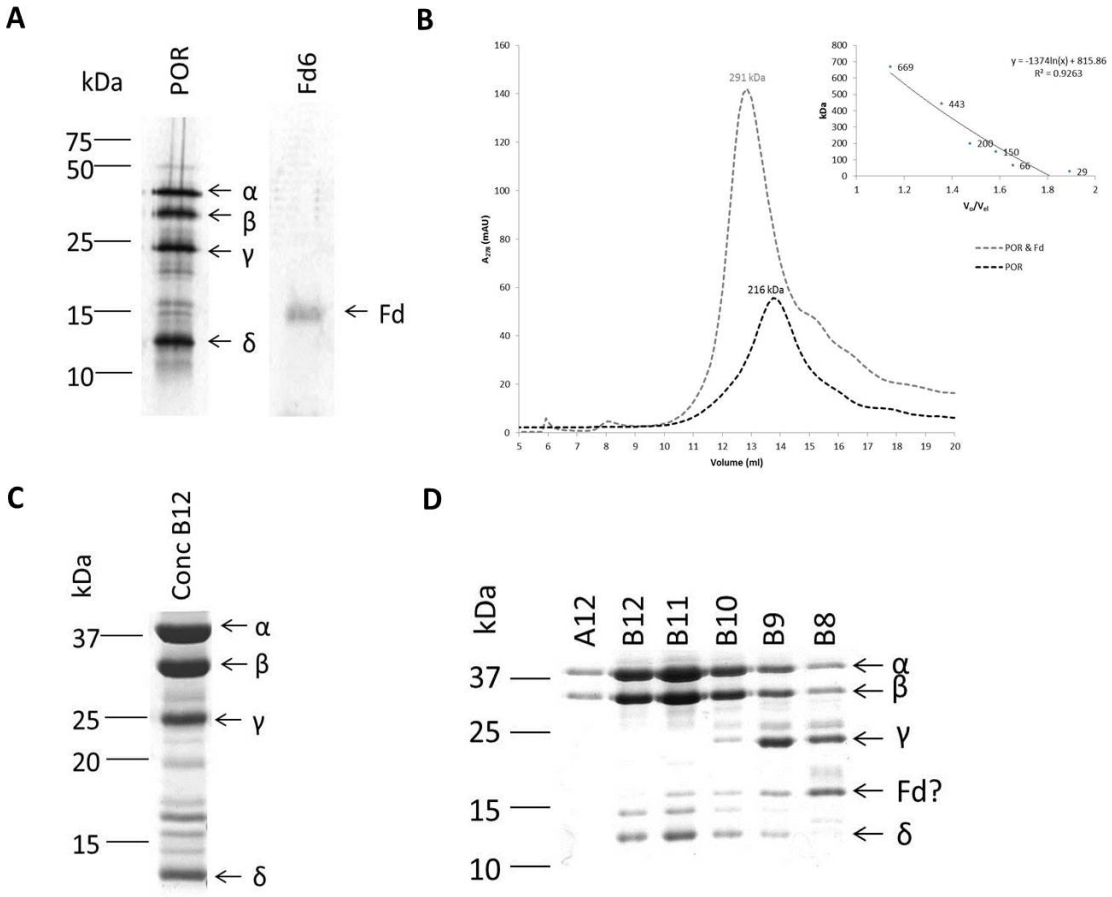


**Figure 2.13 Heterologous expression, purification and characterisation of *Th. maritima* POR and Fd. A.** $^{35}S$ Methionine radiolabelling of pUni-Tma-POR and pUNI-Tma-Fd6 followed by SDS-PAGE and autoradiography. **B.** Size-exclusion chromatography of $Ni^{2+}$-IMAC purified POR enzyme (black dashed lines) and POR & Fd (grey dashed lines) indicates that POR complex purifies as a dimer of the four subunits and also indicates that this POR dimer interacts with 4 Fds. **C.** SDS-PAGE analysis of the peak fraction from size-exclusion chromatography of POR. Each of the four subunits was identified by tryptic-peptide mass fingerprinting. **D.** SDS-PAGE analysis of the peak fraction from size-exclusion chromatography of POR. The band at approximately 16 kDa could be the Fd in complex with POR.

## 2.4 **Discussion**

### 2.4.1 Standardisation of characterisation of parts and systems in synthetic biology

Standardisation in the field of synthetic biology is a major focus of current discussion. The famous "Biobrick" standard developed by the Knight lab has gained most traction in the drive to standardise the construction of standardised genes, promoters, RBSs, etc., in order to permit the true engineering of biology (Shetty*, et al.*, 2008). Standard cloning and expression vectors (Silva-Rocha*, et al.*, 2013) and even standard minimal organisms/chasses (Gibson*, et al.*, 2010) are also under construction.

The standardisation of the characterisation of biological parts and synthetic systems however, is a much more difficult ambition to realise. It has been suggested that a concerted effort to standardise the way synthetic parts, pathways, systems and organisms are characterised would lead to more predictable and effective construction of synthetic pathways and systems. This would allow for true modularity ("plug and play") of biological parts, in much the same way that engineering device standards allow an engineer to evaluate a particular part in the design of predictable complex systems (Arkin, 2008). In synthetic biology however, it is extremely difficult to work out what the "proper characterisation" of a part/system means. Variables such as the plasmids used, the type of growth media used, the temperature the cells were grown at and whether a part has been chromosomally integrated or introduced on expression vectors have to be taken into consideration. More complex systems such as synthetic secretion systems and redox enzyme systems will always require massive tinkering in order to optimise their activity, and this makes standardisation extremely difficult to implement (Arkin, 2008). In addition to these technical obstacles to standardisation, it's very possible that "over-standardisation" could lead to a lack of innovation, where exciting and important serendipitous results/breakthroughs are missed.

Standardisation of characterisation until now has been mostly limited to biological parts that control gene expression/translation, i.e. promoter libraries, RBSs, negative/positive gene expression feedback loops. They typically involve the transcriptional fusion of a promoter/RBS to GFP/RFP/LuxR and in these situations quantitative characterisation of these parts is possible. There are huge limitations and flaws with this type of approach as when these same parts are subsequently placed upstream of another gene, perhaps encoding a structural protein or an enzyme, the codon usage, length and secondary structure of the mRNA transcript is completely different to that of GFP/RFP etc.

Possibly for this reason and others, characterisation of the activity of a more complex system usually relies upon a qualitative yes/or observation of the whole system, rather than true biochemical characterisation of each individual step. Indeed, although *in vitro* reconstruction of a synthetic metabolic pathway is recognised as essential for true meaningful characterisation of a synthetic system (Bayer, 2010), very few synthetic biology studies take this approach. One excellent recent paper outlining this kind of comprehensive approach to the *in vitro* characterisation of each step in a metabolic pathway, was the refactoring of the nitrogen fixation gene cluster performed by the Voigt lab at MIT (Temme*, et al.*, 2012). Building on preliminary work where they constructed huge libraries of promoters and RBSs (characterised using fusions to GFP/RFP etc.), individual refactored (randomised DNA; removes native internal regulation) operons were put under the control of a series of promoters with increasing strength and the activity of the products of each operon measured relative to the WT operons. Through this meticulous method the optimum level of expression for each refactored operon was identified and then operons were combined to construct the final complex synthetic metabolic pathway and the final enzymatic activity measured (Temme*, et al.*, 2012).

Perhaps at this stage of synthetic biology, a more useful standardisation of characterisation would be the comprehensive documentation of both the physical characteristics of constructs (e.g. a detailed file including sequenced constructs with full decoration of features such as promoters, RBSs, ORFs, terminators etc.) and performance characteristics such as expression data (e.g. qPCR or in the near future, RNA sequencing), *in vitro* biochemical characterisation (protein levels, localisation etc.) as well as performance measurements of individual parts (enzymatic activity) and the entire synthetic system. A similar system is proposed by the Endy lab at Berkeley, where the publication of new synthetic systems would require an accompanying datasheet (Canton*, et al.*, 2008).

In the future perhaps a standard growth media, expression plasmid, environmental conditions, buffers and even enzymatic assays can be agreed upon amongst researchers working in a particular field (e.g. secretion, nitrogen fixation, long-chain biofuel fields etc.) and these standards could then be performed as a mandatory yet supplementary standard characterisation.

### 2.4.2 Design and comprehensive testing of a synthetic hydrogenase

In this study a synthetic operon encoding an alien [FeFe]-hydrogenase was constructed and introduced into an *E. coli* chassis. An operon encoding the essential H-cluster maturation proteins was also constructed and its heterologous expression improved. Bioinformatics and

biochemical characterisation of the individual biological parts as well as the overall synthetic system was integral to this project.

A well-characterised promoter ($P_{tat}$), whose activity under a number of relevant physiological conditions has already been measured, was chosen to provide constitutive expression of both constructs (hydrogenase and maturation). A RBS and spacer with strong 16S rRNA binding was used in front of each structural gene, as well as each half of the maturation gene operon, and the successful translation of each hydrogenase subunit predicted. Codon usage of the synthetic hydrogenase operon was optimised for the *E. coli* chassis and the codon usage of the *Sh* maturation genes was assessed for heterologous expression. *In vivo* transcription and translation was tested using radiolabelling experiments and this characterisation data used to improve the expression of the maturation genes in *E. coli*. This data shows the importance of measuring the levels of full length functional proteins and not just rely on the results of transcriptional/translational fusions to fluorescent proteins.

The synthetic hydrogenase enzyme was isolated from its *E. coli* chassis and a number of *in vitro* experiments performed to further characterise it. Basic structural information on the size and molecular weight of the enzyme complex as well as its stability was obtained. Finally, enzymatic activity assays of the purified enzyme were performed to characterise its performance in both catalytic directions ($H_2$ oxidation and $H_2$ production). This detailed biochemical characterisation allows each step to be tested and if necessary corrected so that the activity of the final overall synthetic system can be confidently investigated.

### 2.4.3 Possible reasons behind the lack of NADH-dependent $H_2$ production?

Disappointingly, no NADH-dependent production of $H_2$ was observed under a number of different assay conditions, despite $H_2$ production with the artificial electron donor MV being demonstrated. NADH oxidation when incubated with purified enzyme was also not detected. This clearly does not match the published data on enzyme purified from the native organism (Soboh*, et al.*, 2004).

As the synthetic [FeFe]-hydrogenase, POR and Fd are all extremely sensitive to $O_2$, perhaps these purifications need to be performed in fully anaerobic conditions to determine if this complex redox reaction occurs.

In the original *Tte* hydrogenase paper (Soboh*, et al.*, 2004), 1 mM Ti(III)citrate was added to the NADH-dependent $H_2$ production assay. Ti(III)citrate is a powerful reducing agent ($E°'_{pH7.5}$ = -500 mV), more than powerful enough to replace $Fd^{red}$ as electron donor ($E°'_{pH7.5}$ = -430 mV) in a bifurcating $H_2$-production mechanism similar to that of *Th. maritima* (Schut and Adams, 2009)

(**Error! Reference source not found.**). Perhaps this is why $H_2$ production from NADH was observed in the original assay. Interestingly, it was noted in the original paper that the rate of electron transfer from the diaphorase (NADH-oxidising) subunit to the H-cluster was likely to be the rate-limiting factor (Soboh*, et al.*, 2004). The physiological role of the closely related NADP-reducing hydrogenase from *Desulfovibrio fructosovorans*, HndABCD, was suggested to be $H_2$-dependent NADP reduction, but this has only been demonstrated in crude *D. fructosovorans* cell extracts (containing this hydrogenase and any possible interacting partners, electron carriers etc.) (Malki*, et al.*, 1995; Malki*, et al.*, 1997). When heterologously expressed in *E. coli*, crude cell extracts displayed $H_2$-dependent MV reduction (de Luca*, et al.*, 1998) but no $H_2$-dependent NADP reduction (or $H_2$ production) has been observed from purified enzyme alone has been observed. It is possible this enzyme also requires Fd for NADP reduction in its native organism as has been seen in other [FeFe]-hydrogenases (Huang*, et al.*, 2012; Rydzak*, et al.*, 2012; Schuchmann and Muller, 2012).

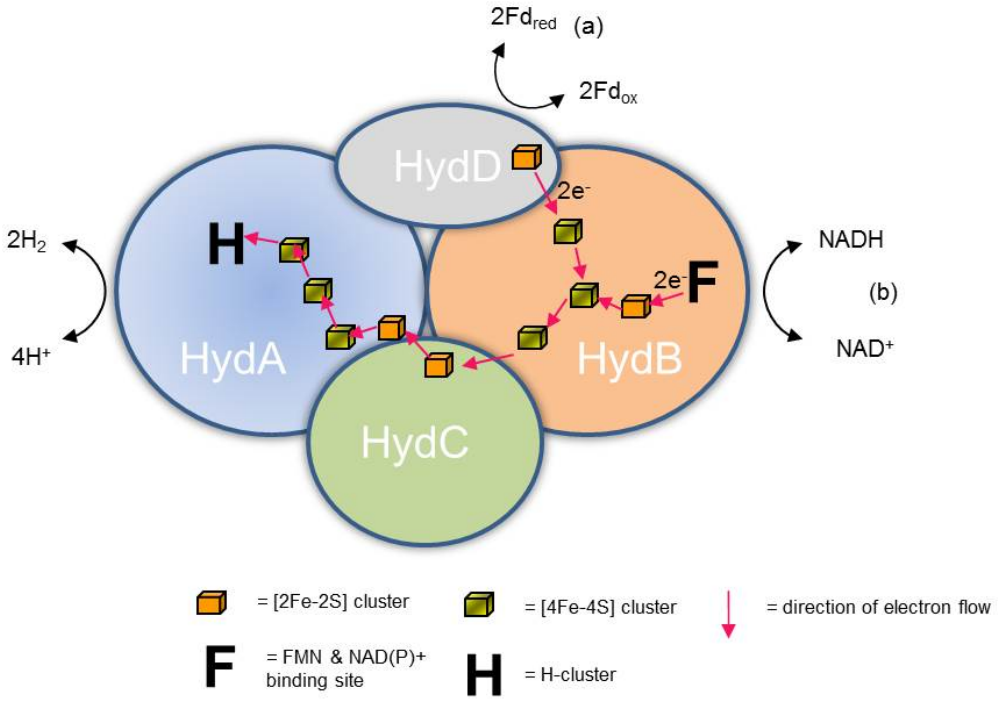


**Figure 2.14 Possible bifurcating mechanism of *Ca tengcongensis* [FeFe]-hydrogenase: HydABCD.** The reduced ferredoxin ($Fd_{red}$) donates electrons in addition to NADH in order to drive the energetically unfavourable production of $H_2$ from NADH. These electrons from $Fd_{red}$ may enter the hydrogenase complex via HydC or HydD (shown here as HydD)

Flavin mononucleotide (FMN) (and not FAD) was identified as the type of flavin cofactor of the *Ca.tengcongensis* NADH-dependent [FeFe]-hydrogenase (Soboh*, et al.*, 2004). Here, FMN (2 mM) was added to lysis buffer, during purification, and to the buffers used during $H_2$ production assays with NADH as the sole electron donor, and during NADH oxidation assays. If FMN is indeed the correct flavin cofactor, then this is unlikely to be a possible reason for the lack of NADH-dependent $H_2$ production.

In this Chapter, all assays were performed at ambient temperature (25 – 30 °C). *T. tengcongensis* is a thermophilic bacterium found at 70 °C. Therefore it is also possible that the lack of NADH-dependent $H_2$ production observed in this chapter is a result of the lower temperatures used during all hydrogenase assays. Thermophilic enzymes are stable at higher temperatures as a result of increased rigidity and stability in the protein backbone. This increased rigidity has been shown to result from extra structurally-stabilising interactions compared to mesophilic homologues, including disulphide bonds (Beeby*, et al.*, 2005) and salt bridges (Lam*, et al.*, 2011), as well as the replacement of certain amino acids with larger residues (Tomazic and Klibanov, 1988). This increased rigidity and stability is inversely proportional to activity of these enzymes at lower temperatures, where increased flexibility allows for greater catalytic activity (Beadle and Shoichet, 2002). In this project, no melting curve could be obtained when standard thermofluor experiments were performed using the purified synthetic enzyme (data not shown), indicating stability of this enzyme at high temperatures.

Interestingly, a huge increase (40 times) in *in vitro* hydrogenase activity was observed when the enzyme was purified from sonicated cell extracts, rather than when BPER was used to lyse the cells.

The SEC-MALLS analysis of the purified enzyme complex indicated that the enzyme purified as a monodisperse dimer of the four subunits. This could be investigated further using analytical ultracentrifugation (AUC).

### 2.4.4 Electrochemical results of purified enzyme

In collaboration with Alison Parkin (University of York) electrochemical experiments were also performed to allow further *in vitro* characterisation of this anaerobically-purified enzyme. Protein-film voltammetry (PFV) is a powerful tool in the study of redox enzymes. Protein molecules are immobilised on a graphite electrode to create a film, varying potentials are applied and any resulting current is measured. Variables such as temperature, pH and substrate concentrations can be sensitively controlled throughout these experiments.

Hydrogenase activity assayed through protein-film voltammetry is substrate independent and [FeFe]-hydrogenases are thought to act bidirectionally (i.e. can carry out both $H_2$ oxidation and evolution).

Initial protein-film voltammetry experiments performed with the purified synthetic *Ca. tengcongensis* [FeFe]-hydrogenase were unsuccessful, probably due to the incorrect orientation on the graphite electrode to allow electron transfer. In an attempt to improve its orientation on the electrode and allow easier access to an FeS cluster for electron transfer, a Δ*hydD* version of the pUNI-Tte-$Hyd_{hisC}$ was constructed and this enzyme was purified. This enzyme displayed $H_2$-dependent BV reduction activity of 561 nmol $H_2$ oxidised $min^{-1}$ $mg^{-1}$. Electrochemical characterisation of this enzyme was possible, but hydrogenase activity was still low compared to other hydrogenases from other organisms described previously.

In protein-film electrochemistry (PFE) positive current arising from enzymatic processes indicates oxidation activity, while negative current is proportional to the rate of electrochemical reduction. When an electrode is modified with a layer/film of adsorbed *Ca. tengcongensis* enzyme, $H_2$ oxidation (100% $H_2$) is observed but no $H_2$ production (100% Ar) (Figure 2.15A). The high potential $H_2$-oxidation activity of the enzyme titrates with pH (Figure 2.15B). As observed with other [FeFe]-hydrogenases, in more alkaline buffer solutions there is a greater proportion of current-loss at potentials more positive than 0 V. This shows that increasing the concentration of hydroxide ions causes a greater amount of anaerobic oxidative-inactivation (formation of the $H_{ox}^{inact}$ state). Lowering the scan rate from 1 mV/s to 3 mV/s allowed the easier observation of the reversible inactivation-reactivation process which occurs at high potential (Figure 2.16A), because the inactivation occurs on a timescale which is too slow to be fully probed at rapid rates. Since *Ca. tengcongensis* is a thermophilic bacterium, the impact of temperature on enzymatic activity was also tested. An increase in $H_2$ oxidation was observed at the higher temperature of 80 °C (Figure 2.16B).

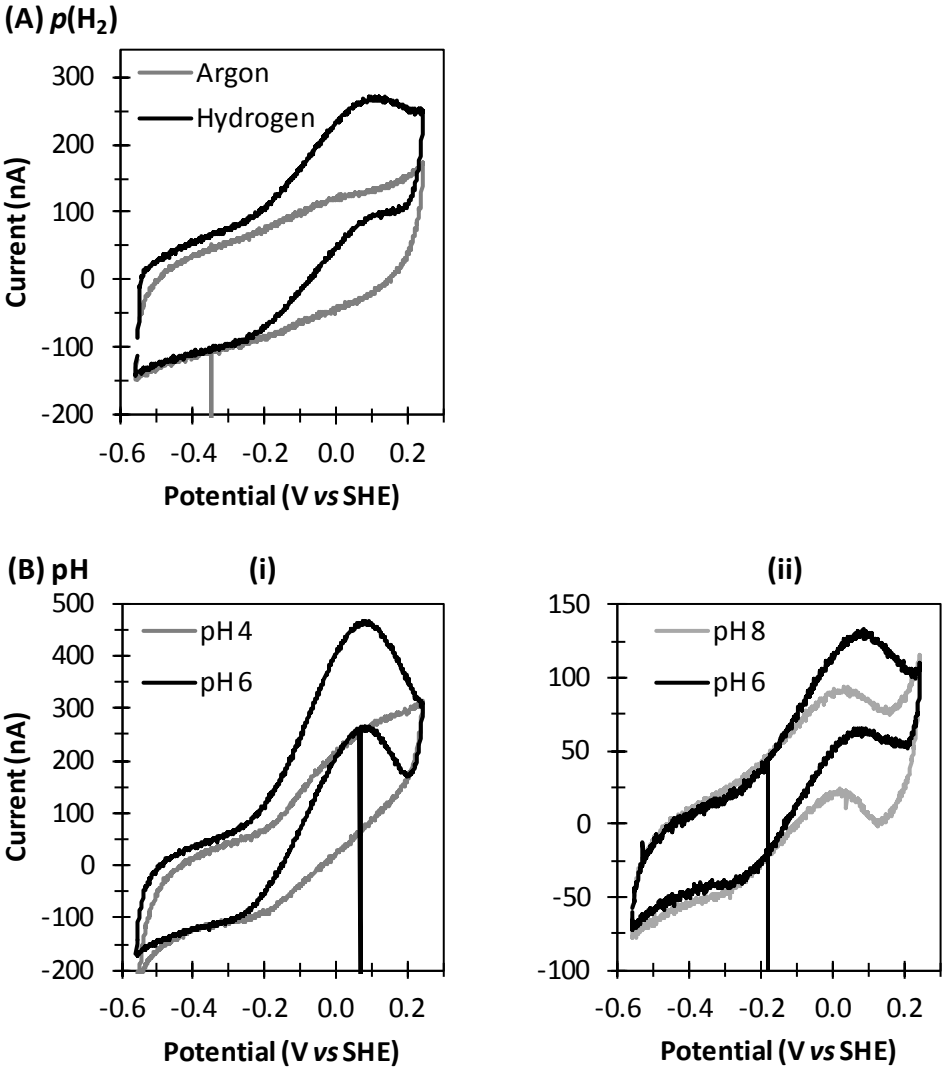


**Figure 2.15 Basic electrochemical characterisation of the catalytic activity of purified ΔHydD enzyme. (A) The impact of hydrogen partial pressure on enzymatic activity:** a 3 mV/s cyclic voltammogram was recorded at pH 6 under a gas atmosphere of Ar, as shown in grey. Hydrogen was then flowed through the electrochemical cell and after an equilibration time of 600 s the black scan was measured at the same scan rate. **(B) The impact of pH on enzymatic activity: (i)** a 3 mV/s cyclic voltammogram was recorded at pH 6 under a gas atmosphere of 100% $H_2$, as shown in black. The buffer solution was then exchanged for pH 4 solution and the grey scan was measured at the same scan rate. **(ii)** a comparison of 1 mV/s voltammograms measured at pH 8 and pH 6. Experimental conditions common to all plots: temperature 60 °C and electrode rotation rate 1000 rpm

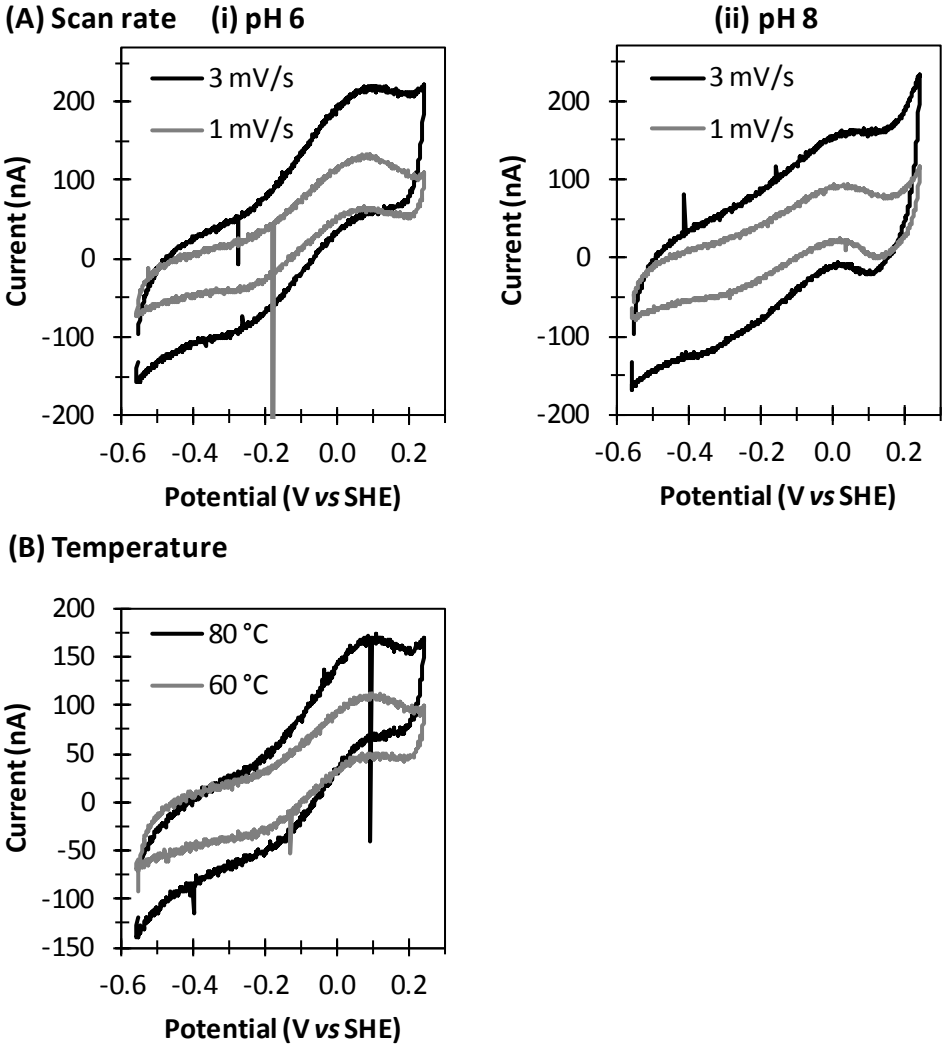


**Figure 2.16 (A) The effect of decreasing the scan rate from 3 to 1 mV/s on the voltammogram shape produced by an adsorbed film of ΔHydD enzyme at pH 6 and pH 8.** The same enzyme film was used for experiments measured at the same pH. Other experimental conditions: temperature 60 °C, gas atmosphere 100% $H_2$ and electrode rotation rate 1000 rpm. **(B) Two 3 $mVs^{-1}$ scans of a ΔHydD enzyme "film" to compare the enzymatic activity at 60 and 80 °C under an atmosphere of 100% $H_2$.** The graphite electrode modified with enzyme remained sealed in the electrochemical cell while a measurement was first made at 60 °C, the potentiostat was then paused at -0.56 V while the temperature of the external water circulator was raised to 80 °C and then the scan was then re-commenced. Other conditions: pH 6, electrode rotation rate of 1000 rpm

### 2.4.5 Future improvements to the synthetic [FeFe]-hydrogenase expression and maturation system

#### 2.4.5.1 Genetic manipulation of native *Sh. oneidensis* maturation gene operon

The correct expression and therefore maturation activity of the cloned *Sh. oneidensis* accessory genes required significant genetic manipulation (Figure 2.6). The hypothesis was that the *Sh. oneidensis* RBS was ineffective at initiating translation in *E. coli* and therefore an optimised Shine-Dalgano sequence and linker was introduced upstream of the *hydE* gene, which rescued translation in *E. coli*. It is also possible that the re-cloning removed some internal transcriptional or translational regulation. The full length *Sh. oneidensis* accessory operon *SO_3923 – SO_3926* was analysed using the Softberry™ BPROM software for putative promoters and ten predicted internal promoters were identified, including well studied promoters such as *lexA*, *fur*, and *rpoD16* & *18* promoters. Six of the ten predicted promoters were had linear discriminant function (LDF) scores that were 10 times over the minimum promoter threshold, indicating the strong likelihood of transcription initiation. Separating the operon into two halves, with the addition of a T7 transcriptional terminator between each half, likely stopped the read through of many of these short transcripts. Alternatively, multiple RBSs or indeed multiple translational start sites might account for the numerous truncated proteins observed in the original radiolabelling experiment (Figure 2.4). Using the EXPASY Translate Tool, over 30 possible ORFs can be identified in the 5'-3' direction alone. The complete removal of spurious internal transcription or translation initiation sites would require the full refactoring (randomisation of codon usage) of the four genes, as performed in the reconstruction of the nitrogen fixation pathway of *Klebsiella* (Temme*, et al.*, 2012).

The function of HydX is still unknown, although it does share 35% sequence identity and 54% sequence similarity with conserved proteins of unknown function in *Desulfovibrio vulgaris* (and other species of this genus), which also encodes an [FeFe]-hydrogenase. HydX shares 30% sequence identity and 47% sequence similarity with a chloroplast phytoene synthase from *Sorghum bicolor*. These are transferase enzymes, involved in the biosynthesis of carotenoids. Perhaps HydX is involved in an additional, previously unreported modification of the H-cluster and/or [FeFe]-hydrogenase complex in *Sh. oneidensis*. In Figure 2.6, a band corresponding to approximately 23 kDa can be observed in the pSU-Sh-GX-EF lane. This band might correspond to HydX, however as *in vitro* hydrogenase activity was observed, no further investigation was deemed necessary.

#### 2.4.5.2 A direct [FeFe]-maturation activity assay

Successful improvement in the expression/translation or even direction evolution of the [FeFe] maturation genes/enzymes can be assessed indirectly by assaying *in vivo*/*in vitro* hydrogenase activity, as carried out in this chapter and used in other previous studies (Brazzolotto*, et al.*, 2006; Nicolet*, et al.*, 2008; Shepard*, et al.*, 2010b). However it would be extremely useful to develop a quantitative assay to determine maturation activity directly. This would allow levels of maturation activity to be optimised precisely, depending on the amount of [FeFe]-hydrogenase protein produced in the cell. It might also allow further elucidation of the fundamental mechanism of these radical SAM and GTPase enzymes in active site construction and insertion. Electron paramagnetic resonance (EPR) spectroscopy can be used to identify the assembly of the H-cluster precursor on HydF (Shepard*, et al.*, 2010b), however this is neither trivial nor high-throughput enough to use as a practical maturation assay. It is now possible however, to perform high-throughput Fourier-transform infrared (FTIR) spectroscopy on numerous samples using either microfluidics (Chan*, et al.*, 2009) or plate-based spectrometers (Thermo Scientific™ Micro Well Plate Reader and Nicolet™ 6700 FT-IR spectrometer). FTIR spectroscopic analysis of HydF with a fully formed H-cluster precursor, shows four distinct bands, two of which correspond to the CO ligand and the other two corresponding to the $CN^-$ ligand (Shepard*, et al.*, 2010b). Absorbance at any of these wavenumbers could be monitored in a cell-free maturation assay similar to that described previously (Boyer*, et al.*, 2008), showing real-time ligand attachment on the 2Fe scaffold and this could then be used as a functional H-cluster maturation assay.

#### 2.4.5.3 Optimising the relative amounts of each hydrogenase subunit and essential maturation proteins for maximal hydrogenase activity

Using either a novel high-throughput [FeFe]-maturation activity assay or indeed by carefully monitoring hydrogenase activity in response to levels of HydEFG protein, the levels of *syn*HydABCD and *Sh*HydEFG, as well as times of induction of each gene could be tuned to allow for maximal hydrogenase activity as well as avoiding issues such as protein toxicity. This could be accomplished through a number of means. Alternative promoters with a range of strengths of induction and physiological requirements for induction of gene expression could be used to control gene expression of each component. Some preliminary work was started towards this end with the replacement of the constitutive $P_{tat}$ promoter on the synthetic [FeFe]-hydrogenase, with one of: $P_{hybO}$ (promoter region of the *E. coli* hydrogenase-2 operon; upregulated under anaerobic conditions; aerobic repression reduced in Δ*iscR* strains – 2.6 fold increase in expression under aerobic conditions); $P_{fadH}$ (promoter region of the *E. coli fadH*

gene; massively upregulated in Δ*iscR* strains under anaerobic conditions – 31 fold increase) (Giel*, et al.*, 2006); and $P_{adhE}$ (promoter region of the *E. coli* alcohol dehydrogenase gene; upregulated under anaerobic conditions – 10 fold increase relative to aerobic conditions and unaffected by deletion of *iscR*) (Leonardo*, et al.*, 1993). A similar approach could also be taken with the *Sh. oneidensis* maturation gene operon. Unfortunately systematic testing of these constructs was not possible due to time constraints.

Alongside testing a variety of promoters, the RBSs before each hydrogenase subunit gene could be changed to normalise the protein levels of each subunit in the cell. This could be carried out using the RBS CALCULATOR (as discussed in 2.3.1), which takes the very important upstream and mRNA transcript secondary structure into consideration. Alternatively, the translation initiation rates for each gene in the synthetic hydrogenase and *Sh* accessory operons could be increased or decreased in order to test for the optimum amount of each protein for hydrogenase activity (and cell survival). In particular, the ratio of HydEFG:HydABCD could be altered to ensure 100% maturation of all expressed hydrogenase.

# 3. Integration of a synthetic [FeFe]-hydrogenase into *E. coli* metabolism

## 3.1 Introduction

Under fermentative conditions, where respiratory electron transport is at a minimum, *E. coli* faces a constant struggle to regenerate $NAD^+$ for glycolysis to continue. The main mechanism for recycling of $NAD^+$ from NADH is through the reduction of acetyl-CoA to ethanol *via* acetylaldehyde (Figure 3.1). In *E. coli* this reaction is catalysed by one protein, alcohol dehydrogenase (AdhE). The other possible routes for the consumption of NADH generated during glycolysis are through the production of lactate and malate (as part of reductive branch of TCA cycle that leads to succinate production); however this are generally confined to late stationary phase and is therefore secondary to ethanol production.

The AdhE protein is essential for *E. coli* growth during fermentation in defined media (Lorowitz and Clark, 1982; Cunningham and Clark, 1986; Gupta and Clark, 1989) and successfully ensures that the cell maintains the correct ratio of $NAD^+$ to NADH (de Graef*, et al.*, 1999). The ratio of $NADH/NAD^+$ is highest during glucose fermentation (~0.75), in comparison with anaerobic respiratory conditions (~0.6) or during aerobic growth (~0.08) (de Graef*, et al.*, 1999).

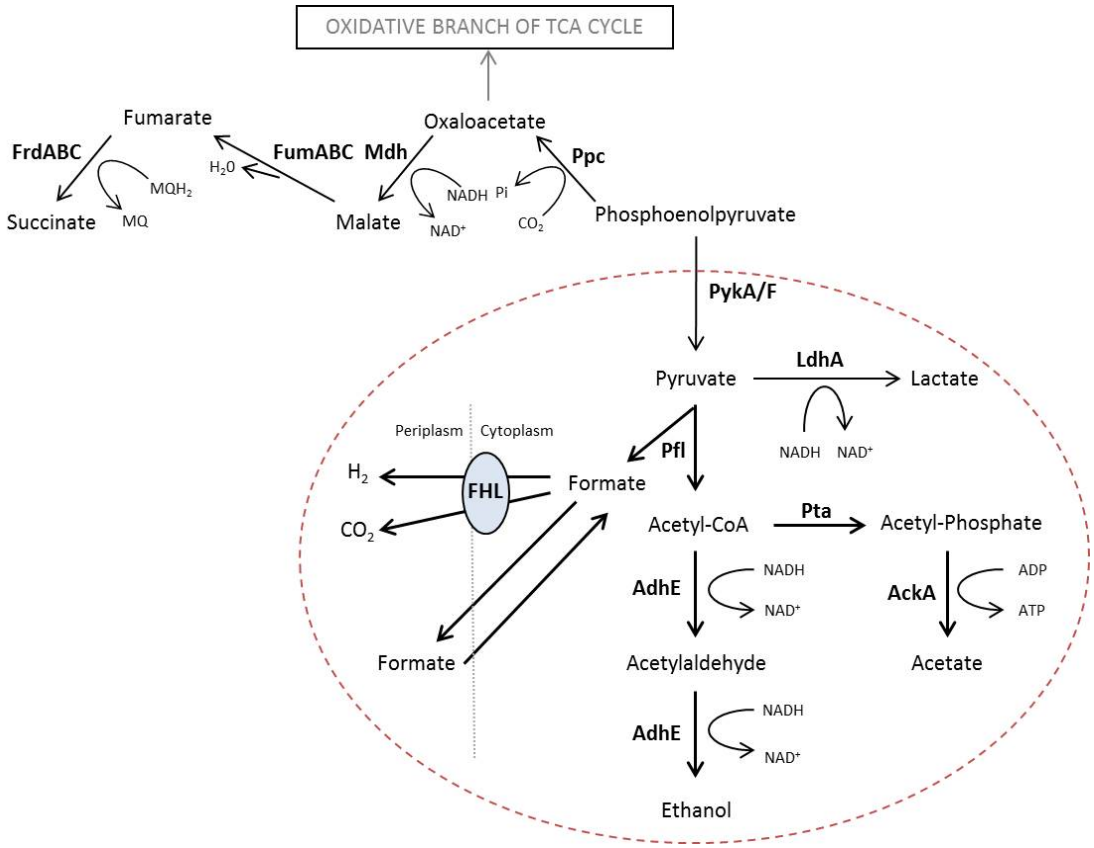


**Figure 3.1 The reductive pathways of mixed-acid fermentation in *E. coli*.** Enzyme abbreviations: PykA/F: pyruvate kinase; LdhA: lactate dehydrogenase; Pta: phosphotransacetylase; AdhE: alcohol dehydrogenase; Pfl: pyruvate formate lyase; Ppc: phosphoenolpyruvate carboxylase; Mdh: malate dehydrogenase; FumABC: fumarase; and FrdABC: fumarate reductase. The oxidative pathway of the TCA cycle halting at α-ketoglutarate is not shown for simplicity

### 3.1.1 A synthetic NADH-dependent [FeFe]-hydrogenase pathway in *E. coli*

Hydrogen production in *E. coli* is not directly coupled to the regeneration of $NAD^+$, as the majority of $H_2$ is generated by the FHL complex. However, a small number of NADH-dependent hydrogenases have been described in other microbes. *Thermoanaerobacter tengcongensis* (recently reclassified as *Caldanaerobacter tengcongensis*) is a thermophilic Gram-negative bacterium isolated from a hot spring in China (Xue*, et al.*, 2001). *Ca. tengcongensis* expresses two hydrogenase activities, one of which has been characterised as a soluble [FeFe]-hydrogenase that produces $H_2$ with NADH as the sole electron donor (Soboh*, et al.*, 2004). In this work, a synthetic operon encoding all structural subunits of this *Ca. tengcongensis* hydrogenase has been constructed, expressed and characterised in *E. coli* (Chapter 2). When co-expressed with the essential H-cluster maturation proteins from *Sh. oneidensis*, (encoded on the pSUtat-Sh-GX-EF vector prepared in this work) the isolated enzyme displays $H_2$-oxidation and $H_2$-production capabilities when assayed *in vitro*. The *Ca. tengcongensis* enzyme is attractive because, as an [FeFe] hydrogenase, it should be biased towards $H_2$ production, and its diaphorase activity could be harnessed in an *E. coli* chassis. Indeed, it is tempting to speculate that coupling a hydrogenase to the essential recycling of NADH during fermentation may boost $H_2$ production.

## 3.2 **Aims**

This Chapter aims to construct a synthetic NADH-dependent $H_2$-production pathway in an engineered *E. coli* chassis. A strain will be engineered that will express a synthetic, active [NADH]-dependent [FeFe]-hydrogenase and metabolic engineering will be performed in order to remove competing $NAD^+$ regeneration pathways. The engineered strains will be characterised for $H_2$ production and changes in metabolic flux during mixed-acid fermentation.

## 3.3 Results

### 3.3.1 Construction of a synthetic [NADH]-dependent $H_2$-production pathway in *E. coli*

A synthetic operon encoding the NADH-dependent [FeFe]-hydrogenase from *Ca. tengcongensis* was integrated onto the chromosome of the *E. coli* strain FTD147 (MC4100 Δ*hyaB,* Δ*hybC,* Δ*hycE*) (Redwood*, et al.*, 2008) in place of *adhE* using the pMAK705 homologous recombination protocol (Hamilton*, et al.*, 1989) (Figure 3.2). This precise replacement of the *adhE* gene with the synthetic [FeFe]-hydrogenase was confirmed using sequencing. The synthetic operon retains the constitutive *tat* promoter, but should also be driven by the native *adhE* promoter itself. The new strain was termed FTD147h3 *E. coli* strains used in this section, including those used as controls, are listed in Table 3.1.

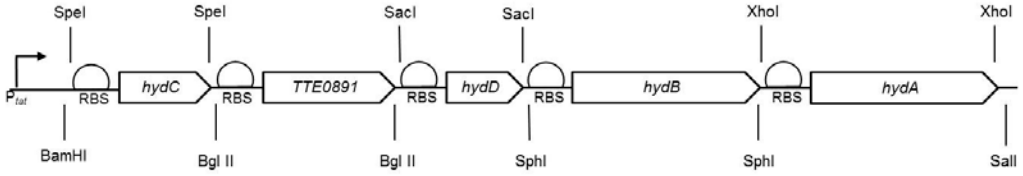


**Figure 3.2 A synthetic operon encoding HydC-A of the *Ca. tengcongensis* NADH-dependent [FeFe]-hydrogenase.** This synthetic operon was integrated onto the chromosome of *E. coli* strain FTD147 in place of *adhE*, which encodes alcohol dehydrogenase. 1000 bp of flanking sequence to *adhE* was amplified by PCR and used to target the insertion of this synthetic operon by homologous recombination using the pMAK705 protocol.

| Strain Name | Genotype | Reference |
|---|---|---|
| MG1655 | wild-type *E. coli* strain<br>F-, λ-, *rph*-1, *ilvG*, *rfb*-50 | (Blattner*, et al.*, 1997) |
| MC4100 | F- [*ara*D139]B/r Δ(*arg*F-lac)169 &lambda- e14- *flh*D5301 Δ(*fruK-yeiR*)725 (*fru*A25)‡ *rel*A1 *rps*L150(*str*R) *rbs*R22 Δ(*fim*B-*fim*E)632(::IS1) *deo*C1 | (Casadaban, 1976) |
| FTD147 | MC4100 Δ*hyaB,* Δ*hybC,* Δ*hycE* | (Redwood*, et al.*, 2008) |
| Teatotal1 | FTD147 Δ*adhE* | This work |
| FTD147h3 | FTD147 Δ*adhE*::*TtehydC-A* | This work |

**Table 3.1 Strains used in the characterisation of a synthetic NADH:$H_2$ production pathway in *E. coli***

### 3.3.2 Characterisation of FTD147h3: growth in liquid media

The ability of FTD147h3 to grow fermentatively in both rich and minimal media was tested and compared with MG1655 and FTD147. Cells were plated freshly from frozen stocks stored at -80 °C and single colonies used to inoculate 5 ml aerobic overnight cultures. These aerobic overnight cultures were used to inoculate (1:1000) 16 ml test tubes filled with L.B. + 0.4% w/v glucose (Figure 3.3A) or M9 + 0.4% w/v glucose (Figure 3.3B). These were sealed to induce anaerobiosis and incubated at 37 °C without shaking. Samples were taken 3, 6, 9, 11, 13, 17, 21 and 38 hours after inoculation and optical density at 600 nm measured (Figure 3.3). In minimal M9 media supplemented with glucose FTD147h3 did not grow anaerobically, whereas MG1655 grew to an $OD_{600}$ of 1.0 after 17 h and then entered stationary phase (Figure 3.3B). FTD147h3 was capable of anaerobic growth in rich media supplemented with glucose (Figure 3.3A), although the final $OD_{600}$ was approximately half (0.57) that of MG1655 (1.07) and FTD147 (0.98) over an identical time course.

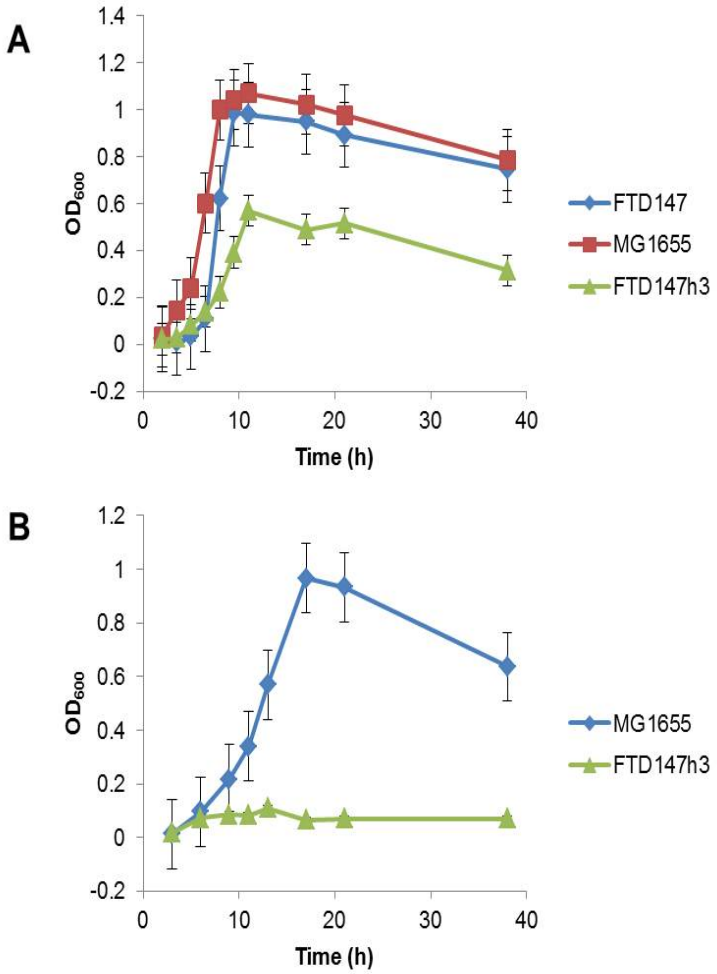


**Figure 3.3 FTD147h3 is capable of growing in rich liquid media supplemented with glucose under fermentative conditions but not in minimal liquid media.** Test tubes filled with 16 ml (A) L.B. + 0.4% w/v glucose or (B) M9 + 0.4% w/v glucose were inoculated 1:1000 with FTD147, FTD147h3 and MG1655 and cultures grown anaerobically. The optical density ($OD_{600}$) of these cultures was recorded at various time points over 38 h. It was decided not to convert $OD_{600}$ to $\log_{10}$ values, to better highlight differences in final cell densities.

### 3.3.3 Characterisation of FTD147h3: organic-acid production

The organic-acid acid content of the extracellular media upon completion of growth was analysed by high-performance liquid chromatography (HPLC) coupled with UV detection. MG1655, FTD147 and FTD147h3 anaerobic cultures of 16 ml LB media supplemented with 0.4 % (w/v) glucose were grown for 72 h (to ensure sufficient FTD147h3 biomass). Cells were harvested by centrifugation and the culture supernatant was passed through a 0.2 μm filter to remove any remaining cells or debris. The spent fermentation broth was analysed with an Aminex HPX-87H organic-acid column at 0.7 ml $min^{-1}$ and 55 °C. Organic acids detected by UV absorption at 210 nm. A standard curve of organic acid standards was prepared ($R^2$: 99.90%) and used to identify and quantify concentrations of pyruvate, succinate, lactate, formate, fumarate and acetate. Sample concentrations were normalised by cell pellet wet weight. The concentrations of compounds in virgin media (LB + 0.4% (w/v) glucose) were subtracted to reveal changes in each metabolite (Figure 3.4).

The extracellular concentration of pyruvate did not increase greatly in any of the three samples tested (Figure 3.4). Succinate concentrations increased slightly in the FTD147h3 sample compared to both MG1655 and FTD147 samples (Figure 3.4). The concentration of lactate also increased relative to the MG1655 sample (Figure 3.4). Formate was not detected with the MG1655 samples (Figure 3.4), presumably as all of the formate is converted to $H_2$ and $CO_2$ following a 72 hour incubation period. No extracellular fumarate was detected in any of the samples (Figure 3.4), however the concentration of acetate increased significantly in both the FTD147 (43 mM; P = 0.0002) and FTD147h3 (58 mM; P = 0.0012).

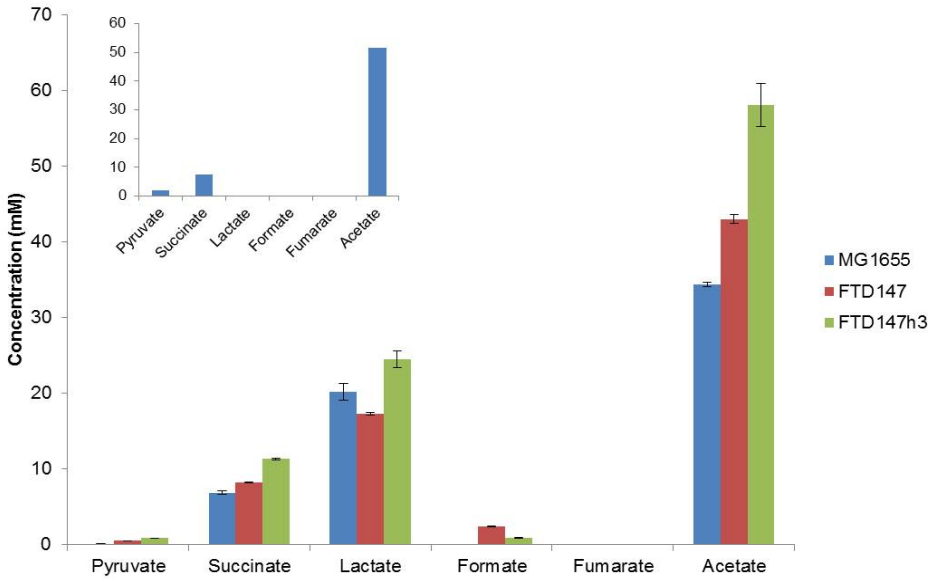


**Figure 3.4 Organic-acid content of MG1655, FTD147 and FTD147h3 fermentation broths.** Test tubes filled with 16 ml L.B. + 0.4% (w/v) glucose were inoculated 1:1000 with MG1655, FTD147 and FTD147h3 and cultures grown anaerobically. Cells were harvested by centrifugation at 4000 rpm before the culture supernatant was passed through a 0.2 µm filter and analysed by HPLC. For HPLC analysis, 5 µl of fermentation broth was separated at 0.7 ml $min^{-1}$ and 55 °C using a Dionex UltiMate 3000 HPLC system, fitted with an Aminex HPX-87H organic acid column and absorbance monitored at 210 nm. Organic acid standards were used all with $R^2$ values greater than 99.90%. Bars represent difference in metabolite concentration between media before and after fermentation. Error bars represent standard error of three biological replicates. The inset graph represents concentration of each metabolite in media before inoculation.

### 3.3.4 Expression of essential maturation proteins in FTD147h3 does not confer a growth advantage during fermentative conditions

Next, FTD147h3 cells were transformed with plasmid pSUtat-Sh-GX-EF (Acc) expressing the H-cluster maturation proteins and was tested for improved growth in both rich and minimal liquid media. No difference was observed between FTD147h3 and FTD147h3 expressing pSUtat-Sh-GX-EF (Acc) in anaerobic LB cultures supplemented with glucose (Figure 3.5A & B). A similar pattern of growth was obtained for TeaTotal1 (FTD147 Δ*adhE*) (Figure 3.5B). No recovery of growth of FTD147h3 expressing pSUtat-Sh-GX-EF was observed in minimal M9 media supplemented with glucose (Figure 3.5C).

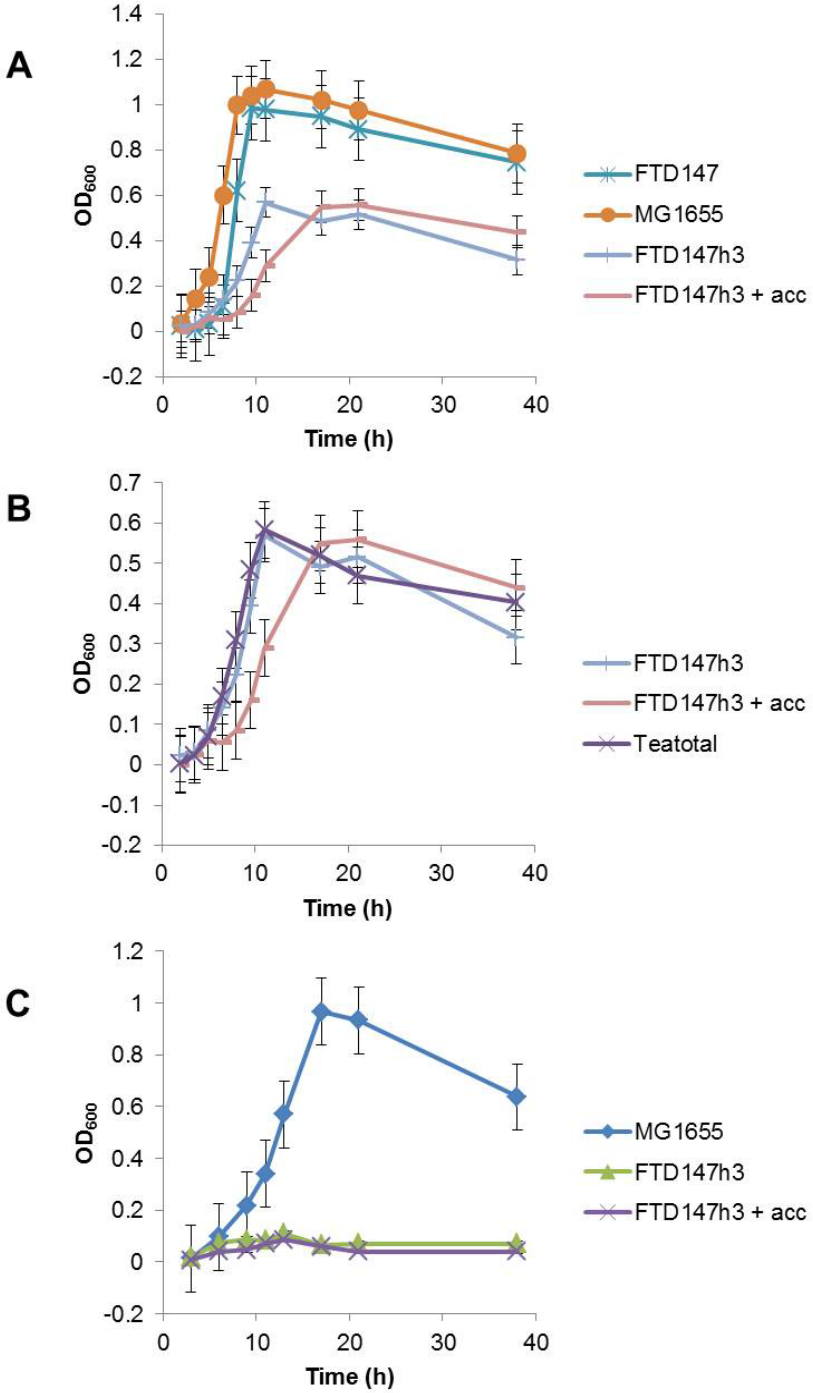


**Figure 3.5 A synthetic *Ca. tengcongensis* hydrogenase provides no growth advantage under fermentative conditions.** Test tubes filled with 16 ml (A & B) L.B. + 0.4% w/v glucose or (C) M9 + 0.4% w/v glucose were inoculated 1:1000 with FTD147, FTD147h3, TeaTotal1 and MG1655, grown anaerobically and the optical density ($OD_{600}$) of these cultures was recorded at various time points over 38 h. It was decided not to convert $OD_{600}$ to $\log_{10}$ values, to better highlight differences in final cell concentrations.

### 3.3.5 Characterisation of FTD147h3: hydrogenase activity when HydEFG are expressed

The next stage in the functional characterisation of FTD147h3 was to assay its ability to either oxidise or evolve $H_2$ with an artificial electron acceptor or donor, when transformed with the optimised H-cluster-accessory plasmid, pSUtat-Sh-GX-EF. Benzyl viologen (BV) was chosen as the electron acceptor as its standard reduction potential ($E^{0'}$ -348 mV) is above that of the $H^+/½\ H_2$ redox couple ($E^{0'}$ -420 mV) and methyl viologen (MV) as the electron donor ($E^{0'}$ -443 mV) as it is a stronger reducing agent. For $H_2$-dependent BV reduction, one activity unit (U) is defined as 1 µmol BV reduced $min^{-1}$ $mg^{-1}$ cells. For MV-dependent $H_2$ production, one unit (U) is defined as 1 µmol $H_2$ evolved $min^{-1}$ $mg^{-1}$ cells.

FTD147h3 was transformed with pSUtat-Sh-GX-EF and this was used to inoculate 500 ml anaerobic LB cultures supplemented with 0.4% (w/v) glucose, 2 mM cysteine, 2 mM ferric ammonium citrate and chloramphenicol. The cultures were incubated at 37 °C for ~16 hours before the cells were harvested, washed, resuspended in anaerobic buffer and lysed by sonication. Cell pellets and crude lysates were flushed with Ar throughout in an attempt to maintain anaerobic conditions. The FTD147h3 + Accessory genes (Acc) crude cell lysate catalysed the reduction of BV with $H_2$ as the electron donor, with a specific activity of 9 U, when assayed in $H_2$-saturated, Tricine pH 8.0 buffer (Figure 3.6B). Assays were repeated in $N_2$-saturated buffer to confirm $H_2$-specific BV reduction. Intact whole cells (in both $H_2$- and $N_2$-saturated buffer) were also used as negative controls, as oxidised BV is believed to be impermeable to the cytoplasmic membrane and therefore should not react with the cytoplasmically-localised [FeFe]-hydrogenase.

The FTD147h3 + Accessory genes (Acc) crude cell lysate demonstrated $H_2$-evolution activity with reduced MV as the artificial electron donor (6 U) (Figure 3.6A). Only a trace of $H_2$-production activity was observed with cell lysates lacking the accessory plasmid, confirming the hydrogenase activity was specific to the chromosomally-encoded [FeFe]-hydrogenase. No NADH-dependent production of $H_2$ was observed from the FTD147h3 + Accessory genes (Acc) crude cell lysate under a number of different assay conditions.

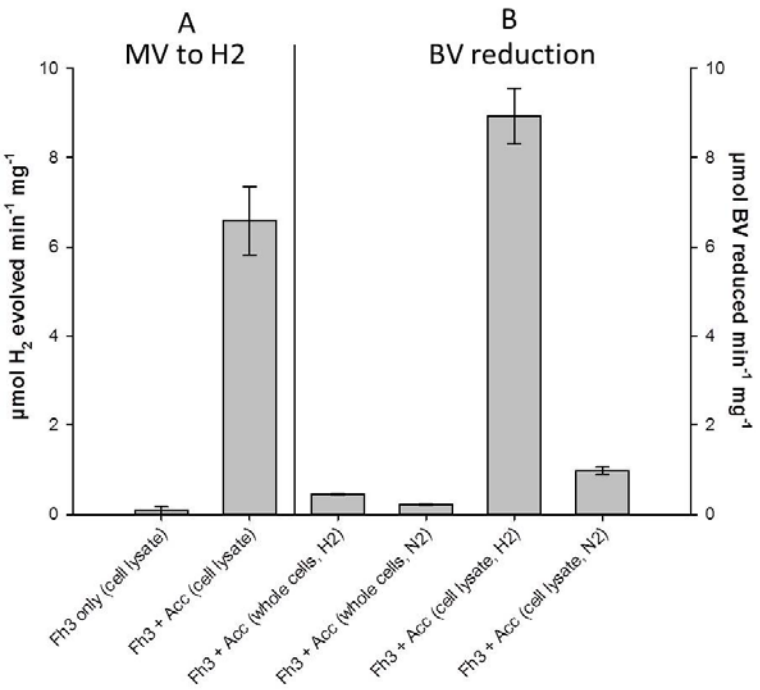


**Figure 3.6 FTD147h3 + Acc displays *in vitro* $H_2$ production and $H_2$ oxidation.** FTD147h3 cells were transformed with pSUtat-Sh-GX-EF, which encodes HydEFG from *Sh. oneidensis*. Transformants were used to inoculate a 5 ml aerobic overnight culture, which was then used to inoculate 500 ml anaerobic L.B. cultures supplemented with 0.4% (w/v) glucose, 2 mM cysteine, 2 mM ferric ammonium citrate and chloramphenicol. The cultures were incubated at 37 °C for ~16 hours, pelleted by centrifugation, washed and resuspended in anaerobic buffer. Cell pellets were flushed with Ar throughout in an attempt to maintain anaerobic conditions, then lysed by sonication and centrifuged to remove cellular debris, resulting in crude cell lysate, which was assayed for hydrogenase activity. **A.** Methyl viologen (MV)-dependent $H_2$ production was measured in a modified Clark-type electrode. 100 mM sodium phosphate buffer pH 6.0 was added to the reaction chamber, to which 12.5 mM MV and 650 µM sodium dithionite was added. The reaction was initiated by the addition of 500 µg of cell lysate. **B.** Benzyl viologen (BV) reduction ($H_2$ oxidation) was monitored at 578 nm in a UV-vis spectrometer. 1 ml quartz cuvettes were filled with $H_2$-saturated buffer (50 mM Tricine pH 8.0) and 13 mM BV. This was titrated with sodium dithionite to an absorbance of 0.4 - 0.7 and the reaction started by the addition of 1 mg of cell lysate. $N_2$-saturation buffer and whole cells were used as controls. Error bars represent the standard error of three independent experiments.

### 3.3.6 Characterisation of FTD147h3 expressing HydEFG: organic-acid production

The organic acids content of the spent culture media from FTD147h3 transformed with pSUtat-Sh-GX-EF (Acc) was measured using HPLC. These samples were compared to samples from MG1655 cultures transformed with pSUtat-Sh-GX-EF (Acc) and pUNI-Tte-Hyd (Tte) or empty control vectors. A standard curve of organic acid standards was prepared ($R^2$: 99.90%) and used to identify and quantify concentrations of pyruvate, succinate, lactate, formate, fumarate and acetate. Sample concentrations were normalised by cell weight, and the concentration of metabolites in starting media (LB + 0.4% (w/v) glucose) was subtracted to reveal changes in each metabolite (Figure 3.7). It is worth noting that the concentration of succinate in the starting L.B. media used in this experiment was almost twice as much as in the media used in the previous organic acid analysis (Section 3.3.3).

The concentrations of succinate, lactate and acetate in the FTD14h3 + pSUtat-Sh-GX-EF samples was higher than either control sample. The MG1655 samples producing the H-cluster maturation proteins and the synthetic hydrogenase showed increased amounts of acetate relative to the control samples, but no other differences could be observed (Figure 3.7).

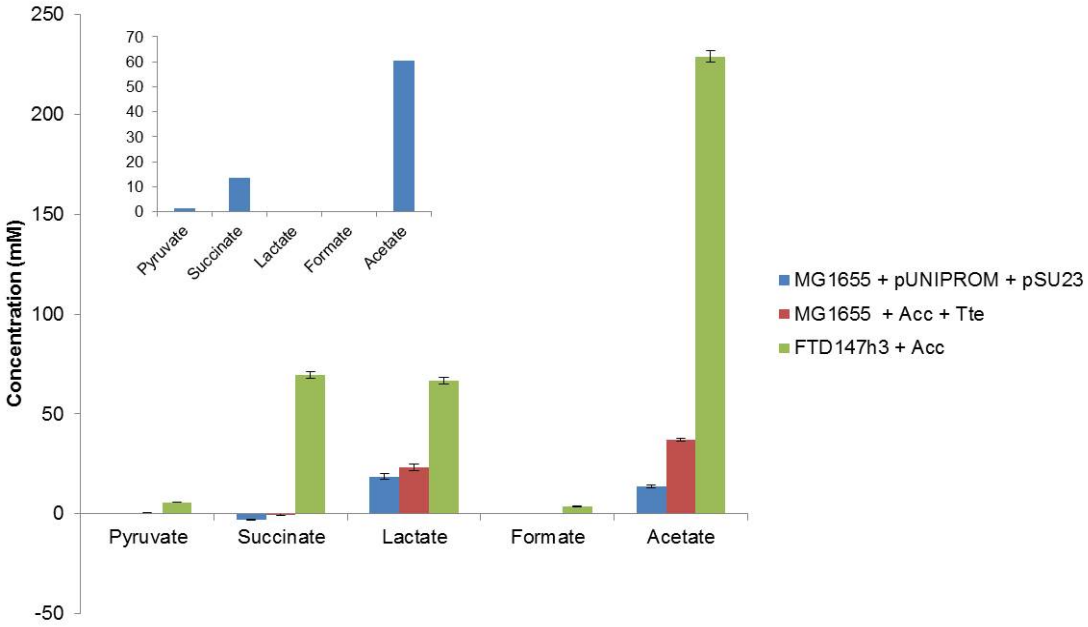


**Figure 3.7 Organic-acid analysis of FTD147h3 + pSUtat-Sh-GXEF fermentation broths relative to wild type samples.** Test tubes filled with 16 ml L.B. + 0.4% (w/v) glucose were inoculated 1:1000 with: MG1655 + pUNIPROM + pSU23; MG1655 + pSUtat-Sh-GX-EF + pUNI-Tte-Hyd; and FTD147h3 + pSUtat-Sh-GX-EF, and cultures grown anaerobically. Cells were pelleted by centrifugation at 4000 rpm, the supernatant was passed through a 0.2 µm syringe filter and analysed by HPLC. For HPLC analysis, 5 µl of fermentation broth was separated at 0.7 ml $min^{-1}$ and 55 °C using a Dionex UltiMate 3000 HPLC system, fitted with an Aminex HPX-87H organic acid column and absorbance monitored at 210 nm. Organic acid standards were used all with $R^2$ values greater than 99.90%. Bars represent difference in metabolite concentration between media before and after fermentation. Error bars represent standard error of three biological replicates. Inset graph represents concentration of each metabolite in media before inoculation.

### 3.3.7 Metabolomic analysis of MC4100, FTD147 and FTD147h3 strains using LC-MS

In an attempt to better understand the fermentation characteristics of FTD147h3, and to better understand changes in *E. coli* metabolism lacking all hydrogenase activity (FTD147), non-targeted liquid chromatography-mass spectroscopy (LC-MS) was performed in collaboration with the Glasgow Polyomics Wolfson Wohl Cancer Research Centre at the University of Glasgow.

FTD147h3, MC4100 and FTD147 were transformed with pSUtat-Sh-GX-EF or pSU23 and transformants used to inoculate 5 ml aerobic overnight cultures. The aerobic overnight cultures were used to inoculate (1:1000) 16 ml test tubes filled with LB + 0.5% (w/v) glucose. These were sealed to induce anaerobiosis and incubated at 37 °C without shaking for 72 h to ensure sufficient FTD147h3 + Acc cell weight. Cells were pelleted by centrifugation at 4000 rpm and the culture supernatant was passed through a 0.2 µm filter to remove any remaining cells. Samples were then extracted using a chloroform:methanol:water (1:3:1) protocol and analysed on an Exactive Orbitrap mass spectrometer (Thermo Fisher) in both positive and negative modes (rapid switching), coupled to a U3000 RSLC HPLC (Dionex) with a ZIC-HILIC column (Sequant) as described previously (Vincent*, et al.*, 2012). Growth media (LB + 0.5% (w/v) glucose) before fermentation was extracted as above and used as a negative control. Concentrations of individual metabolites relative to the concentrations in the control samples are given. In total, 1023 discrete compounds were detected using this method (Figure 3.8). Only compounds scored with an identification confidence value greater than 7/10 are discussed here. Metabolites linked to NADH biochemistry were studied in greater detail.

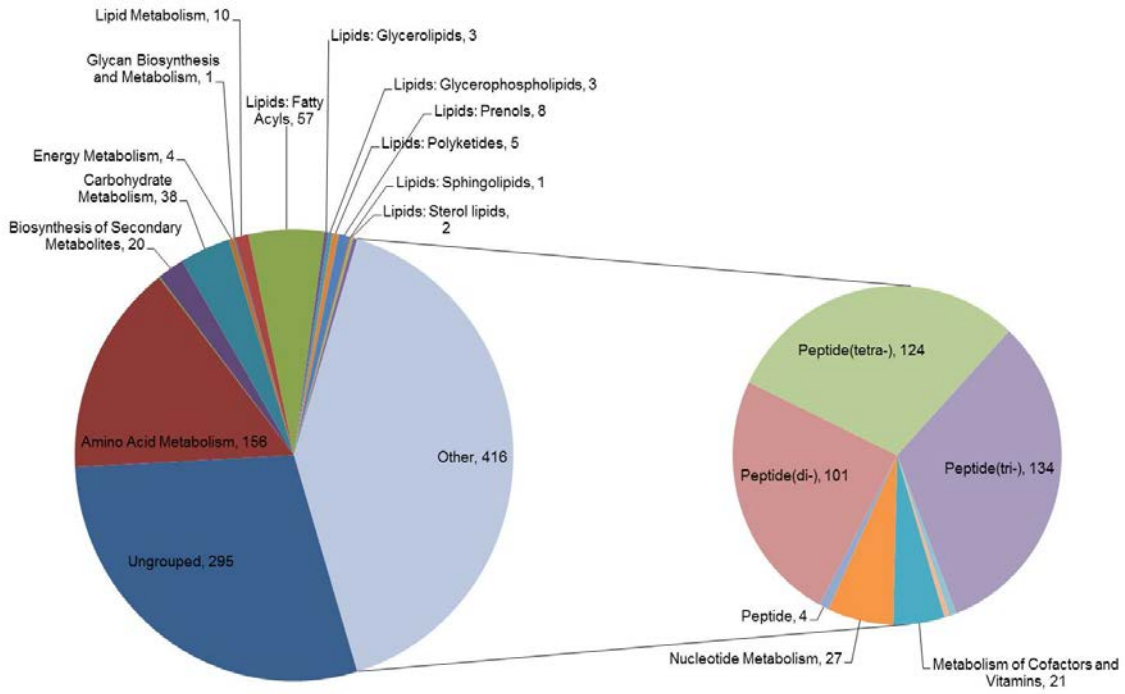


**Figure 3.8 Grouping of compounds identified through non-targeted LC-MS analysis of fermentation broth according to metabolic pathways.**

First, metabolites linked to carbon metabolism were analysed (Figure 3.15). Some of the metabolites that were found in higher concentrations in the FTD147h3 (+ Acc) culture supernatant were sorbitol 6-phosphate, propanoyl phosphate, 3-butynoate and myo-inositol (Figure 3.15). On the other hand, 3-ethylmalate, 3-oxopropanoate and 2-Deoxy-D-ribose 5-phosphate were all found at lower concentrations in FTD147h3 (+ Acc) relative to the MC4100/FTD147 samples (Figure 3.9). Indeed, sorbitol 6-phosphate was not detected in any FTD147 or MC4100 culture supernatant samples.

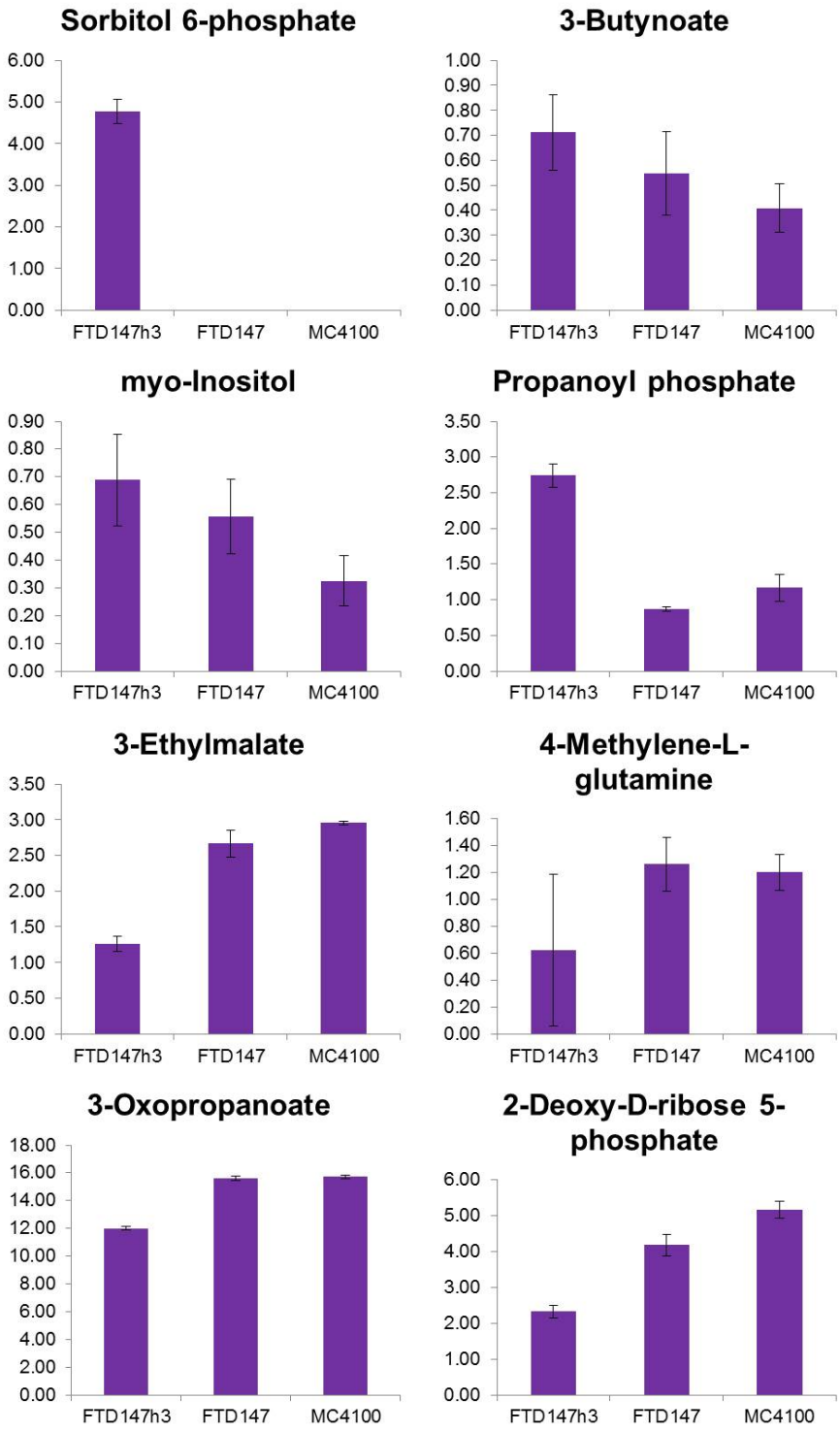


**Figure 3.9 Metabolomic analysis of the spent culture supernatant (1).** Metabolites involved in carbon metabolism were identified through non-targeted LC-MS analysis of spent fermentation supernatants after growth of either FTD147h3 + Acc, FTD147 + pSU23 or MC4100 + pSU23. Samples were extracted using a chloroform:methanol:water (1:3:1) protocol and analysed on an Exactive Orbitrap mass spectrometer (Thermo Fisher) in both positive and negative modes (rapid switching), coupled to a U3000 RSLC HPLC (Dionex) with a ZIC-HILIC column (Sequant). Y-axis represents relative concentration of metabolite in each sample compared to virgin culture media (LB + 0.4% (w/v) glucose).

Next, changes in amino-acid metabolism were also monitored in the FTD147h3 (+ Acc) samples relative to MC4100 or FTD147 (Figure 3.16). An increase in indole-3-acetaldehyde, 2-formylaminobenzaldehyde, urocanate and S-ribosyl-L-homocysteine was observed in these samples (Figure 3.16). A drop in the concentration of 3-methylthio propionic acid, L-3-amino-isobutanoate, indole-3-acetate, N-formyl-L-methionine and 5-hydroxyindolacetate was observed in FTD147h3 strains relative to MC4100 (Figure 3.10). Although only small concentrations of 2-formylaminobenzaldehyde in particular were found, this metabolite was completely absent from FTD147 and MC4100 samples. Small amounts of methylglyoxal were found in all three sample types.

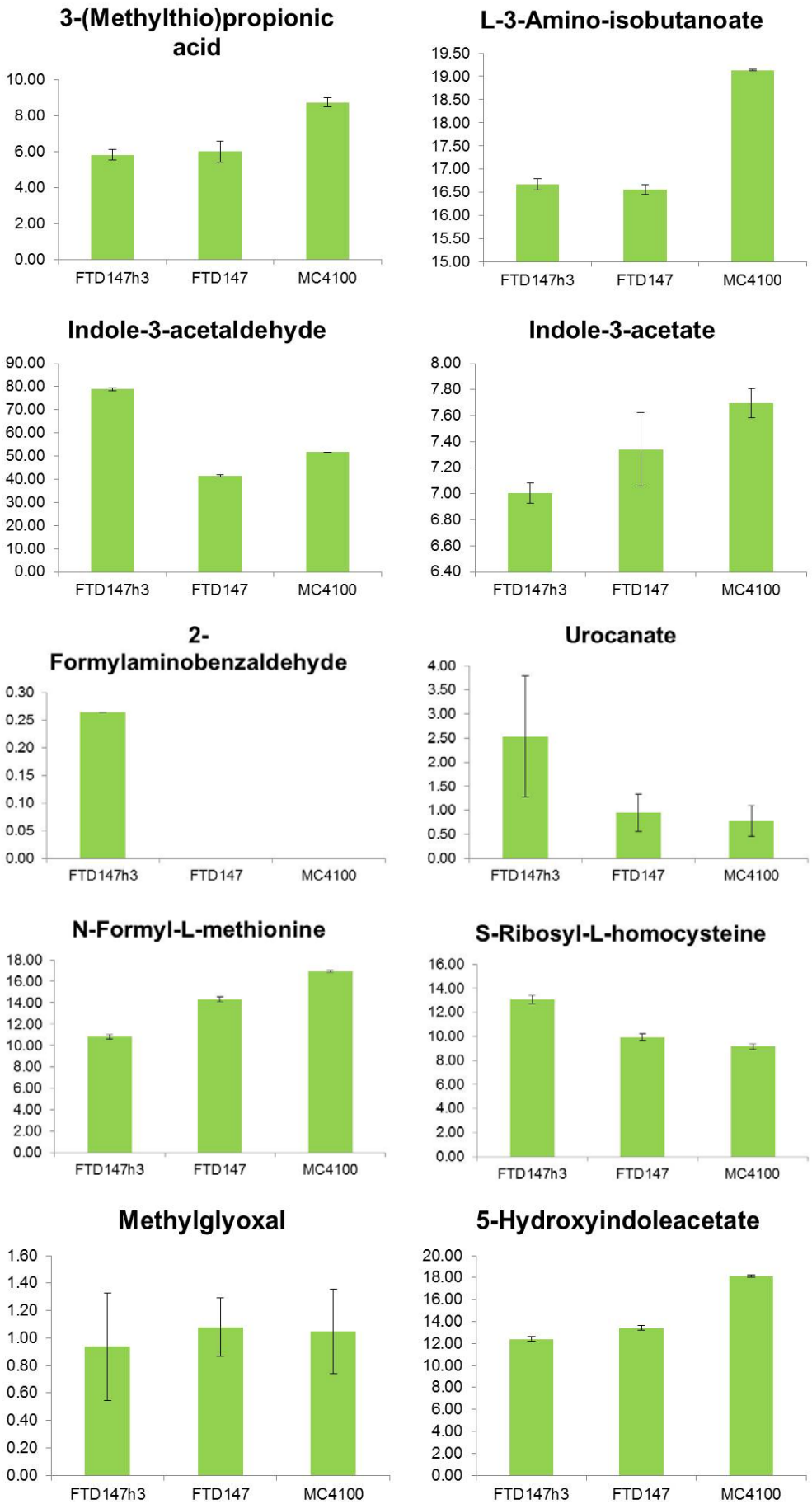


**Figure 3.10 Metabolomic analysis of the spent culture supernatant (2).** Metabolites involved in amino-acid metabolism were identified through non-targeted LC-MS analysis of spent fermentation supernatants after growth of either FTD147h3 + Acc, FTD147 + pSU23 or MC4100 + pSU23. Samples were extracted using a chloroform:methanol:water (1:3:1) protocol and analysed on an Exactive Orbitrap mass spectrometer (Thermo Fisher) in both positive and negative modes (rapid switching), coupled to a U3000 RSLC HPLC (Dionex) with a ZIC-HILIC column (Sequant). Y-axis represents relative concentration of metabolite in each sample compared to virgin culture media (LB + 0.4% (w/v) glucose).

Next, attention turned to energy metabolism (Figure 3.17). Surprisingly, only a small number of metabolites known to play a role in energy metabolism could be identified in the culture supernatant in this experiment. The two metabolites that met the confidence threshold of 7/10 were N-methyl-L-glutamate, which is completely absent from FTD147h3 samples and orthophosphate which was found at a consistent level in all three samples (Figure 3.11).

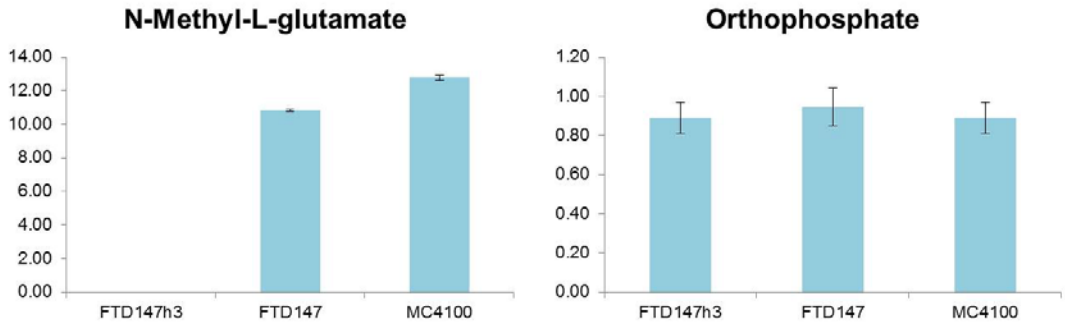


**Figure 3.11 Metabolomic analysis of the spent culture supernatant (3).** Metabolites involved in energy metabolism were identified through non-targeted LC-MS analysis of spent fermentation supernatants after growth of either FTD147h3 + Acc, FTD147 + pSU23 or MC4100 + pSU23. Samples were extracted using a chloroform:methanol:water (1:3:1) protocol and analysed on an Exactive Orbitrap mass spectrometer (Thermo Fisher) in both positive and negative modes (rapid switching), coupled to a U3000 RSLC HPLC (Dionex) with a ZIC-HILIC column (Sequant). Y-axis represents relative concentration of metabolite in each sample compared to virgin culture media (LB + 0.4% (w/v) glucose).

Next, the pathways responsible for cofactor biosynthesis were considered (Figure 3.18). As the [NiFe]-hydrogenases of the *E. coli* strain MC4100 require complex cofactors such as iron, nickel and haem, and as the synthetic strain FTD147h3 +pSUtat-Sh-GX-EF expresses an active [FeFe]-hydrogenase with its own cofactor requirement, changes in extracellular metabolites involved in cofactor metabolism were anticipated. However, the only minor change of note between all three samples was the observation of increase pantothenol in the FTD147h3 samples (Figure 3.12).

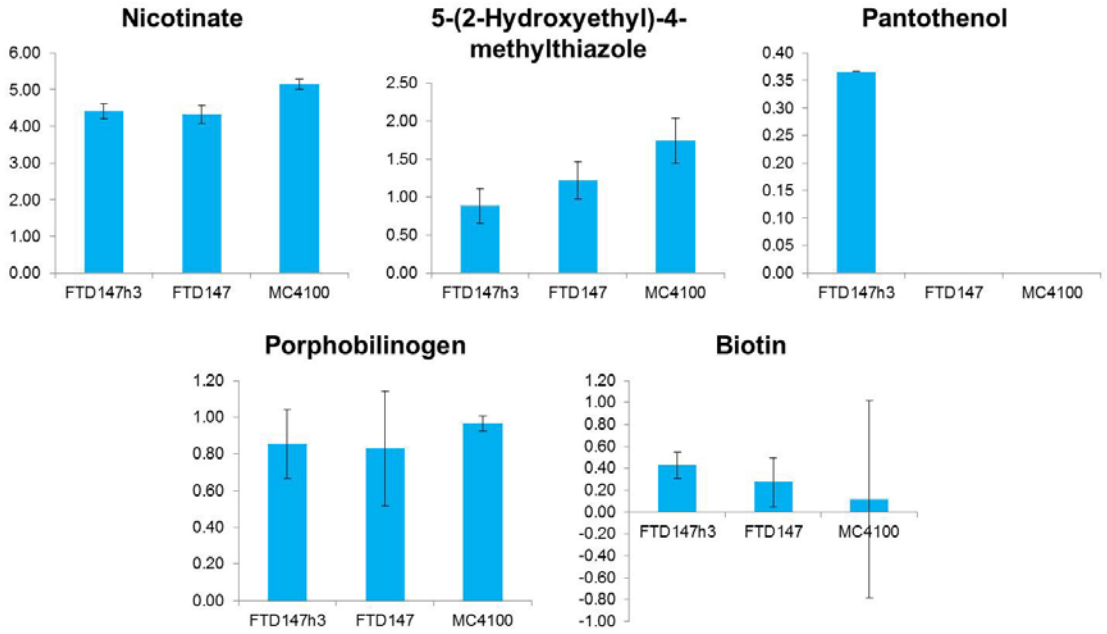


**Figure 3.12 Metabolomic analysis of the spent culture supernatant (4).** Metabolites involved in cofactor metabolism were identified through non-targeted LC-MS analysis of spent fermentation supernatants after growth of either FTD147h3 + Acc, FTD147 + pSU23 or MC4100 + pSU23. Samples were extracted using a chloroform:methanol:water (1:3:1) protocol and analysed on an Exactive Orbitrap mass spectrometer (Thermo Fisher) in both positive and negative modes (rapid switching), coupled to a U3000 RSLC HPLC (Dionex) with a ZIC-HILIC column (Sequant). Y-axis represents relative concentration of metabolite in each sample compared to virgin culture media (LB + 0.4% (w/v) glucose).

Next, compounds involved in fatty acid and lipid metabolism were analysed (Figure 3.19). The important glycolysis metabolites glycerone and glyceraldehyde were found in lower concentrations in the FTD147h3 and FTD147 culture supernatant samples compared to the MC4100 samples (Figure 3.13). The 2-butenoate compound was also found in lower concentrations in FTD147h3 samples (Figure 3.13). A number of metabolites were found in higher concentrations in samples of this mutant, including (R)-3-hydroxybutanoate, traumatic acid, 9-oxononanic acid and FA oxo(5:0)] 3-oxo-4-pentenoic acid (Figure 3.13).

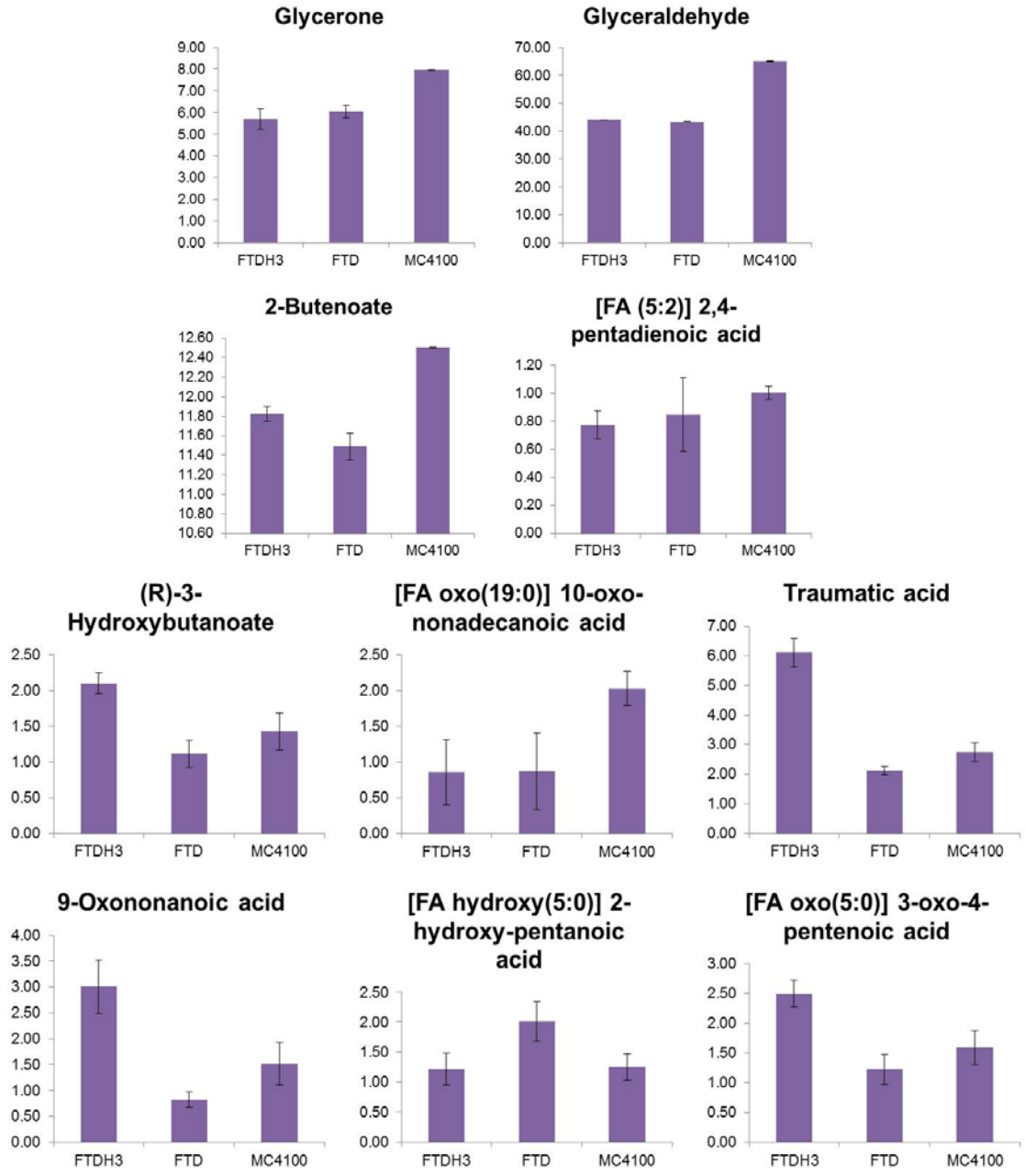


**Figure 3.13 Metabolomic analysis of the spent culture supernatant (5).** Metabolites involved in fatty-acid and lipid metabolism were identified through non-targeted LC-MS analysis of spent fermentation supernatants after growth of either FTD147h3 + Acc, FTD147 + pSU23 or MC4100 + pSU23. Samples were extracted using a chloroform:methanol:water (1:3:1) protocol and analysed on an Exactive Orbitrap mass spectrometer (Thermo Fisher) in both positive and negative modes (rapid switching), coupled to a U3000 RSLC HPLC (Dionex) with a ZIC-HILIC column (Sequant). Y-axis represents relative concentration of metabolite in each sample compared to virgin culture media (LB + 0.4% (w/v) glucose).

As Luria-Bertani media consists of a complex and undefined mixture of yeast-derived peptides, these metabolites were given close attention here (Figure 3.20). A variety of peptides were found in higher concentrations in the FTD147h3 samples, including Leu-Val-Pro; Val-Gly-Pro; Asp-Leu-Pro-Pro and Leu-Gln-Pro (Figure 3.14). No Trp-Asp or Asn-Lys-Cys-Pro peptides were found in the FTD147h3 compared to the other two sample types (Figure 3.14).

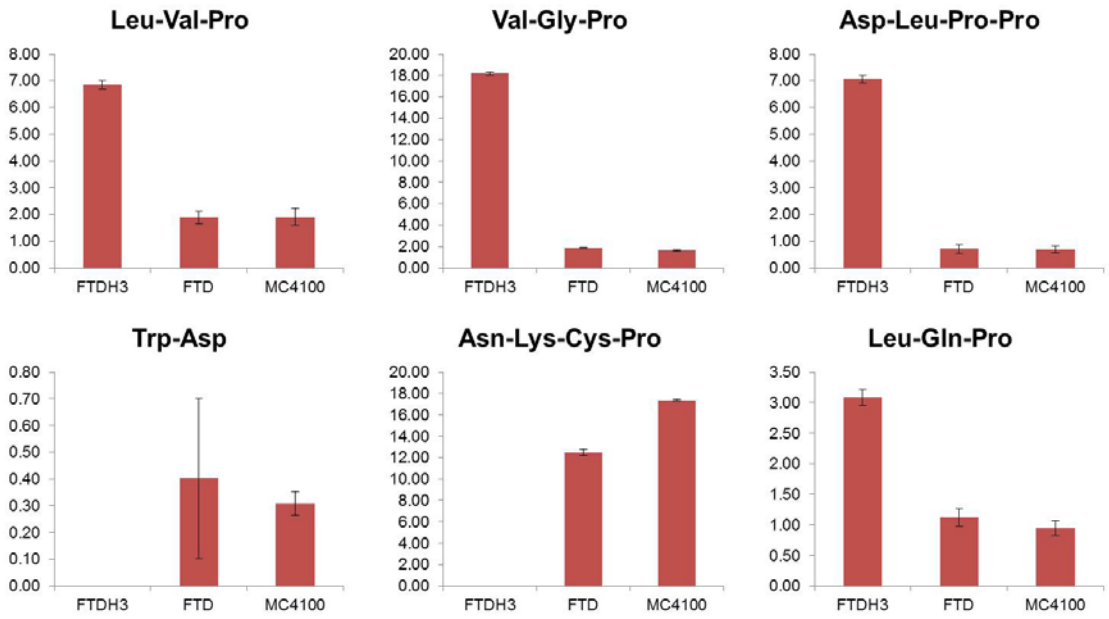


**Figure 3.14 Metabolomic analysis of the spent culture supernatant (6).** Certain short peptides were identified through non-targeted LC-MS analysis of spent fermentation supernatants after growth of either FTD147h3 + Acc, FTD147 + pSU23 or MC4100 + pSU23. Samples were extracted using a chloroform:methanol:water (1:3:1) protocol and analysed on an Exactive Orbitrap mass spectrometer (Thermo Fisher) in both positive and negative modes (rapid switching), coupled to a U3000 RSLC HPLC (Dionex) with a ZIC-HILIC column (Sequant). Y-axis represents relative concentration of metabolite in each sample compared to virgin culture media (LB + 0.4% (w/v) glucose).

Another major group of metabolites studied in this metabolomics experiment were those involved in nucleotide metabolism (Figure 3.21). Methyladenine was found in higher concentrations in the FTD147h3 extracellular environment than the other two culture supernatants, and a fragment of orotate was found at a concentration 7 times higher than either of the other two samples (Figure 3.15). Adenylyl sulphate and 2'3'-cyclic AMP were all found a lower concentrations in the FTD147h3 samples than the MC4100 samples, whereas the concentration of 5,6-dihydrouracil was reduced in both the FTD147h3 and FTD147 samples (Figure 3.15).

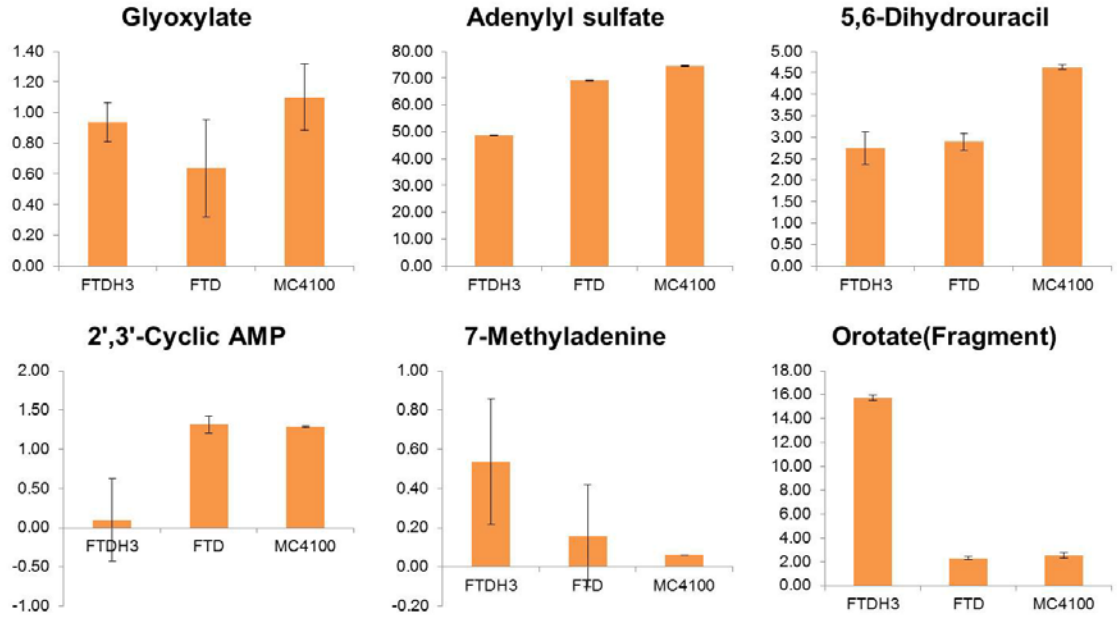


**Figure 3.15 Metabolomic analysis of the spent culture supernatant (7).** Metabolites involved in nucleotide metabolism were identified through non-targeted LC-MS analysis of spent fermentation supernatants after growth of either FTD147h3 + Acc, FTD147 + pSU23 or MC4100 + pSU23. Samples were extracted using a chloroform:methanol:water (1:3:1) protocol and analysed on an Exactive Orbitrap mass spectrometer (Thermo Fisher) in both positive and negative modes (rapid switching), coupled to a U3000 RSLC HPLC (Dionex) with a ZIC-HILIC column (Sequant). Y-axis represents relative concentration of metabolite in each sample compared to virgin culture media (LB + 0.4% (w/v) glucose).

Other interesting metabolites that showed a stark difference between the different culture supernatants included gentianamine, which was completely absent from FTD147h3 and FTD147 samples, and allylcysteine, which was completely absent in FTD147h3 samples (Figure 3.16). Other compounds that were reduced in the FTD147h3 samples included myristic amide/tetradecanamide (reduced in both FTD147 and FTD147h3 samples); fagaronine; ethylpyruvate; hoyrine B; 2-keto-4-hydroxybutyrate (reduced in both FTD147 and FTD147h3 samples); and butylene (Figure 3.16). A number of interesting metabolites were found in higher concentrations in the FTD147h3 supernatant including diethyl adipate; 2-hydroxyadenine; and large amounts of 1-(beta-D-Ribofuranosyl)-1,4-dihydronicotinamide (Figure 3.16).

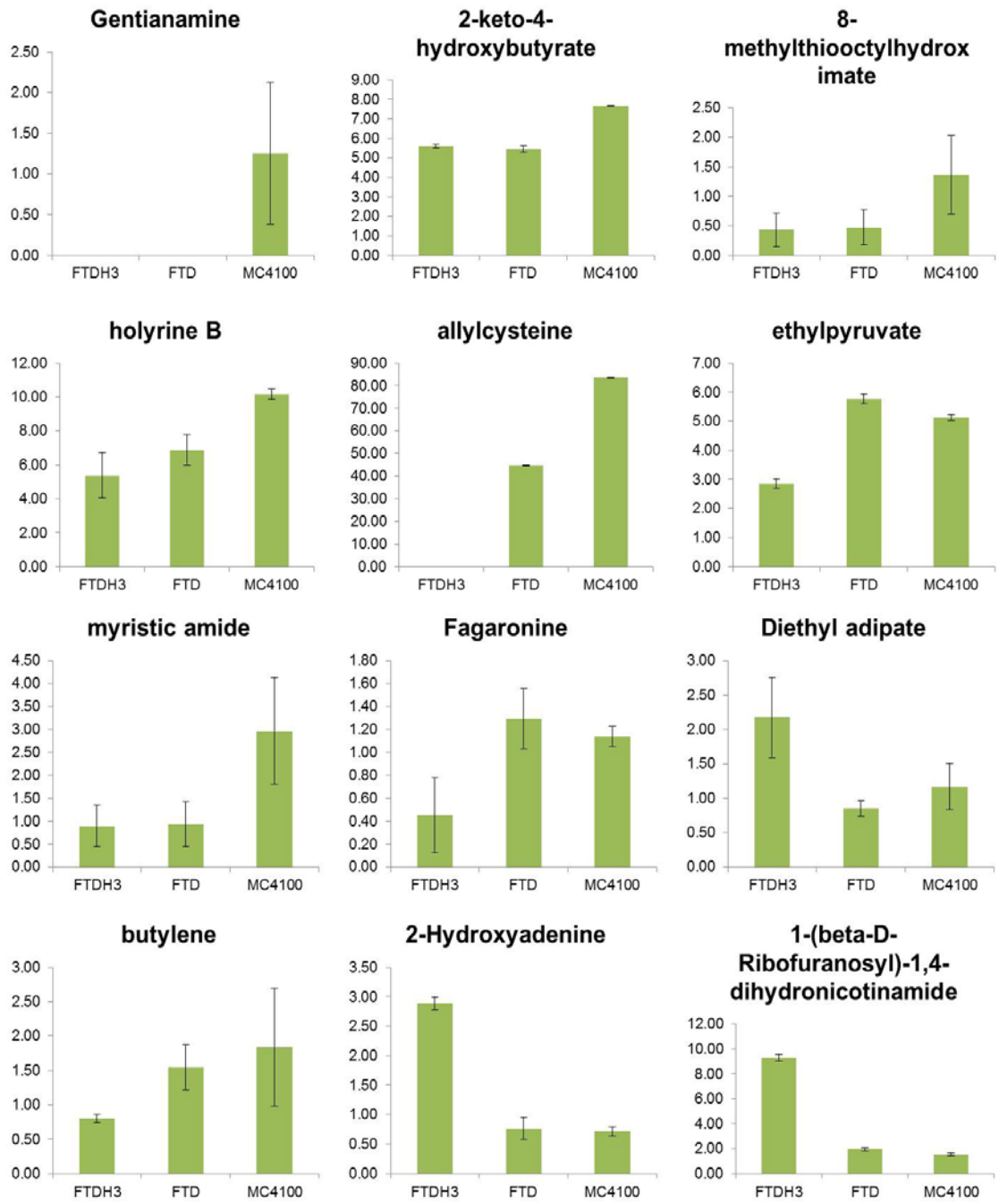


**Figure 3.16 Metabolomic analysis of the spent culture supernatant (8).** Other potentially interesting metabolites were identified through non-targeted LC-MS analysis of spent fermentation supernatants after growth of either FTD147h3 + Acc, FTD147 + pSU23 or MC4100 + pSU23. Samples were extracted using a chloroform:methanol:water (1:3:1) protocol and analysed on an Exactive Orbitrap mass spectrometer (Thermo Fisher) in both positive and negative modes (rapid switching), coupled to a U3000 RSLC HPLC (Dionex) with a ZIC-HILIC column (Sequant). Y-axis represents relative concentration of metabolite in each sample compared to virgin culture media (LB + 0.4% (w/v) glucose).

### 3.3.8 Development of a screen for fully integrated NADH-dependent hydrogenase activity.

The chromosomally-encoded synthetic *Ca. tengcongensis* [FeFe]-hydrogenase was active with redox dyes, but did not demonstrate NADH-dependent $H_2$ production or support growth in the place of alcohol dehydrogenase. It was considered, therefore, that the [FeFe] hydrogenase module was not correctly communicating with the diaphorase module of the enzyme in this synthetic system. In order to tackle this it was decided to prepare a robust strain that could be used to screen for NADH recycling, and to prepare a random mutant library of *hydA*.

As the Δ*adhE*::*TtehydC-A* mutant strain, FTD147h3, retains the ability to produce lactate production, catalysed by the *ldhA* gene product, which is a secondary method of $NAD^+$ regeneration, the *ldhA* gene was specifically deleted from FTD147h (a strain similar to FTD147h3 but lacking an active *Ca. tengcongensis hydA* gene). The resultant strain was named RaisynA1 (Table 3.2). Next, a derivative of RaisynA1 lacking *iscR* (the transcriptional repressor of an iron sulfur cluster biosynthesis operon) was constructed by P1 transduction and termed IronBrew (Table 3.2). A hydrogenase- and alcohol dehydrogenase-positive strain lacking *ldhA*, Maggie1 (Table 3.2), was also constructed to use as a control.

| **Strain Name** | **Genotype** |
|---|---|
| FTD147h | FTD147 Δ*adhE*::*TtehydC-B*, *hydA*$^-$ |
| Maggie1 | MG059e1 (MG1655 *hycE*$^{His}$) Δ*ldhA* |
| RaisynA1 | FTD147h Δ*ldhA* |
| IronBrew | RaisynA1 Δ*iscR* |

**Table 3.2 Strains used in the screening of mutant NADH-dependent [FeFe]-hydrogenase genes**

### 3.3.9 Characterisation of RaisynA1 and IronBrew: growth in liquid media

The ability of RaisynA1 and IronBrew to grow fermentatively in both rich and minimal media was tested and compared with MG1655, FTD147h (the parent strain of RaisynA1), TeaTotal1 (as FTD147 Δ*adhE*) and Maggie1 (Δ*ldhA*). Cells were plated freshly from frozen stocks stored at -80 °C and single colonies used to inoculate 5 ml aerobic overnight cultures. These aerobic overnight cultures were used to inoculate (1:1000) 16 ml test tubes filled with LB + 0.4% w/v glucose (Figure 3.17A, B & C) or M9 + 0.4% w/v glucose (Figure 3.17D). These were sealed to induce anaerobiosis and incubated at 37 °C without shaking. Samples were taken 3, 6, 9, 11, 13, 17, 21 and 38 hours after inoculation and optical density at 600 nm measured.

In minimal M9 media supplemented with glucose, RaisynA1 (essentially Δ*adhE*, Δ*ldhA*) did not grow anaerobically (Figure 3.17D). Indeed, in rich LB medium + glucose RaisynA1 struggled to grow (reaching an $OD_{600}$ of 0.2 after 38 h, with a lag phase of almost 20 h), whereas FTD147h and Teatotal (FTD147 Δ*adhE*) grew to an $OD_{600}$ of approximately 0.7 and 0.6 respectively before entering stationary phase (Figure 3.17B). The MG1655 derivative lacking *ldhA*, Maggie1, grew well in LB + glucose until 11 h ($OD_{600}$ of 0.9) before the cells appeared to lyse since turbidity dropped dramatically ($OD_{600}$ of 0.4 at 17 h) and then stabilised (Figure 3.17C). The Δ*iscR* derivative of RaisynA1, IronBrew grew slightly better than RaisynA1 in rich media (Figure 3.17C).

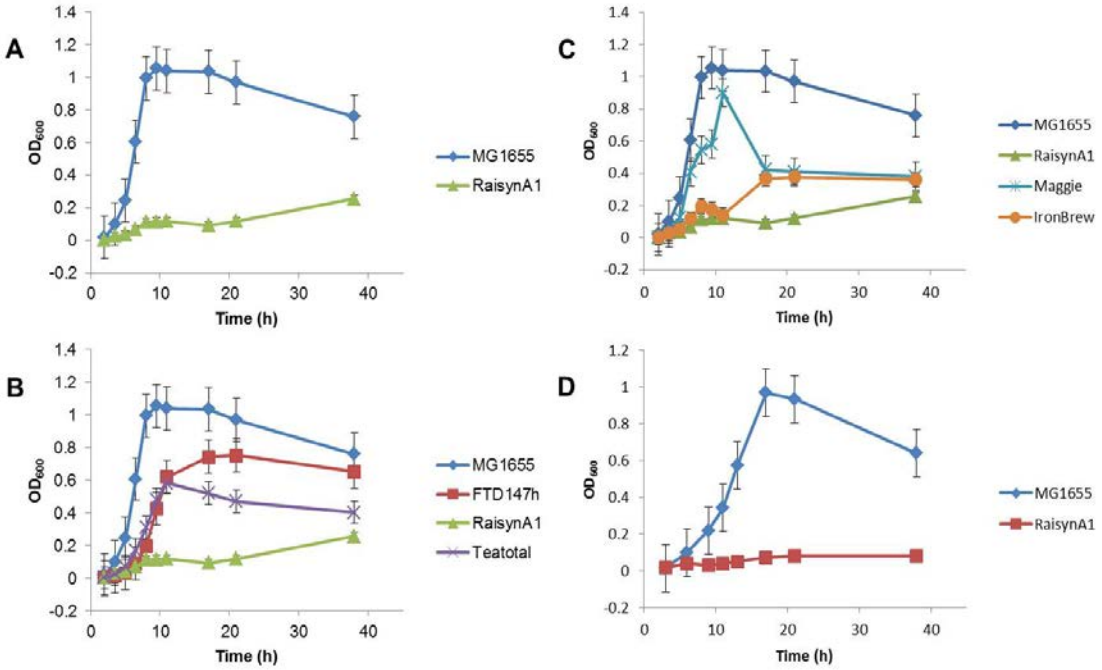


**Figure 3.17 RaisynA1 does not grown in minimal liquid media under fermentative conditions and grows poorly in rich media.** Test tubes filled with 16 ml (A, B & C) L.B. + 0.4% w/v glucose or (D) M9 + 0.4% w/v glucose were inoculated 1:1000 with MG1655, RaisynA1, FTD147h, Teatotal, Maggie and IronBrew and cultures grown anaerobically. The optical density ($OD_{600}$) of these cultures was recorded at various time points over 38 h. It was decided not to convert $OD_{600}$ to $\log_{10}$ values, to better highlight differences in final cell concentrations.

### 3.3.10 Characterisation of RaisynA1: organic acid analysis

In order to characterise the consumption of glucose by the RaisynA1 strain (Δ*adhE*, Δ*ldhA*), and assess the production of other organic acids, HPLC was used. For the detection of glucose and ethanol a refractive index detector was connected downstream of the Aminex HPX-87H column in place of the UV detector. Standard curves of ethanol and glucose were prepared with $R^2$ values of 0.9999% and 0.9997%, respectively. The RaisynA1 culture medium samples containing empty control vectors showed no ethanol production (Figure 3.18B), whereas the MG1655 spent culture supernatants (with or without synthetic hydrogenase and maturation proteins) contained approximately 0.4% (v/v) ethanol (Figure 3.18B). Surprisingly, the amount of glucose in the RaisynA1 samples apparently did not change between initiation and completion of anaerobic growths (Figure 3.18A), suggesting this plentiful carbon source was not used at all by this mutant for anaerobic growth in rich media. By contrast, all added glucose (initially 0.4% (w/v) or 22 mM) was completely consumed in the MG1655 samples (Figure 3.18A).

The production of lactate, and the other main organic acids, was monitored by UV detection at 210 nm. RaisynA1 does not produce lactate when grown on LB + glucose (Figure 3.19). However, the concentrations of succinate, acetate and pyruvate were reduced when the synthetic *Ca. tengcongensis* hydrogenase and the *Sh. oneidensis* maturation proteins were produced in RaiysnA1 (Figure 3.19). The reduction in the secreted concentrations of succinate, acetate and pyruvate was also observed in samples of IronBrew containing the activated hydrogenase (Figure 3.20), perhaps indicating the reduction in these organic acids was related to production of an active version of this enzyme. Note, however, that by comparison the relative concentrations of these organic acids in the growth medium was overall much higher in the IronBrew background than in the corresponding RaisynA1 samples.

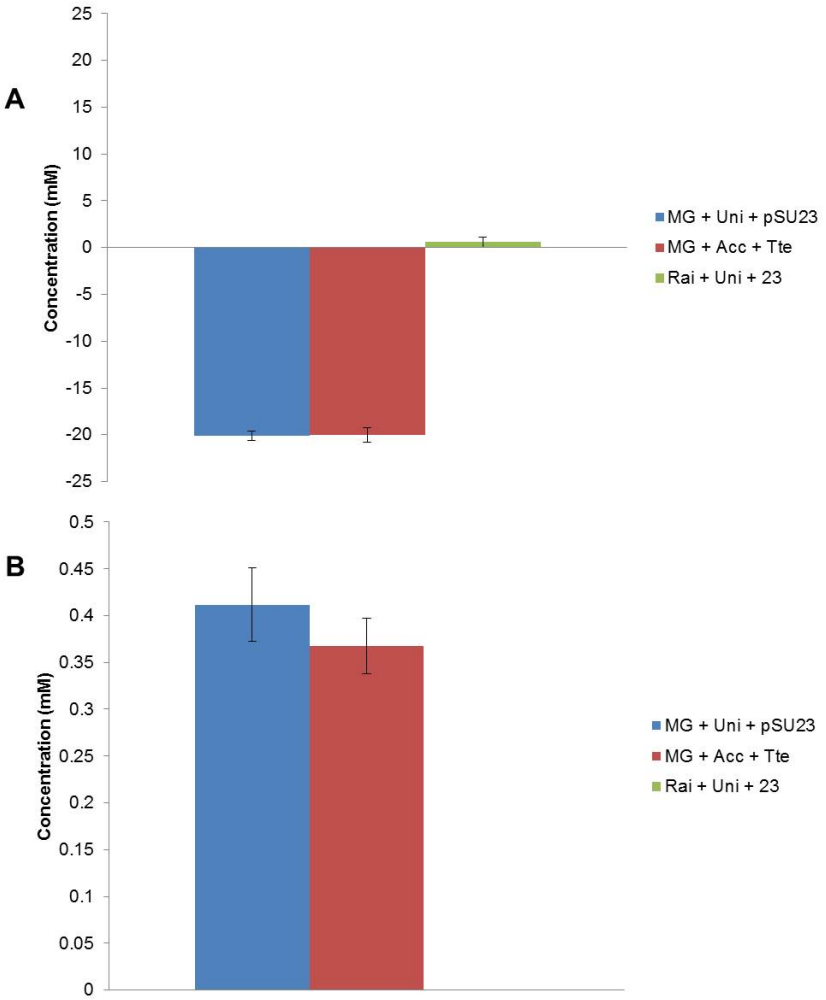


**Figure 3.18 RaisynA1 does not (A) consume glucose or (B) produce ethanol.** Test tubes filled with 16 ml L.B. + 0.4% (w/v) glucose were inoculated 1:1000 with:MG1655 + pUNIPROM + pSU23; MG1655 + pSUtat-Sh-GX-EF + pUNI-Tte-Hyd; or RaisynA1 + pUNIPROM + pSU23, and cultures grown anaerobically. Cells were pelleted by centrifugation at 4000 rpm, the supernatant was passed through a 0.2 µm syringe filter and analysed by HPLC. For HPLC analysis, 5 µl of fermentation broth was separated at 0.7 ml $min^{-1}$ and 55 °C using a Dionex UltiMate 3000 HPLC system, fitted with an Aminex HPX-87H organic acid column and monitored using a refractive index detector. Standards of D-glucose and ethanol were used all with $R^2$ values greater than 99.999%. Bars represent difference in metabolite concentration between media before and after fermentation. Error bars represent standard error of three biological replicates.

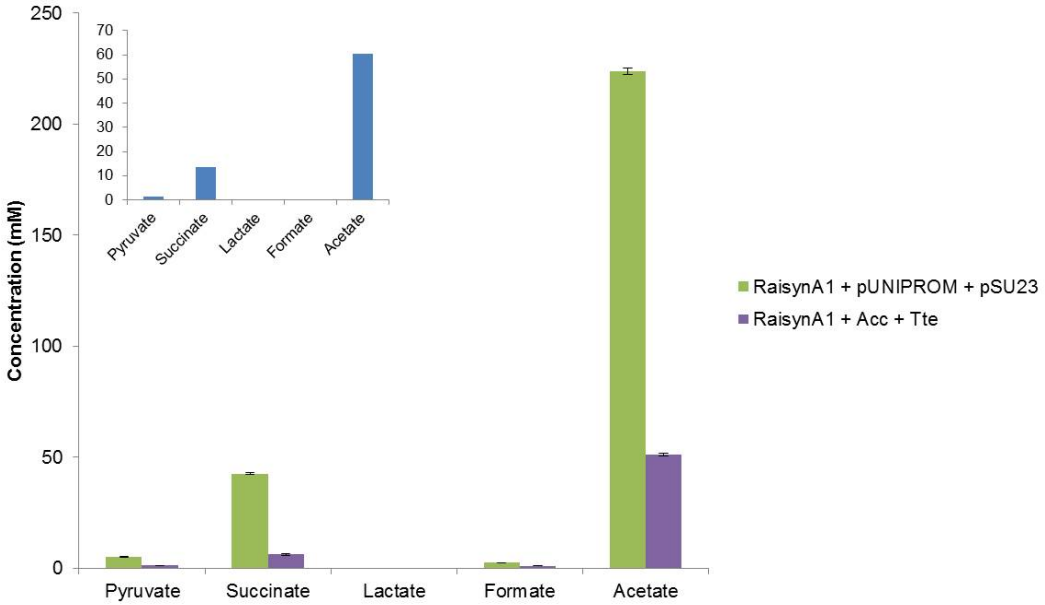


**Figure 3.19 Organic-acid analysis of fermentation broths of RaisynA1 +/- pSUtat-Sh-GXEF and pUNI-Tte-Hyd.** Test tubes filled with 16 ml L.B. + 0.4% (w/v) glucose were inoculated 1:1000 with: RaisynA1 + pUNIPROM + pSU23; or RaisynA1 + pSUtat-Sh-GX-EF + pUNI-Tte-Hyd, and cultures grown anaerobically. Cells were pelleted by centrifugation at 4000 rpm, the supernatant was passed through a 0.2 µm syringe filter and analysed by HPLC. For HPLC analysis, 5 µl of fermentation broth was separated at 0.7 ml $min^{-1}$ and 55 °C using a Dionex UltiMate 3000 HPLC system, fitted with an Aminex HPX-87H organic acid column and absorbance monitored at 210 nm. Organic acid standards were used all with $R^2$ values greater than 99.90%. Bars represent difference in metabolite concentration between media before and after fermentation. Error bars represent standard error of three biological replicates. Inset graph represents concentration of each metabolite in media before inoculation

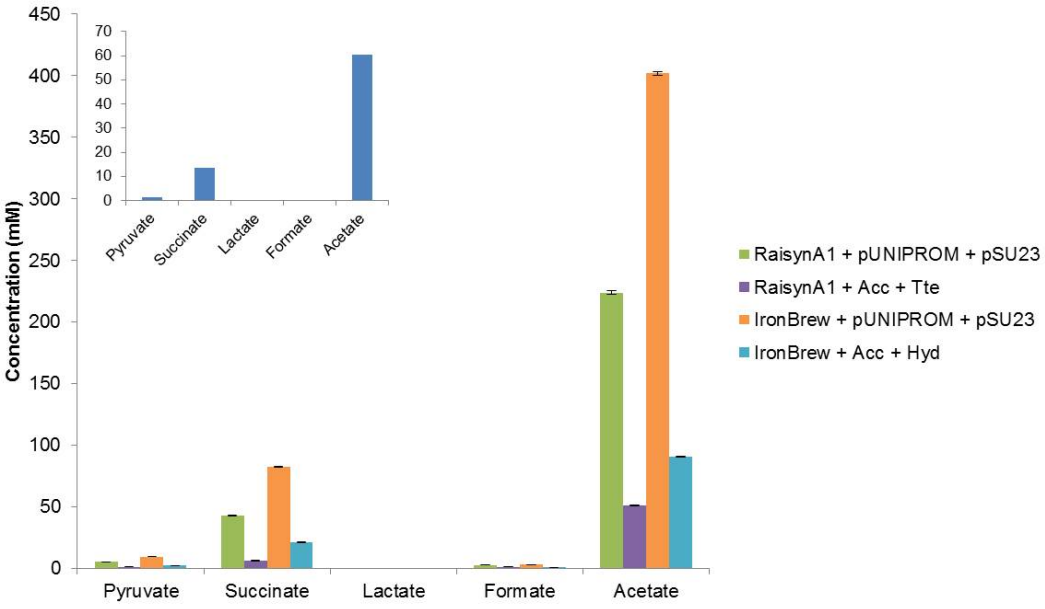


**Figure 3.20 Organic-acid analysis of fermentation broths of RaisynA1/IronBrew +/- pSUtat-Sh-GXEF and pUNI-Tte-Hyd.** Test tubes filled with 16 ml L.B. + 0.4% (w/v) glucose were inoculated 1:1000 with: RaisynA1 + pUNIPROM + pSU23; or RaisynA1 + pSUtat-Sh-GX-EF + pUNI-Tte-Hyd; IronBrew + pUNIPROM + pSU23; or IronBrew + pSUtat-Sh-GX-EF + pUNI-Tte-Hyd, and cultures grown anaerobically. Cells were pelleted by centrifugation at 4000 rpm, the supernatant was passed through a 0.2 µm syringe filter and analysed by HPLC. For HPLC analysis, 5 µl of fermentation broth was separated at 0.7 ml $min^{-1}$ and 55 °C using a Dionex UltiMate 3000 HPLC system, fitted with an Aminex HPX-87H organic acid column and absorbance monitored at 210 nm. Organic acid standards were used all with $R^2$ values greater than 99.90%. Bars represent difference in metabolite concentration between media before and after fermentation. Error bars represent standard error of three biological replicates. Inset graph represents concentration of each metabolite in media before inoculation.

### 3.3.11 Construction and screening of a *hydA* mutant library

Random mutant libraries of *hydA*, which encodes the H-cluster-containing subunit of the synthetic *Ca. tengcongensis* [FeFe]-hydrogenase, were constructed using hypermutagenic PCR with biased dNTPs (Vartanian*, et al.*, 1996a). This protocol is designed to introduce both transitions and transversions. Two libraries of the 1758 bp *hydA* gene were constructed, one with an error rate of 2.8% (considered a 'low' error rate library) and the other with an error rate of 4.5% (considered a 'high' error rate library). Each library consisted of $1.2 \times 10^6$ and $1.5 \times 10^6$ independent clones, respectively, which represented a 682 and 853 times coverage of the *hydA* gene.

Using RaisynA1, which does not grow anaerobically on minimal solid M9 agar plates supplemented with 0.4% (w/v) glucose, both low and high mutant libraries were screened for their ability to recover growth, the hypothesis being that a fully active NADH-linked hydrogenase could complement for the loss of the NADH-linked AdhE and LdhA. RaisynA1 was transformed with pSUtat-Sh-GX-EF and a single colony used to prepare electrocompetent cells (Sambrook*, et al.*, 1989). The resultant RaisynA1 + pSUtat-Sh-GX-EF electrocompetent cells were transformed with 100 or 200 ng of each mutant library and plated on to selection plates, which were incubated at 37 °C for at least one week in anaerobic jars. RaisynA1 transformed with empty plasmids was used as a negative control. Aerobic controls on M9 + glucose plates were used to estimate transformation efficiency and the number of colonies screened. Transformation efficiencies of 200 - 400 transformants per ng plasmid DNA were observed and a total of approximately 270,000 colonies of the 'low' and 280,000 colonies of the 'high' *hydA* libraries were screened. No recovery of anaerobic growth was observed. Other incubation methods were also tested including the use of argon and the maintenance of a mild vacuum (-1 bar), but no recovery of growth was observed.

These negative results indicate that the *Ca. tengcongensis* [FeFe]-hydrogenase cannot complement the RaisynA1 fermentative phenotype and that that lack of complementation is probably not due to a problem with the HydA subunit.

## 3.4 Discussion

In this Chapter, a genetically modified *E. coli* strain (FTD147h3) was constructed that expresses a novel [FeFe]-hydrogenase activity based on the NADH-dependent [FeFe]-hydrogenase from the thermophilic bacterium *Ca. tengcongensis*. This synthetic hydrogenase operon was integrated into the *E. coli* chromosome in place of *adhE*, which encodes alcohol dehydrogenase, the major $NAD^+$ regenerator in *E. coli* during mixed-acid fermentation. In addition to assaying hydrogenase activity, this strain was characterised for growth on a variety of liquid and solid media under fermentative conditions. Organic-acid production by this strain with and without the H-cluster accessory proteins was also characterised. Finally a metabolomics study using LC-MS was used to study changes in other less well characterised metabolites.

### 3.4.1 FTD147h3 displays $H_2$ oxidation and $H_2$ production capabilities

When the essential H-cluster maturation proteins are expressed in the FTD147h3 strain both $H_2$ oxidation and production activities can be detected with redox dyes. The successful integration of genes for a functional [FeFe]-hydrogenase onto the *E. coli* chromosome has not been reported to date. It is possible that the activity of this synthetic hydrogenase could be further improved by also integrating the optimised *Sh. oneidensis hydGX-EF* operon onto the chromosome, as others have recently performed (Yu*, et al.*, 2011). This may help reduce any possible toxic effects resulting from the high level expression of the H-cluster maturation proteins. During the course of this work, it was reported that the deletion of *iscR*, which encodes the transcriptional repressor of the iron-sulphur cluster machinery operon, with the addition of extra cysteine and ferric ammonium citrate, resulted in an increase in [FeFe]-hydrogenase activity in a heterologous system (Kuchenreuther*, et al.*, 2010). A Δ*iscR* version of FTD147h3 was therefore constructed here, however it was not thoroughly tested due to time constraints.

As no *in vivo* $H_2$ production was observed in the FTD147h3 strain expressing the H-cluster maturation proteins, it was hypothesised that directed protein evolution might be required to activate this non-native thermophilic enzyme when expressed in *E. coli* at 37 °C. Indeed, no *in vivo* $H_2$ production was observed in previous studies where the closely-related *Thermotoga maritima* [FeFe]-hydrogenase was heterologously expressed in *E. coli* (Agapakis*, et al.*, 2010), although this was attributed to expression problems by those authors. The hypothesis was that variants of the synthetic enzyme that have increased, or modified, NADH-dependent hydrogenase activity could regenerate $NAD^+$ during fermentation and therefore recover growth of Δ*adhE, ldhA E. coli* strains under these conditions. A variety of mutagenesis

approaches were used in this study. Mutant libraries of *hydA* were constructed using hyper-mutagenic PCR and tested in the RaisynA1 strain, which encodes all of the synthetic *Ca. tengcongensis* [FeFe]-hydrogenase except HydA. No recovery of growth was observed when selected on minimal M9 + glucose agar plates incubated anaerobically.

A number of other mutagenesis approaches were also undertaken. Mutant libraries of both the whole synthetic [FeFe]-hydrogenase plasmid, pUNI-Tte-Hyd, and the accessory plasmid, pSUtat-Sh-GX-EF, were constructed using XL1-Red competent cells, an *E. coli* strain deficient in three of the main *E. coli* DNA repair pathways (Greener*, et al.*, 1996). In addition, chemical mutagenesis using methyl methane sulfonate (MMS) or Captan (Ohta*, et al.*, 2000) was carried out directly on the two plasmids, as well as on the RaisynA1 strain pre-transformed with pUNI-Tte-Hyd and pSUtat-Sh-GX-EF. Finally, mutagenesis using exposure to ultraviolet light was also carried out on this strain. No recovery of growth was observed using any of these mutagenesis approaches.

One possible reason for the lack of recovery of growth could be that the *Ca. tengcongensis* [FeFe]-hydrogenase follows a fundamentally different mechanism of $H_2$ production than postulated in the original work (Soboh*, et al.*, 2004). As now proposed for a number of other multimeric [FeFe]-hydrogenases (Schut and Adams, 2009) (Huang*, et al.*, 2012; Schuchmann and Muller, 2012), it is worth considering that the *Ca. tengcongensis* enzyme produces $H_2$ through a bifurcating mechanism involving two separate electron donors; reduced ferredoxin ($Fd^{red}$) and NADH. Preliminary work to investigate this has been undertaken here and tools are now available for the *Ca. tengcongensis* [FeFe]-hydrogenase and its maturation proteins to be co-expressed with *Th. maritima* pyruvate:ferredoxin oxidoreductase and ferredoxin in the FTD147h3 strain.

The other consideration could be that the major problem lies with the activity of the HydB diaphorase subunit. It should therefore still be possible to perform directed protein evolution on all the other components of this complex system. Indeed, as an alternative to the live/dead selection method, it may be useful to devise a screening mechanism to detect improved hydrogenase activity resulting from any of these mutagenesis approaches such as the high-throughput plate-based assay using redox dyes (Stapleton and Swartz, 2010b; Stapleton and Swartz, 2010a).

Finally, it should be considered that swapping ethanol production for $H_2$ production would not provide the correct redox balance for growth. However, in the course of this work, it was demonstrated that a *bona fide* NADH-dependent $H_2$-producing enzyme (the soluble [NiFe]-hydrogenase of the mesophilic organism *Ralstonia eutropha* H16) is introduced into an *E. coli*

strain lacking *adhE*, recovery of growth is reported as possible together with $H_2$ yields of approximately 2 mol $H_2$ *per* mol glucose (Ghosh*, et al.*, 2013). During this project a synthetic operon encoding the *R. eutropha* SH was prepared but was shown to fail at the protein production stage.

### 3.4.2 Differences in growth of FTD147h3 and RaisynA1 in different types of media

It has been shown that *adhE* is essential for *E. coli* survival during the fermentation of glucose and hexoses more reduced than glucose, such as sorbitol (Lorowitz and Clark, 1982; Cunningham and Clark, 1986; Gupta and Clark, 1989). These experiments were all performed in minimal M9 media supplemented with the carbon source of choice. In this work, it was confirmed that FTD147h3 (FTD147 Δ*adhE*::*TtehydC-A*) did not grow anaerobically in minimal media with glucose as the sole carbon source. However, slow growth occurred in rich liquid media, supplemented with glucose, under anaerobic conditions. The growth of FTD147h3 was almost identical to that of Teatotal1 (FTD147 Δ*adhE*) in both rich liquid and minimal solid media. This implies that in rich liquid media, strains lacking alcohol dehydrogenase are capable or metabolising other carbon sources (e.g. amino acids) in the media and/or have the capacity to direct their metabolism towards alternative $NAD^+$ regeneration pathways.

RaisynA1 (FTD147h Δ*ldhA*) did not grow in either liquid or solid minimal media supplemented with glucose. Lactate production was abolished in this Δ*ldhA* strain. Interestingly, even in rich media RaisynA1 grew poorly, displaying a long lag phase of 17 h, but after 72 h growth sufficient biomass had accumulated to allow characterisation of the organic acid content of the extracellular media. No ethanol was produced by RaisynA1 (it carries a deletion in *adhE*). Very surprisingly, it was shown that RaisynA1 does not consume any of the glucose supplied in the starting culture media. It is likely that the yeast extract in LB broth is being used as the primary C source for growth under these conditions, and leading to ultimate secretion of acetate. Further evidence in support of this hypothesis can be found in the LC-MS metabolomics study comparing samples of growth media after “fermentation”, where the usage of peptides varied greatly between FTD147h3 and the other samples.

### 3.4.3 Identification of putative $NAD^+$-regeneration pathways upregulated in FTD147h3

Although focused solely on secreted metabolites, the results of the metabolomics study give some indications as to possible mechanisms of $NAD^+$ regeneration in FTD147h3 when grown anaerobically in rich media. Sorbitol-6-phosphate is only found in the FTD147h3 + pSUtat-Sh-GX-EF samples and not in FTD147 or MC4100 samples and is likely produced from D-fructose 6-phosphate in a reaction catalysed by sorbitol-6-phosphate dehydrogenase (SrlD; also known

as glucitol-6-phosphate dehydrogenase), which oxidises NADH to $NAD^+$ (Lengeler, 1975). No sorbitol-6-phosphate was present in the culture media at the start of the experiment, suggesting that the build-up of this metabolite was not a result of product (D-fructose-6-phosphate) inhibition, but rather the build-up of D-fructose-6-phosphate ($K_m$: 568 μM) initiated this reaction in the direction of sorbitol 6-phosphate production ($K_m$ for sorbitol-6-phosphate: 3.3 mM) (Novotny*, et al.*, 1984; Roux*, et al.*, 2006).

1-(beta-D-ribofuranosyl)-1,4-dihydronicotinamide (reduced nicotinamide riboside) is a similar pyrimidine cofactor to $NAD^+$ and was found outside the cell at a concentration > 8 times higher in FTD147h3 samples. This compound can be used by 'NAD$^+$ salvage pathway III' of *E. coli* to regenerate $NAD^+$. One multi-domain enzyme, NadR, catalyses both the ribosylnicotinamide kinase (1-(β-D ribofuranosyl)nicotinamide + ATP ↔ β-nicotinamide D-ribonucleotide + ADP + $H^+$; $K_m$ for 1-(β-D ribofuranosyl)nicotinamide: 80 μM) and the NMN adenylyltransferase (β-nicotinamide D-ribonucleotide + ATP + $H^+$ ↔ $NAD^+$ + diphosphate; $K_m$ for β-nicotinamide D-ribonucleotide: 700 μM) reactions (Raffaelli*, et al.*, 1999; Kurnasov*, et al.*, 2002; Grose*, et al.*, 2005).

Reactions involving the $NAD^+$/NADH redox couple in the tryptophan-metabolism pathway also showed statistically-significant changes between the FTD147h3 samples and the other two sample types (P = 0.0001 in both cases). Indole-3-acetaldehyde was found at much higher concentrations than the other two sample types, whereas indole-3-acetate was found at much lower levels. Neither of these metabolites have been well studied in *E. coli*, however in a reaction independent of oxygen in plants and other organisms, indole-3-acetalydehyde is oxidised to indol-3-acetate, with the concurrent reduction of $NAD^+$. This reaction is catalysed by an indole-3-acetalydehyde:$NAD^+$ oxidoreductase. In this mutant and in these growth conditions, it's possible that a similar $NAD^+$-dependent reaction is inhibited by the lack of $NAD^+$ and therefore indole-3-acetalydehyde accumulates. No other significant differences in metabolites of the tryptophan metabolic pathway were observed.

The concentrations of glycerone (dihydroxyacetone) and glyceraldehyde recorded outside the cells were reduced in FTD147h3 samples. Each of these metabolites can be produced through reactions that involve the reduction of $NAD^+$/$NADP^+$ (e.g. glycerone can be produced anaerobically by glycerol:$NAD^+$ 2-oxidoreductase, GldA), and therefore this reaction ceases or reverses in $NAD^+$-limited conditions. It is interesting, however, that the amounts of glycerone and glyceraldehyde are also reduced in FTD147 samples compared to MC4100 samples, suggesting that other factors are involved in the lower amount of these metabolites (perhaps

as a result of a build-up of pyruvate, which in turn results from the inability to dispose of formate in strains defective in formate hydrogenlyase activity).

Another interesting metabolite that showed significant changes between the samples was 2-butenoate (crotonic acid). The amount of this metabolite was reduced in the FTD147 and FTD147h3 samples compared to the MC4100 samples and this difference was statistically significant in both cases ($P = 0.0003$). The metabolism of 2-butenoate in *E. coli* is not well characterised, but it has been studied in various Clostridia species (Bader*, et al.*, 1980). In these organisms, the reduction of 2-butenoate is catalysed by a 2-enoate reductase, which oxidises NADH to $NAD^+$. Crotonic acid is associated with both L-carnitine production (Elssner*, et al.*, 2001) and glutamate fermentation (Buckel, 2001), as it is the precursor to crotonyl-CoA, which plays a key role in both pathways. Interestingly, the concentrations of (R)-3-hydroxybutanoate, itself a precursor to crotonyl-CoA in the glutamate fermentation pathway of various Clostridia species (Buckel, 2001), was higher in FTD147h3 samples than both FTD147 and MC4100 samples, indicating differential flux through these pathways. In a separate provisional metabolomics experiment, an increase in the amount of an unidentified metabolite was noticed in all Δ*adhE* mutant samples (Figure 3.21). This was tentatively identified as an analogue of carnitine ($C_{19}H_{40}N_3O_3$ or $C_{17}H_{36}N_3O_3$) through follow-up LC-MS analysis, adding weight to the hypothesis that carnitine metabolism is altered in these mutants.

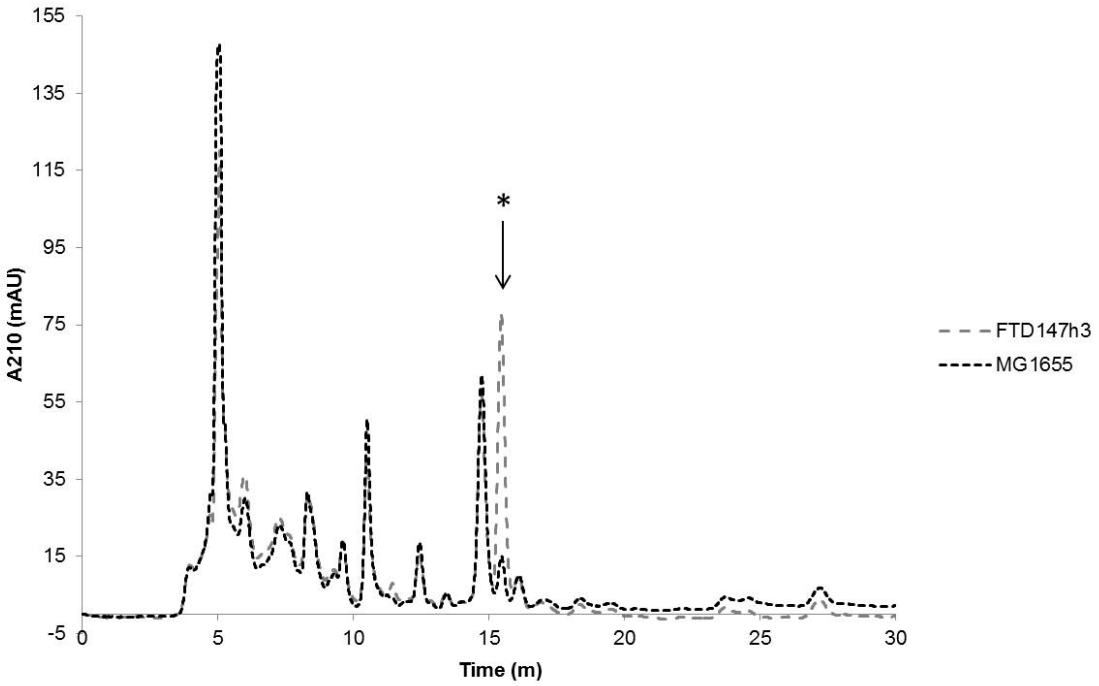


**Figure 3.21 An unknown metabolite found at a much higher level in Δ*adhE* mutant samples.** Test tubes filled with 16 ml L.B. + 0.4% (w/v) glucose were inoculated 1:1000 with MG1655 and FTD147h3 and cultures grown anaerobically. Cells were harvested by centrifugation at 4000 rpm before the culture supernatant was passed through a 0.2 µm filter and analysed by HPLC. For HPLC analysis, 5 µl of fermentation broth was separated at 0.7 ml $min^{-1}$ and 55 °C using a Dionex UltiMate 3000 HPLC system, fitted with an Aminex HPX-87H organic acid column and absorbance monitored at 210 nm. The asterix (*) denotes the mystery peak noticed in the spent media all Δ*adhE* mutant samples. This was analysed by non-targeted LC-MS and putatively identified as a carnitine analogue.

### 3.4.4 Redirection of metabolic flux towards increased acetate production

A large increase in acetate production was noticed in FTD147 and FTD147h3 samples (+/- pSUtat-Sh-GX-EF). One possible reason for this is implied by the lower amounts of 2-deoxy-D-ribose 5-phosphate, an intermediate in the pentose phosphate pathway, in the extracellular environment of both of these samples. In the cytoplasm, 2-deoxy-D-ribose 5-phosphate is cleaved into acetaldehyde and D-glyceraldehyde 3-phosphate by deoxyribose-phosphate aldolase, DeoC (Racker, 1952). The D-glyceraldehyde 3-phosphate produced can enter glycolysis or other metabolic pathways, while the acetaldehyde can be further oxidised to either acetate by an NADP-dependent acetaldehyde dehydrogenase, AldB (Ho and Weiner, 2005), or *via* a second acetaldehyde dehydrogenase, MhpF to acetyl-CoA (Ferrandez*, et al.*, 1997). Note that the latter reaction requires the oxidation of $NAD^+$ and is therefore unlikely in $NAD^+$-limited conditions. Presumably this excess acetate production is necessary for ATP production in these conditions. It is interesting, however, that a reduction in the concentration of 2-deoxy-D-ribose 5-phosphate and an increase in acetate is observed in FTD147 samples, which have functional AdhE. Perhaps the loss of $H_2$ production, or build-up of intracellular

formate, requires compensation in ATP production, again suggesting a link between formate efflux, influx or $H_2$ production and energy conservation.

### 3.4.5 Other changes in metabolite concentrations

Small amounts of 2-formylaminobenzaldehyde were found in the FTD147h3 samples. This is likely to result from the oxidation of indole, which is a derivative of tryptophan breakdown. Interestingly, this reaction, catalysed by an indole:oxygen 2,3-oxidoreductase, requires $O_2$ in other biological systems. The use of tryptophan as a nitrogen and/or carbon source by this mutant is likely. Another strange metabolite found in the FTD147h3 samples was pantothenol (dexpanthenol). This is usually used as a substrate in the pantothenate and CoA biosynthesis pathways, which is linked to the metabolism of various amino acids. The mechanism for its production in *E. coli* is unknown, however. Increasing the amount of pantothenol might therefore aid Coenzyme A production, which might be useful for the cell in these stressed conditions.

Two other metabolites were increased in FTD147h3 samples. The concentration of 2-hydroxyadenine (isoguanine) was approximately two and a half times that of the control sample. It is mutagenic to bacterial cells and therefore is normally quickly converted to xanthine by cytosine deaminase ($K_m$ for isoguanine: 72µM; $K_m$ for cytosine: 302 µM) (Hitchcock*, et al.*, 2011). The second metabolite found at much higher levels in the FTD147h3 samples was the aptly named traumatic acid. This metabolite is produced by many species of plants in response to wounding and has been shown to promote cell proliferation (Van Overbeek, 1940), but its production has not been characterised in *E. coli* previously. It was observed in cultures of *Ralstonia sp.*, which produce it from the oxidation of a fatty acid α-ketol (Schneider*, et al.*, 1997).

A number of metabolites were either completely absent or at lower concentrations in the FTD147h3 samples, yet found in large concentrations in the FTD147 and MC4100 controls. N-methyl-L-glutamate and allylcysteine were completely absent from FTD147h3 samples and adenylyl sulphate was found at much lower concentrations then the other two sample types. The lack of N-methyl-L-glutamate could be explained by either the consumption of all of this metabolite in order to produce L-glutamate and methylamine which could be used as a carbon and nitrogen source, or alternatively its consumption could be linked to the production of L-glutamate and formaldehyde. Both reactions are characterised in *Pseudomonas sp.* but not in *E. coli* (Shaw*, et al.*, 1966; Hersh*, et al.*, 1972). Allylcysteine is another poorly characterised metabolite, but is proposed to be produced from L-cysteine in combination with cyclopropene. It is found in high concentrations in the MC4100 samples and at half that concentration in the

FTD147 samples, but completely absent from the FTD147h3 + pSUtat-Sh-GX-EF samples. This is likely due to the consumption of L-cysteine to support the expression of the synthetic [FeFe]-hydrogenase and HydEFG, which puts a strain on both the cellular iron-sulfur cluster machinery and the raw materials required (e.g. iron and cysteine).

### 3.4.6 Improvements in the design of future experiments

First, MC4100 should have been used as the wild-type control for all experiments as both FTD147h3 and RaisynA1 are derivatives of this strain. For all growth, organic acid and metabolomics analysis, the use of a fully defined rich media such as the EZ Rich Defined Medium from Teknova would be preferential. As the HPLC experiments demonstrate, the starting concentrations of various carbon and nitrogen sources vary dramatically from one batch of LB to another. This would allow the results from these experiments performed on different days to be compared directly. This is not possible with results from experiments in this chapter using LB as different starting concentrations of a carbon sources such as succinate, could potentially influence the direction of metabolic flux in *E. coli* strains. Finally, the use of an anaerobic chamber for some of the procedures in these experiments would be advantageous. No loss of hydrogenase activity from cell lysates of FTD147h3, containing the synthetic [FeFe]-hydrogenase, would occur as a result of oxygen inactivation. $O_2$-sensitive metabolites would also be protected in this environment.

# 4. A synthetic chimeric metalloenzyme for hydrogen production

## 4.1 Introduction

### 4.1.1 Glycerol metabolism in *E. coli*

Glycerol has long been regarded as a "non-fermentable carbon source" in *Escherichia coli* K12 and was thought to require respiratory electron acceptors for its metabolism (Miki and Lin, 1973; Lin, 1976). A glycerol transporter GlpF (a member of the aquaporin [AQP] channel family) is known to transport glycerol into the cytoplasm (Stroud*, et al.*, 2003) where GlpK, a glycerol kinase encoded by an operon that includes *glpF*, phosphorylates glycerol in an ATP-dependent manner resulting in glycerol-3-phosphate (Glyc-3-P). Alternatively, Glyc-3-P itself can be used directly as a carbon source and transported into the cell by the UgpBAEC uptake system (Schweizer*, et al.*, 1982). Under aerobic or anaerobic respiratory conditions, Glyc-3-P is oxidised by one of two membrane-bound respiratory glycerol dehydrogenases: GlpD, the aerobic Glyc3PDH enzyme; or GlpABC, the anaerobic glycerol dehydrogenase, which is loosely attached to the cytoplasmic membrane). In both scenarios, dihydroxyacetone phosphate (DHAP; an intermediate compound in the Emden-Meyerhof glycolytic pathway) and quinol are the products of Glyc-3-P oxidation. DHAP can then be converted to D-glyceraldehyde 3-phosphate (G-3-P) by the enzyme triose-phosphate isomerase (TIM, encoded by *tpiA*).

### 4.1.2 Glycerol would be an ideal substrate for biohydrogen production

Glycerol is a potentially excellent carbon source for the production of biochemicals. Glycerol is the major waste product of biodiesel production (4.5 kg of glycerol *per* 45 kg of biodiesel) and bioethanol production (Yazdani and Gonzalez, 2007). Glycerol is now produced in such large quantities worldwide that its price has plummeted. If a sustainable carbon source could be used for the initial production of the fatty acids required for biodiesel production, glycerol would represent an even more attractive, affordable and sustainable substrate for commercial biochemical production. In addition, the higher degree of reduction ($_K$) of glycerol (4.7) compared to glucose (4) or other carbohydrate sources means that it has the potential to produce higher yields of highly reduced fermentation products such as ethanol and $H_2$, than other carbon sources.

### 4.1.3 A synthetic glycerol $H_2$-producing enzyme

It would be extremely advantageous to construct a synthetic, insulated pathway for hydrogen production from glycerol in *E. coli*. Such a pathway would ideally only produce hydrogen and be unable to reoxidise this hydrogen, and so should also avoid the possible inhibitory effects resulting from a high p($H_2$) atmosphere. One design strategy for such a synthetic pathway

might involve the construction of a non-natural hydrogen-producing enzyme, capable of accepting electrons from the oxidation of glycerol and subsequently reducing protons directly. Such an enzyme could be constructed from the fusion of two unrelated polypeptides, each of which catalyses the desired half reaction, i.e. quinol oxidation and $H_2$ production.

### 4.1.4 Properties of parts for construction of a synthetic glycerol-dependent $H_2$-producing enzyme

In order to construct a synthetic hydrogen-evolving enzyme that is capable of accepting electrons released during glycerol oxidation, individual components or parts with important properties are required. Firstly, such a synthetic enzyme must display the ability to accept electrons directly from the cytoplasmic membrane quinol pool and transfer these electrons to its target substrate efficiently. Thiosulfate reductase, a well-studied and characterised redox enzyme found in *Salmonella enterica* serovar Typhimerium (*Salmonella* hereafter), is an interesting candidate for use in the desired synthetic hydrogen-producing system as it fulfils a number of the requirements. The thiosulfate reductase enzyme complex is encoded by the *phs* operon (Figure 4.1A) and is a heterotrimer consisting of PhsA, PhsB and PhsC (Heinzinger*, et al.*, 1995). PhsA (83 kDa) is the molybdenum cofactor-containing catalytic subunit; PhsB (21 kDa) is an Fe-S cluster-containing electron transfer subunit; and the hydrophobic PhsC (28.5 kDa) subunit is a haem-containing integral membrane quinol dehydrogenase (Heinzinger*, et al.*, 1995). The PhsAB proteins are positioned at the periplasmic face of the cytoplasmic enzyme by the Tat translocase where they form the final complex with PhsC (Figure 4.1B). The enzyme is therefore tightly membrane-bound and capable of oxidising menaquinol, which is the preferred electron carrier from the anaerobic oxidation of either glycerol or formate (Stoffels*, et al.*, 2012), and transferring electrons to the terminal electron acceptor thiosulfate, thus producing sulphide (HS-) and sulphite. The *phs* operon can be expressed and the enzyme complex overproduced in *E. coli* with no loss in thiosulfate reductase activity (Bang*, et al.*, 2000).

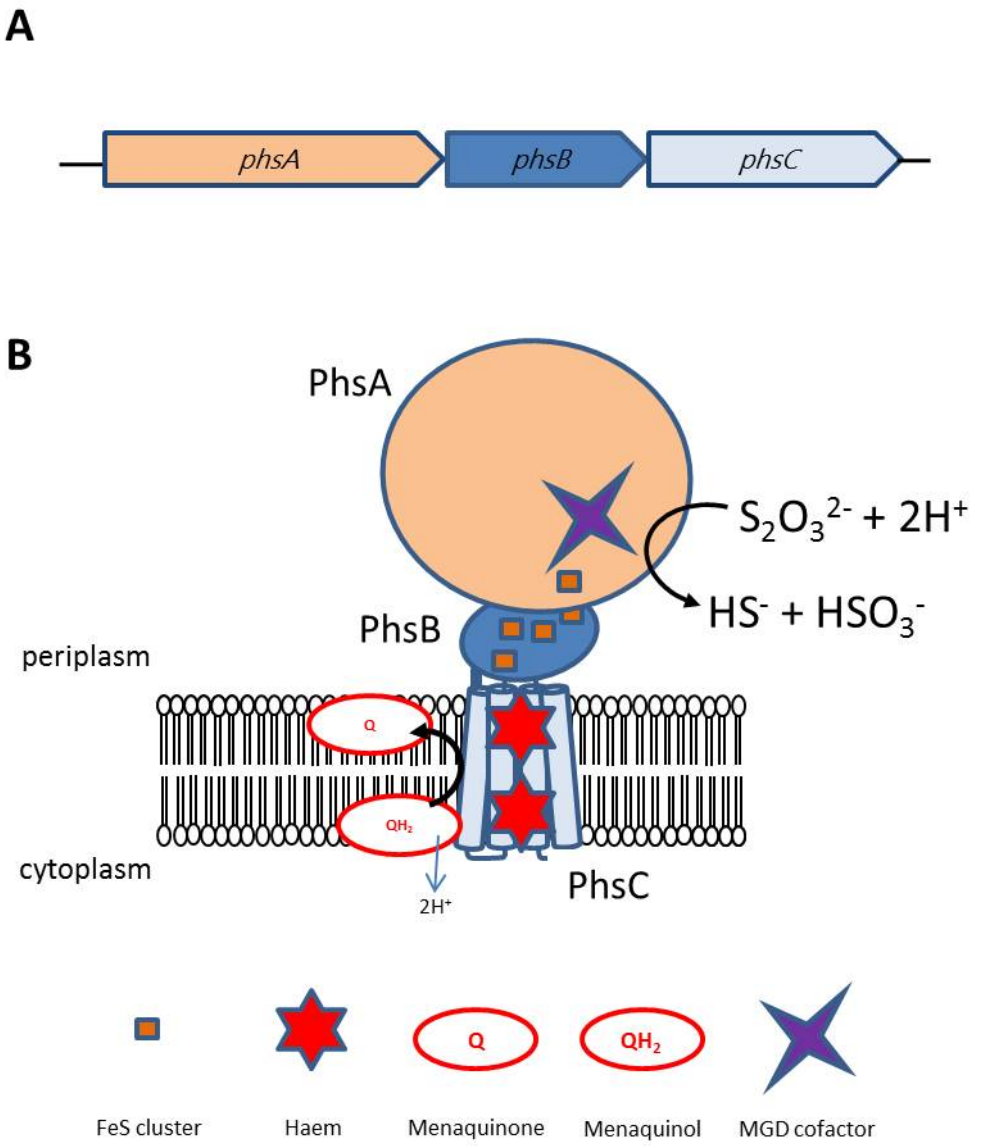


**Figure 4.1 A. The *phsABC* operon of *Salmonella* encodes thiosulfate reductase. B. PhsABC forms a heterotrimeric complex, which is capable of oxidising menaquinol and passing these electrons up an electrochemical potential gradient to reduce thiosulfate ($S_2O_3^{2-}$) to hydrogen sulphite ($HS^-$) and sulphide ($HSO_3^-$).**

It has been shown that thiosulfate reductase is capable of reducing thiosulfate when glycerol is the sole carbon source and is therefore unusually capable of catalysing a highly endergonic reaction (Stoffels*, et al.*, 2012). This ability to pass electrons up a thermodynamic gradient (difference in standard potential, $\Delta E^{0'}$, of menaquinol to thiosulfate under standard conditions = -328 mV) is made possible by the fact that thiosulfate reductase uses the transmembrane electrochemical gradient (or proton motive force [PMF]) to make up this energetic shortfall (Stoffels*, et al.*, 2012). It has been suggested previously that during thiosulfate respiration this PMF is primarily generated by the reverse reaction of the $F_1F_o$ ATP Synthase (Sasahara*, et al.*, 1997). The ability of PhsC to use PMF to drive electrons 'uphill' towards the active site in PhsA would be extremely desirable to have in a glycerol-dependent hydrogen-producing enzyme. The $H_2/2H^+$ couple has a standard potential ($E^{0'}$) of -421 mV (compared with an $E^{0'}$ of -402 mV for the $S_2O_3^{2-}/HS^- + SO_3^{2-}$ couple), therefore if it were possible to combine the menaquinol oxidation properties of thiosulfate reductase and the hydrogen-production activity of a hydrogenase active site in one fusion protein, it should in theory be able to pass electrons from the oxidation of glycerol to the reduction of protons. The final required property of an enzyme to catalyse the production of $H_2$ from glycerol is that it be capable of transferring electrons through FeS clusters to a hydrogen-producing active site at a fast rate. One of the three *E. coli* hydrogenases, Hyd-2, which normally oxidises $H_2$ has previously been shown to be capable of bidirectionality *in vitro*, high catalytic activity in highly reduced conditions, as well displaying low level of inhibition of $O_2$ when producing $H_2$ (Lukey*, et al.*, 2010). It was therefore hypothesised that a novel chimeric metalloenzyme constructed from *Salmonella* thiosulfate reductase and *E. coli* Hyd-2 could be capable of hydrogen production with glycerol as the sole electron donor and carbon source.

## 4.2 **Aims**

This Chapter aims to rationally design and construct a synthetic fusion metalloenzyme capable of accepting electrons from menaquinol generated through the oxidation of glycerol-3-phosphate. Ideally, this chimeric metalloenzyme must also be capable of passing electrons up an electrochemical potential gradient and ultimately reduce protons to produce $H_2$. The parts chosen to form this fusion enzyme are the thiosulfate reductase enzyme from *Salmonella* and hydrogenase-2 (Hyd-2) from *E. coli*. Construction of the fusion enzyme will be guided by structural and functional information available on both enzymes. Expression, stability, localisation and activity of the synthetic enzyme in the *E. coli* chassis will be fully characterised. Attempts to insulate, improve and optimise the synthetic glycerol-dependent hydrogen production pathway will also be performed.

## 4.3 **Results**

### 4.3.1 Examining *Salmonella* thiosulfate reductase as a suitable quinol dehydrogenase for $H_2$ production.

In collaboration with Dr. Jennifer S. McDowall, the genetic requirements for *in vivo* thiosulfate reduction were investigated. Various strains of *E. coli* were transformed with plasmid pAH2 (Stoffels*, et al.*, 2012), which encodes the *phsABC* operon from *Salmonella*, and assessed for thiosulfate reductase activity by their ability to produce iron sulphide (black precipitate), when grown anaerobically for two days in 5 ml PI media (peptone, iron and thiosulfate) cultures containing either formate (final concentration: 0.4% w/v) or glycerol (final concentration: 0.5% v/v) as additional carbon source. *E. coli* strains B1LK0 (as MC4100 Δ*tatC*) and FTD128 (as MC4100 Δ*fdhE*; demonstrated good iron sulphide production in preliminary PI plate experiments) were chosen as negative and positive controls respectively (Figure 4.2A). The addition of tungstate ($WO_4$) to the Δ*fdhE* strain was used to confirm the iron sulphide was the result of the activity of a molybdoenzyme, as excess tungstate can incorrectly inserted in place of molybdenum normally resulting in an inactive enzyme (Figure 4.2A).

It was previously shown that menaquinol was the electron donor for thiosulfate reductase and that the enzyme required PMF to function (Stoffels*, et al.*, 2012) and that the $F_1F_O$ ATP synthase was required (Sasahara*, et al.*, 1997). In agreement with these findings, iron sulphide production is abolished in Δ*menA/D/E* mutants (Figure 4.2B), which are required for the biosynthesis of the napthoquinones (Young, 1975; Kwon*, et al.*, 1996; Jiang*, et al.*, 2007) and in *atpC/D/G/H* mutants (Figure 4.2C), which form subunits of the $F_1$ complex of the $F_1F_0$ ATP synthase (Engelbrecht and Junge, 1990; Senior, 1990; Tang and Capaldi, 1996).

It was also shown recently that glycerol-dependent thiosulfate reductase activity was independent of $H_2$ metabolism (Stoffels*, et al.*, 2012). It was suggested, however, that the formate-dependent reduction of thiosulfate required $H_2$ as an intermediate in the electron chain between formate and thiosulfate and this claim was assessed using this experimental set up. The *E. coli* strain FTD147, lacking all the large catalytic subunits of each of the three *E. coli* hydrogenases (Hyd-1, 2 & 3) and a Δ*hypF* mutant, a maturation protein required for the activity of all three hydrogenases, both showed iron sulphide production, indicating thiosulfate reductase activity (although less iron sulphide was observed in the FTD147 sample).

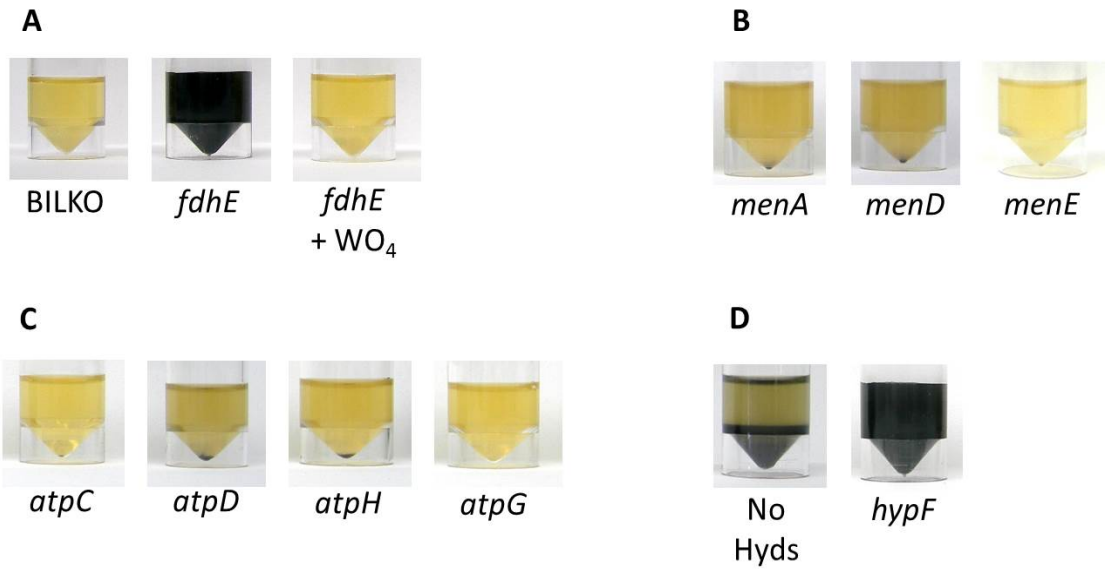


**Figure 4.2 Menaquinone and ATP synthase are essential for formate-dependent thiosulfate reduction, but $H_2$ metabolism is not.** Various strains of *E. coli* were transformed with plasmid pAH2, which encodes *phsABC* from *Salmonella*, and assessed for thiosulfate-reductase activity by their ability to produce iron sulphide (black precipitate), when grown anaerobically for two days in 5 ml PI media (peptone, iron and thiosulfate) cultures containing either formate (final concentration: 0.4% w/v) or glycerol (final concentration: 0.5% v/v) as the sole carbon source. **A.** *E. coli* strains BILKO (as MC4100 Δ*tatC*) and FTD128 (as MC4100 Δ*fdhE*; demonstrated good iron sulphide production in preliminary PI plate experiments) were chosen as negative and positive controls respectively. Tungstate was added to Δ*fdhE* strain to confirm iron sulphide production was specific to molybdenum-containing thiosulfate reductase. **B.** Genes involved in the menaquinone-biosynthesis pathway were shown to be essential for thiosulfate reductase activity. **C.** Genes encoding subunits of the F1F0 ATP synthase were shown to be essential for thiosulfate reductase activity. **D.** $H_2$ metabolism was shown to be non-essential for formate-dependent thiosulfate reductase activity.

### 4.3.2 The design and construction of a synthetic fusion metalloenzyme operon

Initially, the genes encoding the quinol dehydrogenase subunit of *Salmonella* thiosulfate reductase (PhsC) and the electron-transferring subunit PhsB were cloned into a medium-copy *E. coli* expression vector based on pUNI-PROM (Jack*, et al.*, 2004). The pUNI-CFM plasmid in question encodes an unusual fusion protein between the TorA signal peptide, chloramphenicol acetyl transferase, the FdnH transmembrane domain, and maltose binding protein. More importantly, this plasmid contains all the restriction sites necessary to build a Hyd-2/thiosulfate reductase fusion. The natural transcriptional/translational coupling between the *phsB* and *phsC* genes was maintained but the *Salmonella phsB* gene was amplified with a primer containing the DNA sequence that encodes a haemaglutinin (HA) epitope tag. The HA-*phsBC* PCR product was digested with NcoI and HindIII and replaced the *fdnH-malE* fragment in pUNI-CFM. This plasmid was termed pUNI-CPhs and encodes a fusion between TorA-CAT and PhsB *via* an HA linker. Next, the *hybO* gene encoding the *E. coli* Hyd-2 small subunit was amplified and used to replace the *torA-cat* allele as a BamHI-BspLU11I fragment. The HybO protein contains a twin-arginine signal peptide at its N-terminus and a transmembrane domain at its C-terminus. In order to attempt to tightly fuse HybO closely to the modified HA-PhsB polypeptide, HybO must be truncated sufficiently to remove this transmembrane helix but to retain its distal 4Fe-4S cluster. In this case two shortened versions of *hybO*, each with different lengths of 3'-end deletions, were cloned into pUNI-CPhs to produce the two final expression plasmids: pUNI-OSPhs (shortest version of HybO; Figure 4.3A); and pUNI-OLPhs (longer version of HybO; Figure 4.3B). The pUNI-PROM plasmid has two promoters upstream of its MCS, the well characterised $P_{T7lac}$ and the constitutive *E. coli* promoter $P_{tat}$, as well as a Shine Dalgano sequence from the *E. coli tatA* gene. The final plasmids would therefore encode a Tat-dependent fusion protein between HybO and PhsB. The final required catalytic subunit of the synthetic fusion Hyd-2/thiosulfate reductase complex is HybC, the catalytic subunit of Hyd-2. Rather than clone this gene as well, a host strain was designed that the pUNI-OSPhs and pUNI-OLPhs plasmids could be expressed in. An *E. coli* strain was constructed called IC011, which is based on MC4100 but carries Δ*hyaB*, Δ*hycE* and Δ*hybOA* alleles. The IC011 strain is therefore devoid of all endogenous hydrogenase activity but, because the Δ*hybOA* allele has been carefully designed in-frame, should still express the remaining *hybBCDEFG* genes of the operon encoding Hyd-2.

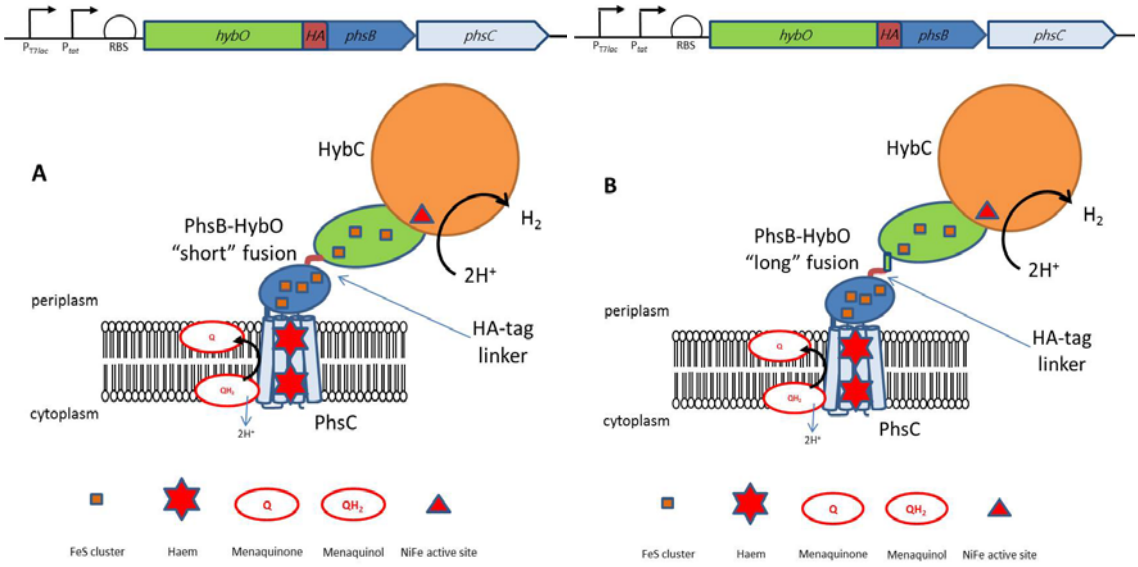


**Figure 4.3 The design and construction of synthetic chimeric metalloenzyme for $H_2$ production from glycerol in *E. coli*.** Two plasmids were constructed that encode a synthetic fusion protein consisting of *E. coli hybO* (the small subunit of Hyd-2) and *Salmonella phsB* (the small subunit of thiosulfate reductase). The two genes were cloned into pUNIPROM (constitutive promoter, $P_{tat}$; optimised RBS) with the sequence that encodes HA tag inserted between the penultimate codon of *hybO* and the second codon of *phsB*. The gene encoding the quinol dehydrogenase subunit of thiosulfate reductase, *phsC*, was cloned in after this fusion gene. **A.** pUNI-OSPhs encodes a shorter fusion protein with most of the C-terminal transmembrane helix removed. **B.** pUNI-OLPhs encodes a longer fusion protein with more of the C-terminal transmembrane helix remaining.

### 4.3.3 The synthetic chimeric metalloenzyme is expressed in *E. coli*

In order to validate that the newly constructed metalloenzyme chimeras were expressed in *E. coli*, radiolabelling experiments were performed. Expression of both the synthetic fusion gene (*hybO-HA-phsB*) and *phsC* was investigated using $^{35}$S-Methionine radiolabelling experiments. *E. coli* strain K38 (containing plasmid pGP1-2, a temperature-sensitive plasmid that encodes T7 polymerase) was transformed with either pUNI-OSPhs or pUNI-OLPhs and minimal M9 cultures lacking cysteine and methionine were labelled *in vivo* for 15 min by the addition of $^{35}$S-methionine. Samples were then analysed by SDS-PAGE (12% w/v polyacrylamide), fixed, and visualised by autoradiography (Figure 4.4A). Distinct prominent bands corresponding to the expected molecular weight of both the shorter fusion protein and the longer fusion protein were observed indicating that both fusion proteins are expressed in *E. coli*.

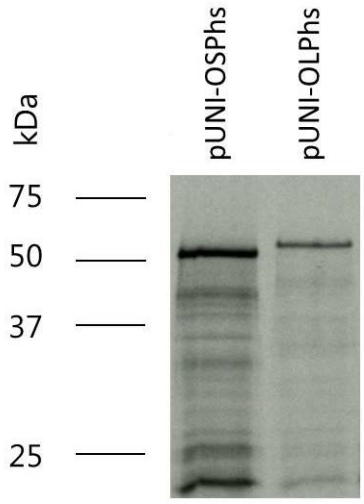


**Figure 4.4 Short and long HybO-PhsB fusion polypeptides are expressed.** $^{35}$S-methionine radiolabelling confirms expression and translation of the synthetic fusion *hybO-HA-phsB* gene. *E. coli* strain K38/pGP1-2 was transformed with plasmids: pUNI-OSPhs; or pUNI-OLPhs, and minimal M9 cultures lacking cysteine and methionine were labelled for 15 min by the addition of $^{35}$S-methionine. Samples were then separated on a 12% SDS-PAGE gel and visualised by autoradiography.

### 4.3.4 The synthetic chimeric metalloenzyme displays *in vitro* hydrogenase activity

Once expression of the synthetic gene encoding the chimeric metalloenzyme in *E. coli* was confirmed, it was now important to answer two essential questions. First, does the plasmid-encoded HybO interact with HybC to form an active enzyme? And second, is the complex transported to the periplasm? The BV-reduction assay can answer both of these questions. As the cytoplasmic membrane is only partially permeable to BV, $H_2$-dependent (equivalent to $H_2$ oxidation) BV reduction would indicate that some of the synthetic fusion enzyme complex has been successfully transported across the inner membrane to the periplasm.

The IC011 (Δ*hyaB*, Δ*hycE*, Δ*hybOA*) reporter strain was transformed separately with either pUNI-PROM, pUNI-OSPhs or pUNI-OLPhs and was assayed for hydrogenase activity using the artificial electron acceptor benzyl viologen (BV). Unbroken, whole-cell samples of IC011 [pUNI-OSPhs] catalysed the $H_2$-dependent reduction of BV with a specific activity of 10.8 ± 0.4 µmol $min^{-1}$ $mg^{-1}$ cells. In comparison, IC011 [pUNI-OLPhs] had a slightly lower activity of 8.7 ± 0.4 µmol $min^{-1}$ $mg^{-1}$ cells. IC011 cells transformed with the empty vector pUNI-PROM displayed only trace activity (Figure 4.5).

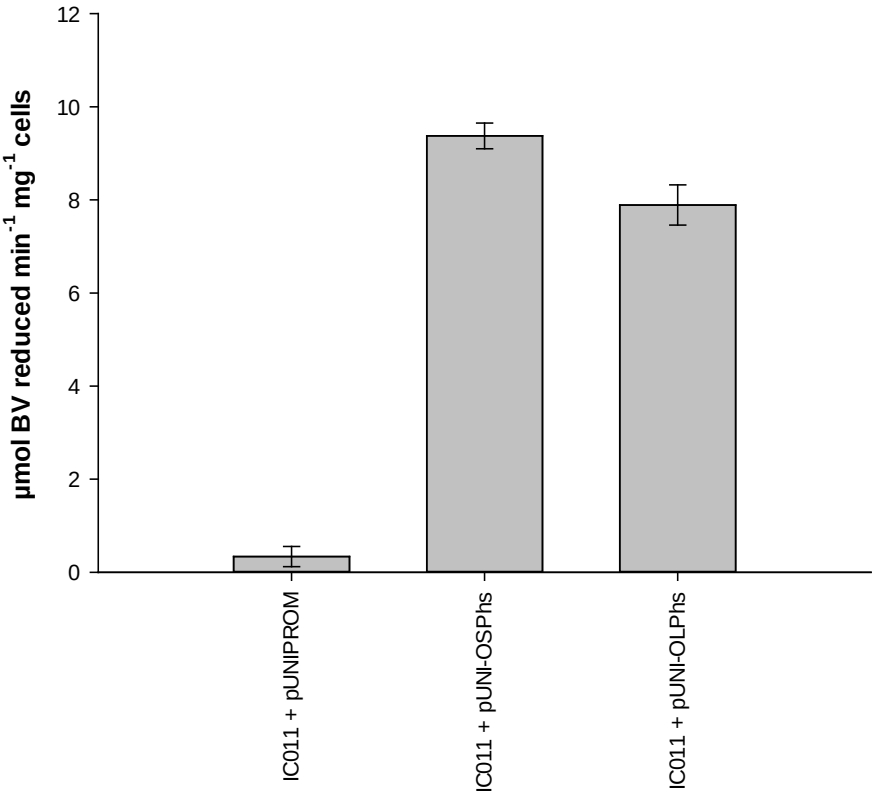


**Figure 4.5 Synthetic chimeric metalloenzyme displays *in vitro* hydrogenase activity.** Benzyl viologen (BV) reduction ($H_2$ oxidation) was monitored at 578 nm in a UV-vis spectrometer. 1 ml quartz cuvettes were filled with $H_2$-saturated buffer (50 mM Tricine pH 8.0) and 13 mM BV. This was titrated with sodium dithionite to an absorbance of 0.4 - 0.7 and the reaction started by the addition of 500 µg of IC011 whole cells expressing either pUNIPROM; pUNI-OSPhs; or pUNI-OLPhs. Error bars represent the standard error of biological replicates

### 4.3.5 The synthetic chimeric metalloenzyme can produce $H_2$ in a glycerol-dependent manner

Next, the synthetic chimeric metalloenzyme was tested for its ability to generate hydrogen when coupled to glycerol-3-phosphate respiration. The IC011 strain harbouring either pUNI-OSPhs or pUNI-OLPhs was grown anaerobically in rich media supplemented with glycerol and fumarate before being harvested and washed under anaerobic conditions. Intact cell samples were introduced into a Clark-type electrode (modified for $H_2$ measurement) and following a period of equilibration, excess glycerol (170 mM final concentration) was added (Figure 4.6). No external electron acceptors were added to the reaction chamber. Under these conditions the IC011 [pUNI-OSPhs] whole cell sample slowly produced hydrogen (22 nmol over ~100 minutes). $H_2$ production notably ceased after approximately 90 minutes, and the rates and durations of $H_2$ production were less in the strain harbouring the pUNI-OSPhs plasmid. IC011 whole cells transformed with pUNI-PROM were assayed as a control and produced no $H_2$ from glycerol, confirming that all of the $H_2$ observed was indeed from the synthetic chimeric metalloenzyme.

When the amount of IC011 + pUNI-OSPhs cells added to the reaction chamber was doubled, the rate and total amount of $H_2$ produced increased and $H_2$ production was sustained for longer. This result demonstrated that the availability of glycerol was not the limiting factor but instead cessation of $H_2$ production must be linked to an internal cellular factor such as depletion of ATP reserves or an inability to generate a proton motive force (PMF). Finally, the synthetic chimeric metalloenzyme was shown to be unable to reoxidise the $H_2$ produced from glycerol, as the addition of a terminal electron acceptor did not reduced the amount of $H_2$ in the reaction chamber (data not shown).

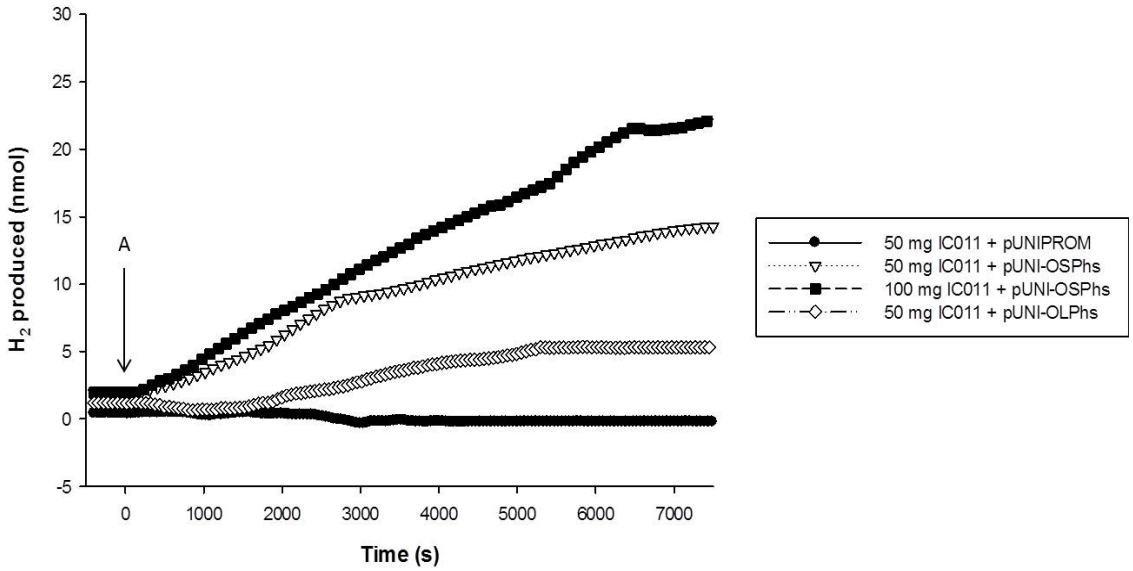


**Figure 4.6. Either version of the synthetic chimeric metalloenzyme is capable of producing $H_2$ directly from glycerol.** Cells were grown for 16 h overnight at 37° C in sealed, stationary 500 ml Duran bottles, containing 500 ml Luria Broth supplemented with 0.5% (v/v) glycerol and 0.4% (w/v) fumarate. Cells were harvested by centrifugation, washed twice in anaerobic buffer (100 mM sodium phosphate, pH 6.8) to remove any trace of growth media, glycerol and fumarate, and resuspended in 2 ml of the same anaerobic buffer per 1 g of cells (wet weight). Assays were carried out using a modified Clark-type electrode (Hansatech Oxygraph). 2 ml of the same anaerobic buffer was added to the reaction chamber and 50 mg of either IC011 + pUNI-PROM (full circle), IC011 + pUNI-OSPhs (open triangle) or IC011 + pUNI-OLPhs (open diamond) whole cells were added. After equilibration, glycerol at a final concentration of 170 mM was added to the reaction chamber (point A; t = 0 s). $H_2$ production was measured by following the current generated following calibration with known amounts of $H_2$. These results show that both the short and long fusion enzyme versions are capable of producing $H_2$ directly from glycerol. The experiment was also performed with the addition of 100 mg of IC011 + pUNI-OSPhs (full square). Representative traces of each sample type are shown.

### 4.3.6 The design and construction of new fusion proteins with alternative peptide linkers

The original plasmids were constructed with a HA-tag linker between PhsB and the truncated HybO. It has been shown recently that varying the length and amino acid composition of the linker can radically alter the properties of fusion proteins (Agapakis*, et al.*, 2010; Chen*, et al.*, 2012). The original HA-tag linker (YPYDVPDYA) of pUNI-OSPhs was therefore replaced with a variety of different peptide linkers to try and improve the stability and activity of the fusion enzyme (Figure 4.7).

It has previously been shown that the optimum distance for spontaneous electron transfer between redox-active centres is 10 - 15 Å (Page*, et al.*, 1999; Page*, et al.*, 2003; Fritsch*, et al.*, 2011). Thus one of the keys to efficient operation of this fusion protein is finding the optimum distance between the PhsB and HybO Fe-S clusters. In order to reduce the distance between the hypothetical N-terminal 4Fe-4S cluster of PhsB (the structure of this protein is not known) and the distal 4Fe-4S cluster of HybO, the sequence encoding the HA-tag linker was replaced with a Sal I restriction enzyme site, which encodes the amino acid sequence EL (Figure 4.7B). The resulting plasmid pUNI-OSSalIPhs should encode a fusion protein where the two subunits are held in a tight rigid conformation with the N- and C-termini of the proteins in the closest possible proximity to each other. Two fusion proteins were next constructed which had well characterised flexible linkers instead of the HA-tag linker. The first of these plasmids, pUNI-OSFlexAPhs, encodes the fusion protein with the flexible linker, GGGGS (Figure 4.7C). The small non-polar glycine residue allows flexibility, therefore allowing these Fe-S cluster-containing subunits to move around, which might be important for efficient electron transfer. The addition of a small polar serine residue is thought to increase solubility of fusion proteins and help stabilise the linker in aqueous solutions (Chen*, et al.*, 2012). The second of these plasmids, pUNI-OSFlexDPhs, encodes the fusion protein with the flexible linker, GGGGGGGG (Figure 4.7D). The next plasmid constructed was pUNI-OS-6aaFLexAPhs and it encodes the same GGGGS flexible linker as used in the FlexA version, but encodes a further truncated version of HybO. Six codons at the 3'-end of the already-shortened *hybO* gene were deleted, which should result in a fusion with PhsB that is very close to the final cysteines predicted to ligate the distal 4Fe-4S cluster of HybO (Figure 4.7E). Finally, in the course of plasmid construction, a derivative of pUNI-OSPhs was isolated with the full *hybOS-HA-phsB* sequence but with mutations in a number of locations in the vector backbone (pUNI-$OS_{mut}$Phs).

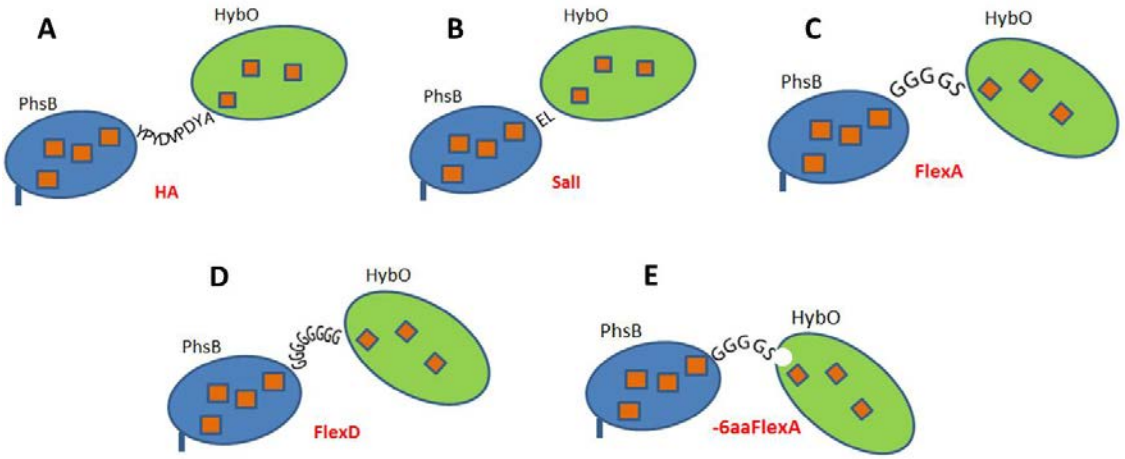


**Figure 4.7 The design of new linker peptides between HybO and PhsB. A.** The original linker peptide used to fuse HybO and PhsB was a *H. influenza* haemaglutinin (HA) tag. A variety of different peptide linkers were selected to replace the HA tag: **B.** a short linker consisting of just two amino acids (EL); **C.** a flexible linker consisting of glycines and a serine residue (GGGS); **D.** a longer flexible linker consisting of just glycines (GGGGGGGG); and **E.** the flexible linker GGGGS was used in the construction of a new fusion protein with a further truncation of the C terminus of HybO.

### 4.3.7 Expression and stability of the synthetic chimeric metalloenzyme with alternative peptide linkers

The expression of the newly constructed metalloenzyme chimeras with alternative peptide linkers was tested in *E. coli* using $^{35}$S-Methionine radiolabelling. The *E. coli* strain K38 (containing plasmid pGP1-2, a temperature-sensitive plasmid that encodes T7 polymerase) was transformed separately with pUNI-OS$_{mut}$Phs, pUNI-OSSalIPhs, pUNI-OSFLexAPhs, pUNI-OSFlexDPhs or pUNI-OS-6aaFlexAPhs. Cultures of M9 minimal medium lacking cysteine and methionine were labelled *in vivo* for 15 min by the addition of $^{35}$S-methionine. Samples were then analysed by SDS-PAGE (12% w/v polyacrylamide), fixed, and visualised by autoradiography (Figure 4.8). Distinct prominent bands corresponding to the expected molecular weight of OSFlexAPhs and OS-6aaFlexPhs (identical to OSPhs) were observed indicating that both fusion proteins are expressed in *E. coli*. No band corresponding to the expected molecular weight of OSSalIPhs was observed, however a prominent band at approximately 34 kDa and a much fainter band at approx. 100 kDa could be seen. pUNI-OSFlexDPhs did not appear to be expressed correctly in *E. coli* as no bands could be detected. Finally, the pUNI-OS$_{mut}$Phs plasmid expressed the main HybO-Phs fusion protein as in pUNI-OSPhs, however another prominent band at approximately 36 kDa and numerous bands of lower molecular weight were also detected. Indeed numerous shorter proteins were expressed in all samples except pUNI-OSFlexDPhs.

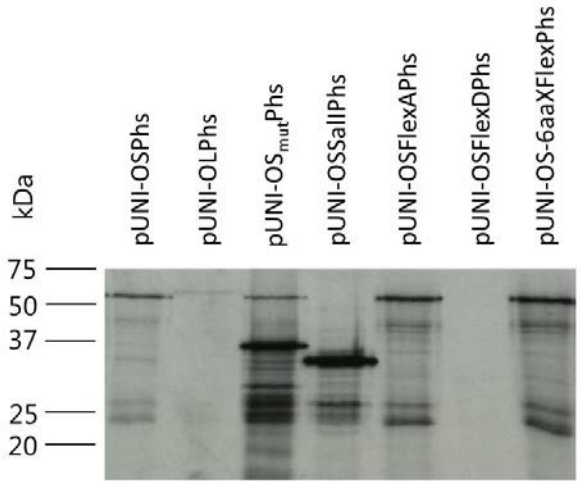


**Figure 4.8 Expression and stability of the new linker fusion enzyme genes in *E. coli*. A.** $^{35}$S-methionine radiolabelling confirms expression and translation of three of the new linker *hybO-phsB* genes in *E. coli*. *E. coli* strain K38/pGP1-2 was transformed with plasmids: pUNI-OSPhs; pUNI-OLPhs; pUNI-OSmutPhs; pUNI-OSSalIPhs; pUNI-OSFlexAPhs; pUNI-OSFlexDPhs; or pUNI-OS-6aaFlexPhs, and minimal M9 cultures lacking cysteine and methionine were labelled for 15 min by the addition of $^{35}$S-methionine. Samples were then run on a 12% SDS-PAGE gel and visualised by autoradiography.

Next, whole cell BV-linked hydrogenase activity was determined (Figure 4.9). IC011 cells transformed with the FlexA, $OS_{mut}$ or SalI plasmid variants displayed slight increases in $H_2$-dependent BV reduction activity compared to the OS plasmid. The FlexD variant as expected showed trace activity, however the -6aaFlex variant only showed trace activity.

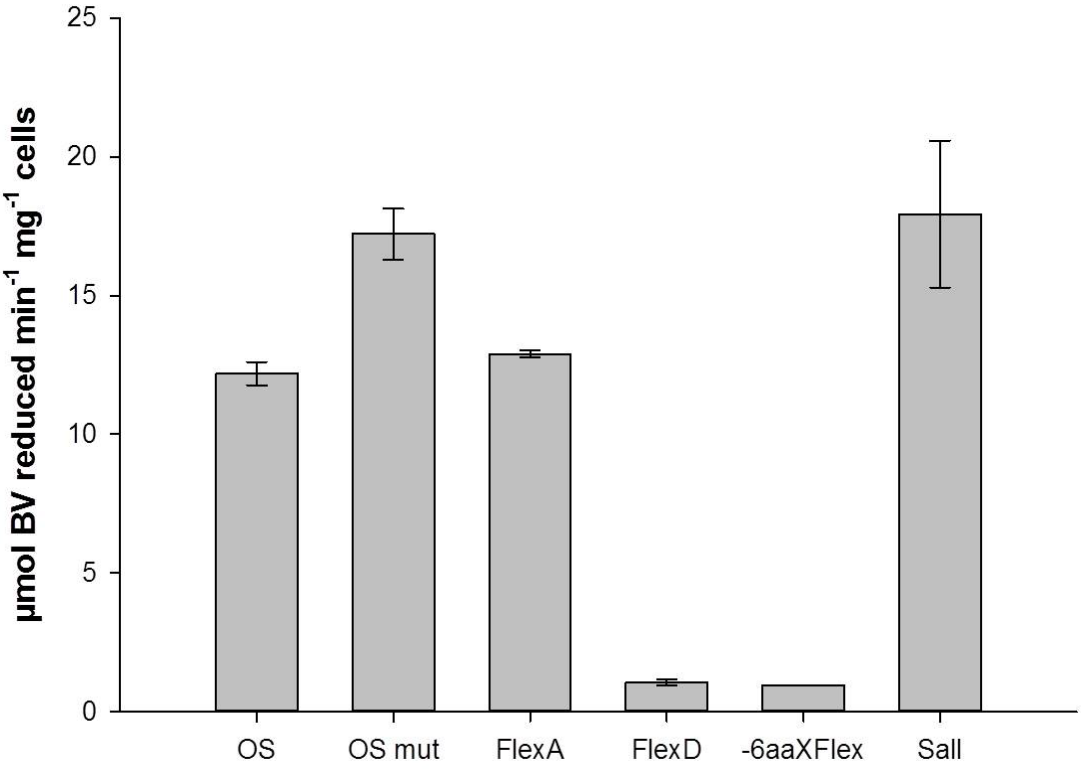


**Figure 4.9 Three of the new linker-peptide versions of the synthetic chimeric metalloenzyme operons show *in vitro* hydrogenase activity.** Benzyl viologen (BV) reduction ($H_2$ oxidation) was monitored at 578 nm in a UV-vis spectrometer. 1 ml quartz cuvettes were filled with $H_2$-saturated buffer (50 mM Tricine pH 8.0) and 13 mM BV. This was titrated with sodium dithionite to an absorbance of 0.4 - 0.7 and the reaction started by the addition of 500 µg of IC011 whole cells expressing either pUNIPROM; pUNI-OSPhs; pUNI-OLPhs; pUNI-OSmutPhs; pUNI-OSSalIPhs; pUNI-OSFlexAPhs; pUNI-OSFlexDPhs; or pUNI-OS-6aaFlexPhs. Error bars represent the standard error of three biological replicates.

### 4.3.8 Localisation of the synthetic chimeric metalloenzymes with alternative peptide linkers

The subcellular localisation of the synthetic chimeric enzymes was analysed using rocket immunoelectrophoresis. The *E. coli* strain IC011 was transformed separately with pUNIPROM (Uni; negative control), pUNI-OSPhs (OS), pUNI-OSSalIPhs (SalI), pUNI-OSFlexAPhs (FlexA), pUNI-OSFlexDPhs (FlexD), pUNI-$OS_{mut}$Phs ($OS_{mut}$) or pUNI-OS-6aaFlexAPhs (-6aaXFlex) and transformants used to inoculate 500 ml anaerobic LB cultures supplemented with glycerol, fumarate and appropriate antibiotics, which were incubated at 37 °C for ~16 h. Cultures were centrifuged and cell pellets used for subcellular fractionation. Cytoplasmic and membrane fractions were isolated and the membranes solubilised using Triton X-100. Cytoplasmic and solubilised membrane samples were then analysed for the presence of active enzyme by rocket immunoelectrophoresis. Samples were separated on a non-denaturing agarose gel containing HybOC antisera, which binds to the corresponding protein as it migrates and eventually stalls its progress. These gels can then be stained for $H_2$-dependent BV-reduction activity in the presence of triphenyl tetrazolium chloride (tetrazolium red; an irreversible redox dye). These experiments give qualitative information on the presence and amount of active enzyme in the specific cellular fractions.

Membrane samples prepared from the OS, FlexA, SalI and $OS_{mut}$ cultures displayed a small amount Hyd-2, indicating that these metalloenzyme chimeras were successfully assembled in the membrane (Figure 4.10A). The corresponding cytoplasmic fractions, however, also contained very large amounts of active enzyme (Figure 4.10B). The membrane and cytoplasmic fractions of FlexD, -6aaXFlex and Uni samples were negative.

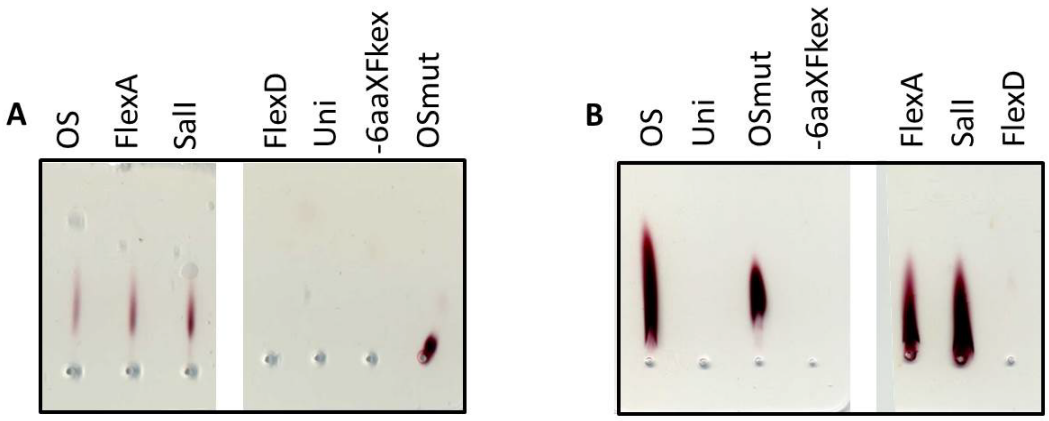


**Figure 4.10 OS, FlexA, SalI and OSmut chimeric metalloenzymes were successfully transported across and inserted into the cytoplasmic membrane. A.** Membrane and **B.** cytoplasmic fractions of overnight 500 ml anaerobic cultures of IC011 transformed with either pUNI-OSPhs, pUNI-OSFlexAPhs, pUNI-OSSalIPhs, pUNI-OSFlexDPhs, pUNIPROM, pUNI-OS-6aaXFlexPhs or pUNI-OSmutPhs plasmids, were analysed by rocket immunoelectrophoresis. Samples were separated for ~8 h on non-denaturing agarose gels containing α-HybOC antibody (A: antibody was diluted 1 in 2 with running buffer before adding to agarose gel; B: antibody was undiluted before adding to agarose gel). Upon completion, each gel was incubated in 25 ml of $H_2$-saturated buffer containing 600 mg BV and 700 mg tetrazolium red and stained for 24 h before photographing.

### 4.3.9 Increasing or maintaining the PMF through heterologous expression of a proteorhodopsin increases $H_2$ production

The data presented in Figure 4.6 show a slow rate of $H_2$ production that tails off and stops. This is similar to what has been observed for the activity of the native thiosulfate reductase as it reaches, what is thought to be, a thermodynamic equilibrium (Stoffels *et al*. 2012). The hypothesis that the production of $H_2$ by the synthetic chimeric metalloenzyme was close to thermodynamic equilibrium was tested by attempting to increase or maintain the proton motive force (PMF) at the cytoplasmic membrane and then monitoring any changes in $H_2$ production activity. A metagene encoding a proteorhodopsin from an uncultured marine γ-proteobacterium was recently discovered and when expressed heterologously in *E. coli* was shown to pump protons, thus increasing PMF in *E. coli* (Tipping*, et al.*, 2013). The gene encoding this proteorhodopsin (PR) was amplified by PCR and cloned into the medium copy *E. coli* expression vector, pSUPROM, which gives constitutive transcription of the PR gene from the *tat* promoter. The resulting plasmid was named pSU-PR.

IC011 cells were co-transformed with pUNI-OSPhs and pSU-PR plasmids and transformants used to inoculate two 500 ml anaerobic LB cultures supplemented with glycerol and fumarate. All-trans retinal, the cofactor necessary for an active proteorhodopsin, is not normally produced by *E. coli*, however it can be supplied exogenously to the culture media and taken up by the cell. All-trans retinal was therefore supplied to one of these cultures and omitted from the other (as a negative control) and both were incubated without shaking at 37 °C for ~ 16 hours in complete darkness (to protect the light-sensitive cofactor). All subsequent steps were performed in complete darkness unless otherwise stated and black light-proof Falcon™ tubes used. Cells were harvested, washed twice in anaerobic buffer and resuspended in anaerobic buffer (100 mM sodium phosphate buffer, pH6.8). The cells that received all-trans retinal were pink in colour indicating the successful expression of the proteorhodopsin and incorporation of the cofactor.

Intact cell samples were introduced into a Clark-type electrode chamber, modified for $H_2$ measurement. Following a period of equilibration, the chamber was illuminated for 10 minutes before an excess of glycerol (170 mM final concentration) was added and the reaction allowed to continue in light until completion. As shown in Figure 4.11, the sample containing no all-trans retinal ('no ret') produced 25 nmol $H_2$ over ~ 40 minutes, whereas the sample containing all-trans retinal ('plus ret') produced more than twice the total amount of $H_2$ and sustained $H_2$ production for longer (60 minutes) (Figure 4.11).

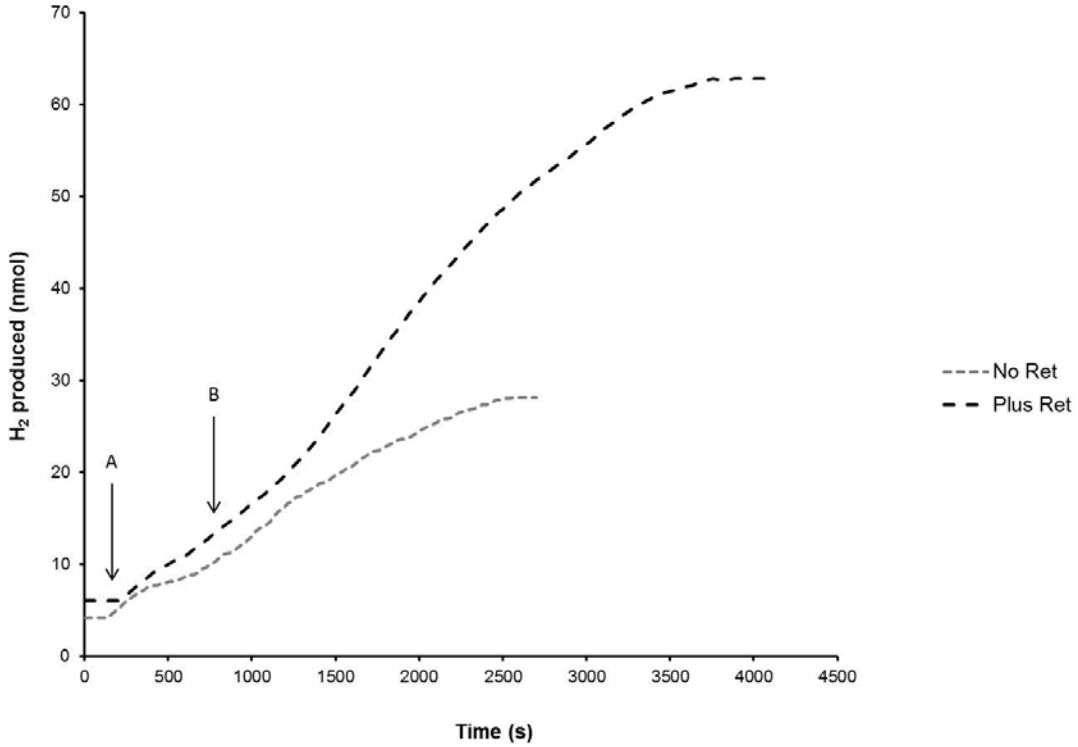


**Figure 4.11 Increasing or maintaining the PMF improves $H_2$ production from synthetic chimeric metalloenzyme.** Cells were grown for 16 h overnight at 37° C in sealed, stationary 500 ml Duran bottles, containing 500 ml Luria Broth supplemented with 0.5% (v/v) glycerol and 0.4% (w/v) fumarate and with/without exogenous all-trans retinal. Cells were harvested by centrifugation, washed twice in anaerobic buffer (100 mM sodium phosphate, pH 6.8) to remove any trace of growth media, glycerol and fumarate, and resuspended in 2 ml of the same anaerobic buffer per 1 g of cells (wet weight). Assays were carried out using a modified Clark-type electrode (Hansatech Oxygraph). 2 ml of the same anaerobic buffer was added to the reaction chamber and 50 mg of IC011 + pUNI-OSPhs + pSU-PR plus/minus all-trans retinal added. After equilibration, the reaction chamber was illuminated for 10 m (point A) before glycerol (at a final concentration of 170 mM) was added to the reaction chamber (point B). $H_2$ production was measured by following the current generated following calibration with known amounts of $H_2$. These results show that increasing the PMF through the heterologous expression of a PR (with required cofactor) is sufficient to increase the amount of $H_2$ produced. Representative traces of each sample type are shown.

## 4.4 **Discussion**

### 4.4.1 Rational design of polypeptides – *in silico*

The rational design of protein domains, long polypeptide chains and ultimately useful functional proteins and enzymes has been a long standing aim of many research groups around the globe. Many groups over the last 15 years have attempted to computationally design artificial enzymes with novel functions. This difficult and highly controversial research area has seen a mixture of successes and failures. The most fundamental requirement for successful *in silico* rational protein design is the development of sophisticated software programs to create accurate models of these artificial proteins based on information in structural databases. This should then be followed by construction of a number of protein models, rigorous characterisation of these artificial proteins and finally the improvement of the original software by feeding back the characterisation data.

In a series of important papers at the start of this century, the lab of Homme Hellinga at Duke University claimed the successful design and construction of artificial enzymes using the computer software DEZYMER. In one of these studies, they used DEZYMER to design the introduction of iron and oxygen binding sites into a thioredoxin scaffold (Benson*, et al.*, 2000). The data showed tight binding of $O_2$ and high specific activity. However in recent years a number of papers from the Hellinga lab, using the same DEZYMER software have been challenged by other research groups who saw no specific binding of these rationally-designed proteins to their supposed ligands/substrates (Schreier*, et al.*, 2009). These papers used more accurate methods to test binding and specific activity, including isothermal titration calorimetry (ITC) and nuclear magnetic resonance (NMR) spectroscopy, which showed no direct/specific binding to any of the protein constructs tested. This has led to the retraction of a number of high profile papers based on this software (Dwyer*, et al.*, 2004).

In a more successful example of rationally designed artificial metalloenzymes, a “designed evolution” approach was adopted, which combines rational design with combinatorial screening (Creus and Ward, 2007). In this study, proteins such as biotin-streptavidin or biotin-avidin were used as scaffolds to hold a diverse range of metal catalysts including non-biological metals such as rhodium. This introduces the possibility of novel catalytic reactions that are not currently found in nature. Libraries of the protein scaffold, protein linker and ligand scaffold can all be screened to optimise activity, selectivity, or stability etc. and thus was described as a “chemogenetic approach”.

However the success *in silico* design of proteins with novel functions is still an unsolved challenge. In a recently published study, the computer program ROSETTA was used to attempt to introduce a D-ala-D-ala binding pocket in an existing protein scaffold (Morin*, et al.*, 2011). Twelve resulting proteins were constructed and characterised and although structurally the designed proteins were as predicted by the software, none of the 12 proteins showed high affinity binding to the target ligand. It is clear, therefore, that the software used in the *de novo* design of proteins requires further development and validation until it reaches the level of reliability necessary to form the backbone of rational protein design projects. Perhaps a better approach for the construction of synthetic enzymes with novel functions is to take existing and well characterised enzymes and construct chimeras of these enzymes using a variety of different protein engineering techniques.

### 4.4.2 Rational design of enzymes - fusion

One of the most famous and earliest examples of a successful construction and application of a fusion protein came from the group of Greg Winter in Cambridge (Riechmann*, et al.*, 1988). They took a human IgGI antibody and replaced the hypervariable regions with those from a rat antibody raised directly against human lymphocytes and the resulting “humanised” antibody (named Campath-1H) showed great efficacy as a clinical therapeutic against lymphoma. Another early example of a fusion protein involved the fusion of the *lacZ* and *galK* genes of *E. coli*. The resulting soluble bifunctional enzyme catalysed both lactose hydrolysis and the phosphorylation of galactose as normal (Bulow, 1987).

More recently a number of more sophisticated approaches to the construction of fusion enzymes have been described. The exponential growth of available protein sequence and structural data allows for greater cognizant design of fusion proteins. Traditionally fusion hydrogenases were constructed in an end-to-end fashion, i.e. the C-terminus of one polypeptide is fused to the N-terminus of the other polypeptide (or vice versa). However if structural knowledge is available, the catalytic domain of one enzyme can be introduced into a non-essential or disordered region of another enzyme, hopefully resulting in a bifunctional enzyme. This approach was used to generate a chimeric bifunctional laccase/gluconase enzyme with improved activity than the wild type enzymes (Furtado*, et al.*, 2013). In a similar recent study, a single-chain protein was constructed from the well characterised and tight-binding rapamycin-binding domain (resulting polypeptide named uniRapR). This synthetic polypeptide was then inserted into a known site of a well characterised kinase (Dagliyan*, et al.*, 2013). The phosphorylation activity of resulting fusion kinase can then be regulated by the binding of rapamycin to the uniRapR domain and this was demonstrated with molecular

dynamics experiments as well as enzymatic activity assays. These examples highlight the successful fusion of two unrelated polypeptides, which linked up both catalytic activities.

Some examples of fusion hydrogenases exist in the literature. In a nice study by the Silver group at Harvard, the [FeFe]-hydrogenase of *Clostridium acetobutylicum* was fused to the ferredoxin from *Spinacea olearcea* and hydrogen production compared to strains expressing both proteins in their non-fused form (Agapakis*, et al.*, 2010). In this study they also systematically altered the length of amino acid linker between the two proteins to increase hydrogenase activity *in vivo*. In an earlier study by another research group, the membrane-bound [NiFe]-hydrogenase of *Ralstonia eutropha* H16 was fused to Photosystem I of the cyanobacteria *Thermosynechococcus elongatus* (Ihara*, et al.*, 2006). This introduced a novel and direct light-to-hydrogen conversion system.

### 4.4.3 A functional synthetic chimeric metalloenzyme for hydrogen production in *E. coli*

In this work a synthetic chimeric metalloenzyme was designed and constructed that was capable of producing hydrogen in an engineered *E. coli* when glycerol was the sole carbon source. The quinol-dehydrogenase and electron-transfer subunits of thiosulfate reductase from *Salmonella* were identified as attractive candidate parts for the synthetic enzyme. Thiosulfate reductase from *Salmonella* is unusually capable of passing electrons up a thermodynamic gradient (Stoffels*, et al.*, 2012) of approximately the same magnitude as would be required to produce hydrogen from menaquinols. It achieves this through its utilisation of the PMF.

In this chapter, it has been shown that $H_2$ oxidation is not essential for electron transfer between formate dehydrogenase (Fdh-O) and the native thiosulfate reductase, as neither a strain devoid of all hydrogenase large subunits (HyaB, HybC and HycE), nor a strain devoid of an essential hydrogenase maturase, HypF, was negative for iron sulphide production in PI indicator media. This is contrary to a previous suggestion (Stoffels*, et al.*, 2012).

Hydrogenase-2 from *E. coli* was an attractive enzyme to mine for the parts required to firstly accept and transfer electrons from the thiosulfate reductase subunits, and finally to reduce protons to molecular hydrogen, as it displays bidirectionality when immobilised to a graphite electrode (Lukey*, et al.*, 2010). These parts from two different organisms were successfully combined to produce a novel, rationally-designed synthetic metalloenzyme. The genes encoding this synthetic enzyme are expressed in *E. coli*, the HybO-PhsB fusion polypeptide is at least partly successfully transported across the cytoplasmic membrane *via* the twin-arginine translocation (Tat) machinery and the subunits form an active complex in the cytoplasmic

membrane. This synthetic enzyme shows unidirectional $H_2$-producing activity, demonstrating that the catalytic bias is radically different to the original *E. coli* Hyd-2 enzyme.

It would be interesting to characterise this synthetic fusion hydrogenase further. Purification of the fusion enzyme would give valuable information on the size, stability and oligomeric state of the entire PhsC-HybOPhsB-HybC complex. If the fusion could be additionally affinity-tagged, IMAC, size-exclusion chromatography and SEC-MALLS could be employed to this end. If successful, the purified enzyme could be entered into crystallisation studies to obtain structural information on the complex. An alternative approach would be to clone and express only the HybO-PhsB fusion gene in an *E. coli* strain lacking the Tat machinery (e.g. DADE). This fusion protein could then be purified and entered into crystallisation studies. This should result in a stable, soluble protein of reduced hydrophobicity, which is desirable in crystallisation studies, as well as removing the requirement for detergents during purification. The information garnered could then be used to design improved versions of the synthetic chimeric metalloenzyme.

### 4.4.4 A novel insulated synthetic glycerol-dependent $H_2$ production pathway in *E. coli*

The introduction of this synthetic chimeric enzyme into a previously engineered *E. coli* strain with no hydrogenases at all (IC011), allowed $H_2$ production to occur when glycerol was the sole carbon source. This is very exciting as glycerol is a cheap and attractive substrate for commercial $H_2$ production. The conversion of glycerol to $H_2$ in this system is however extremely inefficient, as 8.6 mmoles of glycerol added produced only 22 nmoles of $H_2$. It should be noted that anaerobic glycerol metabolism might also produce some formate, which itself could be used as a respiratory electron donor by FdoGHI in this system.

### 4.4.5 Energy depletion as a limiting factor

The collapse of the cytoplasmic membrane PMF, which allows the transfer of electrons from PhsC to the [NiFe] active site of HybC, is the most likely reason for $H_2$ production to cease in this system. The boosting of PMF through the heterologous expression of a proteorhodopsin (PR) and supply of light to the resulting *E. coli* strain was hypothesised to partially overcome this problem (Figure 4.12). In support of this hypothesis, the successful expression of PR (with its essential cofactor, all-trans retinal) increased both the rate and duration of $H_2$ production from this synthetic $H_2$-producing system. A total of 62 nmol of $H_2$ was produced from 8.6 mmol of glycerol using this system. Interestingly, the rate and amount of $H_2$ production in the IC011 + pUNI-OSPhs and pSU-PR sample with no added all-trans retinal (Figure 4.11) was slightly higher than in the earlier experiments without PR (Figure 4.6). Thus may simply be due to increase in

temperature (from 25 °C to 35 °C), as a result of illumination of the reaction chamber with a halogen bulb. Further optimisation of this system is necessary (e.g. by trying light sources with different wavelengths and intensities). Product inhibition, due to a build-up of $H_2$ in the closed environment of the chamber of the $H_2$ electrode, is another possible contributing factor to the premature cessation of $H_2$ production observed in this experimental set up.

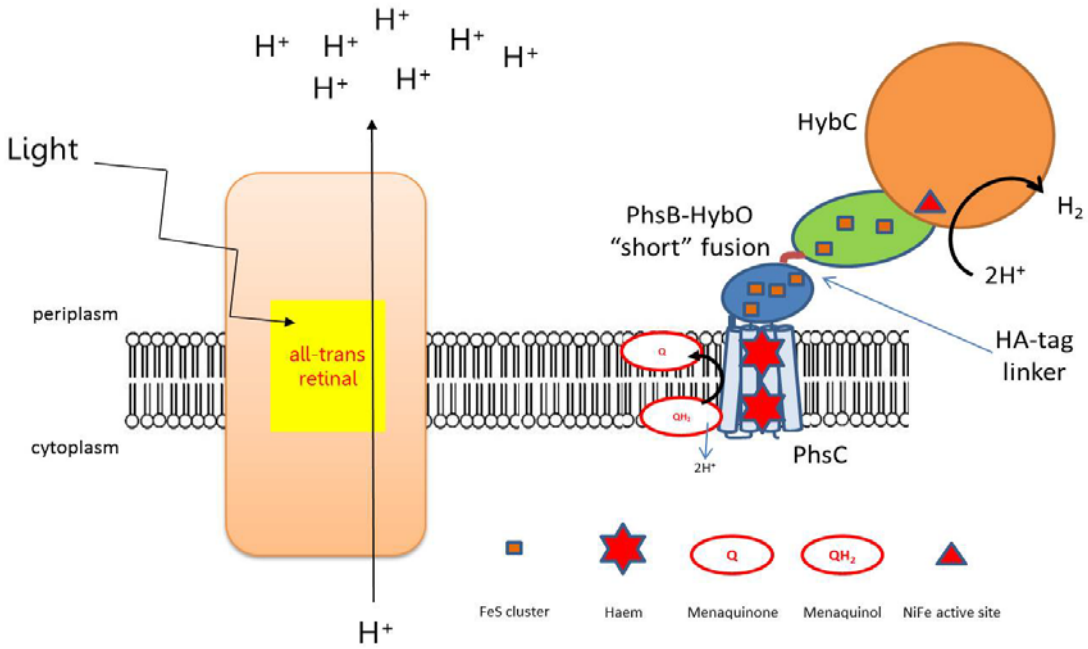


**Figure 4.12 The expression of a proton-pumping proteorhodopsin could increase or maintain PMF and therefore drive sustained $H_2$ production from the synthetic chimeric metalloenzyme.**

### 4.4.6 Enzyme assembly and stability as a limiting factor

Degradation or instability of the HybO-PhsB fusion protein in *E. coli* was proposed as a possible reason for the low level of activity. However, exchange of the HA-tag linker with other well characterised rigid and flexible linker peptides did not drastically improve stability or hydrogenase activity. The -6aaFlex chimera, which has a further C-terminal truncation of HybO (compared to the OS variant), was successfully expressed in *E. coli*, however no active enzyme could be detected in either the cytoplasmic or membrane fractions, indicating that HybO was no longer able to form a stable complex with HybC and is probably degraded. The truncation to the C terminus likely destabilised the protein environment surrounding the distal FeS cluster, causing either protein misfolding and/or the loss of the FeS cluster.

Three of the four genes that encode the subunits of synthetic chimeric enzyme are currently under the control of the constitutive promoter, $P_{tat}$, and expressed from the medium-copy expression vector, pUNI-PROM. The last gene, *hybC* is encoded on the *E. coli* chromosome. It is

probable that this differential level of gene expression results in problems related to the stoichiometry of individual subunits (e.g. HybC may be at too low a level in the cell to match the higher levels of PhsC and HybO-PhsB proteins, therefore resulting in non-functional PhsCHybO-PhsB complexes lacking a catalytic subunit). In addition, high levels of expression of FeS cluster-containing proteins would create a strain on the cellular FeS cluster machinery, as well as deplete cellular iron and sulfur levels. This could lead to incomplete maturation of all FeS clusters in the subunits of the synthetic chimeric metalloenzyme (Pinske and Sawers, 2012a).

Both of these complications might also contribute to the incomplete transport/insertion of the synthetic enzyme complex across/into the cytoplasmic membrane, as shown by the results of the rocket immunoelectrophoresis experiments. These results showed that the majority of enzyme remains in the cytoplasm and is therefore not transported across the cytoplasmic membrane. HybO has been shown to accumulate in the cytoplasm when HybC is missing, as HybC requires the Tat signal sequence of HybO in order to be successfully transported across the inner membrane (Rodrigue*, et al.*, 1999). The Tat proofreading machinery is known to prevent premature transport of proteins lacking their full complement of cofactors (Palmer and Berks, 2012). Even when successfully transported, it can be seen in the membrane-free periplasmic fractions (data not shown), indicating it is either not inserted into the membrane correctly or some subunits dissociate from the membrane-bound subunits.

To attempt to solve these challenges, a number of approaches could be employed. Firstly the synthetic chimeric metalloenzyme operon could be inserted on the chromosome under the control of the native *hybO* promoter, thus ensuring the level of gene expression is similar to that of *hybC*. Secondly an optimised RBS and linker could be inserted upstream of *hybC* on the chromosome to ensure that translation levels are also similar. Finally, it has been shown that *E. coli* strains where the gene encoding the repressor of the iron sulfur cluster machinery operon, *iscR*, has been deleted are able to support over expression of FeS cluster-containing proteins when extra iron and cysteine are supplied (Kuchenreuther*, et al.*, 2010). The construction of a synthetic *E. coli* strain where the iron sulfur cluster machinery is upregulated and the synthetic chimeric metalloenzyme operon is expressed from the chromosome should result in increased rates of $H_2$ production as well as total yields from this synthetic system.

### 4.4.7 Directed protein evolution of the synthetic chimeric metalloenzyme

It is likely that these rational approaches to improve the stability and activity of the synthetic fusion enzyme must be combined with other protein engineering techniques that do not rely on such rational design. Although currently fused C terminus to N terminus, HybO and PhsB

are excellent candidate parts to use in domain shuffling experiment. Similarly, random mutagenesis of *phsC*, and the *hybO-phsB* fusion gene would result in interesting libraries to be screened for improved stability, transport and ultimately hydrogenase activity. However, these ideas would require the development of a high throughput screen or preferably a method of selection, where $H_2$ production was linked to cell survival. One such hypothetical screen could involve the construction of a formate-dependent kill switch, where excess formate induces cell death at a specific threshold concentration and therefore only mutant variants that are capable of increased $H_2$ production from formate survive (either indirectly as in the case of artificial respiration-linked $H_2$ production, or directly as with FHL) (Figure 4.13). This synthetic formate-dependent kill switch would be regulated by FhlA, the well characterised formate-associated transcriptional activator of the formate hydrogenlyase encoding genes (Leonhartsberger*, et al.*, 2000; Sawers, 2005). Formate binds to one domain of FhlA, thus increasing the affinity of its DNA-binding domain, which aids the recruitment of $\sigma^{54}$ polymerase activating the transcription of genes with $\sigma^{54}$-dependent promoters (Leonhartsberger*, et al.*, 2000). The synthetic kill switch construct, would therefore consist of $\sigma^{54}$-dependent promoter inserted upstream of a gene that encode a toxic protein such as RelF (Knudsen and Karlstrom, 1991), Hok (Bej*, et al.*, 1988) or Gef (Bej*, et al.*, 1992). Where no, or poor, $H_2$ production from formate occurs, formate would accumulate in the cell late in growth and bind to FhlA. This would induce *relF* transcription and once a threshold level of RelF is reached, cell death would occur (Figure 4.13A). However, if sufficient formate oxidation occurs, presumably linked to $H_2$ production, expression of *relF* is reduced/inhibited as the majority/all of the formate is oxidised, which directly or indirectly leads to $H_2$ production (Figure 4.13B). Such a synthetic system to select for formate-dependent $H_2$ production would of course require significant tuning of a number of its components. First, consideration would have to be given to the level of *fhlA* expression in the cell as well as the post-transcriptional regulator of FhlA, the sRNA OxyS and may therefore require synthetic regulation. Second, a library of $\sigma^{54}$-dependent promoters and partner RBSs may have to be constructed and screened to allow a range of formate-oxidation/$H_2$-production levels to be selected for. And finally, a variety of genes encoding toxic proteins may have to be screened in order to find one that only exhibits toxicity above a specific concentration.

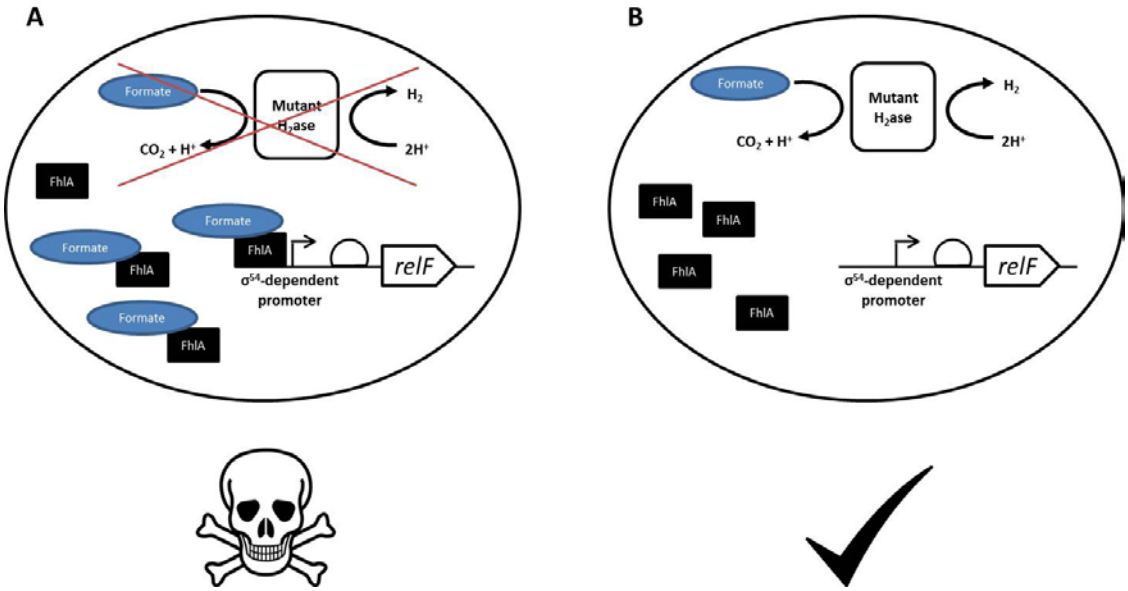


**Figure 4.13 A hypothetical formate-dependent kill switch to allow for selection of formate-dependent $H_2$ producing mutants.** An fhlA-dependent promoter could be inserted upstream of a toxic gene such as *relF* or *hok* protein. Where no/poor $H_2$ production from formate occurs, formate would accumulate in the cell and bind to FhlA. This would induce *relF* transcription and once a threshold level of RelF is reached, cell death would occur. However if sufficient $H_2$ production occurs, expression of *relF* is reduced/inhibited as the majority/all of the formate is oxidised, which directly or indirectly leads to $H_2$ production. *E. coli* cells expressing this synthetic kill switch could be transformed with mutant libraries of hydrogenases and those that produce $H_2$ from the oxidation of formate could be selected for.

# 5. *In vivo* bidirectionality of *E. coli* Hyd-2 and its role in glycerol fermentation

## 5.1 **Introduction**

### 5.1.1 Glycerol respiration by *E. coli*

The glycerol metabolism pathways of *Escherichia coli* K12 were long thought to require quinone-linked respiratory dehydrogenases and therefore the involvement of exogenous electron acceptors (Miki and Lin, 1973; Lin, 1976). Initially, a glycerol transporter GlpF (a member of the aquaporin [AQP] channel family, impermeable to all ions including protons) transports glycerol into the cytoplasm (Stroud*, et al.*, 2003). GlpK, a glycerol kinase (*glpK* found in operon with *glpF*), phosphorylates glycerol in an ATP-dependent manner resulting in glycerol-3-phosphate (Glyc-3-P). Under aerobic conditions, Glyc-3-P is oxidised by the membrane-bound aerobic Glyc-3-P dehydrogenase (aeGlyc3PDH) complex, GlpD, which couples the reaction to quinone reduction and ultimately the reduction of $O_2$ to water. When oxygen is absent, an alternative electron acceptor such as fumarate, TMAO, nitrate or nitrite is required. Under these conditions, an anaerobic Glyc-3-P dehydrogenase (anGlyc3PDH) complex consisting of GlpA, GlpB and GlpC ,and loosely attached to the cytoplasmic membrane, oxidises Glyc-3-P, with the resulting electrons passing to the quinone pool and ultimately to a terminal electron acceptor. In both cases, dihydroxyacetone phosphate (DHAP) is the product of Glyc-3-P oxidation (Figure 5.1). This can then be converted to D-glyceraldehyde 3-phosphate (G-3-P) by the enzyme triose-phosphate isomerase (TIM, encoded by *tpiA*), which can be further oxidised through glycolysis. It was thought that the absence of Glyc-3-P dehydrogenase activity in fermentative growth conditions (i.e. no exogenous electron acceptors present), would lead to a build-up of a dead-end product Glyc-3-P in the cytoplasm that would inhibit cell growth.

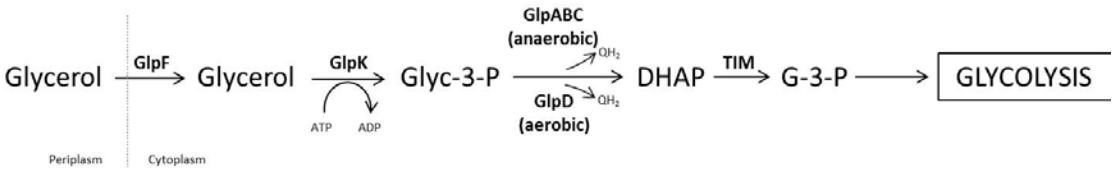


**Figure 5.1 Glycerol respiration by *E. coli* in aerobic or anaerobic conditions.** During respiratory glycerol metabolism, glycerol is phosphorylated to glycerol-3-phosphate (Glyc-3-P) by a glycerol kinase (GlpK). Glyc-3-P is then oxidised by one of two glycerol dehydrogenases depending on the external electron acceptor present. In aerobic conditions this enzyme is GlpD and in anaerobic conditions with an electron acceptor other than $O_2$, GlpABC is the dehydrogenase. The resulting dihydroxyacetone phosphate (DHAP) can then be converted to D-glyceraldehyde 3-phosphate (G-3-P) by a triose isomerase (TIM) which enters glycolysis.

### 5.1.2 $H_2$ respiration by *E. coli*

The *E. coli* chromosome contains genes for four [NiFe]-hydrogenases, three of which have been biochemically characterised: Hyd-1; Hyd-2; and Hyd-3. Hyd-3 forms part of the formate hydrogenlyase (FHL) complex, a large membrane-attached complex of at least seven-proteins, responsible for $H_2$ production during mixed-acid fermentation by *E. coli*. Hyd-1 and Hyd-2 on the other hand are involved in $H_2$ oxidation ($H_2$ uptake). The physiological role of Hyd-1 in *E. coli* is still not fully known, although it is oxygen-tolerant and capable of $H_2$ oxidation coupled to the reduction of nitrate, $O_2$ or DMSO (Laurinavichene and Tsygankov, 2001; Laurinavichene and Tsygankov, 2003).

Hyd-2 appears to oxidise $H_2$ under anaerobic respiratory conditions and this $H_2$ oxidation is coupled to the reduction of fumarate, DMSO and nitrate (Laurinavichene and Tsygankov, 2001). Hyd-2 is a periplasm-facing and membrane-attached enzyme (Ballantine and Boxer, 1986). In its native form, HybOC forms a large respiratory complex with HybA and HybB and this association is essential for $H_2$-dependent fumarate reduction and growth on hydrogen and fumarate alone (Dubini*, et al.*, 2002)

Bidirectionality of Hyd-2 activity has previously been demonstrated *in vitro* through a series of electrochemical and spectrophotometric experiments on the isolated HybOC proteins (Lukey*, et al.*, 2010). Hyd-2 shows higher overall hydrogenase activities than Hyd-1 (Sawers and Boxer, 1986; Menon*, et al.*, 1991) and is optimised for $H_2$ oxidation under more reducing conditions. Hyd-2 is also capable of $H_2$ production *in vitro* and as a result it was postulated that this enzyme may operate as an “electron release valve” operating in reverse to maintain redox balance when the quinone/quinol pool becomes over reduced (Lukey, *et al*., 2010).

## 5.2 **Aims**

This Chapter aims to investigate whether Hyd-2 is capable of both producing and oxidising $H_2$ *in vivo*. This will be done by testing if whole cells expressing Hyd-2 are capable of producing $H_2$ directly from respiratory electron donors such as glycerol, as well as by studying the effect of the addition of exogenous electron acceptors on cellular hydrogenase activity. The other *E. coli* hydrogenases will also be studied for glycerol-dependent $H_2$ production and $H_2$ oxidation activity *in situ*.

## 5.3 **Results**

### 5.3.1 Whole cells producing only Hyd-2 can reduce protons to $H_2$ in a glycerol-dependant manner

*E. coli* Hyd-2 is a well-characterised uptake hydrogenase with homologues in other bacteria. Interestingly, the isolated enzyme is fully reversible when attached to a graphite electrode or platelet (Lazarus*, et al.*, 2009; Lukey*, et al.*, 2010), which led to hypothesis that Hyd-2 may also be reversible *in vivo*. In order to test the reversibility of Hyd-2 in the living cell an experiment was devised using exogenously-added glycerol, which is traditionally regarded as a non-fermentable carbon source, and respiratory electron donor, for *E. coli*.

*In vivo* hydrogen-production assays were performed using a modified Clark-type electrode. *E. coli* strains producing Hyd-2 only (IC010: Δ*hyaB*; Δ*hycE*), Hyd-1 only (IC009: Δ*hybC*; Δ*hycE*), or no hydrogenases at all (IC011: Δ*hyaB*; Δ*hycE;* and Δ*hybOA*), were cultured anaerobically in the presence of glycerol and fumarate before being harvested and washed under anaerobic conditions. Whole cells were added to anaerobic buffer (100 mM sodium phosphate buffer, pH 6.8) within the electrode chamber and $H_2$ production assayed upon addition of 170 mM glycerol. Note that no external electron acceptors (e.g. fumarate, nitrate, etc.) were added to the reaction chamber. Cells producing Hyd-2 only (IC010) produced $H_2$ at a rate of 0.2 nmol $H_2$ $min^{-1}$ $mg^{-1}$ whole cells added (Figure 5.2), while cells producing Hyd-1 only, or none of the well-characterised [NiFe] hydrogenases of *E. coli*, produced no detectable $H_2$ over the time course of this experiment (Figure 5.2). This provides initial direct and genetic evidence that Hyd-2 is indeed capable of accepting electrons, probably *via* the quinol pool, and reducing protons to produce $H_2$ *in vivo* at pH 6.8.

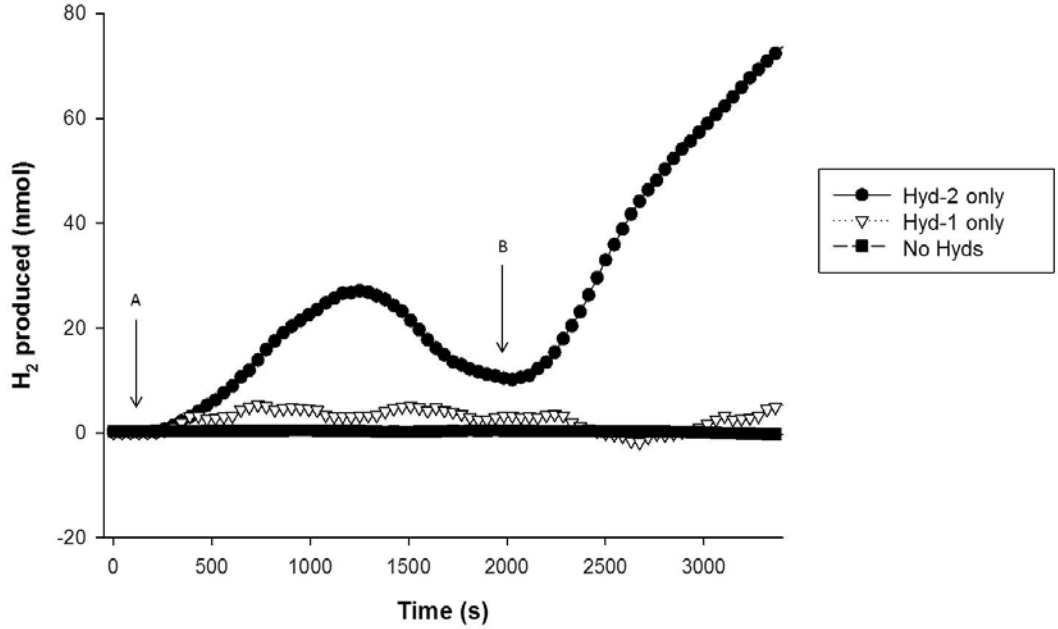


**Figure 5.2. Hyd-2 is capable of producing $H_2$ directly from glycerol.** Cells were grown for 16 h overnight at 37° C in sealed, stationary 500 ml Duran bottles, containing 500 ml Luria Broth supplemented with 0.5% (v/v) glycerol and 0.4% (w/v) fumarate. Cells were harvested by centrifugation, washed twice in anaerobic buffer (100 mM sodium phosphate, pH 6.8) to remove any trace of growth media, glycerol and fumarate, and resuspended in 2 ml of the same anaerobic buffer per 1 g of cells (wet weight). Assays were carried out using a modified Clark-type electrode (Hansatech Oxygraph). 2 ml of the same anaerobic buffer was added to the reaction chamber and 25 mg of either IC010 (full circle), IC009 (open triangle) or IC011 (full square) whole cells were added (point A). After approximately 30 m, glycerol at a final concentration of 170 mM was added to the reaction chamber (point B). $H_2$ production was measured by following the current generated following calibration with known amounts of $H_2$. Hyd-2 only cells (IC010: Δ*hyaB*; Δ*hycE*) are capable of producing $H_2$ directly from glycerol *in vivo*. Hyd-1 only cells (IC009: Δ*hybC*; Δ*hycE*) and cells with no active hydrogenases (IC011: Δ*hyaB*; Δ*hycE;* and Δ*hybOA*) produced no $H_2$ from glycerol. These results show that Hyd-2 is capable of producing $H_2$ from menaquinol, which results from glycerol oxidation, but Hyd-1 cannot.

### 5.3.2 Evidence that Hyd-2 activity is rapidly reversible *in vivo*.

The ability of Hyd-2 to switch from $H_2$ production to $H_2$ oxidation was assessed using the electrode-based whole cell hydrogenase assay. The IC010 (Hyd-2 only) strain was grown anaerobically in the presence of glycerol and fumarate before being harvested and washed under anaerobic conditions. The cells were introduced to the electrode and Hyd-2-dependent $H_2$ production induced by the addition of excess glycerol (Figure 5.3). After a short time an external electron acceptor (nitrate, fumarate or TMAO) was added to the reaction chamber. The $H_2$ production was immediately observed to cease and the $H_2$ previously produced in the chamber was quickly oxidised (Figure 5.3). Hyd-2 therefore is a true *in vivo* bidirectional enzyme depending on the presence of an external electron acceptor.

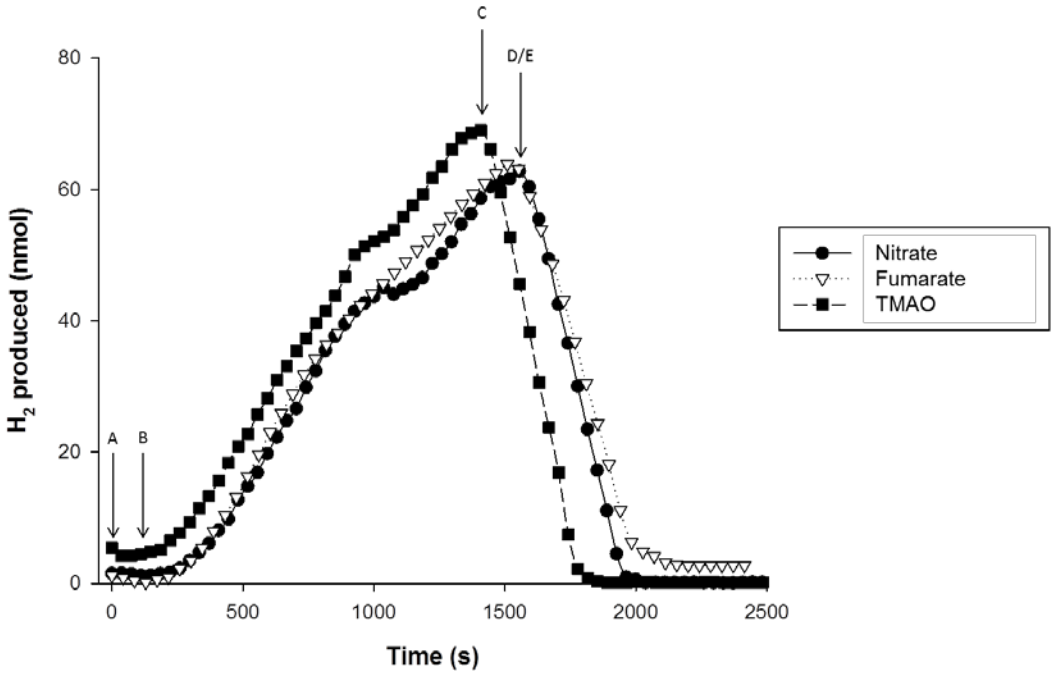


**Figure 5.3. Hyd-2 is a *bona fide* bidirectional enzyme *in vivo*.** Cells were grown for 16 h overnight at 37° C in sealed, stationary 500 ml Duran bottles, containing 500 ml Luria Broth supplemented with 0.5% (v/v) glycerol and 0.4% (w/v) fumarate. Cells were harvested by centrifugation, washed twice in anaerobic buffer (100 mM sodium phosphate, pH 6.8) to remove any trace of growth media, glycerol and fumarate, and resuspended in 2 ml of the same anaerobic buffer per 1 g of cells (wet weight). Assays were carried out using a modified Clark-type electrode (Hansatech Oxygraph), calibrated with known amounts of $H_2$. 2 ml of the same anaerobic buffer was added to the reaction chamber and 25 mg of Hyd-2 only whole cells (IC010) were added (point A). After equilibration, glycerol at a final concentration of 170 mM was added to the reaction chamber (point B). $H_2$ production was measured as previously observed. After approximately 20 m, TMAO (full square, 67.5 mM final), fumarate (open triangle, 25 mM final), or nitrate (full circle, 60 mM final) was added (point C, D and E respectively). Hyd-2 only cells are therefore capable of producing $H_2$ from glycerol, and subsequently reoxidising this $H_2$, passing electrons via membrane quinone pool to a terminal electron acceptor.

### 5.3.3 Hyd-3 is the main $H_2$ producer when glycerol is the sole carbon source

The ability to produce $H_2$ from glycerol, and subsequently reoxidise this $H_2$, was assayed in MC4100 (containing all [NiFe]-hydrogenases) and FTD89 (Hyd-3 only) whole cells. $H_2$ production from glycerol was observed for both MC4100 and FTD89, with more $H_2$ (approx. 300 nmol more) produced by the FTD89 strain lacking the uptake hydrogenases (Figure 5.4). The parent strain MC4100 was capable of oxidising this endogenously-produced $H_2$ immediately upon addition of fumarate, nitrate or TMAO, however the FTD89 uptake mutant was unable to do this (Figure 5.4).

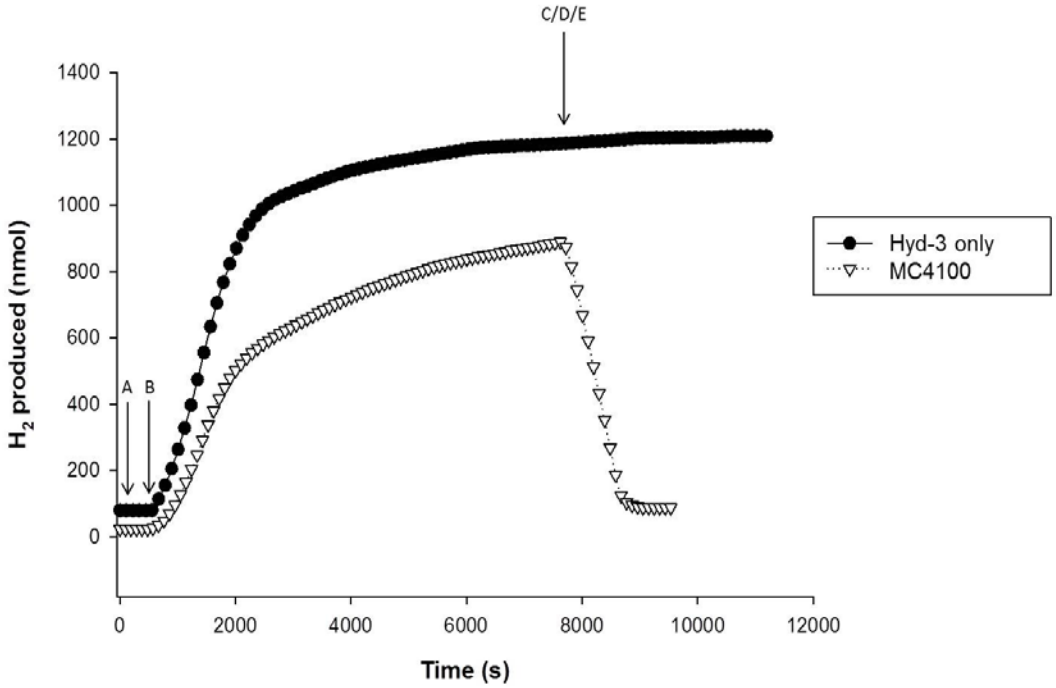


**Figure 5.4. Hyd-3 is the predominant $H_2$ producer with glycerol as the sole substrate.** Cells were grown for 16 h overnight at 37° C in sealed, stationary 500 ml Duran bottles, containing 500 ml Luria Broth supplemented with 0.5% (v/v) glycerol and 0.4% (w/v) fumarate. Cells were harvested by centrifugation, washed twice in anaerobic buffer (100 mM sodium phosphate, pH 6.8) to remove any trace of growth media, glycerol and fumarate, and resuspended in 2 ml of the same anaerobic buffer per 1 g of cells (wet weight). Assays were carried out using a modified Clark-type electrode (Hansatech Oxygraph), calibrated with known amounts of $H_2$. 2 ml of the same anaerobic buffer was added to the reaction chamber and 50 mg of MC4100 (full circle) or FTD89 (Δ*hycB*, Δ*hyaB*, open triangle) whole cells were added (point A). After equilibration, glycerol at a final concentration of 170 mM was added to the reaction chamber (point B) and $H_2$ production was measured. After approximately 120 m, TMAO (67.5 mM final), fumarate (25 mM final), or nitrate (60 mM final) was added (point C, D and E respectively). These results show that Hyd-3 produces $H_2$ from glycerol at a higher rate (need numbers) than Hyd-2. Hyd-3 is not a reversible enzyme as the addition of TMAO, fumarate, or nitrate does not induce $H_2$ oxidation (as was observed with Hyd-2). MC4100 cells however produce less total H2 than FTD89 cells and as they have Hyd-1 and Hyd-2 activity, they are capable of H2 oxidation upon addition of exogenous electron acceptor.

### 5.3.4 Hyd-2 is essential for $H_2$-dependent fumarate or TMAO reduction, but not nitrate reduction.

HybA, a membrane-anchored periplasmic ferredoxin-like protein, and HybB, a large integral membrane protein with a predicted ten transmembrane helices, are peripheral and poorly-characterised components of the membrane-bound Hyd-2 complex. Two *E. coli* strains, FTD671 (Δ*hybA*) and FTD672 (Δ*hybB*), were assessed for their ability to both produce $H_2$ from glycerol and reoxidise this endogenous $H_2$ (Figure 5.5). Both mutant strains retained Hyd-3 activity, thus $H_2$ production from glycerol was observed to proceed at a similar rate to that recorded for the parent strain, MC4100 (Figure 5.4). Interestingly, however FTD672 produced less $H_2$ in total (approx. 200 nmol less) than either MC4100 or FTD671. In the midst of endogenous $H_2$ production, respiratory electron acceptors were added to the reaction chamber (Figure 5.5). Somewhat surprisingly, the addition of fumarate to the reaction chamber did not initiate $H_2$ oxidation, but resulted in a spike in the rate of $H_2$ production (Figure 5.5). However, the addition of nitrate immediately started $H_2$ oxidation and all of the available $H_2$ was reoxidised (Figure 5.5). The addition of TMAO to the reaction chamber was not sufficient to start $H_2$ oxidation, however it did immediately cease $H_2$ production, presumably as electrons from the remaining electron donors in the chamber (glycerol and glycerol-derived formate) were preferentially passed to TMAO along respiratory chains (Figure 5.6).

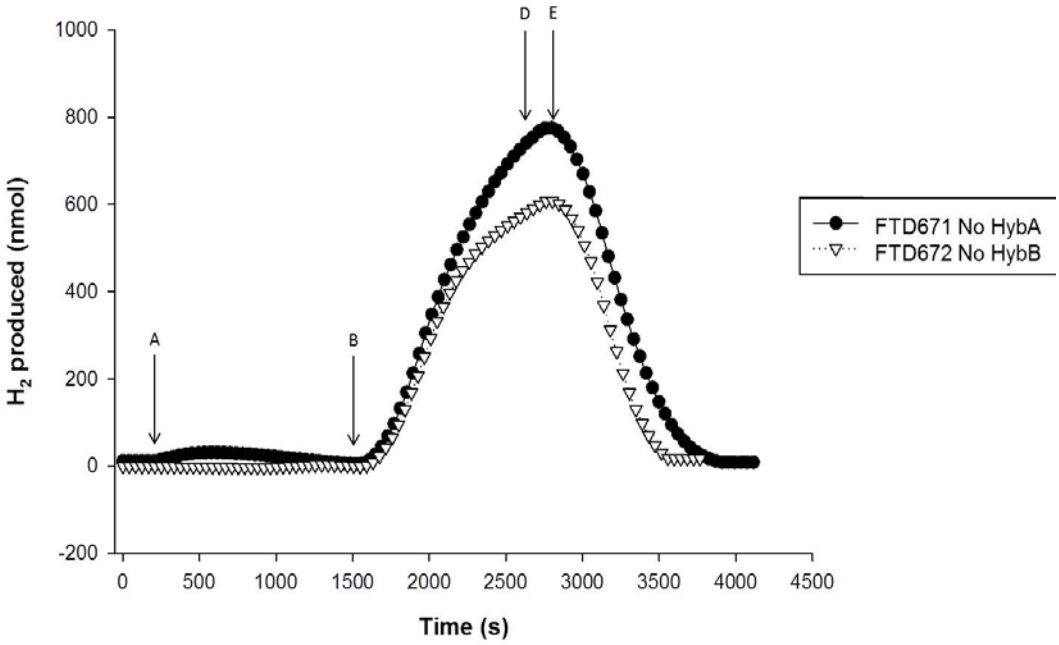


**Figure 5.5. Hyd-2 is essential for $H_2$-dependent fumarate reduction.** Cells were grown for 16 h overnight at 37° C in sealed, stationary 500 ml Duran bottles, containing 500 ml Luria Broth supplemented with 0.5% (v/v) glycerol and 0.4% (w/v) fumarate. Cells were harvested by centrifugation, washed twice in anaerobic buffer (100 mM sodium phosphate, pH 6.8) to remove any trace of growth media, glycerol and fumarate, and resuspended in 2 ml of the same anaerobic buffer per 1 g of cells (wet weight). Assays were carried out using a modified Clark-type electrode (Hansatech Oxygraph), calibrated with known amounts of $H_2$. 2 ml of the same anaerobic buffer was added to the reaction chamber and 50 mg of either FTD671 (Δ*hybA*, full circle) or FTD672 (Δ*hybB*, open triangle) whole cells were added (point A). After equilibration, glycerol at a final concentration of 170 mM was added to the reaction chamber (point B) and $H_2$ production was measured. After approximately 15 m, fumarate (25 mM final) or nitrate (60 mM final) was added (point D and E respectively). HybA, a membrane–anchored periplasmic ferredoxin-like protein and HybB a large integral membrane protein, are therefore not required for $H_2$ production from glycerol. They are however required for reoxidation of this $H_2$ when fumarate is the terminal electron acceptor but not with nitrate.

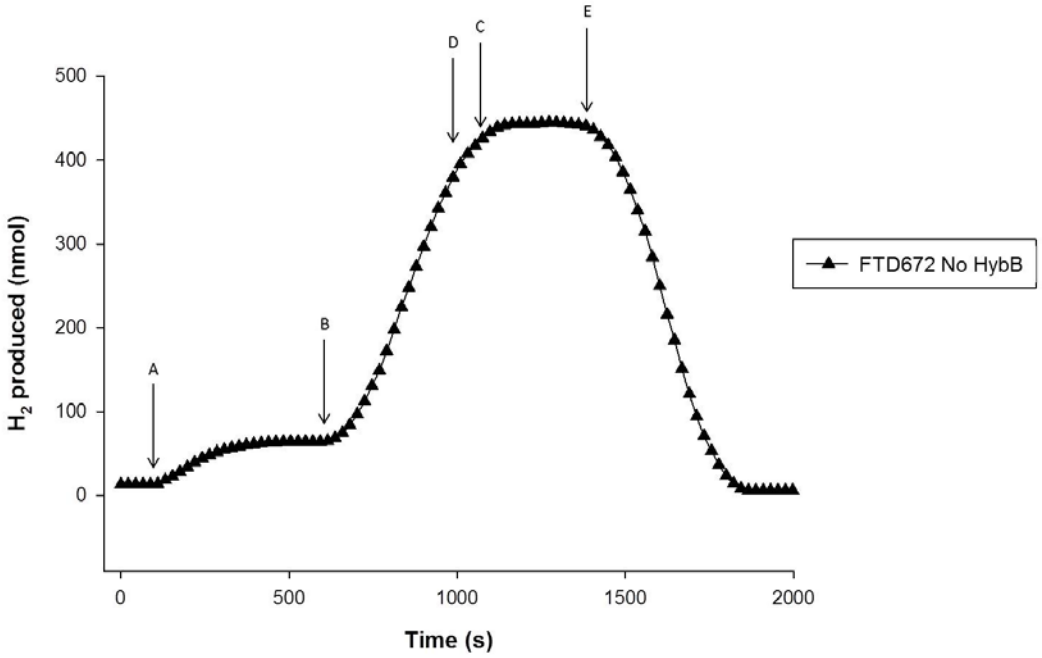


**Figure 5.6. Hyd-2 is involved in $H_2$-dependent fumarate or TMAO reduction.** Cells were grown for 16 h overnight at 37° C in sealed, stationary 500 ml Duran bottles, containing 500 ml Luria Broth supplemented with 0.5% (v/v) glycerol and 0.4% (w/v) fumarate. Cells were harvested by centrifugation, washed twice in anaerobic buffer (100 mM sodium phosphate, pH 6.8) to remove any trace of growth media, glycerol and fumarate, and resuspended in 2 ml of the same anaerobic buffer per 1 g of cells (wet weight). Assays were carried out using a modified Clark-type electrode (Hansatech Oxygraph), calibrated with known amounts of $H_2$. 2 ml of the same anaerobic buffer was added to the reaction chamber and 50 mg of FTD672 (Δ*hybB*, full triangle) whole cells were added (point A). After equilibration, glycerol at a final concentration of 170 mM was added to the reaction chamber (point B) and $H_2$ production was measured. After approximately 7 m, fumarate (25 mM final), TMAO (67.5 mM final), or nitrate (60 mM final) was added (point D, C and E respectively). As previously observed, HybB is not required for $H_2$ production from glycerol but is essential to allow reoxidation of this $H_2$ when fumarate is the terminal electron acceptor but not with nitrate. Interestingly the addition of TMAO as the terminal electron acceptor immediately stops $H_2$ production from glycerol (accepting electrons from oxidised glycerol) but is still unable to initiate $H_2$ oxidation

## 5.4 **Discussion**

In this study, $H_2$ production from glycerol was monitored directly and in real time. This provides an advantage over previous studies where headspace gases of growing cultures were studied after glycerol fermentation, or where hydrogenase activity was measured using artificial electron donors and acceptors, e.g. benzyl viologen. The combination of this real-time $H_2$ production assay with mutant strains defective in different hydrogenases allowed the contribution of each isoenzyme to glycerol-dependent $H_2$ production to be more accurately determined.

### 5.4.1 Hyd-2 is a true bidirectional enzyme, capable of both $H_2$ production and oxidation

It was previously suggested that Hyd-2 may be capable of $H_2$ production in certain conditions (Lukey*, et al.*, 2010), however this study is the first time this has been demonstrated directly. Hyd-2 is therefore a true bidirectional enzyme under physiological conditions. Hyd-2 can switch almost immediately from $H_2$ production to $H_2$ oxidation, upon the addition of an external electron acceptor, e.g. fumarate, nitrate or TMAO. This adds weight to the suggestion in the above electrochemical study that Hyd-2 might act as an "electron-release valve", reducing protons to $H_2$ to blow off excess reducing equivalents when none of the more traditional electron acceptors are present. One peculiarity of the Hyd-2 $H_2$ production assays was that a small spike of $H_2$ production was often observed upon addition of the cells to anaerobic buffer. This could represent the oxidation of trace amounts of an internal electron donor, remaining after harvesting the cells.

### 5.4.2 Hyd-1 is not capable of $H_2$ production from glycerol

These results demonstrate that, at pH 6.8, Hyd-2 and Hyd-3 are the only hydrogenases of *E. coli* K-12 capable of $H_2$ production from glycerol as original substrate. Hyd-1 is not capable of $H_2$ production from glycerol, since IC009 (Hyd-1 only) produced no $H_2$. This contradicts some earlier findings, which suggested both Hyd-1 and Hyd-4 contributed to $H_2$ production from glycerol (Trchounian and Trchounian, 2009; Trchounian*, et al.*, 2013). This conclusion is, however, in perfect agreement with the results in a more recent study (Sanchez-Torres*, et al.*, 2013).

### 5.4.3 FHL/Hyd-3 is the main $H_2$ producer from glycerol (at pH 6.8)

It has been shown that Hyd-3 is the predominant $H_2$ producer at pH 6.8 when glycerol is the sole carbon source, since FTD89 (no Hyd-1 or Hyd-2 activity) whole cells produced > 10 times more $H_2$ from the same amount of exogenous glycerol than IC010 (no Hyd-1 or Hyd-3 activity)

cells. What is the link between glycerol and Hyd-3? The FHL complex disproportionates formate into $CO_2$ and $H_2$ (Sawers, 2005). These data suggest *E. coli* is capable of metabolising glycerol, and so producing some formate, in the absence of an external electron acceptor. Indeed, it has been previously suggested that *E. coli* could ferment glycerol (Gonzalez*, et al.*, 2008) and others have suggested that the $CO_2$ product of FHL actually feeds back into the new glycerol fermentation pathway (Dharmadi*, et al.*, 2006). As the Hyd-3 only strain (FTD89) was unable to reoxidise the $H_2$ produced, upon addition of fumarate, nitrate or TMAO, it is unlikely that Hyd-3 is a physiologically reversible enzyme capable of $H_2$ uptake as surprisingly claimed in another study, which used the artificial electron acceptor, MV (Maeda*, et al.*, 2007b). Indeed, it has been known for some years that Hyd-3 can reduce redox dyes in crude cell extracts (Sawers, *et al*., 1985).

### 5.4.4 Glycerol fermentation in *E. coli* and other bacteria

A few microorganisms are capable of true fermentative glycerol metabolism coupled to cell growth and proliferation. These include certain species of the genera *Klebsiella*, *Enterobacter* and *Citrobacter* (Bouvet*, et al.*, 1995). In these organisms, fermentative dissimilation of glycerol occurs through a reductive and parallel oxidative branch. In the oxidative branch, glycerol is oxidised directly to dihydroxyacetone (DHA) by a type I $NAD^+$-dependent glycerol dehydrogenase (glyDH-1). DHA is then phosphorylated resulting in dihydroxyacetone phosphate (DHAP) and this reaction is catalysed by an ATP/PEP-dependent DHA kinase (DHAK). In the reductive branch, glycerol can be converted into 3-hydroxypropionaldehyde (3-HPA), through its dehydration catalysed by a coenzyme $B_{12}$-dependent glycerol dehydratase (encoded by *glyD*). 3-HPA can then act as a sink for the reducing equivalents generated by the parallel branch, regenerating $NAD^+$ as it is reduced to the major fermentation product 1,3-propanediol (1,3-PDO) by the NADH-dependent 1,3-PDO dehydrogenase (1,3-PDODH). The presence and activity of both glyDH-1 and 1,3-PDODH is therefore essential for the fermentative metabolism of glycerol in these organisms.

Fermentation of glycerol ($C_3H_8O_2$) by *E. coli*, instead of glucose ($C_6H_{12}O_6$) or other sugars is extremely desirable, as the more highly reduced state (degree of reduction) of its carbons would allow the production of larger yields of reduced fermentation products such as ethanol and hydrogen. Recent studies demonstrated that *E. coli* is in fact capable of metabolising glycerol when either exogenous electron acceptors are absent, or when respiratory glycerol metabolism pathways are disrupted (i.e. in Δ*glpA*, Δ*glpD*, Δ*frdA* strains) (Dharmadi*, et al.*, 2006; Gonzalez*, et al.*, 2008; Murarka*, et al.*, 2008). In contrast to the 1,3-PDO/DHA pathway in other bacteria, glycerol fermentation in *E. coli* involves a type II glycerol dehydrogenase and

requires the production of 1,2-PDO (as the sink for reducing equivalents). Note, however, that there is a difference here in that *E. coli* remains incapable of anaerobic growth with glycerol as the sole carbon source: *E. coli* K-12 will not grow under fermentative conditions in true minimal media with glycerol as the sole carbon source. Instead, it has been shown that *E. coli* K-12 cells can metabolise glycerol by a previously unsuspected route.

In this newly described glycerol fermentation pathway of *E. coli*, a type II $NAD^+$-dependent glycerol dehydrogenase (glyDH-II), GldA, is one of two main enzymes required. This enzyme has been studied for many years, yet its true physiological role in *E. coli* remained a mystery. An $NAD^+$-dependent glyDH-II (now identified as GldA) was originally purified from Δ*glpK E. coli* mutants (Asnis and Brodie, 1953; St Martin*, et al.*, 1977; Tang*, et al.*, 1979). It was shown to have specific dehydrogenation activity with glycerol and 1,2-propanediol as substrates, as well as the ability to reduce DHA and hydroxyacetone (HA) (St Martin*, et al.*, 1977; Kelley and Dekker, 1985). More recently in an attempt to elucidate the *in vivo* role of GldA in *E. coli*, it was demonstrated that at neutral pH, the enzyme's affinity towards DHA, methylglyoxal (MG) and glycolaldehyde was much higher than glycerol ($K_m$ values of 0.30, 0.50, 0.85 and 56 mM respectively) (Subedi*, et al.*, 2008). Based on these findings it was concluded that the primary role of GldA is to remove the toxic intermediates DHA and MG, and not to oxidise glycerol. Indeed, in all of the older studies where GldA was identified and its properties investigated, no anaerobic growth on glycerol in the absence of external electron acceptors was observed (St Martin*, et al.*, 1977; Tang*, et al.*, 1982). Finally, in a series of papers from the Gonzalez group in Rice University, Texas (Dharmadi*, et al.*, 2006; Murarka*, et al.*, 2008), anaerobic fermentative growth of *E. coli* on glycerol was demonstrated, although it should be noted that the growth medium was supplemented with tryptone. A new model of glycerol fermentation, based on genetic, biophysical and environmental studies, was proposed (Gonzalez*, et al.*, 2008). There is no doubt that *E. coli* can metabolise glycerol by this alternative pathway. This new model of fermentative glycerol metabolism in *E. coli* is summarised (Figure 5.7). In this model, glycerol is directly oxidised by GldA to DHA, which in turn is phosphorylated by a phosphoenolpyruvate-dependent DHA kinase (DHAK, encoded by *dhaKLM*), resulting in DHAP. The essential role of these enzymes in glycerol fermentation was demonstrated convincingly. Δ*gldA* strains and Δ*dhaKLM* strains were both unable to grow fermentatively on glycerol. The Δ*gldA* mutant also demonstrated no glycerol dehydrogenase activity compared to the WT strain (MG1655). Fermentative growth in Δ*gldA* strain was partially complemented by reintroducing this gene into the strain on a plasmid. Full complementation of the Δ*dhaKLM* strain was achieved by transforming with plasmids encoding these genes. Finally full complementation was achieved

in the Δ*gldA* mutant when transformed with both of these plasmids (*gldA* and *dhaKLM* containing plasmids).

In addition to being able to enter into glycolysis as discussed previously, it was demonstrated that DHAP must be converted to 1,2-PDO. This reaction involves the synthesis of two intermediates: MG (catalysed by methylglyoxal synthase (MGS); encoded by *mgs*); and HA (catalysed by aldo-keto reductase (AKR), encoded by *yeaE*, *yghZ* and *yafB*, regenerates $NAD^+$). The final conversion of HA to 1,2-PDO is catalysed by GldA (regenerates $NAD^+$), which neatly resolves historical observations of its ability to carry out both glycerol oxidation and HA reduction *in vitro*. In addition to 1,2-PDO synthesis, ethanol production (and therefore the regeneration of $NAD^+$, as well as the generation of 1 ATP per glycerol metabolised) is essential for glycerol fermentation (Δ*adhE* strain is unable to ferment glycerol) (Murarka*, et al.*, 2008). This is reflected by the observation that the major fermentation product (97% of products found in fermentation broth) is ethanol.

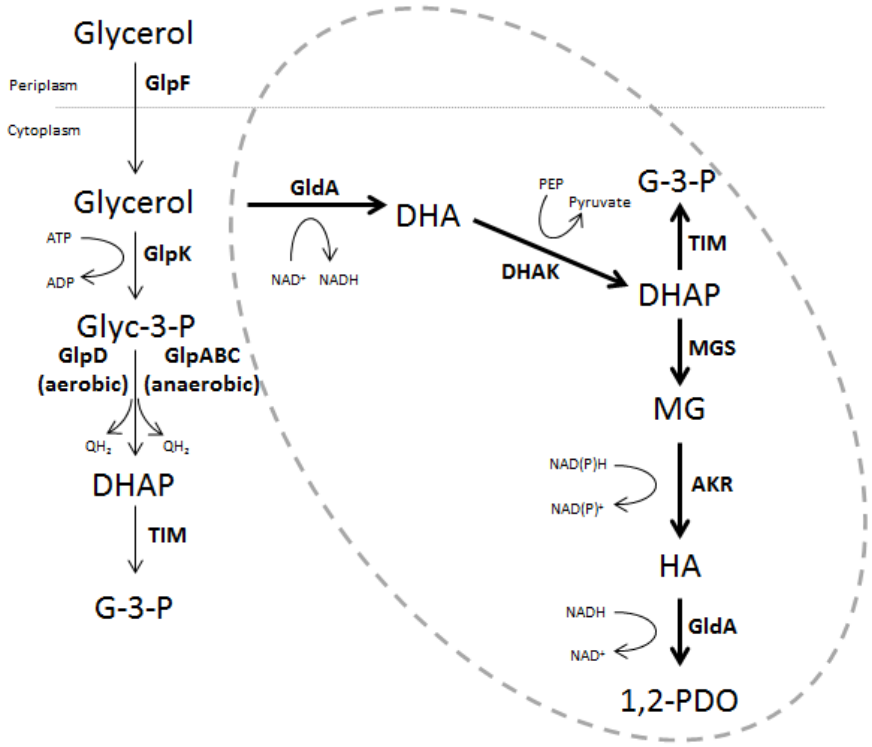


**Figure 5.7. New model of glycerol metabolism by *E. coli* under different physiological conditions.** Glycerol metabolism in the presence or absence of an external electron acceptor is shown above. During respiratory glycerol metabolism, glycerol is phosphorylated to glycerol-3-phosphate (Glyc-3-P) by a glycerol kinase (GlpK). Glyc-3-P is then oxidised by one of two glycerol dehydrogenases depending on the external electron acceptor present. In aerobic conditions this enzyme is GlpD and in anaerobic conditions with an electron acceptor other than $O_2$, GlpABC is the dehydrogenase. The resulting dihydroxyacetone phosphate (DHAP) can then be converted to D-glyceraldehyde 3-phosphate (G-3-P) by a triose isomerase (TIM) which enters glycolysis. In the recently described fermentative pathway of glycerol metabolism (in grey oval), glycerol is oxidised directly by a class II type of glycerol dehydrogenase, GldA. The resulting DHA is subsequently phosphorylated in a phosphoenolpyruvate (PEP)-dependent manner to DHAP. And through a number of intermediates, methylglyoxal (MG) and hydroxyacetone (HA), DHAP is then converted to 1,2-propanediol (1,2-PDO), a reaction also catalysed by GldA.

### 5.4.5 Glycerol fermentation and $H_2$ production

The roles of the individual *E. coli* hydrogenases: Hyd-1; Hyd-2; and Hyd-3, in $H_2$ metabolism during glycerol fermentation has been studied recently. Some of these studies suffered from sub-optimal experimental design (e.g. whole cell hydrogenase-activity assays using the artificial electron acceptor BV) and jumped to premature conclusions, some of which contradicted the published data detailed in the aforementioned glycerol fermentation studies (e.g. no influence of FHL on $H_2$ production from glycerol). In later papers, they further contradict the results documented in their own earlier papers (Trchounian and Trchounian, 2009; Trchounian*, et al.*, 2011; Trchounian*, et al.*, 2013).

Formate produced by glycerol fermentation, in the absence of both an active FHL complex and external electron acceptors, could be oxidised by FdnO, which results in an overly reduced quinone pool. This excess of reduced quinones is subsequently oxidised by Hyd-2 and the reducing equivalents used for proton reduction (Figure 5.8B). This theory could be tested using Δ*fdhO* strains. Alternatively if either the respiratory anaerobic GlpABC enzyme, or even more unlikely, the aerobic GlpD enzyme are oxidising Glyc-3-P in the absence of a terminal electron acceptor, and Hyd-2 is reducing protons as a last resort (Figure 5.8A), this could be tested by using Δ*glpABC* or Δ*glpD* strains. Another approach could be to test $H_2$ production in Δ*tpiA* strains with/without FHL (lacking triose-phosphate isomerase, which converts DHAP to D-glyceraldehyde 3-phosphate) which would halt glycolysis. It is unclear however, if Hyd-2 produces $H_2$ when an active FHL complex is present, however it has been shown that Hyd-2 and Hyd-3 are required for optimum glycerol fermentation (Δ*hycE* & Δ*hybC* strains showed decreased cell fitness, glycerol consumption and increased the production of oxidised fermentation products e.g. acetate) (Sanchez-Torres*, et al.*, 2013).

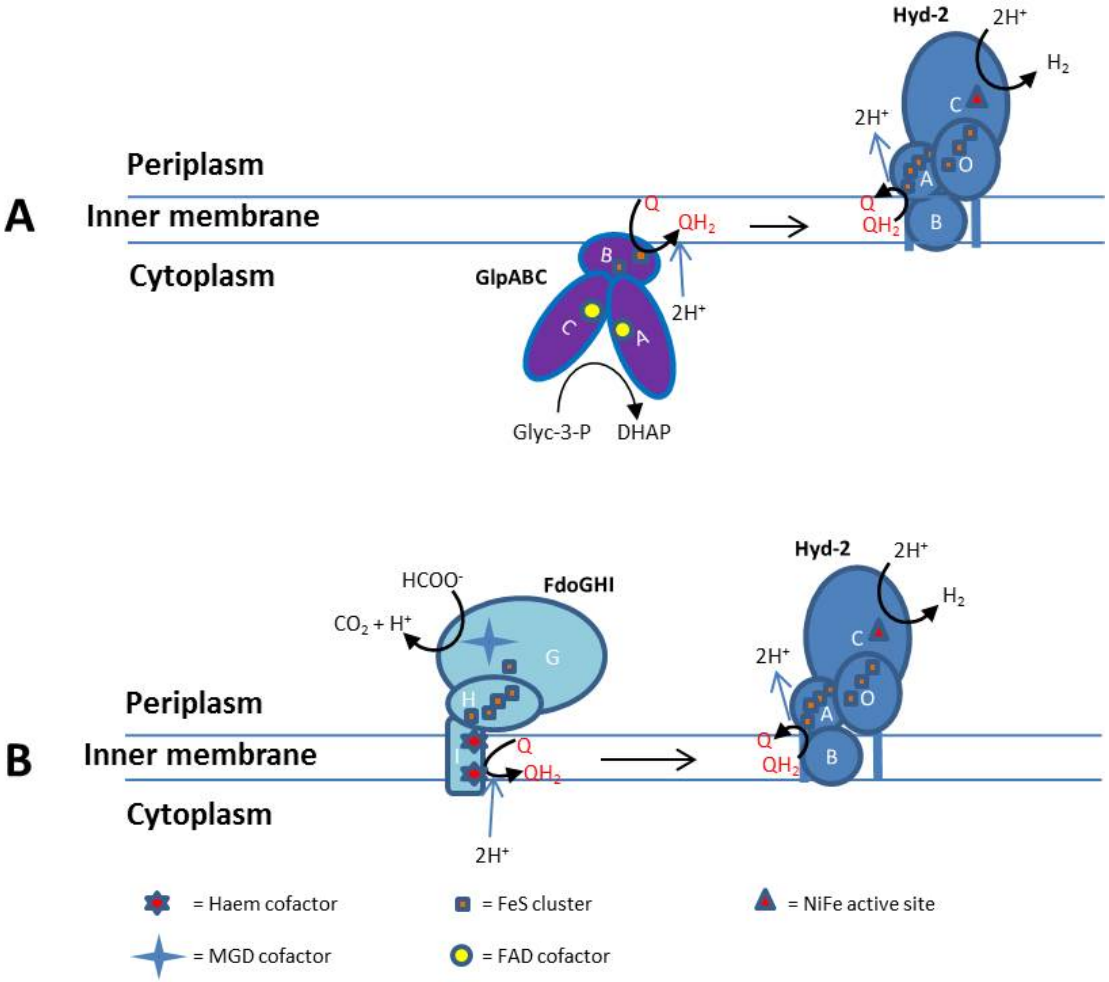


**Figure 5.8. Possible reductant sources for Hyd-2 catalysed $H_2$ production during glycerol metabolism. A.** Glycerol-3-phosphate is oxidised using respiratory glycerol dehydrogenase (GlpABC) and the resulting quinol is oxidised by Hyd-2 to produce $H_2$. **B.** During glycerol fermentation excess formate produced during glycolysis is oxidised by FdO, with the resulting quinol being oxidised by Hyd-2 to produce $H_2$.

If Hyd-2 does produce $H_2$ in WT *E. coli* cells during glycerol fermentation, one possible reason for this might be to maintain redox balance and ensure the cell does not become over reduced which would halt glycerol fermentation. The level of 1,2-PDO production is thought to be low in WT *E. coli* cells and therefore the transfer of excess reductant through proton reduction by Hyd-2 might be a previously uncharacterised facilitative pathway in glycerol fermentation. This could be tested by repeating these real-time $H_2$ production assays in *E. coli* strains lacking two essential genes for 1,2-PDO synthesis: *mgs*; and *gldA*. Perhaps this would compensate for the absolute requirement for tryptone supplementation for glycerol fermentation shown previously (Gonzalez*, et al.*, 2008). It has been suggested that tryptone does not act as an electron acceptor and only as a supplement to provide materials for cell biomass (Gonzalez*, et al.*, 2008). However this could be tested by adding tryptone (of HA, shown to compensate for tryptone deficiency) to the $H_2$ production and oxidation assays used in this chapter and noting any significant differences.

Alternatively the transport or oxidation of various amino acids could be coupled to glycerol metabolism. To test whether this plays any role in glycerol fermentation the assays could be repeated in Δ*dadA* strains. Differences in pH have been shown to be important in both glycerol fermentation and $H_2$ production from glycerol. All of these assays were carried out using a mild acidic buffer (pH 6.8). These assays should be repeated over a range of pH, from pH 4.0 to pH 9.0 to see what differences are observed. Indeed if FHL activity is impaired at more alkaline pH, it might be expected to see an increase in $H_2$ production from Hyd-2. On a related note, one suggestion as to why glycerol fermentation was thought impossible in *E. coli* for so long was that the minimal media contained high levels of potassium and phosphate ions, which inhibited key enzymes in the glycerol fermentation pathways (including GldA), which resulted in toxicity (Truniger and Boos, 1994). In this study, 100 mM sodium phosphate buffer was used in all experiments. It would be interesting to test a number of different buffers to see if they impact $H_2$ production from glycerol.

$H_2$ itself has been suggested as an inhibitory factor to allow glycerol fermentation to continue (Dharmadi*, et al.*, 2006). The historical use of sealed Hungate tubes, filled almost completely with media, in previous studies of *E. coli* glycerol metabolism (i.e. a closed system where $H_2$ accumulates in the minimal headspace) has been suggested as a key factor in why glycerol fermentation was not previously thought possible in *E. coli*. The addition of known amounts of $H_2$ to the reaction chamber before the addition of cells and/or glycerol might give interesting information on whether a high $H_2$ atmosphere can inhibit $H_2$ production by Hyd-2. Electrochemical studies have shown that $H_2$ had a low inhibitory effect on Hyd-2 $H_2$ production activity (Lukey*, et al.*, 2010). In this study, a large difference was observed in the amount of $H_2$ produced by MC4100 and FTD89 whole cells (FTD89 produced 50% more $H_2$ than MC4100). The reasons for this are unclear at this stage. It's possible that small amounts of fumarate are being produced internally and subsequently used as an electron acceptor from the oxidation of $H_2$ as catalysed by either Hyd-1 or Hyd-2. This could explain the lower amount of total $H_2$ produced by MC4100. Alternatively the reoxidation of $H_2$ and reduction of fumarate by the fumarate reductase (FRD) could result in redox imbalance as suggested previously (Murarka*, et al.*, 2008), which stops glycerol fermentation and therefore $H_2$ production. Both of these could be tested by assessing the glycerol-dependent $H_2$ production of a Δ*frdA* mutant (unable to reduce fumarate). Measuring changes in the amount of fermentation by-products (e.g. ethanol, succinate, acetate, lactate, formate etc.) might also give some indication of changes in redox balance etc.

### 5.4.6 Specialised respiratory supercomplexes in *E. coli*

It is unclear from this study, whether HybA or HybB, the two other membrane-associated subunits that form the larger respiratory complex of Hyd-2 (HybO and HybC being the main structural catalytic subunits), are involved in $H_2$ production from Hyd-2, as the total amount of $H_2$ produced (and the rate of $H_2$ production) was much higher in strains containing an active FHL complex (FTD89 or MC4100). This could be investigated by deleting *hybA* and/or *hybB* from the chromosome of IC010 and repeating these experiments. It was however shown that HybA and HybB were essential for $H_2$ oxidation when fumarate or TMAO are the terminal electron acceptors indicating that Hyd-2 is unable to reduce quinones from $H_2$ without these subunits. This is in perfect agreement with the an earlier study (Dubini*, et al.*, 2002), which showed that these strains were unable to grow anaerobically on fumarate and glycerol and that FTD671 had no $H_2$ oxidation activity with fumarate as sole electron acceptor (similar levels to Δ*hybC* mutant). Furthermore whereas the addition of TMAO at least stopped $H_2$ production from glycerol (i.e. accepting electrons generated from glycerol/glycerol-3-phosphate oxidation via the quinone/quinol pool), the addition of fumarate did not halt $H_2$ production.

One interpretation of this could be that perhaps fumarate reductase (FRD) and Hyd-2, although not forming protein-protein interactions between subunits, are functionally organised in the bacterial membrane (i.e. are spatially colocalised to the same parts of the cytoplasmic membrane to form a modular respiratory microdomain). And as both FTD671 and FTD672 were capable of $H_2$ oxidation when nitrate was the terminal electron acceptor, presumably catalysed by Hyd-1 and not Hyd-2, perhaps Hyd-1 is therefore similarly associated with nitrate reductase A (NRA).

The idea of supramolecular organisation of the bacterial membrane has gained momentum in recent years, and has now been accepted in mitochondria. In contrast to the random diffusion model of bacterial membranes (Singer and Nicolson, 1972), where respiratory complexes are randomly distributed throughout the membrane and only linked by the diffusion of electron carriers such as quinones etc., this new model is based on the idea of lipid rafts/microdomains, such as those spingolipid–cholesterol rafts found in eukaryotic cells (Simons and Ikonen, 1997). These are areas of highly organised lipid-protein complexes that function to compartmentalise related functional proteins, in effect forming supercomplexes. Indeed all mitochondrial respiratory complexes except Complex II have been shown to be capable of associating in three supercomplexes: the respirasome (Complexes I, III and IV); Complex I and III; and Complexes III and IV (Lapuente-Brun*, et al.*, 2013). It has also been shown that supercomplex

formation is advantageous in preventing the formation of reactive oxygen species (ROS) from the respiratory chain, implicated in aging and major chronic diseases (Maranzana*, et al.*, 2013)

Cardiolipin (CL), an anionic phospholipid that makes up 5–10% of total lipid content in *E. coli*, has been suggested to play a role in the organisation of the cytoplasmic membrane into microdomains (Arias-Cartin*, et al.*, 2011), as was demonstrated in the mitochondria of yeast (Bazan*, et al.*, 2013). CL has been shown to bind tightly to a number of respiratory complexes, e.g. formate dehydrogenase (FdnGHI) (Arias-Cartin*, et al.*, 2012), nitrate dehydrogenase (NarGHI) (Arias-Cartin*, et al.*, 2011) and succinate dehydrogenase (SdhABCD) (Arias-Cartin*, et al.*, 2012). CL is required for activity of some respiratory enzyme complexes and it has also been suggested that CL localises in discreet foci of the bacterial cell. It is proposed that CL found in these foci, hold related functional enzyme complexes closely together in the same area of the cytoplasmic membrane (Arias-Cartin*, et al.*, 2011). The advantage of such an arrangement is obvious as quinol and quinone binding sites within physiologically-related enzymes would be in close proximity to each other, resulting in short and very efficient electron transfer and allowing higher activities than in the random diffusion model (Singer and Nicolson, 1972). Furthermore, specific proteins may be required to segregate the lipid content of the cytoplasmic membrane. One such protein has been described, flotillin-like proteins with a flotillin domain as well as prohibitin (PHB) or stomatin/prohibitin/flotillin/HflKC (SPFH) domains. In *Bacillus subtilis* 168, YuaG has been shown to be essential for lateral segregation of membrane domains (Bach and Bramkamp, 2013). Through pull-down experiments it was shown to interact with a number of distinct classes of proteins, including those involved in cell-wall machinery, protein transport and secretion (Sec), signalling and finally energy metabolism (e.g. Nag, SdhA etc.). A final related observation on possible mechanisms for spatial organisation of related functional respiratory complexes in bacteria, is that in yeast, almost all membrane proteins segregate into distinct domains based on their membrane anchors (Spira*, et al.*, 2012).

Through a bioinformatics search, only two homologs of *B. subtilis* 168 YuaG are found in the *E. coli* genome: YqiK, a PHB family protein with periplasmic, transmembrane and cytoplasmic domains (28% identity and 47% similarity); and YbbK, a multicopy suppressor of *ftsH hypX*/membrane-anchored predicted protease (22% identity and 44% similarity). Both homologs contain band 7 flotillin-like domains and therefore might be involved in the organisation of the *E. coli* membrane into functional microdomains. In a recent study YqiK has been shown to cluster in discreet foci along the cytoplasmic membrane (Lopez and Kolter, 2010), which is consistent with the hypothesis that the organisation of membrane microdomains is coordinated by flotillin-like proteins.

This formation of a supercomplex or respiratory module consisting of Hyd-2 and FRD (with their menaquinone/menaquinol binding sites in very close proximity) could therefore explain why the loss of HybA or HybB leads to an inability to transfer electrons from $H_2$ to fumarate reductase. This hypothesis is outlined below (Figure 5.9). The idea that Hyd-1 and NRA (both specific for menaquinone/menaquinol) could colocalise to the same membrane microdomain is complicated by two factors. Firstly previous gene expression studies have shown that nitrate represses hydrogenase operon expression (Richard*, et al.*, 1999), however it has also been shown that both Hyd-1 and NRA are expressed in the absence of nitrate, suggesting they could form a functional supercomplex in physiological conditions. And secondly in this study, IC010 (deletion of *hyaB*, encoding the [NiFe] active site containing large subunit of Hyd-1) cells are still capable of nitrate reduction from $H_2$ oxidation.

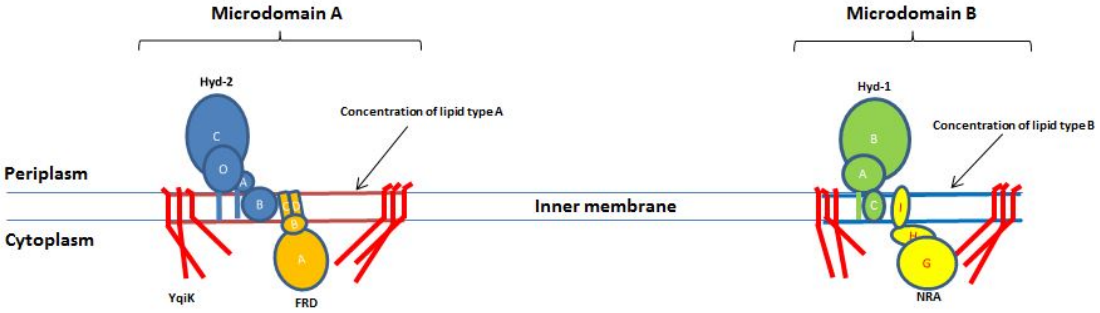


**Figure 5.9. Possible organisation of cytoplasmic membrane into microdomains.** It is proposed that bacterial membranes are organised into microdomains. Certain types of lipids as well as specific proteins containing band 7 flotillin-like domains (YqiK in *E. coli*) are thought to play a key role in these microdomains. Functionally-related protein complexes (e.g. respiratory enzymes) might therefore concentrate in these microdomains, allowing increased enzymatic activities due to the close proximity of their quinone/quinol binding sites. Hydrogenase-2 (Hyd-2) and fumarate reductase (FRD) are proposed to form a respiratory module, whereas hydrogenase-1 (Hyd-1) might reside in another microdomain where nitrate reductase A (NRA) is also localised.

It would be very interesting therefore, to repeat the $H_2$ production and oxidation assays in a Δ*yqiK* mutant. Deletion of this gene has already been shown to be non-lethal (Hinderhofer*, et al.*, 2009). If physiologically/functional respiratory complex microdomains are really formed in *E. coli*, and if YqiK is involved in the organisation of these microdomains, differences in these assays may be observed. For example, if Hyd-2 and FRD are found closely packed in the same microdomain, the rate of $H_2$ oxidation in a Δ*hyaB*, Δ*hycE*, Δ*yqiK* strain (as IC010 but lacking *yqiK*) may be significantly lower than in IC010, as the two enzyme complexes may be randomly distributed along the membrane. Similarly in a Δ*yqiK*, Δ*hybA* or Δ*yqiK*, Δ*hybB* strain, Hyd-1 may now be able to oxidise $H_2$ in the presence of fumarate, as FRD would be randomly distributed across the membrane and not tied up in microdomains. Similar experiments could be carried out with mutants lacking the cardiolipin synthase genes, *clsA*, *clsB* or *clsC* to investigate if cardiolipin played a role in organising these respiratory complexes and resulted in differences

in $H_2$ production and oxidation. The hypothesis that electrons could be conducted along hydrogenase/reductase small subunits lacking the large catalytic subunit and back into the quinone/quinol pool could be tested through deletions of the genes encoding the small subunits, e.g. *hyaA*, *hybO* etc. It would be interesting for example to perform $H_2$ oxidation assays in IC009 (Hyd-1 only) with fumarate as the sole electron acceptor, and compare these results to assays performed with IC009 lacking *hybO*. If $H_2$-dependent fumarate reduction activity was abolished, this would infer both a tight association between Hyd-2 and FRD, as well as suggesting that HybOAB is possible of electron transfer along the membrane.

And finally, the observation that the plasma membrane proteins of *Saccharomyces cerevisiae* with similar or identical transmembrane sequences colocalised to membrane microdomains and furthermore that protein relocation to another microdomain was possible by swapping their transmembrane sequence is very exciting (Spira*, et al.*, 2012). If a similar phenomenon was found in bacteria and in particular with respiratory enzyme complexes, then it can be imagined that manipulation of the transmembrane anchor sequences might result in relocation of these enzymes to another microdomain. If proven, this ability to colocalise and compartmentalise related enzymes in the cytoplasmic membrane could increase reaction rates and higher yields of specific products. In addition this would be extremely useful as a basic tool in the biochemical study of many membrane proteins.

# 6. Future Perspectives

## 6.1 Synthetic biology approaches to the synthesis of natural and synthetic bio-products

Tools developed by synthetic biology have the potential to contribute to the solution of many global grand challenges, including the production of cheap, sustainable and environmentally-friendly biofuels, as well as new and inexpensive drugs to fight disease and antibiotic resistance. One of the most famous and successful examples of a synthetic biology application in this area was in the production of artemisinic acid, an inexpensive precursor to the most effective anti-malarial drug Artemisinin (Paddon*, et al.*, 2013). This I.P.-free project used a variety of synthetic biology tools to engineer *E. coli* to produce high yields (100 mg/l) of artemisinic acid, which could then be converted into Artemisinin in a cost-effective and reliable manner.

Many research groups and pharmaceutical companies are currently engaged in the development of new antibiotic and antibacterial drugs in a frantic attempt to combat the global emergency of antibiotic resistance. Synthetic biology approaches are being used to expand upon the four main categories of broad spectrum antibiotics: cephalosporins; penicillins; quinolones; and macrolides, thus enabling libraries of completely novel antibiotics to be synthesised (Medema*, et al.*, 2011; Thaker and Wright, 2012). Other groups are also engaged in engineering bacteriophage for use as anti-biofilm therapeutics which increases the susceptibility of certain bacteria to antibiotics (Lu and Collins, 2009).

Important and high-value chemicals can also be produced using a variety of synthetic biology approaches such as heterologous enzyme expression, metabolic pathway engineering and the directed evolution of enzymes. Advanced biofuels are one such high-value commodity and indeed are the driving motivation of many synthetic biologist's research (reviewed in Rabinovitch-Deere*, et al.*, 2013). High yields of 2,3-butanediol (and mannitol) were produced using strains of *Lactococcus lactis* engineered to overexpress desired $NAD^+$- regeneration enzymes (Gaspar*, et al.*, 2011). In another example n-butanol was produced with high yields (28% w/w) from glucose through the introduction of synthetic heterologous enzymes, which drive the normally reversible reaction in a unidirectional manner (Bond-Watts*, et al.*, 2011). This study also attempted to ensure that the redox balance of the host chassis was maintained during fermentation. A variety of higher alcohols (C4 and C5 alcohols such as isobutanol, 1-butanol and 2-phenylethanol) were produced in high yields in another study, through the re-engineering of the amino acid biosynthetic pathway of *E. coli*, into which two non-native 2-keto-acid decarboxylases were introduced (Atsumi*, et al.*, 2008). Engineered cyanobacteria are another promising chassis for the production of biofuels such as alkanes (Wang*, et al.*, 2013)

and ethylene (Guerrero*, et al.*, 2012). Other biofuels produced using synthetic biology approaches include isopropanol (Hanai*, et al.*, 2007; Jojima*, et al.*, 2008), fatty-acid based biofuels from plant biomass (Steen*, et al.*, 2010) and bisabolene (a terpene-based biofuel) (Peralta-Yahya*, et al.*, 2011). These examples and the many others in the literature show the great potential of synthetic biology to cheaper, sustainable and biologically-produced fuels.

## 6.2 Metabolic engineering approaches to increase fermentative biohydrogen production in *E. coli*

Many groups have performed metabolic engineering of *E. coli* strains in order to increase overall biohydrogen yields and/or biohydrogen production rates during mixed-acid fermentation. The Hallenbeck group studied the effect of deletions to the *hyaB* and *hybC*, which encode the two uptake hydrogenases of *E. coli*: Hyd-1 and Hyd-2. They also disrupted *ldhA* and expressed a mutant *fhlA* that encodes a truncated version of the transcriptional activator known to constitutively induce all genes in the formate regulon (Bisaillon*, et al.*, 2006). The strains lacking both Hyd-1 and Hyd-2 produced 37% more $H_2$ (48.1 µmol $H_2$; in batch fermentations) than the wild type strain (35 µmol $H_2$). The *ldhA* and *fhlA* mutants showed 18% (41.4 µmol $H_2$) and 11% (39.1 µmol $H_2$) increases respectively in $H_2$ yield relative to wild type, and when these mutations were combined in the same strain, a 47% increase in $H_2$ (51.5 µmol $H_2$) was observed. The group also studied the effect of limiting various nutrients and found that they could increase fermentative $H_2$ production to close to 2 mol $H_2$ $mol^{-1}$ glucose (in 0.03% glucose) in an engineered strain expressing neither Hyd-1, Hyd-2 nor LdhA and expressing the mutant (active) FhlA (Bisaillon*, et al.*, 2006). This increase in $H_2$ yields upon deletion of the genes encoding Hyd-1 and Hyd-2 was also observed in another study (Redwood*, et al.*, 2008).

The Chatterjee group engineered the *E. coli* strain W3110 by deleting the individual genes encoding FocA, NarL (the global nitrate-dependent transcriptional regulator), Ppc and HybC, but only modest increases in $H_2$ yields were achieved (Fan*, et al.*, 2009). The overexpression of *fnr* (the global anaerobic transcriptional regulator) in the Δ*focA* mutant however, led to a large increase in $H_2$ yield from 1 µmol $H_2$ $mg^{-1}$ dry cell mass in the W3110 strain and 6 µmol $H_2$ $mg^{-1}$ dry cell mass in the W3110 strain overexpressing *fnr*, to over 10 µmol $mg^{-1}$ dry cell mass (Fan*, et al.*, 2009). Increases in $H_2$ production rates do not always equate to increased yields of $H_2$ per mol of substrate. The Wood group have performed numerous metabolic engineering studies on *E. coli* in order to boost $H_2$ production during fermentation (Maeda*, et al.*, 2007a; Maeda*, et al.*, 2008). And although 141 fold increases in the rate of $H_2$ production from formate were observed, overall $H_2$ yields from glucose only increased from 0.47 to 0.70 mol $H_2$

per mol of glucose (Maeda*, et al.*, 2008). A final example of metabolic engineering to increase $H_2$ production was combined with metabolic flux analyses of mutants (Kim*, et al.*, 2009). $H_2$ production rates and total $H_2$ yields were increased in mutants no longer expressing lactate dehydrogenase or fumarate reductase (30.6 mmol $H_2$ $g^{-1}$ cell $h^{-1}$ and 1.20 mol $H_2$ $mol^{-1}$ glucose for the wild type strain BW25113; 45.6 mmol $H_2$ $g^{-1}$ cell $h^{-1}$ and 1.61 mol $H_2$ $mol^{-1}$ glucose for the Δ*ldhA* mutant; and 52.2 mmol $H_2$ $g^{-1}$ cell $h^{-1}$ and 1.80 mol $H_2$ $mol^{-1}$ glucose for the Δ*frd* mutant) (Kim*, et al.*, 2009). Metabolic flux analysis confirmed that most of the carbons from glucose were being directed through the FHL complex as predicted *in silico* (Kim*, et al.*, 2009).

It is clear from these examples that metabolic engineering of *E. coli* strains to delete or interrupt pathways competing for electrons with FHL alone, is not sufficient to reach the yields of $H_2$ required for commercial biohydrogen production (Section 1.6.3) (Benemann, 1996). For this reason, many commentators have suggested the integration of dark/heterotrophic fermentative biohydrogen production from substrates such as glucose, and photo-fermentation by purple-photosynthetic bacteria such as *Rhodobacter sphaeroides*, which can convert organic acids produced during fermentation into further $H_2$ (Vardar-Schara*, et al.*, 2008; Kim*, et al.*, 2009).

## 6.3 Heterologous hydrogenase expression and other synthetic biology approaches to increase biohydrogen production

Another approach to boosting $H_2$ yields during heterotrophic fermentation is the construction of synthetic hydrogen-production pathways in a suitable chassis. This can then be combined with directed enzyme evolution and pathway engineering in order to increase overall $H_2$ production rates and yields. These synthetic pathways can be designed so they are insulated from or fully integrated into the metabolism of the chassis. A number of interesting examples are described below.

It had been shown that *in vitro* $H_2$ production systems could be constructed from purified mesophilic enzymes of the oxidative pentose phosphate cycle in combination with a purified NADPH-dependent hydrogenase from the thermophilic bacterium *Pyrococcus furiosus* (Woodward*, et al.*, 2000). Using this *in vitro* enzymatic system 11.6 mol $H_2$ $mol^{-1}$ from glucose 6-phosphate were achieved (which is close to the theoretical maximum yield), however the rate of $H_2$ production was very slow. In order to increase the reaction rates, thermally stable enzymes of the pentose phosphate pathway would be required (Woodward*, et al.*, 2000). A completely cell-free system for the transcription, translation and maturation of hydrogenases was demonstrated using the [FeFe]-hydrogenase from *Clostridium pasteurianum* (Boyer, et al., 2008). H-cluster maturation was accomplished using HydEFG-containing crude cell extracts

from *Shewanella oneidensis*. Active synthetic enzyme constituted 44% of the synthesised protein, and this could be increased through the addition of Fe and S to cell extracts prior to maturation. It is worth noting that the authors used oxidised MV as an artificial electron acceptor from $H_2$, as no physiological electron donor/acceptor was synthesised (Boyer*, et al.*, 2008). Building upon this newly-developed technique, high-throughput screening of mutant [FeFe]-hydrogenase libraries for increased hydrogenase activity could be performed (Stapleton and Swartz, 2010b; Stapleton and Swartz, 2010a; Bingham*, et al.*, 2012). Microfluidics techniques were utilised to develop an *in vitro* compartmentalisation method for the synthesis, maturation and screening of mutant hydrogenase libraries for properties such as $O_2$ tolerance in [FeFe]-hydrogenase (Stapleton and Swartz, 2010a; Stapleton and Swartz, 2010b).

Another interesting protein evolution approach to increase $H_2$ production during fermentation was performed on FhlA, the transcriptional regulator of the *E. coli* formate regulon (including FHL/Hyd-3) (Sanchez-Torres*, et al.*, 2009). Random mutagenesis of *fhlA* followed by screening identified a number of FhlA variants that led to an increase of up to nine fold in total $H_2$ yields.

Before the identities of the essential [FeFe] active site maturation proteins, HydE, HydF and HydG were known, many groups expressed these hydrogenases in a chassis known to encode [FeFe]-hydrogenases. *Clostridium acetobutylicum* is one such organism and was used to overexpress its own [FeFe]-hydrogenase, as well as the heterologous expression of those from *Chlamydomonas reinhardtii* and *Scenedesmus obliquus* (Girbal*, et al.*, 2005). Enzyme could be purified with high specific activities indicating this strategy was successful. The *C. reinhardtii* hydrogenase was also heterologously expressed in a *Shewanella oneidensis* chassis with active enzyme purified (Sybirna*, et al.*, 2008). Metagenomics offers an exciting bioprospecting tool for synthetic biologists as DNA sequences from unculturable organisms can now be cloned/synthesised and novel enzymes hopefully identified. One of the first uses of this metagenomic approach in the hydrogenase field involved the cloning of environmental DNA from Sargasso Sea that was suspected to encode a [NiFe]-hydrogenase (Maroti*, et al.*, 2009). The sequence shared 60% sequence identity with a [NiFe]-hydrogenase found in *Thiocapsa roseopersicina* and therefore this synthetic hydrogenase was expressed in this organism. Only two extra accessory genes: *hyaD*; and *hupH* from the putative operon identified in the metagenomic study were required for full maturation of the [NiFe] active site as the rest could be performed by host maturation machinery. $H_2$ uptake and production were observed confirming the successful expression and maturation of this synthetic hydrogenase sequence in a new chassis (Maroti*, et al.*, 2009).

Once the maturation proteins required for [FeFe] active site maturation were identified, synthetic biologists could immediately use this information to express [FeFe]-hydrogenases in *E. coli*, which does not contain any of these accessory genes. This could then lead to the construction of more complex synthetic devices incorporating the fast $H_2$-producing [FeFe]-hydrogenases in a wide variety of chasses. High-yields of heterologously-expressed [FeFe]-hydrogenases from *C. pasteurianum* and *C reinhardtii* can now be expressed in *E. coli* along with *hydEFG* (Kuchenreuther*, et al.*, 2010). These enzymes were purified and displayed high specific $H_2$ production and oxidation activities with artificial and physiologically-relevant electron donors and acceptors (MV and ferredoxin respectively). More complex synthetic $H_2$-production pathways have also been constructed in *E. coli*, which are capable of expressing not only the [FeFe]-hydrogenase and accessory genes but also the genes encoding the physiological electron donor in their native organism, ferredoxin and the oxidoreductase responsible for reducing this electron donor from pyruvate. One such study expressed *Clostridium acetobutylicum hydA*, *hydE*, *hydF* and *hydG* in addition to the gene encoding the [4Fe–4S]-ferredoxin from *Clostridium pasteurianum* (Akhtar and Jones, 2009). The authors tested the ability of the putative *E. coli* pyruvate ferredoxin oxidoreductase (PFOR) homolog, YdbK, to oxidise pyruvate and concurrently reduce the *C. pasteurianum* ferredoxin. If successful this should pass electrons to the [FeFe]-hydrogenase and produce $H_2$. Yields of up to 1.46 mol $H_2$ $mol^{-1}$ glucose were obtained (measured using gas chromatography) and this was improved further through nutritional supplementation to the growth media (Akhtar and Jones, 2009).The additional introduction of AmyE from *Bacillus subtilis* enabled starch-dependent $H_2$ synthesis in minimal media (Akhtar and Jones, 2009).

In a study by the Silver lab at Harvard, an insulated synthetic $H_2$-producing pathway was constructed in *E. coli* (Agapakis*, et al.*, 2010). Various combinations of ferredoxins, PFORs, HydEFG-encoding synthetic operons and [FeFe]-hydrogenases were tested for high levels of $H_2$ production and the best combination selected. Synthetic codon-optimised genes encoding the ferredoxin and [FeFe]-hydrogenase from *Clostridium acetobutylicum* along with the PFOR from *Desulfovibrio africans* and HydEFG from *C. reinhardtii* were designed, constructed and successfully expressed in *E. coli* (Agapakis*, et al.*, 2010). A number of insulation strategies were tested including: the deletion of competing native FeS proteins (Δ*ydbK* = 1.4 fold increase in $H_2$ production); the physical linking of the [FeFe]-hydrogenase to the ferredoxin protein with flexible peptide linkers (14 aa = 5 fold increase in $H_2$ yields relative to non-linked); the attachment of the hydrogenase and ferredoxin to a protein scaffold with different peptide linkers (3 fold increase in $H_2$ when scaffolded; closer scaffolding = better; 2:1 ratio of linked hydrogenase molecules to ferredoxin = 1.5 fold increase over 1:1 ratio); and finally attempts to

improve the interaction between the ferredoxin and hydrogenase through the mutation of specific surface residues (Agapakis*, et al.*, 2010). In another study by the Silver lab, rationally designed RNA aptamer scaffolds with distinct docking sites were used to spatially organise a [FeFe]-hydrogenase and a ferredoxin (Delebecque*, et al.*, 2011). The three different RNA scaffold types increased total $H_2$ yield by 4, 11 and 48 times respectively (Delebecque*, et al.*, 2011).

## 6.4 Concluding remarks

This project used a number of synthetic biology approaches to produce biohydrogen in *E. coli*. A synthetic [FeFe]-hydrogenase operon was successfully constructed, expressed and the enzyme complex characterised in *E. coli*. A synthetic *E. coli* strain was then constructed to host this synthetic hydrogenase and fully integrate the envisaged synthetic $H_2$-production pathway into mixed-acid fermentation. This integration into central metabolism would allow for the directed evolution of the enzyme coupled with selection or screening for variants with increased catalytic activity and/or reaction specificity. An active, synthetic, chimeric metalloenzyme capable of producing $H_2$ in *E. coli* was also constructed in this project. This fusion-protein approach, where the catalytic activities of two unrelated enzymes were combined, has not been widely explored in the hydrogenase field and could lead to new $H_2$ production pathways. New pathways for $H_2$ production will be essential to achieve the biohydrogen yields required to make it commercially viable.

Synthetic biology projects utilising hydrogenase enzymes require fundamental biochemical research for a number of reasons. Firstly identify new candidate biological parts and secondly the comprehensive characterisation of these enzymes (in a number of different environmental conditions) is essential to fully elucidate the mechanisms of biosynthesis and catalysis, which can be used in biotechnological projects. With this motivation, novel $H_2$ production by *E. coli* Hyd-2 was also demonstrated and investigated in this project.

In the future, it is likely that commercial biohydrogen production will require a combination of natural hydrogenase enzymes and new artificial biomimetic catalysts. These artificial chemical catalysts mimic the active site of hydrogenase enzymes and can perform $H_2$ catalysis at high rates (Helm*, et al.*, 2011; Berggren*, et al.*, 2013). Electrons of course are still required and perhaps it would be advantageous in the future to use *de novo* protein scaffolds (such as those designed by the Baker lab at Washington State University; e.g. Tinberg*, et al.*, 2013), which have been optimised for efficient and rapid electron transfer to such a synthetic catalyst. Furthermore it would be amazing if these catalysts and scaffolds could be genetically encoded using novel synthetic nucleic-acid code and then fully assembled in a chassis. Such a truly

“synthetic” organism could produce cheap and plentiful biohydrogen for use as the future fuel of the planet.

# 7. Materials and Methods

## 7.1 Table of Bacterial Strains

| Bacterial Strain | Genotype | Antibiotic Resistance | Reference |
|---|---|---|---|
| MG1655 | wild-type *E. coli* strain F-, λ-, *rph*-1, *ilvG*, *rfb*-50 | None | (Blattner*, et al.*, 1997) |
| MC4100 | F- [*ara*D139]B/r Δ(*arg*F-lac)169 &lambda- e14- *flh*D5301 Δ(*fruK*-*yeiR*)725 (*fru*A25)‡ *rel*A1 *rps*L150(*str*R) *rbs*R22 Δ(*fim*B-*fim*E)632(::IS1) *deo*C1 | None | (Casadaban, 1976) |
| K38 (pGP1-2) | *HfrC phoA4 pit-10, tonA22 ompF 627, relA1 spoT1* $\lambda^+$ pGP1-2 encodes T7 RNA polymerase | Kan | (Tabor and Richardson, 1985) |
| FTD147 | As MC4100 but Δ*hyaB, hybC, hycE* | None | (Redwood*, et al.*, 2008) |
| FTD89 | As MC4100 but Δ*hyaB, hybC* | None | (Sargent*, et al.*, 1999) |
| DH5α | F-, ϕ80d*lacZ*ΔM15, Δ(*lacZYA*-*argF*)U169, *deoR*, *recA1*, *endA1*, hsdR17($r_K$-, $m_K$+), *phoA*, *supE44*, λ-, *thi*-1, *gyr*A96, *rel*A1 | None | (Grant*, et al.*, 1990) |
| FTD147h | As FTD147 but Δ*adhE*::*TtehydC-B* | None | This work |
| FTD147h3 | As FTD147 but Δ*adhE*::*TtehydC-A* | None | This work |
| RaisynA1 | As FTD147h but *ΔldhA* | None | This work |
| Teatotal1 | As FTD147 Δ*adhE* | None | This work |
| MG059e1 | MG1655 that encodes a version of HycE with an internal 6xHis epitope tag | None | (McDowall, Palmer and Sargent, unpublished) |
| Maggie1 | As MG059e1 but *ΔldhA* | None | This work |
| IronBrew | As RaisynA1 but *ΔiscR* | None | This work |
| FTD147h3Δ*iscR* | As FTD147h3 but *ΔiscR* | None | This work |
| PK4854 | As MG1655 but *ΔiscR* | None | (Schwartz*, et al.*, 2001) |
| PK4854Δ*hypF* | As PK4854 but *ΔhypF* | None | This work |
| PK4854Δ*metJ* | As PK4854 but *ΔmetJ* | None | This work |

| | | | |
|---|---|---|---|
| FTD147(DE3)Δ*metJ* | As FTD147(DE3) but *ΔmetJ* | None | This work |
| IC010 | As MC4100 but *ΔhyaB, hycE* | None | (Deplanche*, et al.*, 2010) |
| IC009 | As MC4100 but *ΔhybC, hycE* | None | (Deplanche*, et al.*, 2010) |
| IC011 | As MC4100 but *ΔhyaB, hycE, hybOA* | None | This work |
| FTD671 | As MC4100 but *ΔhybA* | None | (Dubini*, et al.*, 2002) |
| FTD672 | As MC4100 but *ΔhybB* | None | (Dubini*, et al.*, 2002) |
| XL1-Red | *endA1 gyrA96 thi-1 hsdR17 supE44 relA1 lac mutD5 mutS mutT* Tn10 | Tet | Stratagene |
| XL10-Gold | *(mcrA)183 Δ(mcrCB-hsdSMR-mrr)173 endA1 supE44 thi-1 recA1 gyrA96 relA1 lac* Hte [F´ *proAB* $lacI^{q}ZΔM15$ Tn10] | Tet, Cml | Stratagene |

**Table 7.1 Table of bacterial strains used in this study**

## 7.2 Media and Additives

| Medium | Components | Sterilised | Quantity ($L^{-1}$) |
|---|---|---|---|
| Cohen-Rickenberg (CR) media | $K_2HPO_4$ | | 4.8 g |
| | $KH_2PO_4$ | | 9.8 g |
| | Peptone | | 5 g |
| | $(NH_4)_2SO_4$ | | 2 g |
| | Trace elements * | autoclave | 1 ml |
| | 100 mM MoSes * | filtered | 1 ml |
| | 1% Thiamine * | filtered | 1 ml |
| | 1 M $MgCl_2$ * | filtered | 2 ml |
| | 10% casamino acids * | autoclave | 2 ml |
| LB-agar | NaCl | | 10 g |
| | Tryptone | | 10 g |
| | Yeast Extract | | 5 g |
| | Agar | | 15 g |
| LBMC soft agar | NaCl | | 10 g |
| | Tryptone | | 10 g |
| | Yeast Extract | | 5 g |
| | Agar | | 6.5 g |
| | 0.5 M $CaCl_2$ * | filtered | 10 ml |
| | 1 M $MgSO_4$ * | filtered | 10 ml |
| Luria Bertani medium (LB) | NaCl | | 10 g |
| | Tryptone | | 10 g |
| | Yeast Extract | | 5 g |
| M9 medium | 100 mM $CaCl_2$ * | filtered | 1 ml |
| | 10x M9 salts * | autoclave | 100 ml |
| | 1 M $MgSO_4$ * | filtered | 2 ml |
| | 1% Thiamine * | filtered | 2 ml |
| | MoSe's * | filtered | 1 ml |
| M9 agar | As M9 medium | | |
| | + Agar | | 16 g |
| R-medium | NaCl | | 5 g |
| | Tryptone | | 10 g |
| | Yeast Extract | | 5 g |
| | Agar | | 15 g |
| | 20% Glucose * | filtered | 5 ml |
| | 0.5 M $CaCl_2$ * | filtered | 4 ml |
| TYGES | NaCl | | 5 g |
| | Tryptone | | 10 g |
| | Yeast Extract | | 5 g |
| | 20% Glucose * | filtered | 20 ml |
| SOB medium | Tryptone | | 20 g |
| | Yeast extract | | 5 g |
| | NaCl | | 5 g |

| Medium | Components | Sterilised | Quantity ($L^{-1}$) |
|---|---|---|---|
| | 1 M $MgCl_2$ | filtered | 10 ml |
| | 1 M $MgSO_4$ | filtered | 10 ml |
| SOC medium | As SOB medium + 0.4% Glucose | filtered | 20 ml |

**Table 7.2 Growth media used in this study.**

Constituents were sterilised by autoclaving unless indicated by an asterisk in which case it was sterilised individually and then added to the media afterwards

| Media Supplement | Stock concentration | Final concentration |
|---|---|---|
| Glucose | 20% | 0.4% |
| Glycerol | 50% | 0.5% |
| IPTG | 1 M | 2 mM |
| SDS | 20% | 2% |
| Sodium formate | 50% | 0.5% |
| Sodium fumarate | 16% | 0.4% |
| Sodium nitrate | 20% | 0.4% |
| Sodium pyrophosphate | 250 mM | 3.125 mM |
| Ferric ammonium citrate | 1 M | 2 mM |
| Cysteine | 1 M | 2 mM |
| L-arabinose | 1 M | 2 mM |
| Trace elements ($g\ L^{-1}$)<br>0.48 g $FeCl_3.6H_2O$<br>0.33 g $MnCl_2.4H_2O$<br>0.36 g $CaCl_2.2H_20$<br>2 g $ZnCl_2$<br>0.2 g $H_3BO_3$<br>0.1 g $CoSO_4$ | 1000x | 1x |
| M9 salts ($g\ L^{-1}$)<br>10 g $NH_4Cl$<br>5 g NaCl<br>30 g $KH_2PO_4$<br>64 g $NaH_2PO_4.7H_2O$ | 10x | 1x |

**Table 7.3 Media supplements**

| Antibiotic | Stock concentration | Prepared in | Final concentration |
|---|---|---|---|
| Ampicillin | 125 mg $ml^{-1}$ | Water | 100 µg $ml^{-1}$ |
| Chloramphenicol | 25 mg $ml^{-1}$ | 80% ethanol | 25 µg $ml^{-1}$ |
| Kanamycin | 50 mg $ml^{-1}$ | Water | 50 µg $ml^{-1}$ |

**Table 7.4 Antibiotics**

## 7.3 Culture conditions

Aerobic growth of *E. coli* strains was achieved by culturing the bacteria in Luria Bertani (LB) medium at 37 °C with shaking at 200 rpm. A minimum liquid to air ratio of 1:4 was maintained in each case. Anaerobic growth of *E. coli* was ensured by completely filling the growth vessel with LB medium and incubating, without agitation, at 37 °C. 500 ml volumes were typically used for $H_2$ oxidation/production assays with whole cells/cell lysates.

For growth on solid media, LB containing 1.5% agar was utilised and incubated at 37 °C. Two methods were tested to generate anaerobic conditions for solid agar plate experiments. Plates were incubated in Oxoid anaerobic jars with either Oxoid Anaerogen sachets or by 5 cycles of filling and evacuation of Argon gas. Merck Anaerotest strips were used to confirm anaerobiosis.

Inoculated plates were stored at 4 °C for no more than 14 days. Strains and plasmid stocks (in DH5α) were stored in cryogenic vials at -80°C long term. Long term, strain and plasmid stocks (in DH5α) were flash frozen in liquid nitrogen and then stored at -80°C as 25% (v/v) glycerol stock cultures in cryogenic vials.

## 7.4 Buffers and solutions

| Buffer/Solution | Component |
|---|---|
| APS | 10% ammonium persulphate |
| Carbonate transfer buffer | 10 mM $NaCHO_3$ pH 9.9<br>3 mM $Na_2CO_3$<br>20% (v/v) methanol |
| Sodium dithionite | 1% (w/v) dithionite<br>Dissolved in 1mM NaOH |
| DNA loading buffer | 0.25% (w/v) bromophenol blue<br>0.25% (w/v) xylene cyanol blue<br>40% (w/v) sucrose |
| Laemmli sample buffer (2x) | 62.5 mM Tris HCl pH 6.8<br>2% (w/v) SDS<br>5% (v/v) β-mercaptoethanol<br>25% (v/v) glycerol<br>0.01% (w/v) bromophenol blue |
| Lysozyme<br>(60 mg $ml^{-1}$) | 6% lysozyme (from chicken egg white)<br>Dissolved in 1 ml Tris (HCl) pH 7.5 |
| MC Buffer | 100 mM $MgSO_4$<br>5 mM $CaCl_2$ |
| Mg buffer (10x) | 100 mM Tris HCl pH 7.5<br>12 mM $MgCl_2$ |
| Phosphate buffer pH 7.0 | $Na_2HPO_4$ to desired molarity<br>(pH in $NaH_2PO_4$) |
| SDS-running buffer (5x) | 25 mM Tris HCl pH 8.3<br>192 mM glycine<br>0.5% (w/v) SDS |

| Buffer/Solution | Component |
|---|---|
| TAE buffer | 40 mM Tris HCl pH 8.0<br>1.142% (v/v) acetic acid<br>1 mM EDTA |
| TBS-Tween (TBS-T) | 1x TBS<br>0.1% (v/v) Tween 20 |
| Transformation Buffer (TSB) | 20 ml LB<br>1 ml 1 M $MgSO_4$<br>1 ml DMSO<br>2 g PEG 6000 |
| Tris buffered saline (TBS) | 20 mM Tris HCl pH 7.6<br>137 mM NaCl |
| Rocket immunoelectrophoresis running buffer | 20 mM Sodium barbitone HCl pH 8.6<br>0.1% (v/v) Triton X-100 |
| Tris-sucrose buffer | 50 mM Tris HCl, pH 7.5<br>40% (w/v) Sucrose |
| Tris HCl | 50 mM Tris HCl<br>Adjusted to required pH by the addition of HCl |
| Ni-purification resuspension buffer | 50 mM Tris HCl pH7.5<br>1 mM DTT<br>2 mM flavin mononucleotide<br>150 mM NaCl<br>25 mM imidazole |
| Ni-purification buffer A | 50 mM Tris HCl pH7.5<br>1 mM DTT<br>150 mM NaCl<br>25 mM imidazole |

| Buffer/Solution | Component |
|---|---|
| Ni-purification buffer B | 50 mM Tris HCl pH7.5<br>1 mM DTT<br>150 mM NaCl<br>1 M imidazole |
| SEC buffer | 50 mM Tris HCl pH7.5<br>1 mM DTT<br>150 mM NaCl |
| Benzyl viologen (BV) | 250 mM (stock) |
| Methyl viologen (MV) | 250 mM (stock) |

**Table 7.5 Buffers and solutions used**

## 7.5 **Molecular Biology Techniques**

### 7.5.1 Table of Plasmids

| Plasmid | Details | Antibiotic resistance | Reference |
|---|---|---|---|
| pUNIPROM | Medium copy expression vector with promoter and RBS from *tat* operon | Amp | (Jack*, et al.*, 2004) |
| pSUPROM | Low copy expression vector with promoter and RBS from *tat* operon | Kan | |
| pUNI-Tte-Hyd | Synthetic *Tte hydC-A* cloned *Bam*HI – *Hind*III into pUNIPROM | Amp | This work |
| pUNI-Tte-$Hyd_{hisC}$ | As pUNI-Tte-Hyd but encodes a 6 x His tag on HydC | Amp | This work |
| pUNI-Tte-$Hyd_{hisC}$ Δ*hydD* | As pUNI-Tte-$Hyd_{hisC}$ but Δ*hydD* | Amp | This work |
| pUNI-Tte-$Hyd_{hisC}$ Δ*Tte0891* | As pUNI-Tte-$Hyd_{hisC}$ but Δ*Tte0891* | Amp | This work |
| pSU-Sh-EFG | *Sh. oneidensis hydGXEF* operon cloned *Bam*HI – *Hind*III into pSUPROM | Kan | This work |
| pSU-Tte-EFG | Synthetic operon encoding *Ca. tengcongensis hydEFG* homologs cloned *Bam*HI – *Sal*I into pSUPROM | Kan | This work |
| pACYCDuet1 | Medium copy expression vector with two separate MCS, $T7_{lac}$ promoters and T7 terminators | Cml | Novagen |
| pAC-Tte-EFG | Synthetic operon encoding *Ca. tengcongensis hydEFG* homologs cloned *Bam*HI – *Sal*I into pACYCDuet-1 | Cml | This work |
| pAC-Duet-Sh-GX-EF | *Sh. oneidensis hydGX* (*Eco*RI - *Hind*III) and *hydEF* (*Bgl*II - *Aat*II) cloned in two MCS of pACYCDuet-1 | Cml | This work |
| pAC-Duet-Sh-GX | *Sh. oneidensis hydGX* cloned *Eco*RI - *Hind*III into the first MCS of pACYCDuet-1 | Cml | This work |
| pSU23 | Medium copy expression vector | Cml | (Bartolome*, et al.*, 1991) |
| pUNI-Tte-EFG | Synthetic operon encoding *Ca. tengcongensis hydEFG* homologs cloned *Bam*HI – *Sal*I into | Amp | This work |

| | | | |
|---|---|---|---|
| | pUNIPROM | | |
| pUNI-Sh-EFG | *Sh. oneidensis hydGXEF* operon cloned *Bam*HI – *Hind*III into pUNIPROM | Amp | This work |
| pSU23-Sh-GX-EF | Two MCS of pAC-Duet-Sh-GX-EF cloned *Eco*RI – *Kpn*I into pSU23 | Cml | This work |
| pSUtat-Sh-GX-EF | As pSU23-Sh-GX-EF but with *tat* promoter upstream of first MCS | Cml | |
| pSU23-Sh-GXEF-TM | As pSU23-Sh-GX-EF but with *Th. maritima hydF* homolog *TM0445* cloned in downstream of *hydEF* | Cml | This work |
| pSUtat-Sh-GXEF-TM | pSU23-Sh-GX-EF-TM but with *tat* promoter upstream of first MCS | Cml | This work |
| pCP20 | Temp$^{s}$ vector containing FLP recombinase | Amp / Cml | (Datsenko and Wanner, 2000) |
| pUNI-Tm-Fd6 | *Th. maritima TM0927* ferredoxin gene cloned *Bam*HI – *Sal*I into pUNIPROM so it encodes a N-terminal His tag | Amp | This work |
| pUNI-Tm-Fd8 | *Th. maritima TM0927* ferredoxin gene cloned *Bam*HI – *Sal*I into pUNIPROM so it encodes a C-terminal His tag | Amp | This work |
| pUNI-Tm-POR$_{his}$ | *Th. maritima* PFOR operon (*TM0015-0018*) cloned *Xba*I – *Hind*III into pUNIPROM | Amp | This work |
| pUNI-Tm-Fd-POR$_{his}$ | *Th. maritima* Fd gene (*TM0927*; *Xba*I - *Hind*III) and PFOR operon (*TM0015-0018*; *Bam*HI - *Xba*I) cloned into pUNIPROM | Amp | This work |
| pKS II $^{+}$ | pBluescript, high copy expression vector | Amp | Stratagene |
| pMAK705 | low copy temperature sensitive plasmid | Cml | (Hamilton*, et al.*, 1989) |
| pKSmetJ | 500 bp up and downstream sequence of *metJ* cloned *Kpn*I – *Hind*III into pKS II$^{+}$ | Amp | This work |
| pMAKmetJ | 500 bp up and downstream sequence of *metJ* cloned *Kpn*I – *Hind*III into pMAK705 | Cml | This work |
| pKSiscR | 500 bp up and downstream sequence of *iscR* cloned *Kpn*I – *Hind*III into pKS II$^{+}$ | Amp | This work |
| pBAD33 | medium copy expression vector with P$_{ara}$ | Kan | <WHO MAKES THIS?> |
| pBAD33-PR | Proteorhodopsin gene cloned *Sal*I | Cml | This work |

| | | | |
|---|---|---|---|
| | - *Hind*III into pBAD33 expression vector | | |
| pSU-PR | Proteorhodopsin gene cloned *Sal*I - *Hind*III into pSUPROM | Kan | This work |
| pGP1-2 | Temp$^{s}$ plasmid that expresses T7 polymerase when induced at 42 °C | Kan | (Tabor and Richardson, 1985) |
| pUNI-Tte-Hyd(*adhE*prom) | As pUNI-Tte-Hyd but with *adhE* promoter instead of *tat* promoter | Amp | This work |
| pUNI-Tte-Hyd(*fadh*prom) | As pUNI-Tte-Hyd but with *fadh* promoter instead of *tat* promoter | Amp | This work |
| pUNI-Tte-Hyd(*fadh*prom)$_{hisC}$ | As pUNI-Tte-Hyd$_{hisC}$ but with f*adh* promoter instead of *tat* promoter | Amp | This work |
| pUNI-Tte-Hyd(*hyaA*prom) | As pUNI-Tte-Hyd but with *hyaA* promoter instead of *tat* promoter | Amp | This work |
| pUNI-Tte-Hyd(*hyaA*prom)$_{hisC}$ | As pUNI-Tte-Hyd$_{hisC}$ but with *hyaA* promoter instead of *tat* promoter | Amp | This work |
| pUNI-Tte-Hyd(*hybO*prom) | As pUNI-Tte-Hyd but with *hybO* promoter instead of *tat* promoter | Amp | This work |
| pUNI-Tte-Hyd(*hybO*prom)$_{hisC}$ | As pUNI-Tte-Hyd$_{hisC}$ but with *hybO* promoter instead of *tat* promoter | Amp | This work |
| pAH2 | Plasmid encoding *phsABC* from *Salmonella* | Amp | (Stoffels*, et al.*, 2012) |
| pUNI-OSPhs | Fusion gene of highly-truncated *hybO* and *phsB* with HA-tag linker peptide and *phsC* cloned *Bam*HI - *Hind*III into pUNIPROM | Amp | This work |
| pUNI-OLPhs | Fusion gene of a less-truncated *hybO* and *phsB* with HA-tag linker peptide and *phsC* cloned into pUNIPROM | Amp | This work |
| pUNI-OS$_{SalI}$Phs | As pUNI-OSPhs but HA-tag linker replaced with two amino acid linker | Amp | This work |
| pUNI-OS$_{FLexA}$Phs | As pUNI-OSPhs but HA-tag linker replaced with a flexible peptide linker | Amp | This work |
| pUNI-OS$_{FlexD}$Phs | As pUNI-OSPhs but HA-tag linker replaced with flexible peptide linker | Amp | This work |
| pUNI-OS$_{-6aaFlexA}$Phs | As pUNI-OSPhs but HA-tag linker replaced with flexible peptide linker and a further truncation to *hybO* | Amp | This work |
| pUNI-OS$_{mut}$Phs | As pUNI-OSPhs but mutations to backbone of vector | Amp | This work |

**Table 7.6 Table of plasmids used in this study**

### 7.5.2 Plasmid DNA preparation

Plasmids were extracted from cell pellets of 5 ml overnight aerobic cultures of *E. coli* strains transformed with the plasmid of interest using the QIAprep® Spin Miniprep Kit (Qiagen), which is based on the alkaline lysis method of extracting plasmid DNA developed by Birnboim and Doly (Birnboim and Doly, 1979). Plasmid DNA was then eluted in the elution buffer supplied. Plasmids used in this study are listed in Table 7.6. DNA was quantified spectrophotometrically using a NanoDrop ND-1000 system (Thermo Scientific) and by recording the absorbance peak of nucleic acid at 260 nm.

### 7.5.3 Polymerase Chain Reaction (PCR)

DNA fragments were amplified using the polymerase chain reaction (PCR). Standard reaction mixtures used are shown in Table 7.7. GoTaq DNA polymerase (BioRad) was typically used for diagnostic PCRs using genomic DNA from bacterial colonies as the template (one colony in 60 µl Milli-Q water; 3 µl used). Herculase II (Agilent Technologies) was used for high fidelity PCR and to amplify DNA fragments used for cloning, and approximately 200 ng of plasmid or genomic DNA was used as the template. Standard reaction cycling conditions are detailed in Table 7.8. Annealing temperature varied depending on the melting temperature of the primers used (50 – 60 °C) and 30 cycles were typically performed.

| **Component** | **Volume** |
|---|---|
| 10 x buffer (Herc)/5 x buffer (GoTaq) | 5 µl (Herc)/10 µl (GoTaq) |
| Forward primer (10 µM) | 1.5 µl |
| Reverse primer (10 µM) | 1.5 µl |
| dNTPs (20 µM) | 1.0 µl |
| Polymerase | 1.0 µl (Herc)/0.5 µl (GoTaq) |
| DNA template | 1.0 µl |
| $ddH_2O$ | 39.0 µl (Herc)/34.5 µl (GoTaq) |
| **Total** | **50 µl** |

**Table 7.7 PCR reaction mixtures**

| Step | Temperature | Time |
|---|---|---|
| Initial denaturation | 95 °C | 5 m |
| Denaturation | 95 °C | 30 s |
| Annealing | 50 – 60 °C | 30 s |
| Elongation | 72 °C | 1 m/kb |
| Final elongation | 72 °C | 5 m |

**Table 7.8 PCR reaction cycling conditions**

7.5.4 Table of Primers

| Name | Sequence 5' to 3' | Details |
|---|---|---|
| hyaAPROMfor | GCGCGAATTCGATGCGGCGTGTAAACC | Used to amplify promoter sequence of *hyaA* to clone in front of *Tte* Hyd operon |
| hyaAPROMrev | GCGCGGATCCCTCCTTGCGACACCGGCAGG | Used to amplify promoter sequence of *hyaA* to clone in front of *Tte* Hyd operon |
| hybOPROMfor | GCGCGAATTCAATTCTGTGCCGATTATAAACG | Used to amplify promoter sequence of *hybO* to clone in front of *Tte* Hyd operon |
| hybOPROMrev | GCGCGGATCCTTGCGAAGACCTGGCATATATTTTGC | Used to amplify promoter sequence of *hybO* to clone in front of *Tte* Hyd operon |
| adhEPROMfor | GCGCGAATTCGGTTAGCTCCGAAGCAAAAG | Used to amplify promoter sequence of *adhE* to clone in front of *Tte* Hyd operon |
| adhEPROMrev | GCGCGGATCCAATGTTAAACTTTTTTAGTAAATCATCTGC | Used to amplify promoter sequence of *adhE* to clone in front of *Tte* Hyd operon |
| fadhPROMfor | GCGCGAATTCCAAGGCGCACCAAATTTCTCCTGG | Used to amplify promoter sequence of *fadh* to clone in front of *Tte* Hyd operon |
| fadhPROMrev | GCGCGGATCCTGTAAAATAATTGTTATGTGGTCG | Used to amplify promoter sequence of *fadh* to clone in front of *Tte* Hyd operon |
| EcoRIT5PROMfor | GCGCGAATTCAAATCATAAAAAATTTATTTGCTTTGTGAGC | Used to amplify promoter sequence of T5 to clone in front of *Tte* Hyd operon |

| | | |
|---|---|---|
| EcoRIT5promrev | GCGCGAATTCTTTCTCCTCTTTAATGTATTCTGTGTGAAATTGTTATC | Used to amplify promoter sequence of T5 to clone in front of *Tte* Hyd operon |
| NdeIT5promfor | GCGCCATATGAAATCATAAAAAATTTATTTGCTTTGTGAGC | Used to amplify promoter sequence of T5 to clone in front of *Tte* Hyd operon |
| NdeIT5promrev | GCGCAGATCTTTTCTCCTCTTTAATGTATTCTGTGTGAAATTGTTATC | Used to amplify promoter sequence of T5 to clone in front of *Tte* Hyd operon |
| TtehydCNTermHisfor | GCGCACTAGTAGGAGGAAAAAAAAATGCACCATCACCATCACCATCAAGGTATGAAAGAGGCG | Used to introduce a C-terminal 6xHis epitope tag onto HydC of synthetic *Tte* Hyd operon |
| TtehydCNTermHisrev | GCGCACTAGTTTATTCGAACTTTTTCAGGATTTCG | Used to introduce a C-terminal 6xHis epitope tag onto HydC of synthetic *Tte* Hyd operon |
| TtehydANTermHisfor | GCGCCTCGAGTCAATGGTGATGGTGATGGTGTTTTACCAGCGGGTACAGTTCTTTACG | Used to introduce a C-terminal 6xHis epitope tag onto HydA of synthetic *Tte* Hyd operon |
| TtehydANTermHisrev | GCGCCTCGAGAGGAGGAAAAAAAAATGGACAAAGTCCG | Used to introduce a C-terminal 6xHis epitope tag onto HydA of synthetic *Tte* Hyd operon |
| SSMAfor | CTATAAGAAGTAAGCATACATCGAGAGGAGG | Quikchange™ primers used to change the first two bases of four that was needed to be changed |
| SSMArev | CCTCCTCTCGATGTATGCTTACTTCTTATAG | Quikchange™ primers used to change the first two bases of four that was needed to be changed |
| SSMBfor | CTATAAGAAGTAAGCATAGATCTAGAGGAGG | Quikchange™ primers used to change the second two bases of four that was needed to be changed |

| | | |
|---|---|---|
| SSMBrev | CCTCCTCTAGATCTATGCTTACTTCTTATAG | Quikchange™ primers used to change the second two bases of four that was needed to be changed |
| pBAD33PRfor | GCGCGTCGACAGGAGGAAAAAAAAATGGGTAAATTATTACTGATATTAGGTAGTG | Used to amplify proteorhodopsin gene from an pBAD21-PR to clone into pBAD33 and pSUPROM |
| pBAD33PRrev | GCGCAAGCTTTCATCCGCCAAAACAGCCAAGCTGGAG | Used to amplify proteorhodopsin gene from an pBAD21-PR to clone into pBAD33 and pSUPROM |
| SalIonlylinkrev | GTCGACGGCAAGCTGATGGATGCCTTTATGGAAGC | Used to exchange the HA-tag linker between HybO and PhsB of fusion enzyme with just two amino acids |
| SalIonlylinkfor | GTCGACAATCATTTAACGAATCAGTACGTCATGC | Used to exchange the HA-tag linker between HybO and PhsB of fusion enzyme with two amino acids |
| FlexASacIfor | GAGCTCGGTGGTGGTGGTTCTAATCATTTAACGAATCAGTACG | Used to exchange the HA-tag linker between HybO and PhsB of fusion enzyme with a flexible linker |
| FlexASacIrev | GAGCTCAATCATTTAACGAATCAGTACGTCATGC | Used to exchange the HA-tag linker between HybO and PhsB of fusion enzyme with a flexible linker |
| FlexDSacIfor | GAGCTCGGTGGTGGTGGTGGTGGTGGTAATCATTTAACGAATCAGTACG | Used to exchange the HA-tag linker between HybO and PhsB of fusion enzyme with a different |

| | | |
|---|---|---|
| | | flexible linker |
| FlexDSacIrev | GAGCTCAATCATTTAACGAATCAGTACGTCATGC | Used to exchange the HA-tag linker between HybO and PhsB of fusion enzyme with a different flexible linker |
| 6shortaaFlexfor | TCTAGATACCCATACGATGTTCCAGATTACGCTAATCATTTAACG | Used to exchange the HA-tag linker between HybO and PhsB of fusion enzyme with a flexible linker and a C-terminal truncation of HybO |
| 6shortaaFlexrev | TCTAGAGATACCTTCTTCGTTACAGCCATAGCAAGG | Used to exchange the HA-tag linker between HybO and PhsB of fusion enzyme with a flexible linker and a C-terminal truncation of HybO |
| DRGXfor | GCGCGAATTCAGGAGGAAAAAAAAATGAGCACACACGAGC | Used to amplify the *Sh. oneidensis* hydGX genes to clone into pACYC-Duet |
| DuetShGtoXrev | CGCGAAGCTTTCATCTGTTAAACCC | Used to amplify the *Sh. oneidensis* hydGX genes to clone into pACYC-Duet |
| DREFfor | GCGCAGATCTAGGAGGAAAAAAAAATGATCACTCGCCCTAGC | Used to amplify the *Sh. oneidensis* hydEF genes to clone into pACYC-Duet |
| newDuetShEtoFrev | CGCGGACGTCCTATTGCTGAGGATTGCGG | Used to amplify the *Sh. oneidensis* hydEF genes to clone into pACYC-Duet |
| rmhydB1 | ATGAGAGCTCGCATGCAGG | Used to amplify the *Tte hydB* gene for the construction of a random mutant library |

| | | |
|---|---|---|
| rmhydB2 | TTTTCCTCCTCTAGATCTATGC | Used to amplify the *Tte hydB* gene for the construction of a random mutant library |
| rmhydA1 | GAAGTAAGCATAGATCTAGAGGAGG | Used to amplify the *Tte hydA* gene for the construction of a random mutant library |
| rmhydA2 | GCTGCAGGTCGACCTCGAG | Used to amplify the *Tte hydA* gene for the construction of a random mutant library |
| iscRupfor | GCGCGGTACCCCGTTACGCTGCGGTGCCAGGTAGG | Used to amplify 500 bp sequence upstream of *iscR* to clone into pKS II $^{+}$ |
| iscRuprev | GCGCGTCGACTAAAAAGAATTCAGAATCAGGC | Used to amplify 500 bp sequence upstream of *iscR* to clone into pKS II $^{+}$ |
| iscRdownfor | GCGCGTCGACGTCTTACTTCACCTCAAACTCGC | Used to amplify 500 bp sequence downstream of *iscR* to clone into pKS II $^{+}$ |
| iscRdownrev | GCGCGCGCAAGCTTGGATTCTGGCTTCTATTGAGCAGC | Used to amplify 500 bp sequence downstream of *iscR* to clone into pKS II $^{+}$ |
| metJupfor | GCGCGGTACCGTTTGCGCCAGTTTTTGC | Used to amplify 500 bp sequence upstream of *metJ* to clone into pKS II $^{+}$ |
| metJuprev | GCGCGTCGACAGCAAAAAAGAGCGG | Used to amplify 500 bp sequence upstream of *metJ* to clone into pKS II $^{+}$ |
| metJdownfor | GCGCGTCGACGAGATACTTAATCCTCTTCG | Used to amplify 500 bp sequence downstream of *metJ* to clone into pKS II $^{+}$ |

| | | |
|---|---|---|
| metJdownrev | GCGCAAGCTTGTATTAGTAAGTACTGCACC | Used to amplify 500 bp sequence downstream of *metJ* to clone into pKS II $^{+}$ |
| Tma0927for1 | GCGCGGATCCAGGAGGAAAAAAAAATGAAGGTAAGAGTTGACGC | Used to amplify *Th. maritima* ferredoxin gene *TM0927* to clone into pUNIPROM |
| Tma0927rev1 | GCGCGTCGACTCACTCTTCTACGCTGATAGC | Used to amplify *Th. maritima* ferredoxin gene *TM0927* to clone into pUNIPROM |
| Tma0927Hisfor2 | GCGCGGATCCAGGAGGAAAAAAAAATGCACCATCACCATCACCATAAGGTAAGAGTTGACGC | Used to amplify *Th. maritima* ferredoxin gene *TM0927* to clone into pUNIPROM so it will encode an N-terminal 6xHis tag |
| Tma0927Hisrev2 | GCGCGTCGACTCAATGGTGATGGTGATGGTGCTCTTCTACGCTGATAGC | Used to amplify *Th. maritima* ferredoxin gene *TM0927* to clone into pUNIPROM so it will encode a C-terminal 6xHis tag |
| POR1for | GCGCTCTAGAAGGAGGAAAAAAAAATGCCCGTTGCGAAGAAATACTTTGAAATACG | Used to amplify *Th. maritima* PFOR operon clone into pUNIPROM |
| POR1forHis | GCGCTCTAGAAGGAGGAAAAAAAAATGCACCATCACCATCACCATCCCGTTGCGAAGAAATACTTTGAAATACG | Used to amplify *Th. maritima* PFOR operon to clone into pUNIPROM so it will encode an N-terminal 6xHis tag |
| POR1rev | GCGCAAGCTTTTATCTAATCGGTTTGTCCTTTGTAACC | Used to amplify *Th. maritima* PFOR operon to clone into pUNIPROM |
| POR1revHis | GCGCAAGCTTTTAATGGTGATGGTGATGGTGTCTAATCGGTTTGTCCTTTGTAACC | Used to amplify *Th. maritima* PFOR operon to |

| | | |
|---|---|---|
| | | clone into pUNIPROM so it will encode a C-terminal 6xHis tag |
| adhEdelcheckfor | GGCCACAGACAGGTTGGCTGTAAGG | Used to check for successful deletion of *adhE* allele |
| adhEdelcheckrev | CGATATCAGCCGCTTTGTTGGTGGC | Used to check for successful deletion of *adhE* allele |

**Table 7.9 of primers used in this study**

### 7.5.5 Quikchange™ (site-directed mutagenesis) PCR

Site-directed mutagenesis of pUNI-Tte-Hyd was carried out to change the upstream restriction site of the *hydA* gene on the synthetic *Tte* hydrogenase operon. This restriction site was changed from *Xho*I to *Xba*I, in two steps, using the Quikchange® protocol (Agilent) and the following primers: SSMAfor and SSMArev; SSMBfor and SSMBrev.

### 7.5.6 Random Mutagenesis through hyper-mutagenic PCR

Hyper-mutagenic PCR was used to construct two libraries of the 1758 bp *hydA* gene, one with an error rate of 2.8 % per clone (low) and the other with an error rate of 4.5 % per clone (high). The method used is based on the use of biased dNTPs (Vartanian*, et al.*, 1996b). The primers used were rmhydA1 and rmhydA2. The elongation step of each PCR cycle was lengthened to 10 m and $MnCl_2$ added to the reaction mix, to allow full amplification of mismatch-containing PCR fragments (). Each library consisted of plasmid DNA prepared from $1.2 \times 10^6$ and $1.5 \times 10^6$ colonies respectively, a 682 and 853 times coverage of the *hydA* gene. Thus, each base in the *hydA* gene could theoretically be mutated 38 times per mutant library.

| **Component** | **Volume** |
|---|---|
| 5 x buffer (GoTaq) | 20 µl |
| $MgCl_2$ (25 mM) | 10 µl |
| $MnCL_2$ (5 mM) | 10 µl |
| Forward primer (10 µM) | 1.5 µl |
| Reverse primer (10 µM) | 1.5 µl |
| dTTP (100 mM) | 1.0 µl |
| dGTP (100 mM) | 1.0 µl |
| dATP (10 mM) | 0.75 µl (low)/0.6 µl (high) |
| dCTP (10 mM) | 0.75 µl (low)/0.6 µl (high) |
| GoTaq polymerase | 1.0 µl |
| DNA template | 1.0 µl |
| $ddH_2O$ | 51.5 µl (low)/ 51.8 µl (high) |
| **Total** | **100 µl** |

**Table 7.10 Random mutagenesis PCR reaction mixtures**

### 7.5.7 Chimeric protein linker-exchange PCR

Amplification of the entire chimeric metalloenzyme-containing plasmid was performed in order to change the peptide linkers between HybO and PhsB. The cloning strategy employed is detailed in Figure 7.1. This allowed the rapid exchange of a number of different peptide linkers of different lengths. Normal PCR cycling conditions and reaction mixtures were used.

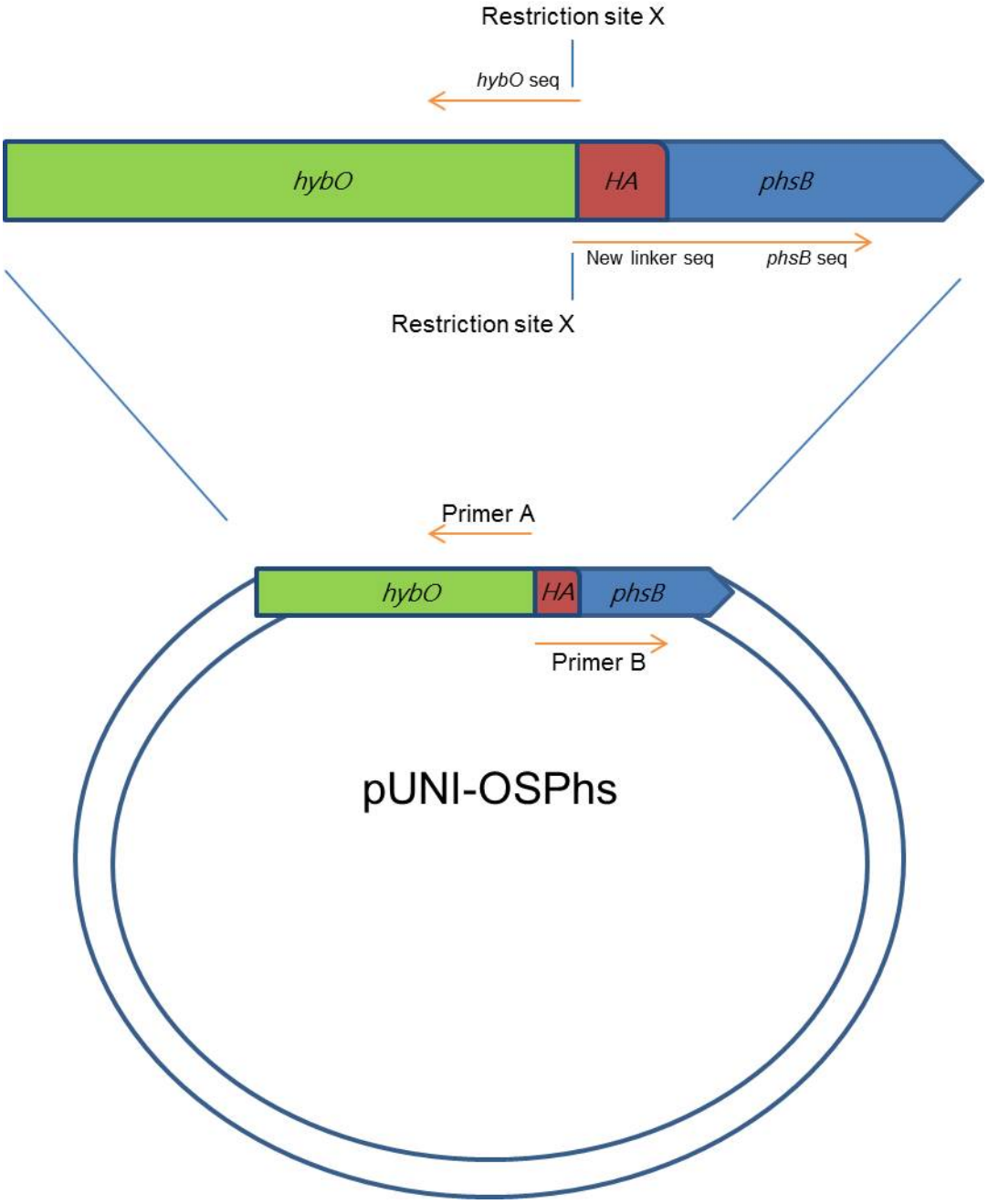


**Figure 7.1 Fusion protein linker-exchange PCR schematic**

### 7.5.8 Competent cell preparation and transformation of with plasmid DNA

Standard transformations were carried out using chemically-competent cells prepared using the TSB method (DMSO) as described (Chung and Miller, 1988). XL10-Gold competent cells (Stratagene) were used in the construction of the *hydA* mutant libraries due to their extremely high transformation efficiency, as per manufacturer's instructions. Electrocompetent cells were prepared as described previously (Sambrook*, et al.*, 1989) and used in the screening of the *hydA* mutant libraries. 200 ml of LB media was inoculated 1 in 100 with aerobic RaisynA1 cultures and grown aerobically with agitation at 37 ˚C to an optical density ($OD_{600}$) of 0.6 – 0.8. Cell cultures were then cooled rapidly at 0 ˚C for 15 min, before pelleting at 3,000 g for 20 min. Cell pellets were washed twice in ice-cold MilliQ water before a final wash in 75 ml 10% ice-cold glycerol. Cell pellets were then resuspended by vortexing in 400 µl 10% ice-cold glycerol. Aliquots of 40 µl were used immediately in transformations, to which approximately 200 ng of plasmid DNA was added. After 10 – 30 min incubation, the cells were transferred to an ice-cold 2 mm electroporation cuvette (Molecular BioProducts) and an electrical pulse applied (2.5 kV voltage, 25 µF capacitance, 200 Ω resistance, 2 mm cuvette length) using a GenePulser Xcell® electroporator (BioRad). 1 ml of LB medium at room temperature was added to the electroporation cuvette and the cells mixed by gentle pipetting. Cells were then transferred to an Eppendorf tube and incubated at 37 ˚C for 1 h. 100 µl of the cells was spread onto appropriate selective media (M9 minimal agar media) supplemented with the required antibiotics and grown anaerobically at 37 ˚C.

### 7.5.9 Design of synthetic operon

A BLAST search of the *Thermoanaerobacter tengcongensis* was performed to obtain the amino acid sequences of the gene products encoded by the hydrogenase operons. These sequences were reverse-translated using OPTIMIZER, which optimises genes for *E. coli* codon usage (Puigbo*, et al.*, 2007). An optimised RBS and linker sequence was inserted upstream of each gene and suitable restriction sites were then inserted before and after every gene. This synthetic gene was then synthesised as a service by Biomatik Corporation, Ontario, Canada and cloned into suitable vectors.

### 7.5.10 Digestion of DNA by restriction endonucleases for cloning

Digestion of DNA using restriction endonucleases was carried out in the manufacturer supplied buffer. Where two enzymes were used, an appropriate buffer was selected to permit efficient activity of both enzymes. If this was not possible then two separate digestions were. A typical restriction digestion used 1 µl of each enzyme, buffer diluted to 1x concentration,

approximately 1 µg DNA, and water up to 40 µl final volume. Digestions were carried out at 37 ˚C for 3 h or overnight for certain PCR products. Digested PCR products for cloning were purified by QIAquick® PCR Purification (Qiagen) according to kit instructions to remove restriction endonucleases. Digested vectors for cloning were purified using the QIAquick® gel-extraction kit (Qiagen). In this case, the digestion product was separated agarose gel electrophoresis and the cut band of the correct size excised from the gel and purified according to kit instructions. Following purification by gel-extraction the cut vector was treated with alkaline phosphatase (Roche). This enzyme removes phosphate groups from the 5' end of DNA molecules, preventing re-ligation of the cut vector without the addition of insert. 1 µl of alkaline phosphatase was added to the cut vector and incubated at 37 ˚C for 30 min before addition of another 1 µl of alkaline phosphatase for a further 30 min. The cut vector was then finally purified using PCR clean-up or by heat inactivation at 75 ˚C for 2 min.

### 7.5.11 DNA ligation

Digested DNA fragments were quantified using a Nanodrop® spectrophotometer (Labtech). Vector and insert were typically mixed in a 10 ng:30 ng ratio and incubated in 1x ligation buffer and 1 unit of T4 DNA ligase (Roche) in a final volume of 10 µl and incubated at 16 ˚C overnight. Following ligation, the entire 10 µl ligation mixture was used for transformations of *E. coli* strain DH5α. For troublesome ligations (e.g. random mutant library construction), molar ratios of 1:1, 1:3 and 1:5 were used with much higher starting amounts of DNA (e.g. 50 ng of vector).

### 7.5.12 Agarose gel electrophoresis

Agarose gel electrophoresis was used both for diagnostic and to separate DNA fragments for cloning. DNA fragments were typically separated 1% (w/v) agarose gels prepared in 1 x TAE and containing a 1:10,000 dilution of GelRed® (Biotium). DNA samples were mixed with 10 x DNA loading dye before electrophoresis. A DNA standard (1 kb ladder, Roche) was loaded adjacent to the DNA samples to allow for estimation of fragment size. Electrophoresis and fragment separation was then performed at 100 V for 20-45 min. DNA fragments were visualised by exposure to UV light using a Gel Doc XR+ system (BioRad). For use in further applications, DNA was extracted from agarose gels using the QIAquick® Gel Extraction Kit (Qiagen) as described in Section 7.5.10.

### 7.5.13 Random Mutagenesis using XL1-Red competent cells

XL1-Red mutator cells were transformed with the plasmids to be mutated as per the manufacturer's instructions. The transformation mixture were plated onto LB agar plates

containing the appropriate antibiotic and the plates incubated at 37 °C for 24 – 30 h. 1 ml of LB medium was added to the plate, swirled for 30 s and then all colonies were scraped off into a 15 ml Falcon tube. LB medium containing the appropriate antibiotics was added to a final volume of 10 ml and this tube was incubated aerobically with shaking overnight at 37 °C. Mutated plasmid DNA was isolated using the QIAprep® Spin Miniprep Kit (Qiagen) and eluted into 100 ul $dH_2O$ to give the mutant library for screening.

### 7.5.14 Chemical mutagenesis using Captan and MMS

5 ml of LB media was inoculated 1 in 1000 with *E. coli* strains to be mutated and these were grown aerobically overnight. These overnight cultures were then used to inoculate 5 ml aerobic cultures of LB media, which were grown to OD600 of approximately 0.6 – 0.8. 0.1 ml of bacterial culture was added to 10 µl, 50 µl, 75 µl, 100 µl of mutagen (Captan/MMS) and 0.5 ml of 100 mM sodium phosphate buffer (pH 7.4) was added. This reaction was allowed to proceed at 37 °C for 20 min, 40 min and 1 h with gentle shaking (100 rpm), before the cells were pelleted by centrifugation at 13,000 rpm for 2 min, washed twice with buffer and resuspended in LB medium, before being plated out onto selective media (M9 minimal agar media) supplemented with the required antibiotics and grown anaerobically at 37 ˚C.

### 7.5.15 pMAK705 homologous recombination protocol for chromosomal gene deletions and insertions

The pMAK705 allelic exchange protocol was used to generate gene replacements and deletions of various *E. coli* strains as described (Hamilton*, et al.*, 1989). DNA sequence (500 bp upstream and downstream) surrounding the chromosomal target to be replaced/deleted was amplified and cloned into the suicide vector pMAK705. The resulting plasmid was then transformed into the target strain and an overnight culture grown in LB media supplemented with chloramphenicol (Cml), at 30 °C. Serial dilutions ($10^{-3}$, $10^{-4}$ and $10^{-5}$) were then spread onto the LB agar media supplemented with Cml and incubated at 44 °C overnight. As pMAK705 is temperature sensitive and only replicates at 30 °C, any $Cml^R$ colonies must be the result of cointegrate formation. A control was also included where cells were diluted at 1 $x10^{-7}$ and incubated at 30 °C. Next, five cultures, each containing five colonies were incubated in the relevant antibiotic containing LB medium at 30 °C for 24 h to allow plasmid replication within the cell. Two more cycles of this growth was carried out by transferring a loopful of culture into fresh antibiotic containing medium. A loopful of each culture was then streaked onto the relevant LB media containing Cml and incubated at 30 °C overnight. The final step involved curing plasmid from the strain. Twelve cultures containing single colonies were grown in the relevant LB media, without any added antibiotic at 44 °C for at least 16 h. A loopful from each

culture was then streaked onto the relevant LB agar medium (without antibiotic) and incubated at 44 °C overnight. Single colonies were then patched onto LB agar and LB agar medium containing Cml and then incubated at 30 °C overnight. $Cml^S$ colonies were tested for successful integration or deletion by PCR using primers with homology to DNA sequence upstream and downstream of the selected region. PCR products were then analysed following agarose gel electrophoresis and DNA sequencing.

### 7.5.16 Construction of individual gene knockout strains: P1 transduction

P1 transduction was performed as described previously (Thomason*, et al.*, 2007) using a P1 lysate prepared from aerobic cultures of various *E. coli* Keio collection strains (e.g. JW1228 [Δ*adhE*]). The remaining $Kan^R$ cassette was removed using the plasmid pCP-20 and FLP recombination as described (Datsenko and Wanner, 2000). Confirmation of deletion was done by PCR amplification of the chromosomal region using flanking and internal primers. gDNA prepared from wild-type *E. coli* strains was used as a negative control.

## 7.6 Protein Methods

### 7.6.1 SDS-PAGE

SDS polyacrylamide gel electrophoresis (SDS-PAGE) was employed to separate proteins under denaturing conditions according to their molecular weight (Laemmli, 1970) using the Bio-Rad Mini-PROTEAN II System. The resolving gel (12-14% typically) was prepared as indicated in Table 7.11 and was poured between two glass plates, leaving enough room for comb insertion. Water was then poured on top of the resolving gel, which was left to polymerise. Following polymerisation, the water was removed and the stacking gel added. This was prepared as detailed in Table 7.11. A comb was immediately inserted into the stacking gel to create sample wells.

| **Resolving Gel constituents** | **Concentration/%** | **Stacking Gel constituents** | **Concentration/%** |
|---|---|---|---|
| Acrylamide/bisacrylamide (37:5:1) | 12-14% | Acrylamide/bisacrylamide (37:5:1) | 6% |
| Tris.HCl pH 8.8 | 0.375 M | Tris.HCl pH 6.8 | 0.125 M |
| SDS | 0.1% (w/v) | SDS | 0.1% (w/v) |
| APS | 0.1% (w/v) | APS | 0.1% (w/v) |
| TEMED | 0.1% (v/v) | TEMED | 0.1% (v/v) |

Table 7.11 The constituents of the resolving and stacking gels used in SDS-PAGE.

### 7.6.2 $^{35}$S-Met Radiolabelling

*E. coli* strain K38/pGP1-2 (pGP1-2 is a temperature sensitive plasmid that encodes T7 polymerase when heat activated) (Tabor and Richardson, 1985) was transformed with plasmids containing the gene(s) to be analysed. These plasmids must have a T7 promoter upstream of the gene(s) of interest. Successful transformants were used to inoculate aerobic 5 ml LB media cultures, which were incubated for approximately 16 h, with shaking, at 30 °C. These cultures were then subcultured into minimal M9 media containing all amino acids added except Met and Cys. This was incubated for one hour at 30 °C and then transcription of T7 RNA polymerase was initiated by heatshocking at 42 °C. Rifampicin was then added to the culture to inhibit native RNA polymerase transcription and 0.01 µCi of $^{35}$S-Met was added to a 1 ml aliquot of cells. Following 15 min incubation, the samples were boiled in Laemmli buffer to lyse the cells and denature the protein. The protein samples were then separated by SDS-PAGE and visualised by autoradiography using an SRX-101A medical film processor (Konica Minolta).

### 7.6.3 Protein Purification

Aerobic cultures of *E. coli* strains expressing the His-affinity tagged protein were used to inoculate 5 L of LB supplemented with 0.4 % (w/v) glucose, 2 mM cysteine and 2 mM ferric ammonium citrate and antibiotics. The cultures were grown anaerobically overnight at 37 °C. Cells were harvested by centrifugation at 5009 x g for 20 min in a Beckman J6-MI centrifuge. All buffers used throughout purification had been bubbled with $N_2$ for at least 1 h prior to resuspension to remove $O_2$ and cell pellets, cell-containing buffers or crude extracts were flushed with argon to protect from $O_2$. Cell pellets were resuspended in either 50 ml of B-PER® solution (Thermo Scientific) or 50 ml of 50 mM Tris HCl pH7.5, 1 mM DTT, 2 mM flavin mononucleotide, 150 mM NaCl and 25 mM imidazole. B-PER lysis was achieved by the addition of lysozyme and DNAse I followed by agitation at room temperature for 1 h. Lysis by sonication was achieved by the addition of lysozyme and DNAse I, followed by agitation and bubbling with $N_2$ at 0 °C for 30 min followed by sonication. The following conditions were used to lyse the cells using a 102-C sonication horn (Branson) and Digital 450 Digital Sonifier (Branson): 20% amplitude; 5 s pulse on/off; and lysis duration of 20 min (40 min total). Following either method of lysis, unbroken cells were pelleted by centrifugation resulting in a crude cell extract.

Nickel-affinity chromatography was used to isolate His-tagged proteins using an ÄKTA FPLC system (Amersham Biosciences). Crude extracts were applied to 5 ml HisTrap HP affinity columns (GE Healthcare) at a flow rate of 1 ml $min^{-1}$, which had been previously equilibrated with anaerobic buffer A. Ten column volumes of Ni-purification buffer A were used to wash any unbound protein from the column. A linear gradient of 0-100% Ni-purification buffer B was then applied to the column to elute bound proteins over a time period of 30 min. Eluted protein was collected in 1 ml fraction tubes, flushed with argon and sealed with rubber stoppers to prevent $O_2$ damage. Individual peak fractions could then be aliquoted under argon, flash frozen in liquid nitrogen and stored under argon at -80 °C in Pyrex® tubes.

### 7.6.4 Size-exclusion chromatography

Size exclusion chromatography was performed using a Superdex 200 10/300 GL gel filtration column (GE Healthcare) in order to further purify protein for crystallisation trials. The column was first equilibrated with 1.5 column volumes of SEC buffer. A small volume of concentrated protein (< 500 µl) was then applied to the column at a flow rate of 0.5 ml $min^{-1}$ and eluted fractions collected in 5 ml fraction collection tubes. Samples were mixed with Laemmli sample buffer at a ratio of 2:1 and then analysed following SDS-PAGE. Fractions containing the desired protein were concentrated using Vivaspin 20, 50 kDa cut-off spin concentrators (Sartorius Stedim).

### 7.6.5 SEC-MALLS

In collaboration with Colin Hammond of Prof. Tom Owen-Hughes group at the University of Dundee, purified hydrogenase was analysed using SEC-MALLS. This couples size-exclusion chromatography with multi-angle laser light scattering and refractive index detection. After resolution of the purified enzyme using a Dionex Ultimate 3000 HPLC system and a MAbPac SEC–1 (Dionex) column, an inline miniDAWN TREOS (Wyatt) multi-angle laser light scattering detector, fires a laser continuously at the eluent, which scatters the beam and then the detector measures the intensity of the scattered beam at different angles. And a T-rEX (Optilab) refractive-index detector determines accurate relative sample concentration. This allows information such as molecular mass, polydispersity and the radius of the complex to be accurately calculated using ASTRA v6.0.0.108 (Wyatt) software. SEC buffer was used to equilibrate and resolve protein complexes.

### 7.6.6 Semi-dry western immunoblotting

Samples for western immunoblotting were first separated by SDS-PAGE. The gel was soaked for 15 min in CTB buffer, which was then placed onto a nitrocellulose membrane that had also been soaked in CTB buffer, with both then in turn placed between two pieces of 3 MM filter paper also soaked in CTB buffer. Protein bands were transferred to the membrane using a semi-dry blotting system (BioRad), at 175 mA for 45 min. The membrane was then blocked in 1 x TBS plus 1% milk powder overnight at 4 °C with shaking. The blocked membrane was then washed in ~100 ml 1xTBS-T for 10 min with shaking at room temperature. The membrane was incubated with an appropriate dilution of the primary antibody serum in 1x TBS-T for 1 h with shaking. Following antibody binding, the membrane was washed three times in ~100 ml 1x TBS-T to remove excess antibody. The membrane was then incubated with an appropriate dilution of the secondary antibody in 1x TBS-T for 1 h with shaking. The membrane was again washed three times in ~100 ml 1x TBS-T to remove excess antibody. Immunoreactive protein bands were detected using ECL Western Blotting Detection Reagents (Amersham). Kodak BioMax MR scientific imaging film (Sigma) was used to detect reacted bands and was developed with an SRX-101A medical film processor (Konica Minolta).

### 7.6.7 Protein concentration determination

Protein concentrations were determined using the DC Protein Assay (BioRad) using the manufacturer's instructions and a microplate reader by recording absorbance at $A_{750}$. A standard curve of bovine serum albumin (BSA) was prepared freshly each time and used as the reference protein standard.

### 7.6.8 Rocket immunoelectrophoresis

Samples of periplasmic, cytoplasmic and membrane fractions were used directly for analysis by rocket immunoelectrophoresis. 1% (w/v) agarose gels containing rocket immunoelectrophoresis buffer and antisera specific to the protein being investigated were assembled on small glass plates and small wells introduced. Plates were then placed in an electrophoresis tank containing rocket immunoelectrophoresis buffer and 1-2 µl samples added to the wells. Two Whatman™ paper electrode wicks were then placed in the buffer, at both the cathode and the anode, ensuring contact with the gels. Samples were electrophoresed at 2 mA per plate for 16 h at 4 °C. As the protein migrates through the gel, antibody begins to bind forming a precipitin, which eventually stalls electrophoresis of the complex. Plates were then removed, blotted dry and placed in petri dishes where they were immersed in a 50 mM Tris HCl pH 7.5 buffer containing 600 mg benzyl viologen (BV) and 700 mg tetrazolium red. BV acts as an artificial electron acceptor while tetrazolium red is an irreversible redox dye, which can accept electrons from BV and therefore precipitin arcs positive for hydrogenase activity can be stained red. Plates were then enclosed within an Equitron anaerobic jar and incubated under an $H_2$ for 16 h. $H_2$ oxidation was detected as red precipitin arcs.

### 7.6.9 UV-Vis spectroscopy of purified enzyme

Purified enzyme was diluted 1:1 with 100 mM sodium phosphate buffer pH 6.0 and analysed over wavelengths from 330 to 710 nm using a Lambda 35 UV/VIS spectrometer (Perkin Elmer). Buffer was used as a blank control and subtracted from protein spectra.

## 7.7 **Oxidoreductase/Hydrogenase Activity Assays**

### 7.7.1 Large-scale gas production experiments during fermentations of various *E. coli* strains

10 ml of an aerobic overnight culture of the *E. coli* strain to be assessed was added to 3.6 l of CR-Hyd media pH 6.4 (plus additional nutrients and appropriate antibiotics), in a 5 l Minifors™ bioreactor. A weak vacuum was applied to degas the media and remove oxygen from the headspace of the fermenter. The culture was incubated at 37 ˚C with gentle stirring (200 rpm). The gas output pipe was connected to the gas flow meter and gas produced was measured over 16 h.

### 7.7.2 Small-scale gas production experiments

Test-tubes containing an upturned Durham tube and 20 ml of CR-Hyd media pH 6.4 (with additional nutrients and appropriate antibiotics) were inoculated with 50 µl of an aerobic overnight culture of the *E. coli* strain to be assessed. These were sealed and incubated for 3 days at 37 °C without agitation and then assessed for presence and size of gas bubble produced in the upturned Durham tube.

### 7.7.3 Hydrogen-dependent BV reduction assays

The oxidation of electron donors such as $H_2$ or pyruvate can be enzymatically-coupled *in vitro* to the reduction of certain artificial electron acceptors, such as methyl viologen (MV) and benzyl viologen (BV). These redox dyes are colourless when oxidised and dark blue/violet when reduced. BV was used as electron acceptor for these assays as its standard reduction potential ($E^{0'}$ -348 mV) is above that of the $H^+/½\ H_2$ redox couple ($E^{0'}$ -420 mV). For BV reduction, one activity unit (U) is defined as 1 µmol BV reduced $min^{-1}$ $mg^{-1}$ cells. Hydrogenase activity was therefore measured spectroscopically by monitoring the reduction of BV at $A_{578}$. Quartz cuvettes were filled with 1.8 ml of an anaerobic $H_2$-saturated buffer (50 mM Tricine pH 8.0 or 50 mM Tris HCl pH 8.0) and 14 mM BV, which was titrated to $A_{578}$ of approximately 0.4 - 0.6. The reaction was initiated by the addition of whole cells (washed and resuspended in anaerobic buffer), crude cell lysates or purified enzyme and the initial velocity of the reaction measured using a millimolar extinction coefficient for BV at 578 nm of 8.65 $cm^{-1}$ $mM^{-1}$ and the following equation:

$$= \frac{\textbf{(Slope*D.F.)}}{\textbf{(E.C.*2*L)}}$$

- Slope = $\Delta A_{578}$ $min^{-1}$
- D.F. = $Vol_{buff}/Vol_{enz}$ added
- E.C. = extinction coefficient
- *2 = because there are 2 electrons passed from $H_2$ to 2 BV molecules
- L = path length

### 7.7.4 MV-dependent hydrogen-production assays using Clark-type electrode

$H_2$-production from purified enzyme or crude cell lysate can be artificially driven *in vitro* by using the electron donor methyl viologen (MV; $E^{0'}$ -443 mV, which is lower than that of the $H^+/½\ H_2$ redox couple ($E^{0'}$ -420 mV) and a modified Clark-type electrode. The modified Clark-type electrode consists of an electrode disc with a platinum chloride-plated anode and a silver chloride-plated cathode, which are connected via a potassium chloride electrolyte. The electrode is separated from the reaction chamber by a P.T.F.E. membrane. Current resulting from the oxidation of $H_2$ at the anode surface is recorded and can be easily converted to µmol of $H_2$ following calibration with known amounts of $H_2$. For MV-dependent $H_2$ production, one unit (U) is defined as 1 µmol $H_2$ evolved $min^{-1}$ $mg^{-1}$ cells. 2 ml of anaerobic buffer (100 mM sodium phosphate pH 6.0 or 6.8) was added to the reaction chamber and allowed to equilibrate. 12.5 mM of MV is then added to the reaction chamber in addition to 650 µM sodium dithionite to fully reduce all MV in the chamber and again this is allowed to equilibrate. The reaction is initiated by the addition of enzyme or cell lysate and the reaction allowed to proceed to completion.

### 7.7.5 Hydrogen production/oxidation assays with Clark-type electrode

$H_2$-production assays with physiological electron donors and acceptors were also performed using the Clark-type electrode as described in Section 7.7.4. 2 ml of 100 mM anaerobic buffer was added to the reaction chamber and after equilibration, whole cells, cell lysate or purified enzyme was added to the reaction chamber and allowed to equilibrate. Finally the reaction was initiated by the addition of an excess of substrate (e.g. glycerol, formate, NADH etc.). Alternatively, a small volume of $H_2$-saturated buffer could be added to the reaction chamber and cells/enzyme added to the reaction chamber followed by the addition of an external electron donor such as nitrate, fumarate or $NAD^+$, and the uptake/oxidation of $H_2$ monitored.

A modified set-up was used in the experiments where a proteorhodopsin was coexpressed in order to boost proton motive force (PMF) at the cytoplasmic membrane. The reaction chamber was maintained in complete darkness, while buffer and cell equilibration occurred. Light from a 100 W halogen bulb and green light (λ: 550 nm) was used to illuminate the reaction chamber for 5/10 min to charge the PMF, before the substrates were added.

### 7.7.6 BV-linked pyruvate: ferredoxin oxidoreductase activity assay

BV was used as the artificial electron acceptor from the oxidation of pyruvate as catalysed by pyruvate:ferredoxin oxidoreductase. For BV reduction, one activity unit (U) is defined as 1

µmol BV reduced $min^{-1}$ $mg^{-1}$ cells. Quartz cuvettes were filled with 1.8 ml of an anaerobic $H_2$-saturated buffer (50 mM Tricine pH 8.0) and 14 mM BV. 5 mM pyruvate and 100 µM coenzymeA (required to accept acetyl group from pyruvate) was added to the cuvette and BV was titrated to $A_{578}$ of approximately 0.4 - 0.6. The reaction was initiated by the addition of known amounts of purified enzyme.

### 7.7.7 $H_2$-production assays to investigate a possible bifurcating mechanism

$H_2$-production assays with purified hydrogenase, ferredoxin and pyruvate:ferredoxin oxidoreductase were carried out using the Clark-type electrode as described in Section 7.7.5. 5 mM pyruvate, 100 µM coenzyme A and 20 mM NADH were added to 2 ml of anaerobic 100 mM sodium phosphate pH 7.0 buffer in the reaction chamber and the reaction initiated by the addition of the purified protein.

## 7.8 Growth curve analysis

Test tubes filled with 16 ml L.B. + 0.4% (w/v) glucose or M9 + 0.4% (w/v) glucose were inoculated 1:1000 with aerobic cultures of the *E. coli* strains to be analysed and cultures grown anaerobically. The optical density ($OD_{600}$) of these cultures was recorded at various time points over 38 h. It was decided not to convert $OD_{600}$ to $\log_{10}$ values, to better highlight differences in final cell densities.

## 7.9 Cell Fractionation

Subcellular fractionation was performed on *E. coli* cultures, grown anaerobically 500 ml LB media supplemented with 0.5% glycerol and 0.4% fumarate anaerobic at 37 °C. Cells were harvested at 2773 x g, washed in 50 mM Tris HCl pH 7.5 and resuspended in Tris-sucrose buffer at 10 ml $g^{-1}$ wet weight. EDTA and lysozyme were added to a final concentration of 5 mM and 0.6 mg/ml respectively and the suspension incubated, without agitation, at 37 °C for 30 min. The suspension was centrifuged at 17,387 x g for 12 min in a Beckman Avanti J-26 XP centrifuge to pellet sphaeroplasts. The resultant supernatant is the periplasmic fraction. Sphaeroplasts were resuspended in 50 mM Tris HCl pH 7.5 at a volume of 10 ml $g^{-1}$ of original wet weight and DNase I added. Cell suspensions were lysed at 8,000 psi using a French® Press cell disruptor (Thermo Scientific) and the sample then centrifuged at 27,000 x g for 20 min to remove cell debris. The supernatant was then centrifuged at 278,000 x g for 30 min in an OptimaTM TLX ultracentrifuge (Beckman) to pellet membranes. The upper 200 µl of the supernatant was retained as the cytoplasmic fraction. Membrane pellets were resuspended in 50 mM Tris HCl pH 7.5 and 250 mM NaCl and suspensions centrifuged again at 278,000 x g for

30 min. For Western immunoblotting, pellets were resuspended in 50 mM Tris HCl pH 7.5 following removal of the supernatant and then re-centrifuged. For rocket immunoelectrophoresis, membranes were solubilised in 50 mM Tris HCl pH 7.6 containing 0.4% Triton X-100 (v/v), incubated on ice for 20 min and then centrifuged at 278,000 x g for a further 30 min. Supernatants containing membranes were added to an equal volume of Laemmli sample buffer and flash frozen in liquid nitrogen.

## 7.10 High-performance liquid chromatography (HPLC) analysis of organic acids

16 ml of LB media supplemented with 0.4 % (w/v) glucose was inoculated with various *E. coli* strains to be analysed and grown anaerobically for 72 h. Cells were harvested by centrifugation and the culture supernatant was passed through a 0.2 µm filter to remove any remaining cells or debris. The spent fermentation broth was analysed with using a Dionex Ultimate 3000 HPLC system and an Aminex HPX-87H organic-acid column, which was operated at 0.7 ml $min^{-1}$ and 55 °C (to reduce viscosity of complex media and improve resolution). Organic acids were detected by UV absorption at 210 nm, except for ethanol and glucose, which were detected using an Optilab T-rEX refractive index detector. A standard curve of organic acid standards was prepared for each experiment ($R^2$: 99.90%) and used to identify and quantify concentrations of pyruvate, succinate, lactate, formate, fumarate, ethanol, glucose and acetate. Sample concentrations were normalised by cell pellet wet weight. The concentrations of compounds in virgin media (LB + 0.4% (w/v) glucose) were subtracted to reveal changes in each metabolite.

## 7.11 Metabolomics Sample Preparation

16 ml of LB media supplemented with 0.4 % (w/v) glucose was inoculated with various *E. coli* strains to be analysed and grown anaerobically for 72 h. Cells were harvested by centrifugation and the culture supernatant was passed through a 0.2 µm filter to remove any remaining cells or debris. The supernatant was mixed and then 5 µl of supernatant added to 200 ul of $CHCl_3$:$CH_3OH$:$dH_20$ (ratio 1:3:1) and mixed vigorously at 4 $^oC$ for 1 h. Samples were then centrifuged for 3 min at 13,000 rpm at 4 $^oC$ and the supernatant flash-frozen in liquid nitrogen and stored at -80 $^oC$ before sending for LC-MS analysis at the Glasgow Polyomics Wolfson Wohl Cancer Research Centre at the University of Glasgow.

# 8. Bibliography

F. B. Abeles (1964) "Cell-free Hydrogenase from *Chlamydomonas*", Plant physiology, 39: 169-76

B. A. Ackrell, R. N. Asato and H. F. Mower (1966) "Multiple forms of bacterial hydrogenases", Journal of bacteriology, 92: 828-38

M. W. Adams and L. E. Mortenson (1984) "The physical and catalytic properties of hydrogenase II of *Clostridium pasteurianum*. A comparison with hydrogenase I", The Journal of biological chemistry, 259: 7045-55

M. W. Adams, E. Eccleston and J. B. Howard (1989) "Iron-sulfur clusters of hydrogenase I and hydrogenase II of *Clostridium pasteurianum*", Proceedings of the National Academy of Sciences of the United States of America, 86: 4932-6

M. W. Adams (1990) "The structure and mechanism of iron-hydrogenases", Biochimica et biophysica acta, 1020: 115-45

C. M. Agapakis, D. C. Ducat, P. M. Boyle, E. H. Wintermute, J. C. Way and P. A. Silver (2010) "Insulation of a synthetic hydrogen metabolism circuit in bacteria", Journal of biological engineering, 4: 3

M. K. Akhtar and P. R. Jones (2009) "Construction of a synthetic YdbK-dependent pyruvate:H2 pathway in *Escherichia coli* BL21(DE3)", Metabolic engineering, 11: 139-47

K. Y. Alam and D. P. Clark (1989) "Anaerobic fermentation balance of *Escherichia coli* as observed by in vivo nuclear magnetic resonance spectroscopy", Journal of bacteriology, 171: 6213-7

M. M. Altamirano, J. M. Blackburn, C. Aguayo and A. R. Fersht (2000) "Directed evolution of new catalytic activity using the alpha/beta-barrel scaffold", Nature, 403: 617-22

R. Arias-Cartin, S. Grimaldi, J. Pommier, P. Lanciano, C. Schaefer, P. Arnoux, G. Giordano, B. Guigliarelli and A. Magalon (2011) "Cardiolipin-based respiratory complex activation in bacteria", Proceedings of the National Academy of Sciences of the United States of America, 108: 7781-6

R. Arias-Cartin, S. Grimaldi, P. Arnoux, B. Guigliarelli and A. Magalon (2012) "Cardiolipin binding in bacterial respiratory complexes: structural and functional implications", Biochimica et biophysica acta, 1817: 1937-49

A. Arkin (2008) "Setting the standard in synthetic biology", Nature biotechnology, 26: 771-4

J. A. Arpino, E. J. Hancock, J. Anderson, M. Barahona, G. B. Stan, A. Papachristodoulou and K. Polizzi (2013) "Tuning the dials of Synthetic Biology", Microbiology, 159: 1236-53

R. E. Asnis and A. F. Brodie (1953) "A glycerol dehydrogenase from *Escherichia coli*", The Journal of biological chemistry, 203: 153-9

M. R. Atkinson, M. A. Savageau, J. T. Myers and A. J. Ninfa (2003) "Development of genetic circuitry exhibiting toggle switch or oscillatory behavior in *Escherichia coli*", Cell, 113: 597-607

S. Atsumi, T. Hanai and J. C. Liao (2008) "Non-fermentative pathways for synthesis of branched-chain higher alcohols as biofuels", Nature, 451: 86-9

M. J. Axley, D. A. Grahame and T. C. Stadtman (1990) "*Escherichia coli* formate-hydrogen lyase. Purification and properties of the selenium-dependent formate dehydrogenase component", The Journal of biological chemistry, 265: 18213-8

C. Ayala-Castro, A. Saini and F. W. Outten (2008) "Fe-S cluster assembly pathways in bacteria", Microbiology and molecular biology reviews : MMBR, 72: 110-25, table of contents

J. N. Bach and M. Bramkamp (2013) "Flotillins functionally organize the bacterial membrane", Molecular microbiology, 88: 1205-17

J. Bader, H. Gunther, E. Schleicher, H. Simon, S. Pohl and W. Mannheim (1980) "Utilization of (E)-2-butenoate (crotonate) by *Clostridium kluyveri* and some other Clostridium species", Archives of microbiology, 125: 159-65

S. P. Ballantine and D. H. Boxer (1986) "Isolation and characterisation of a soluble active fragment of hydrogenase isoenzyme 2 from the membranes of anaerobically grown *Escherichia coli*", European journal of biochemistry / FEBS, 156: 277-84

S. W. Bang, D. S. Clark and J. D. Keasling (2000) "Engineering hydrogen sulfide production and cadmium removal by expression of the thiosulfate reductase gene (phsABC) from *Salmonella enterica* serovar Typhimurium in *Escherichia coli*", Applied and environmental microbiology, 66: 3939-44

A. Bar-Even, E. Noor, Y. Savir, W. Liebermeister, D. Davidi, D. S. Tawfik and R. Milo (2011) "The moderately efficient enzyme: evolutionary and physicochemical trends shaping enzyme parameters", Biochemistry, 50: 4402-10

A. Bar-Even, A. Flamholz, E. Noor and R. Milo (2012) "Rethinking glycolysis: on the biochemical logic of metabolic pathways", Nature chemical biology, 8: 509-17

R. Baradaran, J. M. Berrisford, G. S. Minhas and L. A. Sazanov (2013) "Crystal structure of the entire respiratory complex I", Nature, 494: 443-8

R. Bartha and E. J. Ordal (1965) "Nickel-Dependent Chemolithotrophic Growth of Two Hydrogenomonas Strains", Journal of bacteriology, 89: 1015-9

B. Bartolome, Y. Jubete, E. Martinez and F. de la Cruz (1991) "Construction and properties of a family of pACYC184-derived cloning vectors compatible with pBR322 and its derivatives", Gene, 102: 75-8

T. S. Bayer and C. D. Smolke (2005) "Programmable ligand-controlled riboregulators of eukaryotic gene expression", Nature biotechnology, 23: 337-43

T. S. Bayer (2010) "Grand challenge commentary: Transforming biosynthesis into an information science", Nature chemical biology, 6: 859-61

S. Bazan, E. Mileykovskaya, V. K. Mallampalli, P. Heacock, G. C. Sparagna and W. Dowhan (2013) "Cardiolipin-dependent reconstitution of respiratory supercomplexes from purified *Saccharomyces cerevisiae* complexes III and IV", The Journal of biological chemistry, 288: 401-11

B. M. Beadle and B. K. Shoichet (2002) "Structural bases of stability-function tradeoffs in enzymes", Journal of molecular biology, 321: 285-96

M. Beeby, B. D. O'Connor, C. Ryttersgaard, D. R. Boutz, L. J. Perry and T. O. Yeates (2005) "The genomics of disulfide bonding and protein stabilization in thermophiles", PLoS biology, 3: e309

A. K. Bej, M. H. Perlin and R. M. Atlas (1988) "Model suicide vector for containment of genetically engineered microorganisms", Applied and environmental microbiology, 54: 2472-7

A. K. Bej, S. Molin, M. Perlin and R. M. Atlas (1992) "Maintenance and killing efficiency of conditional lethal constructs in Pseudomonas putida", Journal of industrial microbiology, 10: 79-85

J. Benemann (1996) "Hydrogen biotechnology: progress and prospects", Nature biotechnology, 14: 1101-3

D. E. Benson, M. S. Wisz and H. W. Hellinga (2000) "Rational design of nascent metalloenzymes", Proceedings of the National Academy of Sciences of the United States of America, 97: 6292-7

G. Berggren, A. Adamska, C. Lambertz, T. R. Simmons, J. Esselborn, M. Atta, S. Gambarelli, J. M. Mouesca, E. Reijerse, W. Lubitz, T. Happe, V. Artero and M. Fontecave (2013) "Biomimetic assembly and activation of [FeFe]-hydrogenases", Nature, 499: 66-9

B. C. Berks, F. Sargent, E. De Leeuw, A. P. Hinsley, N. R. Stanley, R. L. Jack, G. Buchanan and T. Palmer (2000) "A novel protein transport system involved in the biogenesis of bacterial electron transfer chains", Biochimica et biophysica acta, 1459: 325-30

Y. Berlier, G. D. Fauque, J. LeGall, E. S. Choi, H. D. Peck, Jr. and P. A. Lespinat (1987) "Inhibition studies of three classes of Desulfovibrio hydrogenase: application to the further characterization of the multiple hydrogenases found in *Desulfovibrio vulgaris* Hildenborough", Biochemical and biophysical research communications, 146: 147-53

S. Bhatia and D. Densmore (2013) "Pigeon: A Design Visualizer for Synthetic Biology", ACS synthetic biology, Epub

L. Bilitchenko, A. Liu, S. Cheung, E. Weeding, B. Xia, M. Leguia, J. C. Anderson and D. Densmore (2011) "Eugene--a domain specific language for specifying and constraining synthetic biological parts, devices, and systems", PloS one, 6: e18882

Alyssa S. Bingham, Phillip R. Smith and James R. Swartz (2012) "Evolution of an [FeFe] hydrogenase with decreased oxygen sensitivity", International Journal of Hydrogen Energy, 37: 2965-2976

Ariane Bisaillon, Jonathan Turcot and Patrick C. Hallenbeck (2006) "The effect of nutrient limitation on hydrogen production by batch cultures of *Escherichia coli*", International Journal of Hydrogen Energy, 31: 1504-1508

F. R. Blattner, G. Plunkett, 3rd, C. A. Bloch, N. T. Perna, V. Burland, M. Riley, J. Collado-Vides, J. D. Glasner, C. K. Rode, G. F. Mayhew, J. Gregor, N. W. Davis, H. A. Kirkpatrick, M. A. Goeden, D. J. Rose, B. Mau and Y. Shao (1997) "The complete genome sequence of *Escherichia coli* K-12", Science, 277: 1453-62

M. Blokesch, A. Paschos, E. Theodoratou, A. Bauer, M. Hube, S. Huth and A. Bock (2002) "Metal insertion into NiFe-hydrogenases", Biochemical Society transactions, 30: 674-80

M. Blokesch, S. P. Albracht, B. F. Matzanke, N. M. Drapal, A. Jacobi and A. Bock (2004) "The complex between hydrogenase-maturation proteins HypC and HypD is an intermediate in the supply of cyanide to the active site iron of [NiFe]-hydrogenases", Journal of molecular biology, 344: 155-67

J. D. Bloom, M. M. Meyer, P. Meinhold, C. R. Otey, D. MacMillan and F. H. Arnold (2005) "Evolving strategies for enzyme engineering", Current opinion in structural biology, 15: 447-52

J. D. Bloom and F. H. Arnold (2009) "In the light of directed evolution: pathways of adaptive protein evolution", Proceedings of the National Academy of Sciences of the United States of America, 106 Suppl 1: 9995-10000

A. Böck and G. Sawers (1996) Ch 18 "Fermentation", F. C. Neidhardt, R. Curtiss III, C. C. Lin, K. B. Low, B. Magasanik, W. S. Reznikoff, M. Riley, M. Schaechter and H. E. Umbarger (ed.), *EcoSal - Escherichia coli* and *Salmonella*: Cellular and Molecular Biology, ASM Press, Washington DC.

W. Bonacci, P. K. Teng, B. Afonso, H. Niederholtmeyer, P. Grob, P. A. Silver and D. F. Savage (2012) "Modularity of a carbon-fixing protein organelle", Proceedings of the National Academy of Sciences of the United States of America, 109: 478-83

B. B. Bond-Watts, R. J. Bellerose and M. C. Chang (2011) "Enzyme mechanism as a kinetic control element for designing synthetic biofuel pathways", Nature chemical biology, 7: 222-7

J. Bonnet, P. Subsoontorn and D. Endy (2012) "Rewritable digital data storage in live cells via engineered control of recombination directionality", Proceedings of the National Academy of Sciences of the United States of America, 109: 8884-9

T. L. Born and J. S. Blanchard (1999) "Enzyme-catalyzed acylation of homoserine: mechanistic characterization of the *Escherichia coli* metA-encoded homoserine transsuccinylase", Biochemistry, 38: 14416-23

O. M. Bouvet, P. Lenormand, E. Ageron and P. A. Grimont (1995) "Taxonomic diversity of anaerobic glycerol dissimilation in the Enterobacteriaceae", Research in microbiology, 146: 279-90

M. E. Boyer, J. A. Stapleton, J. M. Kuchenreuther, C. W. Wang and J. R. Swartz (2008) "Cell-free synthesis and maturation of [FeFe] hydrogenases", Biotechnology and bioengineering, 99: 59-67

J. C. Boyington, V. N. Gladyshev, S. V. Khangulov, T. C. Stadtman and P. D. Sun (1997) "Crystal structure of formate dehydrogenase H: catalysis involving Mo, molybdopterin, selenocysteine, and an Fe4S4 cluster", Science, 275: 1305-8

X. Brazzolotto, J. K. Rubach, J. Gaillard, S. Gambarelli, M. Atta and M. Fontecave (2006) "The [Fe-Fe]-hydrogenase maturation protein HydF from *Thermotoga maritima* is a GTPase with an iron-sulfur cluster", The Journal of biological chemistry, 281: 769-74

R. C. Brewster, D. L. Jones and R. Phillips (2012) "Tuning promoter strength through RNA polymerase binding site design in *Escherichia coli*", PLoS computational biology, 8: e1002811

L. Brondsted and T. Atlung (1994) "Anaerobic regulation of the hydrogenase 1 (hya) operon of *Escherichia coli*", Journal of bacteriology, 176: 5423-8

S. Brown (2009) "The new deficit model", Nature nanotechnology, 4: 609-11

W. Buckel (2001) "Unusual enzymes involved in five pathways of glutamate fermentation", Applied microbiology and biotechnology, 57: 263-73

L. Bulow (1987) "Characterization of an artificial bifunctional enzyme, beta-galactosidase/galactokinase, prepared by gene fusion", European journal of biochemistry / FEBS, 163: 443-8

G. Butland, J. W. Zhang, W. Yang, A. Sheung, P. Wong, J. F. Greenblatt, A. Emili and D. B. Zamble (2006) "Interactions of the *Escherichia coli* hydrogenase biosynthetic proteins: HybG complex formation", FEBS letters, 580: 677-81

D. Campbell-Lendrum and R. Woodruff (2007) "Climate change: quantifying the health impact at national and local levels.", WHO Environmental Burden of Disease Series, World Health Organization, Geneva

V. A. Campos-Bermudez, F. P. Bologna, C. S. Andreo and M. F. Drincovich (2010) "Functional dissection of *Escherichia coli* phosphotransacetylase structural domains and analysis of key compounds involved in activity regulation", The FEBS journal, 277: 1957-66

B. Canton, A. Labno and D. Endy (2008) "Refinement and standardization of synthetic biological parts and devices", Nature biotechnology, 26: 787-93

R. Carlson (2009) "The changing economics of DNA synthesis", Nature biotechnology, 27: 1091-4

M. L. Cartron, S. Maddocks, P. Gillingham, C. J. Craven and S. C. Andrews (2006) "Feo--transport of ferrous iron into bacteria", Biometals : an international journal on the role of metal ions in biology, biochemistry, and medicine, 19: 143-57

M. J. Casadaban (1976) "Transposition and fusion of the lac genes to selected promoters in *Escherichia coli* using bacteriophage lambda and Mu", Journal of molecular biology, 104: 541-55

K. H. Chan, K. M. Lee and K. B. Wong (2012a) "Interaction between hydrogenase maturation factors HypA and HypB is required for [NiFe]-hydrogenase maturation", PloS one, 7: e32592

K. H. Chan, T. Li, C. O. Wong and K. B. Wong (2012b) "Structural basis for GTP-dependent dimerization of hydrogenase maturation factor HypB", PloS one, 7: e30547

K. L. Chan, S. Gulati, J. B. Edel, A. J. de Mello and S. G. Kazarian (2009) "Chemical imaging of microfluidic flows using ATR-FTIR spectroscopy", Lab on a chip, 9: 2909-13

D. Chandran, F. T. Bergmann and H. M. Sauro (2009) "TinkerCell: modular CAD tool for synthetic biology", Journal of biological engineering, 3: 19

Wen-Ming Chen, Ze-Jing Tseng, Kuo-Shing Lee and Jo-Shu Chang (2005) "Fermentative hydrogen production with *Clostridium butyricum* CGS5 isolated from anaerobic sewage sludge", International Journal of Hydrogen Energy, 30: 1063-1070

X. Chen, J. L. Zaro and W. C. Shen (2012) "Fusion protein linkers: Property, design and functionality", Advanced drug delivery reviews

Y. J. Chen, P. Liu, A. A. Nielsen, J. A. Brophy, K. Clancy, T. Peterson and C. A. Voigt (2013) "Characterization of 582 natural and synthetic terminators and quantification of their design constraints", Nature methods, 10: 659-64

J. W. Chin, A. B. Martin, D. S. King, L. Wang and P. G. Schultz (2002a) "Addition of a photocrosslinking amino acid to the genetic code of *Escherichia coli*", Proceedings of the National Academy of Sciences of the United States of America, 99: 11020-4

J. W. Chin, S. W. Santoro, A. B. Martin, D. S. King, L. Wang and P. G. Schultz (2002b) "Addition of p-azido-L-phenylalanine to the genetic code of *Escherichia coli*", Journal of the American Chemical Society, 124: 9026-7

J. W. Chin (2011) "Reprogramming the genetic code", The EMBO journal, 30: 2312-24

Mei-Ling Chong, Vikineswary Sabaratnam, Yoshihito Shirai and Mohd Ali Hassan (2009) "Biohydrogen production from biomass and industrial wastes by dark fermentation", International Journal of Hydrogen Energy, 34: 3277-3287

C. T. Chung and R. H. Miller (1988) "A rapid and convenient method for the preparation and storage of competent bacterial cells", Nucleic Acids Res, 16: 3580

D. P. Clark, P. R. Cunningham, S. G. Reams, F. Mat-Jan, R. Mohammedkhani and C. R. Williams (1988) "Mutants of *Escherichia coli* defective in acid fermentation", Applied biochemistry and biotechnology, 17: 163-73

W. M. Coco, W. E. Levinson, M. J. Crist, H. J. Hektor, A. Darzins, P. T. Pienkos, C. H. Squires and D. J. Monticello (2001) "DNA shuffling method for generating highly recombined genes and evolved enzymes", Nature biotechnology, 19: 354-9

Christophe Collet, Nevenka Adler, Jean-Paul Schwitzguébel and Paul Péringer (2004) "Hydrogen production by *Clostridium thermolacticum* during continuous fermentation of lactose", International Journal of Hydrogen Energy, 29: 1479-1485

M. Creus and T. R. Ward (2007) "Designed evolution of artificial metalloenzymes: protein catalysts made to order", Organic & biomolecular chemistry, 5: 1835-44

P. R. Cunningham and D. P. Clark (1986) "The use of suicide substrates to select mutants of *Escherichia coli* lacking enzymes of alcohol fermentation", Molecular & general genetics : MGG, 205: 487-93

O. Dagliyan, D. Shirvanyants, A. V. Karginov, F. Ding, L. Fee, S. N. Chandrasekaran, C. M. Freisinger, G. A. Smolen, A. Huttenlocher, K. M. Hahn and N. V. Dokholyan (2013) "Rational design of a ligand-controlled protein conformational switch", Proceedings of the National Academy of Sciences of the United States of America, 110: 6800-4

F. Danielsen, H. Beukema, N. D. Burgess, F. Parish, C. A. Bruhl, P. F. Donald, D. Murdiyarso, B. Phalan, L. Reijnders, M. Struebig and E. B. Fitzherbert (2009) "Biofuel plantations on forested lands: double jeopardy for biodiversity and climate", Conservation biology : the journal of the Society for Conservation Biology, 23: 348-58

J. Dassa, H. Fsihi, C. Marck, M. Dion, M. Kieffer-Bontemps and P. L. Boquet (1991) "A new oxygen-regulated operon in *Escherichia coli* comprises the genes for a putative third cytochrome oxidase and for pH 2.5 acid phosphatase (appA)", Molecular & general genetics : MGG, 229: 341-52

K. A. Datsenko and B. L. Wanner (2000) "One-step inactivation of chromosomal genes in *Escherichia coli* K-12 using PCR products", Proceedings of the National Academy of Sciences of the United States of America, 97: 6640-5

Gustavo Davila-Vazquez, Sonia Arriaga, Felipe Alatriste-Mondragón, Antonio León-Rodríguez, LuisManuel Rosales-Colunga and Elías Razo-Flores (2008) "Fermentative biohydrogen production: trends and perspectives", Reviews in Environmental Science and Bio/Technology, 7: 27-45

J. H. Davis, A. J. Rubin and R. T. Sauer (2011) "Design, construction and characterization of a set of insulated bacterial promoters", Nucleic acids research, 39: 1131-41

L. Davis and J. W. Chin (2012) "Designer proteins: applications of genetic code expansion in cell biology", Nature reviews. Molecular cell biology, 13: 168-82

M. R. de Graef, S. Alexeeva, J. L. Snoep and M. J. Teixeira de Mattos (1999) "The steady-state internal redox state (NADH/NAD) reflects the external redox state and is correlated with catabolic adaptation in *Escherichia coli*", Journal of bacteriology, 181: 2351-7

G. de Luca, P. de Philip, M. Rousset, J. P. Belaich and Z. Dermoun (1998) "The NADP-reducing hydrogenase of *Desulfovibrio fructosovorans*: evidence for a native complex with hydrogen-dependent methyl-viologen-reducing activity", Biochemical and biophysical research communications, 248: 591-6

C. J. Delebecque, A. B. Lindner, P. A. Silver and F. A. Aldaye (2011) "Organization of intracellular reactions with rationally designed RNA assemblies", Science, 333: 470-4

K. Deplanche, I. Caldelari, I. P. Mikheenko, F. Sargent and L. E. Macaskie (2010) "Involvement of hydrogenases in the formation of highly catalytic Pd(0) nanoparticles by bioreduction of Pd(II) using *Escherichia coli* mutant strains", Microbiology, 156: 2630-40

Y. Dharmadi, A. Murarka and R. Gonzalez (2006) "Anaerobic fermentation of glycerol by *Escherichia coli*: a new platform for metabolic engineering", Biotechnology and bioengineering, 94: 821-9

G. Diekert, U. Konheiser, K. Piechulla and R. K. Thauer (1981) "Nickel requirement and factor F430 content of methanogenic bacteria", Journal of bacteriology, 148: 459-64

A. Dubini, R. L. Pye, R. L. Jack, T. Palmer and F. Sargent (2002) "How bacteria get energy from hydrogen: a genetic analysis of periplasmic hydrogen oxidation in *Escherichia coli*", International Journal of Hydrogen Energy, 27: 1413-1420

A. Dubini and F. Sargent (2003) "Assembly of Tat-dependent [NiFe] hydrogenases: identification of precursor-binding accessory proteins", FEBS letters, 549: 141-6

J. E. Dueber, G. C. Wu, G. R. Malmirchegini, T. S. Moon, C. J. Petzold, A. V. Ullal, K. L. Prather and J. D. Keasling (2009) "Synthetic protein scaffolds provide modular control over metabolic flux", Nature biotechnology, 27: 753-9

M. A. Dwyer, L. L. Looger and H. W. Hellinga (2004) "Computational design of a biologically active enzyme", Science, 304: 1967-71

W. R. Edwards, K. Busse, R. K. Allemann and D. D. Jones (2008) "Linking the functions of unrelated proteins using a novel directed evolution domain insertion method", Nucleic acids research, 36: e78

R. G. Efremov and L. A. Sazanov (2012) "The coupling mechanism of respiratory complex I - a structural and evolutionary perspective", Biochimica et biophysica acta, 1817: 1785-95

T. Eitinger and M. A. Mandrand-Berthelot (2000) "Nickel transport systems in microorganisms", Archives of microbiology, 173: 1-9

D. A. Elias, J. M. Suflita, M. J. McInerney and L. R. Krumholz (2004) "Periplasmic cytochrome c3 of *Desulfovibrio vulgaris* is directly involved in H2-mediated metal but not sulfate reduction", Applied and environmental microbiology, 70: 413-20

M. B. Elowitz and S. Leibler (2000) "A synthetic oscillatory network of transcriptional regulators", Nature, 403: 335-8

T. Elssner, C. Engemann, K. Baumgart and H. P. Kleber (2001) "Involvement of coenzyme A esters and two new enzymes, an enoyl-CoA hydratase and a CoA-transferase, in the hydration of crotonobetaine to L-carnitine by *Escherichia coli*", Biochemistry, 40: 11140-8

S. Engelbrecht and W. Junge (1990) "Subunit delta of H(+)-ATPases: at the interface between proton flow and ATP synthesis", Biochimica et biophysica acta, 1015: 379-90

C. Engler, R. Gruetzner, R. Kandzia and S. Marillonnet (2009) "Golden gate shuffling: a one-pot DNA shuffling method based on type IIs restriction enzymes", PloS one, 4: e5553

U.S. Environmental Protection Agency (2008) "Technical Support Document for Hydrogen Production: Proposed Rule for Mandatory Reporting of Greenhouse Gases", Government Printing Office, Washington D.C.

R. M. Evans, A. Parkin, M. M. Roessler, B. J. Murphy, H. Adamson, M. J. Lukey, F. Sargent, A. Volbeda, J. C. Fontecilla-Camps and F. A. Armstrong (2013) "Principles of sustained enzymatic hydrogen oxidation in the presence of oxygen--the crucial influence of high potential Fe-S clusters in the electron relay of [NiFe]-hydrogenases", Journal of the American Chemical Society, 135: 2694-707

Z. Fan, L. Yuan and R. Chatterjee (2009) "Increased hydrogen production by genetic engineering of *Escherichia coli*", PloS one, 4: e4432

G. Fauque, H. D. Peck, Jr., J. J. Moura, B. H. Huynh, Y. Berlier, D. V. DerVartanian, M. Teixeira, A. E. Przybyla, P. A. Lespinat, I. Moura and et al. (1988) "The three classes of hydrogenases from sulfate-reducing bacteria of the genus Desulfovibrio", FEMS microbiology reviews, 4: 299-344

M. Ferchichi, E. Crabbe, G. H. Gil, W. Hintz and A. Almadidy (2005) "Influence of initial pH on hydrogen production from cheese whey", Journal of biotechnology, 120: 402-9

A. Ferrandez, J. L. Garcia and E. Diaz (1997) "Genetic characterization and expression in heterologous hosts of the 3-(3-hydroxyphenyl)propionate catabolic pathway of *Escherichia coli* K-12", Journal of bacteriology, 179: 2573-81

C. Fichtner, C. Laurich, E. Bothe and W. Lubitz (2006) "Spectroelectrochemical characterization of the [NiFe] hydrogenase of *Desulfovibrio vulgaris* Miyazaki F", Biochemistry, 45: 9706-16

M. Filipiak, W. R. Hagen and C. Veeger (1989) "Hydrodynamic, structural and magnetic properties of *Megasphaera elsdenii* Fe hydrogenase reinvestigated", European journal of biochemistry / FEBS, 185: 547-53

A. Flamholz, E. Noor, A. Bar-Even, W. Liebermeister and R. Milo (2013) "Glycolytic strategy as a tradeoff between energy yield and protein cost", Proceedings of the National Academy of Sciences of the United States of America, 110: 10039-44

M. Fontecave and S. Ollagnier-de-Choudens (2008) "Iron-sulfur cluster biosynthesis in bacteria: Mechanisms of cluster assembly and transfer", Archives of biochemistry and biophysics, 474: 226-37

J. C. Fontecilla-Camps, A. Volbeda, C. Cavazza and Y. Nicolet (2007) "Structure/function relationships of [NiFe]- and [FeFe]-hydrogenases", Chemical reviews, 107: 4273-303

L. Forzi, P. Hellwig, R. K. Thauer and R. G. Sawers (2007) "The CO and CN(-) ligands to the active site Fe in [NiFe]-hydrogenase of *Escherichia coli* have different metabolic origins", FEBS letters, 581: 3317-21

L. Forzi and R. G. Sawers (2007a) "Maturation of [NiFe]-hydrogenases in *Escherichia coli*", Biometals, 20: 565-78

L. Forzi and R. G. Sawers (2007b) "Maturation of [NiFe]-hydrogenases in *Escherichia coli*", Biometals : an international journal on the role of metal ions in biology, biochemistry, and medicine, 20: 565-78

Biobricks Foundation "The registry of standard biological parts", Cambridge, Massachusetts, http://parts.igem.org/wiki/index.php/Main_Page

D. K. Fox and S. Roseman (1986) "Isolation and characterization of homogeneous acetate kinase from Salmonella typhimurium and *Escherichia coli*", The Journal of biological chemistry, 261: 13487-97

D. G. Fraenkel (1996) Ch 14 "Glycolysis", F. C. Neidhardt, R. Curtiss III, C. C. Lin, K. B. Low, B. Magasanik, W. S. Reznikoff, M. Riley, M. Schaechter and H. E. Umbarger (ed.), *EcoSal - Escherichia coli* and *Salmonella*: Cellular and Molecular Biology, ASM Press, Washington DC.

K. Francis, P. Patel, J. C. Wendt and K. T. Shanmugam (1990) "Purification and characterization of two forms of hydrogenase isoenzyme 1 from *Escherichia coli*", Journal of bacteriology, 172: 5750-7

S. Frank, A. D. Lawrence, M. B. Prentice and M. J. Warren (2013) "Bacterial microcompartments moving into a synthetic biological world", Journal of biotechnology, 163: 273-9

M. Frey (2002) "Hydrogenases: hydrogen-activating enzymes", Chembiochem : a European journal of chemical biology, 3: 153-60

A. E. Friedland, T. K. Lu, X. Wang, D. Shi, G. Church and J. J. Collins (2009) "Synthetic gene networks that count", Science, 324: 1199-202

J. Fritsch, P. Scheerer, S. Frielingsdorf, S. Kroschinsky, B. Friedrich, O. Lenz and C. M. Spahn (2011) "The crystal structure of an oxygen-tolerant hydrogenase uncovers a novel iron-sulphur centre", Nature, 479: 249-52

E. Fung, W. W. Wong, J. K. Suen, T. Bulter, S. G. Lee and J. C. Liao (2005) "A synthetic gene-metabolic oscillator", Nature, 435: 118-22

G. P. Furtado, L. F. Ribeiro, M. R. Lourenzoni and R. J. Ward (2013) "A designed bifunctional laccase/beta-1,3-1,4-glucanase enzyme shows synergistic sugar release from milled sugarcane bagasse", Protein engineering, design & selection : PEDS, 26: 15-23

M. Galdzicki, C. Rodriguez, D. Chandran, H. M. Sauro and J. H. Gennari (2011) "Standard biological parts knowledgebase", PloS one, 6: e17005

E. Garcin, X. Vernede, E. C. Hatchikian, A. Volbeda, M. Frey and J. C. Fontecilla-Camps (1999) "The crystal structure of a reduced [NiFeSe] hydrogenase provides an image of the activated catalytic center", Structure, 7: 557-66

T. S. Gardner, C. R. Cantor and J. J. Collins (2000) "Construction of a genetic toggle switch in *Escherichia coli*", Nature, 403: 339-42

P. Gaspar, A. R. Neves, M. J. Gasson, C. A. Shearman and H. Santos (2011) "High yields of 2,3-butanediol and mannitol in *Lactococcus lactis* through engineering of NAD(+) cofactor recycling", Applied and environmental microbiology, 77: 6826-35

U.S. Geological Survey (2011) "Mineral Commodity Summaries", Governmental Printing Office, Washington D.C.

H. Gest (1952) "Properties of cell-free hydrogenases of *Escherichia coli* and *Rhodospirillum rubrum*", Journal of bacteriology, 63: 111-21

M. L. Ghirardi, A. Dubini, J. Yu and P. C. Maness (2009) "Photobiological hydrogen-producing systems", Chemical Society reviews, 38: 52-61

D. Ghosh, A. Bisaillon and P. C. Hallenbeck (2013) "Increasing the metabolic capacity of *Escherichia coli* for hydrogen production through heterologous expression of the *Ralstonia eutropha* SH operon", Biotechnology for biofuels, 6: 122

D. G. Gibson (2009) "Synthesis of DNA fragments in yeast by one-step assembly of overlapping oligonucleotides", Nucleic acids research, 37: 6984-90

D. G. Gibson, J. I. Glass, C. Lartigue, V. N. Noskov, R. Y. Chuang, M. A. Algire, G. A. Benders, M. G. Montague, L. Ma, M. M. Moodie, C. Merryman, S. Vashee, R. Krishnakumar, N. Assad-Garcia, C. Andrews-Pfannkoch, E. A. Denisova, L. Young, Z. Q. Qi, T. H. Segall-Shapiro, C. H.

Calvey, P. P. Parmar, C. A. Hutchison, 3rd, H. O. Smith and J. C. Venter (2010) "Creation of a bacterial cell controlled by a chemically synthesized genome", Science, 329: 52-6

J. L. Giel, D. Rodionov, M. Liu, F. R. Blattner and P. J. Kiley (2006) "IscR-dependent gene expression links iron-sulphur cluster assembly to the control of O2-regulated genes in *Escherichia coli*", Molecular microbiology, 60: 1058-75

L. Girbal, G. von Abendroth, M. Winkler, P. M. Benton, I. Meynial-Salles, C. Croux, J. W. Peters, T. Happe and P. Soucaille (2005) "Homologous and heterologous overexpression in *Clostridium acetobutylicum* and characterization of purified clostridial and algal Fe-only hydrogenases with high specific activities", Applied and environmental microbiology, 71: 2777-81

J. C. Gonzalez, R. V. Banerjee, S. Huang, J. S. Sumner and R. G. Matthews (1992) "Comparison of cobalamin-independent and cobalamin-dependent methionine synthases from *Escherichia coli*: two solutions to the same chemical problem", Biochemistry, 31: 6045-56

R. Gonzalez, A. Murarka, Y. Dharmadi and S. S. Yazdani (2008) "A new model for the anaerobic fermentation of glycerol in enteric bacteria: trunk and auxiliary pathways in *Escherichia coli*", Metabolic engineering, 10: 234-45

T. Goris, A. F. Wait, M. Saggu, J. Fritsch, N. Heidary, M. Stein, I. Zebger, F. Lendzian, F. A. Armstrong, B. Friedrich and O. Lenz (2011) "A unique iron-sulfur cluster is crucial for oxygen tolerance of a [NiFe]-hydrogenase", Nature chemical biology, 7: 310-8

S. G. Grant, J. Jessee, F. R. Bloom and D. Hanahan (1990) "Differential plasmid rescue from transgenic mouse DNAs into *Escherichia coli* methylation-restriction mutants", Proceedings of the National Academy of Sciences of the United States of America, 87: 4645-9

C. T. Gray and H. Gest (1965) "Biological Formation of Molecular Hydrogen", Science, 148: 186-92

D. E. Green and L. H. Stickland (1934) "Studies on reversible dehydrogenase systems: The reversibility of the hydrogenase system of Bact. coli", The Biochemical journal, 28: 898-900

A. Greener, M. Callahan and B. Jerpseth (1996) "An efficient random mutagenesis technique using an E. coli mutator strain", Methods in molecular biology, 57: 375-85

J. H. Grose, U. Bergthorsson and J. R. Roth (2005) "Regulation of NAD synthesis by the trifunctional NadR protein of *Salmonella enterica*", Journal of bacteriology, 187: 2774-82

F. Guerrero, V. Carbonell, M. Cossu, D. Correddu and P. R. Jones (2012) "Ethylene synthesis and regulated expression of recombinant protein in *Synechocystis sp.* PCC 6803", PloS one, 7: e50470

S. Gupta and D. P. Clark (1989) "*Escherichia coli* derivatives lacking both alcohol dehydrogenase and phosphotransacetylase grow anaerobically by lactate fermentation", Journal of bacteriology, 171: 3650-5

P. C. Hallenbeck and D. Ghosh (2012) "Improvements in fermentative biological hydrogen production through metabolic engineering", Journal of environmental management, 95 Suppl: S360-4

C. M. Hamilton, M. Aldea, B. K. Washburn, P. Babitzke and S. R. Kushner (1989) "New method for generating deletions and gene replacements in *Escherichia coli*", Journal of bacteriology, 171: 4617-22

T. Hanai, S. Atsumi and J. C. Liao (2007) "Engineered synthetic pathway for isopropanol production in *Escherichia coli*", Applied and environmental microbiology, 73: 7814-8

T. Happe, K. Schutz and H. Bohme (2000) "Transcriptional and mutational analysis of the uptake hydrogenase of the filamentous cyanobacterium *Anabaena variabilis* ATCC 29413", Journal of bacteriology, 182: 1624-31

G. C. Hartmann, A. R. Klein, M. Linder and R. K. Thauer (1996) "Purification, properties and primary structure of H2-forming N5 ,N10 -methylenetetrahydromethanopterin dehydrogenase from *Methanococcus thermolithotrophicus*", Archives of microbiology, 165: 187-93

J. Hasty, D. McMillen and J. J. Collins (2002) "Engineered gene circuits", Nature, 420: 224-30

N. K. Heinzinger, S. Y. Fujimoto, M. A. Clark, M. S. Moreno and E. L. Barrett (1995) "Sequence analysis of the phs operon in *Salmonella* Typhimurium and the contribution of thiosulfate reduction to anaerobic energy metabolism", Journal of bacteriology, 177: 2813-20

M. L. Helm, M. P. Stewart, R. M. Bullock, M. R. DuBois and D. L. DuBois (2011) "A synthetic nickel electrocatalyst with a turnover frequency above 100,000 s(-)(1) for H(2) production", Science, 333: 863-6

L. B. Hersh, M. J. Stark, S. Worthen and M. K. Fiero (1972) "N-methylglutamate dehydrogenase: kinetic studies on the solubilized enzyme", Archives of biochemistry and biophysics, 150: 219-26

Y. Higuchi, T. Yagi and N. Yasuoka (1997) "Unusual ligand structure in Ni-Fe active center and an additional Mg site in hydrogenase revealed by high resolution X-ray structure analysis", Structure, 5: 1671-80

N. J. Hillson, R. D. Rosengarten and J. D. Keasling (2012) "j5 DNA assembly design automation software", ACS synthetic biology, 1: 14-21

M. Hinderhofer, C. A. Walker, A. Friemel, C. A. Stuermer, H. M. Moller and A. Reuter (2009) "Evolution of prokaryotic SPFH proteins", BMC evolutionary biology, 9: 10

D. S. Hitchcock, A. A. Fedorov, E. V. Fedorov, L. J. Dangott, S. C. Almo and F. M. Raushel (2011) "Rescue of the orphan enzyme isoguanine deaminase", Biochemistry, 50: 5555-7

K. K. Ho and H. Weiner (2005) "Isolation and characterization of an aldehyde dehydrogenase encoded by the aldB gene of *Escherichia coli*", Journal of bacteriology, 187: 1067-73

E. L. Holbrook, R. C. Greene and J. H. Krueger (1990) "Purification and properties of cystathionine gamma-synthase from overproducing strains of *Escherichia coli*", Biochemistry, 29: 435-42

K. Hollands, S. Proshkin, S. Sklyarova, V. Epshtein, A. Mironov, E. Nudler and E. A. Groisman (2012) "Riboswitch control of Rho-dependent transcription termination", Proceedings of the National Academy of Sciences of the United States of America, 109: 5376-81

S. Hopper and A. Bock (1995) "Effector-mediated stimulation of ATPase activity by the sigma 54-dependent transcriptional activator FHLA from *Escherichia coli*", Journal of bacteriology, 177: 2798-803

D. C. Howarth and G. A. Codd (1985) "The Uptake and Production of Molecular Hydrogen by Unicellular Cyanobacteria", Journal of General Microbiology, 131: 1561-1569

H. Huang, S. Wang, J. Moll and R. K. Thauer (2012) "Electron bifurcation involved in the energy metabolism of the acetogenic bacterium *Moorella thermoacetica* growing on glucose or H2 plus CO2", Journal of bacteriology, 194: 3689-99

B. H. Huynh, M. H. Czechowski, H. J. Kruger, D. V. DerVartanian, H. D. Peck, Jr. and J. LeGall (1984) "*Desulfovibrio vulgaris* hydrogenase: a nonheme iron enzyme lacking nickel that exhibits anomalous EPR and Mossbauer spectra", Proceedings of the National Academy of Sciences of the United States of America, 81: 3728-32

IEA (2012) "World Energy Outlook 2012", OECD Publishing, Paris

IEA (2013) "Redrawing the Energy-Climate Map", World Energy Outlook Special Report, OECD Publishing, Paris

M. Ihara, H. Nishihara, K. S. Yoon, O. Lenz, B. Friedrich, H. Nakamoto, K. Kojima, D. Honma, T. Kamachi and I. Okura (2006) "Light-driven hydrogen production by a hybrid complex of a [NiFe]-hydrogenase and the cyanobacterial photosystem I", Photochemistry and photobiology, 82: 676-82

R. L. Jack, F. Sargent, B. C. Berks, G. Sawers and T. Palmer (2001) "Constitutive expression of *Escherichia coli tat* genes indicates an important role for the twin-arginine translocase during aerobic and anaerobic growth", Journal of bacteriology, 183: 1801-4

R. L. Jack, G. Buchanan, A. Dubini, K. Hatzixanthis, T. Palmer and F. Sargent (2004) "Coordinating assembly and export of complex bacterial proteins", The EMBO journal, 23: 3962-72

M. Jiang, Y. Cao, Z. F. Guo, M. Chen, X. Chen and Z. Guo (2007) "Menaquinone biosynthesis in *Escherichia coli*: identification of 2-succinyl-5-enolpyruvyl-6-hydroxy-3-cyclohexene-1-carboxylate as a novel intermediate and re-evaluation of MenD activity", Biochemistry, 46: 10979-89

D. C. Johnson, D. R. Dean, A. D. Smith and M. K. Johnson (2005) "Structure, function, and formation of biological iron-sulfur clusters", Annual review of biochemistry, 74: 247-81

T. Jojima, M. Inui and H. Yukawa (2008) "Production of isopropanol by metabolically engineered *Escherichia coli*", Applied microbiology and biotechnology, 77: 1219-24

W. K. Joklik (1950a) "The hydrogenase of *E. coli* in the cell-free state. II. The effect of certain inhibitors on hydrogenase", The Australian journal of experimental biology and medical science, 28: 331-8

W. K. Joklik (1950b) "The hydrogenase of *E. coli* in the cell-free state. I. Concentration, properties and activation", The Australian journal of experimental biology and medical science, 28: 320-9

D. T. Jones and D. R. Woods (1986) "Acetone-butanol fermentation revisited", Microbiological reviews, 50: 484-524

M. Kammler, C. Schon and K. Hantke (1993) "Characterization of the ferrous iron uptake system of *Escherichia coli*", Journal of bacteriology, 175: 6212-9

J. J. Kelley and E. E. Dekker (1985) "Identity of *Escherichia coli* D-1-amino-2-propanol:NAD+ oxidoreductase with *E. coli* glycerol dehydrogenase but not with *Neisseria gonorrhoeae* 1,2-propanediol:NAD+ oxidoreductase", Journal of bacteriology, 162: 170-5

D. Kessler, I. Leibrecht and J. Knappe (1991) "Pyruvate-formate-lyase-deactivase and acetyl-CoA reductase activities of *Escherichia coli* reside on a polymeric protein particle encoded by adhE", FEBS letters, 281: 59-63

Seohyoung Kim, Eunhee Seol, You-Kwan Oh, G. Y. Wang and Sunghoon Park (2009) "Hydrogen production and metabolic flux analysis of metabolically engineered *Escherichia coli* strains", International journal of hydrogen energy, 34: 7417-7427

P. W. King, M. C. Posewitz, M. L. Ghirardi and M. Seibert (2006) "Functional studies of [FeFe] hydrogenase maturation in an *Escherichia coli* biosynthetic system", Journal of bacteriology, 188: 2163-72

R. Kitney and P. Freemont (2012) "Synthetic biology - the state of play", FEBS letters, 586: 2029-36

J. Knappe and G. Sawers (1990) "A radical-chemical route to acetyl-CoA: the anaerobically induced pyruvate formate-lyase system of *Escherichia coli*", FEMS microbiology reviews, 6: 383-98

T. F. Knight (2003) "Idempotent Vector Design for Standard Assembly of BioBricks", MIT Synthetic Biology Working Group Technical Reports, http://hdl.handle.net/1721.1/21168

S. M. Knudsen and O. H. Karlstrom (1991) "Development of efficient suicide mechanisms for biological containment of bacteria", Applied and environmental microbiology, 57: 85-92

A. I. Krasna, E. Riklis and D. Rittenberg (1960) "The purification and properties of the hydrogenase of *Desulfovibrio desulfuricans*", The Journal of biological chemistry, 235: 2717-20

N. J. Kruger and A. von Schaewen (2003) "The oxidative pentose phosphate pathway: structure and organisation", Current opinion in plant biology, 6: 236-46

J. M. Kuchenreuther, C. S. Grady-Smith, A. S. Bingham, S. J. George, S. P. Cramer and J. R. Swartz (2010) "High-yield expression of heterologous [FeFe] hydrogenases in *Escherichia coli*", PloS one, 5: e15491

O. V. Kurnasov, B. M. Polanuyer, S. Ananta, R. Sloutsky, A. Tam, S. Y. Gerdes and A. L. Osterman (2002) "Ribosylnicotinamide kinase domain of NadR protein: identification and implications in NAD biosynthesis", Journal of bacteriology, 184: 6906-17

O. Kwon, D. K. Bhattacharyya and R. Meganathan (1996) "Menaquinone (vitamin K2) biosynthesis: overexpression, purification, and properties of o-succinylbenzoyl-coenzyme A synthetase from *Escherichia coli*", Journal of bacteriology, 178: 6778-81

B. Laber, T. Clausen, R. Huber, A. Messerschmidt, U. Egner, A. Muller-Fahrnow and H. D. Pohlenz (1996) "Cloning, purification, and crystallization of *Escherichia coli* cystathionine beta-lyase", FEBS letters, 379: 94-6

S. Y. Lam, R. C. Yeung, T. H. Yu, K. H. Sze and K. B. Wong (2011) "A rigidifying salt-bridge favors the activity of thermophilic enzyme at high temperatures at the expense of low-temperature activity", PLoS biology, 9: e1001027

C. Lambertz, N. Leidel, K. G. Havelius, J. Noth, P. Chernev, M. Winkler, T. Happe and M. Haumann (2011) "O2 reactions at the six-iron active site (H-cluster) in [FeFe]-hydrogenase", The Journal of biological chemistry, 286: 40614-23

J. R. Lancaster, Jr. (1980) "Soluble and membrane-bound paramagnetic centers in *Methanobacterium bryantii*", FEBS letters, 115: 285-8

E. Lapuente-Brun, R. Moreno-Loshuertos, R. Acin-Perez, A. Latorre-Pellicer, C. Colas, E. Balsa, E. Perales-Clemente, P. M. Quiros, E. Calvo, M. A. Rodriguez-Hernandez, P. Navas, R. Cruz, A. Carracedo, C. Lopez-Otin, A. Perez-Martos, P. Fernandez-Silva, E. Fernandez-Vizarra and J. A. Enriquez (2013) "Supercomplex assembly determines electron flux in the mitochondrial electron transport chain", Science, 340: 1567-70

T. V. Laurinavichene, A. Chanal, L. F. Wu and A. A. Tsygankov (2001) "Effect of O2, H2 and redox potential on the activity and synthesis of hydrogenase 2 in *Escherichia coli*", Research in microbiology, 152: 793-8

T. V. Laurinavichene and A. A. Tsygankov (2001) "H2 consumption by *Escherichia coli* coupled via hydrogenase 1 or hydrogenase 2 to different terminal electron acceptors", FEMS microbiology letters, 202: 121-4

T. V. Laurinavichene and A. A. Tsygankov (2003) "[Role of hydrogenases 1 and 2 in the hydrogen dependent nitrate respiration by *Escherichia coli*]", Mikrobiologiia, 72: 740-5

G. Layer, S. Ollagnier-de Choudens, Y. Sanakis and M. Fontecave (2006) "Iron-sulfur cluster biosynthesis: characterization of *Escherichia coli* CYaY as an iron donor for the assembly of [2Fe-2S] clusters in the scaffold IscU", The Journal of biological chemistry, 281: 16256-63

O. Lazarus, T. W. Woolerton, A. Parkin, M. J. Lukey, E. Reisner, J. Seravalli, E. Pierce, S. W. Ragsdale, F. Sargent and F. A. Armstrong (2009) "Water-gas shift reaction catalyzed by redox enzymes on conducting graphite platelets", Journal of the American Chemical Society, 131: 14154-5

T. S. Lee, R. A. Krupa, F. Zhang, M. Hajimorad, W. J. Holtz, N. Prasad, S. K. Lee and J. D. Keasling (2011) "BglBrick vectors and datasheets: A synthetic biology platform for gene expression", Journal of biological engineering, 5: 12

J. Legall, D. V. DerVartanian, E. Spilker, J. P. Lee and H. D. Peck, Jr. (1971) "Evidence for the involvement of non-heme iron in the active site of hydrogenase from *Desulfovibrio vulgaris*", Biochimica et biophysica acta, 234: 526-30

J. LeGall, P. O. Ljungdahl, I. Moura, H. D. Peck, Jr., A. V. Xavier, J. J. Moura, M. Teixera, B. H. Huynh and D. V. DerVartanian (1982) "The presence of redox-sensitive nickel in the periplasmic hydrogenase from *Desulfovibrio gigas*", Biochemical and biophysical research communications, 106: 610-6

J. Lengeler (1975) "Mutations affecting transport of the hexitols D-mannitol, D-glucitol, and galactitol in *Escherichia coli* K-12: isolation and mapping", Journal of bacteriology, 124: 26-38

O. Lenz, I. Zebger, J. Hamann, P. Hildebrandt and B. Friedrich (2007) "Carbamoylphosphate serves as the source of CN(-), but not of the intrinsic CO in the active site of the regulatory [NiFe]-hydrogenase from *Ralstonia eutropha*", FEBS letters, 581: 3322-6

M. R. Leonardo, P. R. Cunningham and D. P. Clark (1993) "Anaerobic regulation of the adhE gene, encoding the fermentative alcohol dehydrogenase of *Escherichia coli*", Journal of bacteriology, 175: 870-8

S. Leonhartsberger, A. Ehrenreich and A. Bock (2000) "Analysis of the domain structure and the DNA binding site of the transcriptional activator FhlA", European journal of biochemistry / FEBS, 267: 3672-84

David B. Levin, Lawrence Pitt and Murray Love (2004) "Biohydrogen production: prospects and limitations to practical application", International Journal of Hydrogen Energy, 29: 173-185

R. Lill (2009) "Function and biogenesis of iron-sulphur proteins", Nature, 460: 831-8

E. C. Lin (1976) "Glycerol dissimilation and its regulation in bacteria", Annual review of microbiology, 30: 535-78

D. Lopez and R. Kolter (2010) "Functional microdomains in bacterial membranes", Genes & development, 24: 1893-902

W. Lorowitz and D. Clark (1982) "*Escherichia coli* mutants with a temperature-sensitive alcohol dehydrogenase", Journal of bacteriology, 152: 935-8

C. Lou, B. Stanton, Y. J. Chen, B. Munsky and C. A. Voigt (2012) "Ribozyme-based insulator parts buffer synthetic circuits from genetic context", Nature biotechnology, 30: 1137-42

T. K. Lu and J. J. Collins (2009) "Engineered bacteriophage targeting gene networks as adjuvants for antibiotic therapy", Proceedings of the National Academy of Sciences of the United States of America, 106: 4629-34

W. Lu, J. Du, T. Wacker, E. Gerbig-Smentek, S. L. Andrade and O. Einsle (2011) "pH-dependent gating in a FocA formate channel", Science, 332: 352-4

M. J. Lukey, A. Parkin, M. M. Roessler, B. J. Murphy, J. Harmer, T. Palmer, F. Sargent and F. A. Armstrong (2010) "How *Escherichia coli* is equipped to oxidize hydrogen under different redox conditions", The Journal of biological chemistry, 285: 3928-38

S. Lutz, A. Jacobi, V. Schlensog, R. Bohm, G. Sawers and A. Bock (1991) "Molecular characterization of an operon (hyp) necessary for the activity of the three hydrogenase isoenzymes in *Escherichia coli*", Mol Microbiol, 5: 123-35

T. Maeda, V. Sanchez-Torres and T. K. Wood (2007a) "Enhanced hydrogen production from glucose by metabolically engineered *Escherichia coli*", Applied microbiology and biotechnology, 77: 879-90

T. Maeda, V. Sanchez-Torres and T. K. Wood (2007b) "*Escherichia coli* hydrogenase 3 is a reversible enzyme possessing hydrogen uptake and synthesis activities", Applied microbiology and biotechnology, 76: 1035-42

T. Maeda, V. Sanchez-Torres and T. K. Wood (2008) "Metabolic engineering to enhance bacterial hydrogen production", Microbial biotechnology, 1: 30-9

H. Makui, E. Roig, S. T. Cole, J. D. Helmann, P. Gros and M. F. Cellier (2000) "Identification of the *Escherichia coli* K-12 Nramp orthologue (MntH) as a selective divalent metal ion transporter", Molecular microbiology, 35: 1065-78

S. Malki, I. Saimmaime, G. De Luca, M. Rousset, Z. Dermoun and J. P. Belaich (1995) "Characterization of an operon encoding an NADP-reducing hydrogenase in *Desulfovibrio fructosovorans*", Journal of bacteriology, 177: 2628-36

S. Malki, G. De Luca, M. L. Fardeau, M. Rousset, J. P. Belaich and Z. Dermoun (1997) "Physiological characteristics and growth behavior of single and double hydrogenase mutants of *Desulfovibrio fructosovorans*", Archives of microbiology, 167: 38-45

S. Manish and Rangan Banerjee (2008) "Comparison of biohydrogen production processes", International Journal of Hydrogen Energy, 33: 279-286

E. Maranzana, G. Barbero, A. I. Falasca, G. Lenaz and M. L. Genova (2013) "Mitochondrial Respiratory Supercomplex Association Limits Production of Reactive Oxygen Species from Complex I", Antioxidants & redox signaling,
G. D. Markham, E. W. Hafner, C. W. Tabor and H. Tabor (1980) "S-Adenosylmethionine synthetase from *Escherichia coli*", The Journal of biological chemistry, 255: 9082-92

G. Maroti, Y. Tong, S. Yooseph, H. Baden-Tillson, H. O. Smith, K. L. Kovacs, M. Frazier, J. C. Venter and Q. Xu (2009) "Discovery of [NiFe] hydrogenase genes in metagenomic DNA: cloning and heterologous expression in *Thiocapsa roseopersicina*", Applied and environmental microbiology, 75: 5821-30

S. E. McGlynn, E. M. Shepard, M. A. Winslow, A. V. Naumov, K. S. Duschene, M. C. Posewitz, W. E. Broderick, J. B. Broderick and J. W. Peters (2008) "HydF as a scaffold protein in [FeFe] hydrogenase H-cluster biosynthesis", FEBS letters, 582: 2183-7

M. J. McInerney, J. R. Sieber and R. P. Gunsalus (2009) "Syntrophy in anaerobic global carbon cycles", Current opinion in biotechnology, 20: 623-32

M. H. Medema, M. T. Alam, R. Breitling and E. Takano (2011) "The future of industrial antibiotic production: from random mutagenesis to synthetic biology", Bioengineered bugs, 2: 230-3

A. Melis, L. Zhang, M. Forestier, M. L. Ghirardi and M. Seibert (2000) "Sustained photobiological hydrogen gas production upon reversible inactivation of oxygen evolution in the green alga *Chlamydomonas reinhardtii*", Plant physiology, 122: 127-36

N. K. Menon, J. Robbins, H. D. Peck, Jr., C. Y. Chatelus, E. S. Choi and A. E. Przybyla (1990) "Cloning and sequencing of a putative *Escherichia coli* [NiFe] hydrogenase-1 operon containing six open reading frames", Journal of bacteriology, 172: 1969-77

N. K. Menon, J. Robbins, J. C. Wendt, K. T. Shanmugam and A. E. Przybyla (1991) "Mutational analysis and characterization of the *Escherichia coli* hya operon, which encodes [NiFe] hydrogenase 1", Journal of bacteriology, 173: 4851-61

N. K. Menon, C. Y. Chatelus, M. Dervartanian, J. C. Wendt, K. T. Shanmugam, H. D. Peck, Jr. and A. E. Przybyla (1994) "Cloning, sequencing, and mutational analysis of the hyb operon encoding *Escherichia coli* hydrogenase 2", Journal of bacteriology, 176: 4416-23

B. Meyssignac and A. Cazenave (2012) "Sea level: A review of present-day and recent-past changes and variability", Journal of Geodynamics, 58: 96-109

K. Miki and E. C. Lin (1973) "Enzyme complex which couples glycerol-3-phosphate dehydrogenation to fumarate reduction in *Escherichia coli*", Journal of bacteriology, 114: 767-71

T. Miyake, M. Bruschi, U. Cosentino, C. Baffert, V. Fourmond, C. Leger, G. Moro, L. De Gioia and C. Greco (2013) "Does the environment around the H-cluster allow coordination of the pendant amine to the catalytic iron center in [FeFe] hydrogenases? Answers from theory", Journal of biological inorganic chemistry : JBIC : a publication of the Society of Biological Inorganic Chemistry, 18: 693-700

G. H. Moe-Behrens, R. Davis and K. A. Haynes (2013) "Preparing synthetic biology for the world", Frontiers in microbiology, 4: 5

A. Morin, K. W. Kaufmann, C. Fortenberry, J. M. Harp, L. S. Mizoue and J. Meiler (2011) "Computational design of an endo-1,4-beta-xylanase ligand binding site", Protein engineering, design & selection : PEDS, 24: 503-16

D. W. Mulder, E. S. Boyd, R. Sarma, R. K. Lange, J. A. Endrizzi, J. B. Broderick and J. W. Peters (2010) "Stepwise [FeFe]-hydrogenase H-cluster assembly revealed in the structure of HydA(DeltaEFG)", Nature, 465: 248-51

D. W. Mulder, E. M. Shepard, J. E. Meuser, N. Joshi, P. W. King, M. C. Posewitz, J. B. Broderick and J. W. Peters (2011) "Insights into [FeFe]-hydrogenase structure, mechanism, and maturation", Structure, 19: 1038-52

A. Murarka, Y. Dharmadi, S. S. Yazdani and R. Gonzalez (2008) "Fermentative utilization of glycerol by *Escherichia coli* and its implications for the production of fuels and chemicals", Applied and environmental microbiology, 74: 1124-35

G. Nakos and L. Mortenson (1971) "Purification and properties of hydrogenase, an iron sulfur protein, from *Clostridium pasteurianum* W5", Biochimica et biophysica acta, 227: 576-83

C. Navarro, L. F. Wu and M. A. Mandrand-Berthelot (1993) "The nik operon of *Escherichia coli* encodes a periplasmic binding-protein-dependent transport system for nickel", Molecular microbiology, 9: 1181-91

A. D. Nesbit, A. S. Fleischhacker, S. J. Teter and P. J. Kiley (2012) "ArcA and AppY antagonize IscR repression of hydrogenase-1 expression under anaerobic conditions, revealing a novel mode of O2 regulation of gene expression in *Escherichia coli*", Journal of bacteriology, 194: 6892-9

D. J. Nicholas, D. J. Fisher, W. J. Redmond and M. A. Wright (1960) "Some aspects of hydrogenase activity and nitrogen fixation in Azotobacter spp and in *Clostridium pasteurianum*", Journal of general microbiology, 22: 191-205

Y. Nicolet, C. Piras, P. Legrand, C. E. Hatchikian and J. C. Fontecilla-Camps (1999) "*Desulfovibrio desulfuricans* iron hydrogenase: the structure shows unusual coordination to an active site Fe binuclear center", Structure, 7: 13-23

Y. Nicolet, A. L. de Lacey, X. Vernede, V. M. Fernandez, E. C. Hatchikian and J. C. Fontecilla-Camps (2001) "Crystallographic and FTIR spectroscopic evidence of changes in Fe coordination upon reduction of the active site of the Fe-only hydrogenase from *Desulfovibrio desulfuricans*", Journal of the American Chemical Society, 123: 1596-601

Y. Nicolet, J. K. Rubach, M. C. Posewitz, P. Amara, C. Mathevon, M. Atta, M. Fontecave and J. C. Fontecilla-Camps (2008) "X-ray structure of the [FeFe]-hydrogenase maturase HydE from *Thermotoga maritima*", The Journal of biological chemistry, 283: 18861-72

Y. Nicolet, L. Martin, C. Tron and J. C. Fontecilla-Camps (2010) "A glycyl free radical as the precursor in the synthesis of carbon monoxide and cyanide by the [FeFe]-hydrogenase maturase HydG", FEBS letters, 584: 4197-202

J. Nielsen and J. D. Keasling (2011) "Synergies between synthetic biology and metabolic engineering", Nature biotechnology, 29: 693-5

M. J. Novotny, J. Reizer, F. Esch and M. H. Saier, Jr. (1984) "Purification and properties of D-mannitol-1-phosphate dehydrogenase and D-glucitol-6-phosphate dehydrogenase from *Escherichia coli*", Journal of bacteriology, 159: 986-90

S. E. Oh, S. Van Ginkel and B. E. Logan (2003) "The relative effectiveness of pH control and heat treatment for enhancing biohydrogen gas production", Environmental science & technology, 37: 5186-90

T. Ohta, M. Watanabe-Akanuma and H. Yamagata (2000) "A comparison of mutation spectra detected by the *Escherichia coli* lac(+) reversion assay and the Salmonella typhimurium his(+) reversion assay", Mutagenesis, 15: 317-23

C. J. Paddon, P. J. Westfall, D. J. Pitera, K. Benjamin, K. Fisher, D. McPhee, M. D. Leavell, A. Tai, A. Main, D. Eng, D. R. Polichuk, K. H. Teoh, D. W. Reed, T. Treynor, J. Lenihan, M. Fleck, S. Bajad, G. Dang, D. Dengrove, D. Diola, G. Dorin, K. W. Ellens, S. Fickes, J. Galazzo, S. P. Gaucher, T. Geistlinger, R. Henry, M. Hepp, T. Horning, T. Iqbal, H. Jiang, L. Kizer, B. Lieu, D. Melis, N. Moss, R. Regentin, S. Secrest, H. Tsuruta, R. Vazquez, L. F. Westblade, L. Xu, M. Yu, Y. Zhang, L. Zhao, J. Lievense, P. S. Covello, J. D. Keasling, K. K. Reiling, N. S. Renninger and J. D. Newman (2013) "High-level semi-synthetic production of the potent antimalarial artemisinin", Nature, 496: 528-32

C. C. Page, C. C. Moser, X. Chen and P. L. Dutton (1999) "Natural engineering principles of electron tunnelling in biological oxidation-reduction", Nature, 402: 47-52

C. C. Page, C. C. Moser and P. L. Dutton (2003) "Mechanism for electron transfer within and between proteins", Current opinion in chemical biology, 7: 551-6

T. Palmer and B. C. Berks (2012) "The twin-arginine translocation (Tat) protein export pathway", Nature reviews. Microbiology, 10: 483-96

A. Parkin, L. Bowman, M. M. Roessler, R. A. Davies, T. Palmer, F. A. Armstrong and F. Sargent (2012) "How Salmonella oxidises H(2) under aerobic conditions", FEBS letters, 586: 536-44

A. Parkin and F. Sargent (2012) "The hows and whys of aerobic H2 metabolism", Current opinion in chemical biology, 16: 26-34

J. B. Parsons, S. Frank, D. Bhella, M. Liang, M. B. Prentice, D. P. Mulvihill and M. J. Warren (2010) "Synthesis of empty bacterial microcompartments, directed organelle protein incorporation, and evidence of filament-associated organelle movement", Molecular cell, 38: 305-15

A. Paschos, R. S. Glass and A. Bock (2001) "Carbamoylphosphate requirement for synthesis of the active center of [NiFe]-hydrogenases", FEBS Lett, 488: 9-12

L. Pasotti, N. Politi, S. Zucca, M. G. Cusella De Angelis and P. Magni (2012) "Bottom-up engineering of biological systems through standard bricks: a modularity study on basic parts and devices", PloS one, 7: e39407

N. Peekhaus and T. Conway (1998) "What's for dinner?: Entner-Doudoroff metabolism in *Escherichia coli*", Journal of bacteriology, 180: 3495-502

P. P. Peralta-Yahya, M. Ouellet, R. Chan, A. Mukhopadhyay, J. D. Keasling and T. S. Lee (2011) "Identification and microbial production of a terpene-based advanced biofuel", Nature communications, 2: 483

J. W. Peters, W. N. Lanzilotta, B. J. Lemon and L. C. Seefeldt (1998) "X-ray crystal structure of the Fe-only hydrogenase (CpI) from *Clostridium pasteurianum* to 1.8 angstrom resolution", Science, 282: 1853-8

J. W. Peters and J. B. Broderick (2012) "Emerging paradigms for complex iron-sulfur cofactor assembly and insertion", Annual review of biochemistry, 81: 429-50

S. Petkun, R. Shi, Y. Li, A. Asinas, C. Munger, L. Zhang, M. Waclawek, B. Soboh, R. G. Sawers and M. Cygler (2011) "Structure of hydrogenase maturation protein HypF with reaction intermediates shows two active sites", Structure, 19: 1773-83

V. B. Pinheiro, A. I. Taylor, C. Cozens, M. Abramov, M. Renders, S. Zhang, J. C. Chaput, J. Wengel, S. Y. Peak-Chew, S. H. McLaughlin, P. Herdewijn and P. Holliger (2012) "Synthetic genetic polymers capable of heredity and evolution", Science, 336: 341-4

V. B. Pinheiro, D. Loakes and P. Holliger (2013) "Synthetic polymers and their potential as genetic materials", BioEssays : news and reviews in molecular, cellular and developmental biology, 35: 113-22

C. Pinske, J. S. McDowall, F. Sargent and R. G. Sawers (2012) "Analysis of hydrogenase 1 levels reveals an intimate link between carbon and hydrogen metabolism in *Escherichia coli* K-12", Microbiology, 158: 856-68

C. Pinske and R. G. Sawers (2012a) "Delivery of iron-sulfur clusters to the hydrogen-oxidizing [NiFe]-hydrogenases in *Escherichia coli* requires the A-type carrier proteins ErpA and IscA", PloS one, 7: e31755

C. Pinske and R. G. Sawers (2012b) "A-type carrier protein ErpA is essential for formation of an active formate-nitrate respiratory pathway in *Escherichia coli* K-12", Journal of bacteriology, 194: 346-53

I. Poblete-Castro, J. Becker, K. Dohnt, V. M. dos Santos and C. Wittmann (2012) "Industrial biotechnology of *Pseudomonas putida* and related species", Applied microbiology and biotechnology, 93: 2279-90

B. K. Pohorelic, J. K. Voordouw, E. Lojou, A. Dolla, J. Harder and G. Voordouw (2002) "Effects of deletion of genes encoding Fe-only hydrogenase of *Desulfovibrio vulgaris* Hildenborough on hydrogen and lactate metabolism", Journal of bacteriology, 184: 679-86

M. C. Posewitz, P. W. King, S. L. Smolinski, L. Zhang, M. Seibert and M. L. Ghirardi (2004) "Discovery of two novel radical S-adenosylmethionine proteins required for the assembly of an active [Fe] hydrogenase", The Journal of biological chemistry, 279: 25711-20

M. C. Posewitz, P. W. King, S. L. Smolinski, R. D. Smith, A. R. Ginley, M. L. Ghirardi and M. Seibert (2005) "Identification of genes required for hydrogenase activity in *Chlamydomonas reinhardtii*", Biochemical Society transactions, 33: 102-4

P. Puigbo, E. Guzman, A. Romeu and S. Garcia-Vallve (2007) "OPTIMIZER: a web server for optimizing the codon usage of DNA sequences", Nucleic acids research, 35: W126-31

C. A. Rabinovitch-Deere, J. W. Oliver, G. M. Rodriguez and S. Atsumi (2013) "Synthetic biology and metabolic engineering approaches to produce biofuels", Chemical reviews, 113: 4611-32

E. Racker (1952) "Enzymatic synthesis and breakdown of desoxyribose phosphate", The Journal of biological chemistry, 196: 347-65

O. Rackham and J. W. Chin (2005) "A network of orthogonal ribosome x mRNA pairs", Nature chemical biology, 1: 159-66

N. Raffaelli, T. Lorenzi, P. L. Mariani, M. Emanuelli, A. Amici, S. Ruggieri and G. Magni (1999) "The *Escherichia coli* NadR regulator is endowed with nicotinamide mononucleotide adenylyltransferase activity", Journal of bacteriology, 181: 5509-11

M. D. Redwood, I. P. Mikheenko, F. Sargent and L. E. Macaskie (2008) "Dissecting the roles of *Escherichia coli* hydrogenases in biohydrogen production", FEMS microbiology letters, 278: 48-55

M. R. Reyda, C. J. Fugate and J. T. Jarrett (2009) "A complex between biotin synthase and the iron-sulfur cluster assembly chaperone HscA that enhances in vivo cluster assembly", Biochemistry, 48: 10782-92

D. J. Richard, G. Sawers, F. Sargent, L. McWalter and D. H. Boxer (1999) "Transcriptional regulation in response to oxygen and nitrate of the operons encoding the [NiFe] hydrogenases 1 and 2 of *Escherichia coli*", Microbiology, 145 ( Pt 10): 2903-12

L. Riechmann, J. Foote and G. Winter (1988) "Expression of an antibody Fv fragment in myeloma cells", Journal of molecular biology, 203: 825-8

A. Rodrigue, A. Chanal, K. Beck, M. Muller and L. F. Wu (1999) "Co-translocation of a periplasmic enzyme complex by a hitchhiker mechanism through the bacterial tat pathway", The Journal of biological chemistry, 274: 13223-8

A. H. Romano and T. Conway (1996) "Evolution of carbohydrate metabolic pathways", Research in microbiology, 147: 448-55

R. Rossmann, M. Sauter, F. Lottspeich and A. Bock (1994) "Maturation of the large subunit (HYCE) of *Escherichia coli* hydrogenase 3 requires nickel incorporation followed by C-terminal processing at Arg537", European journal of biochemistry / FEBS, 220: 377-84

C. Roux, L. Salmon and C. Verchere-Beaur (2006) "Preliminary studies on the inhibition of D-sorbitol-6-phosphate 2-dehydrogenase from *Escherichia coli* with substrate analogues", Journal of enzyme inhibition and medicinal chemistry, 21: 187-92

R. J. Rowbury and D. D. Woods (1964) "O-Succinylhomoserine as an Intermediate in the Synthesis of Cystathionine by *Escherichia coli*", Journal of general microbiology, 36: 341-58

J. K. Rubach, X. Brazzolotto, J. Gaillard and M. Fontecave (2005) "Biochemical characterization of the HydE and HydG iron-only hydrogenase maturation enzymes from *Thermatoga maritima*", FEBS letters, 579: 5055-60

T. Rydzak, P. D. McQueen, O. V. Krokhin, V. Spicer, P. Ezzati, R. C. Dwivedi, D. Shamshurin, D. B. Levin, J. A. Wilkins and R. Sparling (2012) "Proteomic analysis of *Clostridium thermocellum* core metabolism: relative protein expression profiles and growth phase-dependent changes in protein expression", BMC microbiology, 12: 214

J. C. Sadana and D. Rittenberg (1963) "Some Observations on the Enzyme Hydrogenase of *Desulfovibrio Desulfuricans*", Proceedings of the National Academy of Sciences of the United States of America, 50: 900-4

J. C. Sadana and D. Rittenberg (1964) "Iron Requirement for the Hydrogenase of *Desulfovibrio Desulfuricans*", Archives of biochemistry and biophysics, 108: 255-7

A. Saini, D. T. Mapolelo, H. K. Chahal, M. K. Johnson and F. W. Outten (2010) "SufD and SufC ATPase activity are required for iron acquisition during in vivo Fe-S cluster formation on SufB", Biochemistry, 49: 9402-12

H. M. Salis, E. A. Mirsky and C. A. Voigt (2009) "Automated design of synthetic ribosome binding sites to control protein expression", Nature biotechnology, 27: 946-50

H. M. Salis (2011) "The ribosome binding site calculator", Methods in enzymology, 498: 19-42

J. Sambrook, E. F. Fritsch and T. Maniatis (1989) "Molecular cloning: a laboratory manual", Cold Spring Harbor Laboratory, Cold Spring Harbor, New York.

V. Sanchez-Torres, T. Maeda and T. K. Wood (2009) "Protein engineering of the transcriptional activator FhlA To enhance hydrogen production in *Escherichia coli*", Applied and environmental microbiology, 75: 5639-46

V. Sanchez-Torres, M. Z. M. Yusoff, C. Nakano, T. Maeda, H. I. Ogawa and T. K. Wood (2013) "Influence of *Escherichia coli* hydrogenases on hydrogen fermentation from glycerol", International Journal of Hydrogen Energy

S. W. Santoro, L. Wang, B. Herberich, D. S. King and P. G. Schultz (2002) "An efficient system for the evolution of aminoacyl-tRNA synthetase specificity", Nature biotechnology, 20: 1044-8

F. Sargent, S. P. Ballantine, P. A. Rugman, T. Palmer and D. H. Boxer (1998a) "Reassignment of the gene encoding the *Escherichia coli* hydrogenase 2 small subunit--identification of a soluble precursor of the small subunit in a hypB mutant", European journal of biochemistry / FEBS, 255: 746-54

F. Sargent, E. G. Bogsch, N. R. Stanley, M. Wexler, C. Robinson, B. C. Berks and T. Palmer (1998b) "Overlapping functions of components of a bacterial Sec-independent protein export pathway", The EMBO journal, 17: 3640-50

F. Sargent, N. R. Stanley, B. C. Berks and T. Palmer (1999) "Sec-independent protein translocation in *Escherichia coli*. A distinct and pivotal role for the TatB protein", The Journal of biological chemistry, 274: 36073-82

K. C. Sasahara, N. K. Heinzinger and E. L. Barrett (1997) "Hydrogen sulfide production and fermentative gas production by *Salmonella* Typhimurium require F0F1 ATP synthase activity", Journal of bacteriology, 179: 6736-40

M. Sauter, R. Bohm and A. Bock (1992) "Mutational analysis of the operon (hyc) determining hydrogenase 3 formation in *Escherichia coli*", Molecular microbiology, 6: 1523-32

R. G. Sawers, S. P. Ballantine and D. H. Boxer (1985) "Differential expression of hydrogenase isoenzymes in *Escherichia coli* K-12: evidence for a third isoenzyme", Journal of bacteriology, 164: 1324-31

R. G. Sawers and D. H. Boxer (1986) "Purification and properties of membrane-bound hydrogenase isoenzyme 1 from anaerobically grown *Escherichia coli* K12", European journal of biochemistry / FEBS, 156: 265-75

R. G. Sawers (2005) "Formate and its role in hydrogen production in *Escherichia coli*", Biochemical Society transactions, 33: 42-6

C. Schneider, M. Wein, D. Harmsen and P. Schreier (1997) "A fatty acid alpha-ketol, a product of the plant lipoxygenase pathway, is oxidized to 3(Z)-dodecendioic acid by a bacterial monooxygenase", Biochemical and biophysical research communications, 232: 364-6

B. Schreier, C. Stumpp, S. Wiesner and B. Hocker (2009) "Computational design of ligand binding is not a solved problem", Proceedings of the National Academy of Sciences of the United States of America, 106: 18491-6

K. Schuchmann and V. Muller (2012) "A bacterial electron-bifurcating hydrogenase", The Journal of biological chemistry, 287: 31165-71

G. J. Schut and M. W. Adams (2009) "The iron-hydrogenase of *Thermotoga maritima* utilizes ferredoxin and NADH synergistically: a new perspective on anaerobic hydrogen production", Journal of bacteriology, 191: 4451-7

C. J. Schwartz, J. L. Giel, T. Patschkowski, C. Luther, F. J. Ruzicka, H. Beinert and P. J. Kiley (2001) "IscR, an Fe-S cluster-containing transcription factor, represses expression of *Escherichia coli* genes encoding Fe-S cluster assembly proteins", Proceedings of the National Academy of Sciences of the United States of America, 98: 14895-900

H. Schweizer, T. Grussenmeyer and W. Boos (1982) "Mapping of two ugp genes coding for the pho regulon-dependent sn-glycerol-3-phosphate transport system of *Escherichia coli*", Journal of bacteriology, 150: 1164-71

P. Schyfter (2013) "How a 'drive to make' shapes synthetic biology", Studies in history and philosophy of biological and biomedical sciences

T. Searchinger, R. Heimlich, R. A. Houghton, F. Dong, A. Elobeid, J. Fabiosa, S. Tokgoz, D. Hayes and T. H. Yu (2008) "Use of U.S. croplands for biofuels increases greenhouse gases through emissions from land-use change", Science, 319: 1238-40

A. E. Senior (1990) "The proton-translocating ATPase of *Escherichia coli*", Annual review of biophysics and biophysical chemistry, 19: 7-41

P. M. Sharp and W. H. Li (1987) "The codon Adaptation Index--a measure of directional synonymous codon usage bias, and its potential applications", Nucleic acids research, 15: 1281-95

W. V. Shaw, L. Tsai and E. R. Stadtman (1966) "The enzymatic synthesis of N-methylglutamic acid", The Journal of biological chemistry, 241: 935-45

E. M. Shepard, B. R. Duffus, S. J. George, S. E. McGlynn, M. R. Challand, K. D. Swanson, P. L. Roach, S. P. Cramer, J. W. Peters and J. B. Broderick (2010a) "[FeFe]-hydrogenase maturation: HydG-catalyzed synthesis of carbon monoxide", Journal of the American Chemical Society, 132: 9247-9

E. M. Shepard, S. E. McGlynn, A. L. Bueling, C. S. Grady-Smith, S. J. George, M. A. Winslow, S. P. Cramer, J. W. Peters and J. B. Broderick (2010b) "Synthesis of the 2Fe subcluster of the [FeFe]-hydrogenase H cluster on the HydF scaffold", Proceedings of the National Academy of Sciences of the United States of America, 107: 10448-53

R. P. Shetty, D. Endy and T. F. Knight, Jr. (2008) "Engineering BioBrick vectors from BioBrick parts", Journal of biological engineering, 2: 5

S. Shima, O. Pilak, S. Vogt, M. Schick, M. S. Stagni, W. Meyer-Klaucke, E. Warkentin, R. K. Thauer and U. Ermler (2008) "The crystal structure of [Fe]-hydrogenase reveals the geometry of the active site", Science, 321: 572-5

D. L. Shis and M. R. Bennett (2013) "Library of synthetic transcriptional AND gates built with split T7 RNA polymerase mutants", Proceedings of the National Academy of Sciences of the United States of America, 110: 5028-33

R. Silva-Rocha, E. Martinez-Garcia, B. Calles, M. Chavarria, A. Arce-Rodriguez, A. de Las Heras, A. D. Paez-Espino, G. Durante-Rodriguez, J. Kim, P. I. Nikel, R. Platero and V. de Lorenzo (2013) "The Standard European Vector Architecture (SEVA): a coherent platform for the analysis and deployment of complex prokaryotic phenotypes", Nucleic acids research, 41: D666-75

K. Simons and E. Ikonen (1997) "Functional rafts in cell membranes", Nature, 387: 569-72

S. J. Singer and G. L. Nicolson (1972) "The fluid mosaic model of the structure of cell membranes", Science, 175: 720-31

P. Siuti, J. Yazbek and T. K. Lu (2013) "Synthetic circuits integrating logic and memory in living cells", Nature biotechnology, 31: 448-52

B. Soboh, D. Linder and R. Hedderich (2004) "A multisubunit membrane-bound [NiFe] hydrogenase and an NADH-dependent Fe-only hydrogenase in the fermenting bacterium *Thermoanaerobacter tengcongensis*", Microbiology, 150: 2451-63

B. Soboh, S. T. Stripp, E. Muhr, C. Granich, M. Braussemann, M. Herzberg, J. Heberle and R. Gary Sawers (2012) "[NiFe]-hydrogenase maturation: isolation of a HypC-HypD complex carrying diatomic CO and CN- ligands", FEBS letters, 586: 3882-7

S. Solomon, D. Qin, M. Manning, Z. Chen, M. Marquis, K.B. Averyt, and M. Tignor and H.L. Miller (eds.) (2007) "Climate Change 2007: The Physical Science Basis. Contribution of Working

Group I to the Fourth Assessment Report of the Intergovernmental Panel on Climate Change", IPCC, Cambridge University Press, 996

F. Spira, N. S. Mueller, G. Beck, P. von Olshausen, J. Beig and R. Wedlich-Soldner (2012) "Patchwork organization of the yeast plasma membrane into numerous coexisting domains", Nature cell biology, 14: 640-8

G. A. Sprenger (1995) "Genetics of pentose-phosphate pathway enzymes of *Escherichia coli* K-12", Archives of microbiology, 164: 324-30

E. J. St Martin, W. B. Freedberg and E. C. Lin (1977) "Kinase replacement by a dehydrogenase for *Escherichia coli* glycerol utilization", Journal of bacteriology, 131: 1026-8

J. A. Stapleton and J. R. Swartz (2010a) "A cell-free microtiter plate screen for improved [FeFe] hydrogenases", PloS one, 5: e10554

J. A. Stapleton and J. R. Swartz (2010b) "Development of an in vitro compartmentalization screen for high-throughput directed evolution of [FeFe] hydrogenases", PloS one, 5: e15275

E. J. Steen, Y. Kang, G. Bokinsky, Z. Hu, A. Schirmer, A. McClure, S. B. Del Cardayre and J. D. Keasling (2010) "Microbial production of fatty-acid-derived fuels and chemicals from plant biomass", Nature, 463: 559-62

G. Stephanopoulos (2012) "Synthetic biology and metabolic engineering", ACS synthetic biology, 1: 514-25

M. Stephenson and L. H. Stickland (1931) "Hydrogenase: a bacterial enzyme activating molecular hydrogen: The properties of the enzyme", The Biochemical journal, 25: 205-14

M. Stephenson and L. H. Stickland (1932) "Hydrogenlyases: Bacterial enzymes liberating molecular hydrogen", The Biochemical journal, 26: 712-24

L. Stoffels, M. Krehenbrink, B. C. Berks and G. Unden (2012) "Thiosulfate reduction in Salmonella enterica is driven by the proton motive force", Journal of bacteriology, 194: 475-85

S. T. Stripp, B. Soboh, U. Lindenstrauss, M. Braussemann, M. Herzberg, D. H. Nies, R. G. Sawers and J. Heberle (2013) "HypD Is the Scaffold Protein for Fe-(CN)CO Cofactor Assembly in [NiFe]-Hydrogenase Maturation", Biochemistry

R. M. Stroud, L. J. Miercke, J. O'Connell, S. Khademi, J. K. Lee, J. Remis, W. Harries, Y. Robles and D. Akhavan (2003) "Glycerol facilitator GlpF and the associated aquaporin family of channels", Current opinion in structural biology, 13: 424-31

K. P. Subedi, I. Kim, J. Kim, B. Min and C. Park (2008) "Role of GldA in dihydroxyacetone and methylglyoxal metabolism of *Escherichia coli* K12", FEMS microbiology letters, 279: 180-7

J. H. Sun, M. R. Hyman and D. J. Arp (1992) "Acetylene inhibition of Azotobacter vinelandii hydrogenase: acetylene binds tightly to the large subunit", Biochemistry, 31: 3158-65

B. Suppmann and G. Sawers (1994) "Isolation and characterization of hypophosphite--resistant mutants of *Escherichia coli*: identification of the FocA protein, encoded by the pfl operon, as a putative formate transporter", Molecular microbiology, 11: 965-82

K. Sybirna, T. Antoine, P. Lindberg, V. Fourmond, M. Rousset, V. Mejean and H. Bottin (2008) "Shewanella oneidensis: a new and efficient system for expression and maturation of heterologous [Fe-Fe] hydrogenase from *Chlamydomonas reinhardtii*", BMC biotechnology, 8: 73

N. Szita, K. Polizzi, N. Jaccard and F. Baganz (2010) "Microfluidic approaches for systems and synthetic biology", Current opinion in biotechnology, 21: 517-23

S. Tabor and C. C. Richardson (1985) "A bacteriophage T7 RNA polymerase/promoter system for controlled exclusive expression of specific genes", Proceedings of the National Academy of Sciences of the United States of America, 82: 1074-8

C. Tang and R. A. Capaldi (1996) "Characterization of the interface between gamma and epsilon subunits of *Escherichia coli* F1-ATPase", The Journal of biological chemistry, 271: 3018-24

C. T. Tang, F. E. Ruch, Jr. and C. C. Lin (1979) "Purification and properties of a nicotinamide adenine dinucleotide-linked dehydrogenase that serves an *Escherichia coli* mutant for glycerol catabolism", Journal of bacteriology, 140: 182-7

J. C. Tang, R. G. Forage and E. C. Lin (1982) "Immunochemical properties of NAD+-linked glycerol dehydrogenases from *Escherichia coli* and *Klebsiella pneumoniae*", Journal of bacteriology, 152: 1169-74

E. M. Tarmy and N. O. Kaplan (1968a) "Kinetics of *Escherichia coli* B D-lactate dehydrogenase and evidence for pyruvate-controlled change in conformation", The Journal of biological chemistry, 243: 2587-96

E. M. Tarmy and N. O. Kaplan (1968b) "Chemical characterization of D-lactate dehydrogenase from *Escherichia coli* B", The Journal of biological chemistry, 243: 2579-86

K. Temme, D. Zhao and C. A. Voigt (2012) "Refactoring the nitrogen fixation gene cluster from *Klebsiella oxytoca*", Proceedings of the National Academy of Sciences of the United States of America, 109: 7085-90

B. Ten Brink and W. N. Konings (1980) "Generation of an electrochemical proton gradient by lactate efflux in membrane vesicles of *Escherichia coli*", European journal of biochemistry / FEBS, 111: 59-66

M. N. Thaker and G. D. Wright (2012) "Opportunities for Synthetic Biology in Antibiotics: Expanding Glycopeptide Chemical Diversity", ACS synthetic biology

K. Thodey and C. D. Smolke (2011) "Cell biology. Bringing it together with RNA", Science, 333: 412-3

L. C. Thomason, N. Costantino and D. L. Court (2007) "*E. coli* genome manipulation by P1 transduction", Curr Protoc Mol Biol, Chapter 1: Unit 1 17

C. E. Tinberg, S. D. Khare, J. Dou, L. Doyle, J. W. Nelson, A. Schena, W. Jankowski, C. G. Kalodimos, K. Johnsson, B. L. Stoddard and D. Baker (2013) "Computational design of ligand-binding proteins with high affinity and selectivity", Nature, 501: 212-6

M. J. Tipping, B. C. Steel, N. J. Delalez, R. M. Berry and J. P. Armitage (2013) "Quantification of flagellar motor stator dynamics through in vivo proton-motive force control", Molecular microbiology, 87: 338-47

S. J. Tomazic and A. M. Klibanov (1988) "Why is one Bacillus alpha-amylase more resistant against irreversible thermoinactivation than another?", The Journal of biological chemistry, 263: 3092-6

K. Trchounian and A. Trchounian (2009) "Hydrogenase 2 is most and hydrogenase 1 is less responsible for H2 production by *Escherichia coli* under glycerol fermentation at neutral and slightly alkaline pH", International Journal of Hydrogen Energy, 34: 8839–8845

K. Trchounian, V. Sanchez-Torres, T. K. Wood and A. Trchounian (2011) "*Escherichia coli* hydrogenase activity and H2 production under glycerol fermentation at a low pH", International journal of hydrogen energy, 36: 4323-4331

K. Trchounian, B. Soboh, R. G. Sawers and A. Trchounian (2013) "Contribution of Hydrogenase 2 to Stationary Phase H2 Production by *Escherichia coli* During Fermentation of Glycerol", Cell biochemistry and biophysics, 66: 103-8

V. Truniger and W. Boos (1994) "Mapping and cloning of gldA, the structural gene of the *Escherichia coli* glycerol dehydrogenase", Journal of bacteriology, 176: 1796-800

J. A. Turner (2004) "Sustainable hydrogen production", Science, 305: 972-4

Population Division UN Department of Economic and Social Affairs (2013) "World Population Prospects: The 2012 Revision, Key Findings and Advance Tables", United Nations, New York

R. C. Valentine and R. S. Wolfe (1963) "Role of Ferredoxin in the Metabolism of Molecular Hydrogen", Journal of bacteriology, 85: 1114-20

S. A. van Hijum, M. H. Medema and O. P. Kuipers (2009) "Mechanisms and evolution of control logic in prokaryotic transcriptional regulation", Microbiology and molecular biology reviews : MMBR, 73: 481-509, Table of Contents

E. W. van Niel, P. A. Claassen and A. J. Stams (2003) "Substrate and product inhibition of hydrogen production by the extreme thermophile, Caldicellulosiruptor saccharolyticus", Biotechnology and bioengineering, 81: 255-62

J. Van Overbeek (1940) "Traumatic Acid and Thiamin as Growth Factors for Algae", Proceedings of the National Academy of Sciences of the United States of America, 26: 441-3

G. Vardar-Schara, T. Maeda and T. K. Wood (2008) "Metabolically engineered bacteria for producing hydrogen via fermentation", Microbial biotechnology, 1: 107-25

J. P. Vartanian, M. Henry and S. Wain-Hobson (1996a) "Hypermutagenic PCR involving all four transitions and a sizeable proportion of transversions", Nucleic acids research, 24: 2627-31

J. P. Vartanian, M. Henry and S. Wain-Hobson (1996b) "Hypermutagenic PCR involving all four transitions and a sizeable proportion of transversions", Nucleic Acids Res, 24: 2627-31

N. Verdoni, M. A. Aon, J. M. Lebeault and D. Thomas (1990) "Proton motive force, energy recycling by end product excretion, and metabolic uncoupling during anaerobic growth of *Pseudomonas mendocina*", Journal of bacteriology, 172: 6673-81

M. F. Verhagen, T. O'Rourke and M. W. Adams (1999) "The hyperthermophilic bacterium, *Thermotoga maritima*, contains an unusually complex iron-hydrogenase: amino acid sequence analyses versus biochemical characterization", Biochimica et biophysica acta, 1412: 212-29

P. M. Vignais and B. Billoud (2007) "Occurrence, classification, and biological function of hydrogenases: an overview", Chemical reviews, 107: 4206-72

I. M. Vincent, D. J. Creek, K. Burgess, D. J. Woods, R. J. Burchmore and M. P. Barrett (2012) "Untargeted metabolomics reveals a lack of synergy between nifurtimox and eflornithine against *Trypanosoma brucei*", PLoS neglected tropical diseases, 6: e1618

D. Vinella, C. Brochier-Armanet, L. Loiseau, E. Talla and F. Barras (2009) "Iron-sulfur (Fe/S) protein biogenesis: phylogenomic and genetic studies of A-type carriers", PLoS genetics, 5: e1000497

A. Volbeda, M. H. Charon, C. Piras, E. C. Hatchikian, M. Frey and J. C. Fontecilla-Camps (1995) "Crystal structure of the nickel-iron hydrogenase from *Desulfovibrio gigas*", Nature, 373: 580-7

A. Volbeda, J. C. Fontecilla-Camps and M. Frey (1996) "Novel metal sites in protein structures", Current opinion in structural biology, 6: 804-12

A. Volbeda, L. Martin, C. Cavazza, M. Matho, B. W. Faber, W. Roseboom, S. P. Albracht, E. Garcin, M. Rousset and J. C. Fontecilla-Camps (2005) "Structural differences between the ready and unready oxidized states of [NiFe] hydrogenases", Journal of biological inorganic chemistry : JBIC : a publication of the Society of Biological Inorganic Chemistry, 10: 239-49

A. Volbeda, P. Amara, C. Darnault, J. M. Mouesca, A. Parkin, M. M. Roessler, F. A. Armstrong and J. C. Fontecilla-Camps (2012) "X-ray crystallographic and computational studies of the O2-tolerant [NiFe]-hydrogenase 1 from *Escherichia coli*", Proceedings of the National Academy of Sciences of the United States of America, 109: 5305-10

A. Volbeda, C. Darnault, A. Parkin, F. Sargent, F. A. Armstrong and J. C. Fontecilla-Camps (2013) "Crystal structure of the O(2)-tolerant membrane-bound hydrogenase 1 from *Escherichia coli* in complex with its cognate cytochrome b", Structure, 21: 184-90

M. Wachsmuth, S. Findeiss, N. Weissheimer, P. F. Stadler and M. Morl (2013) "De novo design of a synthetic riboswitch that regulates transcription termination", Nucleic acids research, 41: 2541-51

A. F. Wait, C. Brandmayr, S. T. Stripp, C. Cavazza, J. C. Fontecilla-Camps, T. Happe and F. A. Armstrong (2011) "Formaldehyde--a rapid and reversible inhibitor of hydrogen production by [FeFe]-hydrogenases", Journal of the American Chemical Society, 133: 1282-5

L. Wang, A. Brock, B. Herberich and P. G. Schultz (2001) "Expanding the genetic code of *Escherichia coli*", Science, 292: 498-500

L. Wang, A. Brock and P. G. Schultz (2002) "Adding L-3-(2-Naphthyl)alanine to the genetic code of E. coli", Journal of the American Chemical Society, 124: 1836-7

T. Wang, X. Ma, H. Zhu, A. Li, G. Du and J. Chen (2012) "Available methods for assembling expression cassettes for synthetic biology", Applied microbiology and biotechnology, 93: 1853-63

W. Wang, X. Liu and X. Lu (2013) "Engineering cyanobacteria to improve photosynthetic production of alka(e)nes", Biotechnology for biofuels, 6: 69

H. S. Waring and C. H. Werkman (1944) "Iron deficiency in bacterial metabolism", Arch. Biochem, 4: 75-87

R. Waugh and D. H. Boxer (1986) "Pleiotropic hydrogenase mutants of *Escherichia coli* K12: growth in the presence of nickel can restore hydrogenase activity", Biochimie, 68: 157-66

J. H. Weiner, P. T. Bilous, G. M. Shaw, S. P. Lubitz, L. Frost, G. H. Thomas, J. A. Cole and R. J. Turner (1998) "A novel and ubiquitous system for membrane targeting and secretion of cofactor-containing proteins", Cell, 93: 93-101

F. H. Westheimer (1987) "Why nature chose phosphates", Science, 235: 1173-8

C. D. Whitfield, E. J. Steers, Jr. and H. Weissbach (1970) "Purification and properties of 5-methyltetrahydropteroyltriglutamate-homocysteine transmethylase", The Journal of biological chemistry, 245: 390-401

J. Woodward, M. Orr, K. Cordray and E. Greenbaum (2000) "Enzymatic production of biohydrogen", Nature, 405: 1014-5

Y. Xue, Y. Xu, Y. Liu, Y. Ma and P. Zhou (2001) "*Thermoanaerobacter tengcongensis* sp. nov., a novel anaerobic, saccharolytic, thermophilic bacterium isolated from a hot spring in Tengcong, China", International journal of systematic and evolutionary microbiology, 51: 1335-41

S. S. Yazdani and R. Gonzalez (2007) "Anaerobic fermentation of glycerol: a path to economic viability for the biofuels industry", Current opinion in biotechnology, 18: 213-9

Y. Yokobayashi, R. Weiss and F. H. Arnold (2002) "Directed evolution of a genetic circuit", Proceedings of the National Academy of Sciences of the United States of America, 99: 16587-91

A. Yoshida, T. Nishimura, H. Kawaguchi, M. Inui and H. Yukawa (2005) "Enhanced hydrogen production from formic acid by formate hydrogen lyase-overexpressing *Escherichia coli* strains", Applied and environmental microbiology, 71: 6762-8

I. G. Young (1975) "Biosynthesis of bacterial menaquinones. Menaquinone mutants of *Escherichia coli*", Biochemistry, 14: 399-406

R. Yu, W. Zong and Z. Zhou (2011) "[Engineering of *Escherichia coli* for convenient expression of [FeFe]-hydrogenase]", Wei sheng wu xue bao = Acta microbiologica Sinica, 51: 1468-75

A. L. Zbell, S. L. Benoit and R. J. Maier (2007) "Differential expression of NiFe uptake-type hydrogenase genes in Salmonella enterica serovar Typhimurium", Microbiology, 153: 3508-16

X. Zhang, K. Jantama, J. C. Moore, L. R. Jarboe, K. T. Shanmugam and L. O. Ingram (2009a) "Metabolic evolution of energy-conserving pathways for succinate production in *Escherichia coli*", Proceedings of the National Academy of Sciences of the United States of America, 106: 20180-5

X. Zhang, K. Jantama, K. T. Shanmugam and L. O. Ingram (2009b) "Reengineering *Escherichia coli* for Succinate Production in Mineral Salts Medium", Applied and environmental microbiology, 75: 7807-13

Z. Zhang, L. Wang, A. Brock and P. G. Schultz (2002) "The selective incorporation of alkenes into proteins in *Escherichia coli*", Angewandte Chemie, 41: 2840-2

C. Zirngibl, W. Van Dongen, B. Schworer, R. Von Bunau, M. Richter, A. Klein and R. K. Thauer (1992) "H2-forming methylenetetrahydromethanopterin dehydrogenase, a novel type of hydrogenase without iron-sulfur clusters in methanogenic archaea", European journal of biochemistry / FEBS, 208: 511-20